UNIVERSITÀ DEGLI STUDI DI NAPOLI FEDERICO II

SCUOLA POLITECNICA E DELLE SCIENZE DI BASE
AREA DIDATTICA DI SCIENZE MATEMATICHE FISICHE E NATURALI

DOTTORATO IN SCIENZE DELLA TERRA, DELL'AMBIENTE E DELLE RISORSE

XXXIV CICLO

PHD THESIS

TRACE ELEMENTS, ORGANIC COMPOUNDS AND INTERSTITIAL GASES (RADON AND CO_2) DISTRIBUTION IN THE NEAR SURFACE ENVIRONMENT OF CAMPANIA REGION: NEW METHODS FOR PATTERNS RECOGNITION OF HIDDEN ASSOCIATIONS.

PhD Candidate

Annalise Guarino

Tutor

Prof.ssa Annamaria Lima
(University of Naples Federico II, Naples)

Co-tutors

Prof. Stefano Albanese
(University of Naples Federico II, Naples)

Prof. Domenico Cicchella
(University of Sannio, Benevento)

2018 - 2022

Index

Introduction to the scientific problem

High concentrations of some chemical elements and compounds in the environment can be attributed either to natural sources or anthropogenic causes (e.g., industrial and residential emissions, uncontrolled spills and waste combustion, etc.) (Antoniadis et al., 2019; Albanese and Breward, 2011). Geochemical mapping can be considered a primary tool to identify portions of the territory affected by potential contamination. It is also a starting point for all the assessment processes focusing on safeguarding public health from repercussions related to the equilibrium of the food chain. A correct determination and interpretation of the geochemical patterns in environmental media can bring to more efficient management of anthropised territories favouring the identification of contaminating sources (Plant et al., 2001).

The contamination of environmental media that is mainly due to potentially toxic elements (PTEs) and organic compounds, such as polycyclic aromatic hydrocarbons (PAHs), polychlorinated biphenyls (PCBs) and organochlorine pesticides (OCPs), is primarily affecting air, water, sediment, and soil; collaterally, agricultural products can also be included in the category of environmental media of interest as they are among the main responsible for the transfer of toxic substances to the biological cycle.

As for PTEs, to interpret the nature of the geochemical anomalies, it is essential to determine those concentration ranges to be taken as a reference for the natural background or baseline, especially in solid and liquid media.

In the last two decades, various international projects have been activated at continental and global scales to establish geochemical baselines and determine background (geogenic) values to be used as a reference to discriminate among natural and anthropic sources (Darnley et al., 1995).

In Europe, in response to the IUGS/IAGC Global Geochemical Baselines Programme (https://www.globalgeochemicalbaselines.eu/), the Eurogeosurvey Geochemistry Expert Group (EGEG), assisted by some local research institutions such as universities and research centres, completed two main surveys:

a) the FOREGS project (Salminen et al., 2005; De Vos and Tarvainen, 2006) (based on topsoil, bottom soil, stream and floodplain sediments, surficial and groundwaters, and humus) aiming at applying standardised methods of sampling, chemical analysis and data management to prepare a geochemical baseline across Europe (http://weppi.gtk.fi/publ/foregsatlas/index.php);
b) The GEMAS project (Reimann et al. 2014a; Reimann et al., 2014b) aiming at generating the geochemical mapping of agricultural and grazing land soil of Europe in response to the new

European Chemicals Regulation (REACH), adopted in December 2006, requiring a sound knowledge of the natural geochemical background variation from industry (http://gemas.geolba.ac.at/).

In Italy, the Environmental Geochemistry Working Group (EGWG), based at the Department of Earth, Environment and Resources Sciences, University of Naples Federico II, has collaborated with the EGEG since the late nineties, taking an active part in both FOREGS and GEMAS projects and several related activities developed at both continental and national level (see Aruta and Guarino, 2020, and reference therein).

Following the experience gained in the international field, the EGWG has also activated various geochemical monitoring projects strictly focusing on the Campania region's territory. In 2006, the Environmental Geochemical Atlas of Campania Region (De Vivo et al., 2006) was published by using data referring to almost 3000 stream sediment samples, and, in 2016, the Environmental Geochemical Atlas of Campania Soils (De Vivo et al., 2016) was also released based on 3535 topsoils. Similarly to the work done in the European framework, also for the regional atlases, one of the main aims was to determine the local reference values (background/baseline) for PTEs and other metals and metalloids. Once the reference values were set, in most cases, it was possible to estimate the degree of environmental contamination due to a single element and discriminate between the burden of the component related to human pressure and that of geogenic origin (Albanese et al., 2007; Cicchella et al., 2005, 2013; Salminen and Gregorauskiene, 2000; Thiombane et al., 2018a, 2018b).

In 2015, the "Campania Trasparente" project (http://www.campaniatrasparente.it), an integrate monitoring plan focused on assessing the environmental conditions of the territory of the Campania region, started thanks to the financial support of the regional government.

The primary scope of the whole project was to explore the existence of a link between the presence of some illnesses in the local population and the status of the environment and generate a reliable database to assess local foodstuff healthiness. In the project framework, the collection and analysis of many environmental and biological samples (including soil and air and human blood specimen) were completed, and the EGWG was in charge of most of the research activities focusing on PTEs and organic contaminants in soils and air. Four volumes were published (De Vivo et al., 2021a, 2021b, 2022a, 2022b), including statistical elaborations and geochemical maps to provide both the regional government and local scientific and professional community with a reliable tool to approach local environmental problems starting from a sound knowledge base.

The integration of all the data generated within the "Campania Trasparente" framework, including the data proceeding from the Susceptible Population Exposure Study (SPES)

(http://spes.campaniatrasparente.it/), focusing on human biomonitoring (based on blood), allowed the development of a regional-wide conceptual model to be used as a base to generate highly specialised risk assessments for regional population and local communities affected by specific environmental problems.

Among the others, one of the specific objectives of the "Campania Trasparente" project in charge to EGWG was to assess the amount of individual substances likely to enter the food chain once their origin in soil was stated. The assessment of bioavailability, tightly connected with crop production and food quality, is today one of the main topics of discussion for the scientific community that deals with environmental risk and health issues (Petruzzelli et al., 2020; Ryu et al., 2010).

The aim of this PhD thesis, partially sharing the "Campania Trasparente" objectives and data, was to address specific scientific problems which are, nowadays, of great relevance and interest in the field of environmental geochemistry and medical geology.

Specifically, the thesis focused on the development of the geochemical mapping of raw and background/baseline values of Campania region territory based on the data of the "Campania Trasparente" project and, subsequently, it addressed some specific environmental topics related to human health, such as the variation of spatial patterns of radon fluxes and the bioavailable fraction of some PTE and major elements in regional soils.

Furthermore, numerous collaborations have been made, always on environmental issues of regional interest, collaborating with other members of the research group with the purpose of pursuing both individual growth and solid scientific results based on knowledge sharing and confrontation.

PhD project development and structure of the thesis

During the completion of the PhD program, I had the opportunity to collaborate in drafting the new geochemical atlases of the Campania region related to the data generated within the framework of "Campania Trasparente", working on nearly all the cartographic and statistical elaborations present in them.

The mapping of background/baseline values of PTEs in regional soils highlighted the inadequacy of the national environmental regulations (D.Lgs 152/2006) for managing site-specific problems, especially for geo-pedologically varied regions such as Campania. Therefore, it was decided to investigate the question relating to the definition of reference baseline values at a sub-regional scale in a delicate area between the alluvial plain of the Sarno river, to the south, and the slopes the Mt. Vesuvius, to the north. In addition, being the plain north of Vesuvius known for being an area featured

by a serious anthropic impact and characterised by a very high population density, a detailed study was conducted on this area to define the sources of contamination of PTEs, PAHs and OCPs.

During the development of the regional cartography, it was also found that the distribution of the bioavailable concentrations (based on an ammonium nitrate leaching) of PTEs and other elements in soils did not follow a linear model when compared to measured total concentration (referring to a modified Aqua Regia leaching); it was, hence, decided to study the behaviour of some of those parameters that are recognized to some extent by the current literature as responsible of the change occurring in the bioavailable fractions.

The high concentrations of uranium (U), thorium (Th) and potassium (K) found in regional soils, mainly due to the volcanic nature of the geologic source materials, gave rise to concern about the exposure of the population to low ionizing radiation and to radon. Therefore, it was made a first attempt to estimate the regional variations of the pedogenic radon flux using the available geochemical data jointly with a radiological database containing data on environmental gamma radiation associated with ^{238}U, ^{232}Th and ^{40}K decay in regional soils. The assessment of the health risk due to ^{222}Rn based on quantitative information rather than observational data such as those retrieved from geological maps was completed. In addition, some considerations were made on the possible use of ^{222}Rn flux as a proxy of the presence of active tectonic lineaments across the Campania region.

The thesis has been structured in chapters following the different topics covered during the PhD program:

- Chapter 1 reports the activities concerning the statistical and cartographic processing of analytical data relating to the presence and distribution of potentially toxic elements (PTEs) and other elements and persistent organic pollutants (POPs) in the soil and air samples collected in the whole Campania region in surveys completed in 2017. The cartography produced made it possible to analyse the discrete (dot map) and spatially continuous (raster map) distribution of all the investigated variables, favoring the process of identifying associations of elements and compounds that have similar behavior in environmental media due to specific processes of natural or anthropogenic accumulation. The results of the geostatistical analysys conducted and the cartographic products generated are reported in four volumes (De Vivo et al., 2021a, 2021b, 2022a, 2022b).
- Chapter 2 describes a follow-up study conducted in the eastern sector of the Campania Plain, correpsonding to a portion of the Vesuvian and the Sarno River Basin areas. The cartography of potential hazard produced at the regional scale led to discriminate areas with high concentrations of some PTEs with a high probability to be geogenic rather than anthropogenic. This latter

condition has highlited the inadequacy of the principle of using a single legislative environmental guideline value for individual elements on a national scale. The local background/baseline values were determined for As, Be, V, Tl, Cu and Zn and reference values were set to be used as local guidelines to assess the real need to start characterisation procedures at site-specific level. The results of the work have been presented at the Goldschmidt Virtual 2021 (Guarino et al., 2021c) and they were submitted, as a scientific article, in a special volume dedicated to contaminated sites and remediation methods published by the Italian Society of Environmental Geology (SIGEA) (Albanese et al., 2022); in addition, a regional decree (Regional Executive Decree no. 735 25/11/2021) was issued to formalise the use of the background/baseline values defined by the study in substitution of the national guideline values for the study area .

- Chapter 3 shows the results of the study conducted on the bioavailable concentrations (based on ammonium nitrate leaching) of some major and in trace elements (i.e., Al, Ca, Cu, K, Mg, Tl) in the topsoil of Campania region. These data were compared with the pseudo-total concentrations (determined via an Aqua Regia leaching) and an analysis has been conducted to assess the relationship between bioavailability of elements and the spatial distribution of some parameters such as the organic matter content (OM) and the grain size. The results of the work have been submitted to the Journal of Geochemical Exploration (Guarino et al., submitted).
- Chapter 4 reports the outcomes of a study of the geochemical-environmental conditions conducted on the territory of the city of Acerra and the neighboring municipalities, in the north-eastern sector of the metropolitan city of Naples. The analytical data relative to the concentrations of PTEs, PAHs and OCPs in the soils of the area were statistically processed in order to carry out an environmental assessment based on a geostatistical approach and a multivariate analysis of the data. The results of the studies conducted on PTEs and PAHs have been presented at the conferences Goldschmidt Virtual 2020 (Guarino et al., 2020a) and GeoHealth 2020 – International Meeting of Geohealth Scientists (Guarino et al., 2020c), and are reported in Guarino et al. (2020b); the results concerning the distribution of OCPs have been presented at the European Geosciences Union (EGU) General Assembly 2021 (Guarino et al., 2021b).
- Chapter 5 illustrates the work made to assess the ^{222}Rn flux in the soil of Campania region. Radiometric and geochemical compositional data analysed in topsoil samples were elaborated to estimate the potential fluctuation of ^{222}Rn across the region. The results obtained from the two different datasets were analysed and compared to discriminate the nature of the different sources that potentially contribute to the surficial Rn fluxes. The results of the studies have been presented at the conferences European Geosciences Union (EGU) General Assembly 2020 (Albanese et al., 2020), Geohealth – the International Meeting of Geohealth Scientists (Guarino et al., 2020d) and

the BeGeo Scientists 2021 (Guarino et al., 2021a). A scientific article has been also published in the international peer-reviewed journal Chemosphere (Guarino et al, 2022).

- Chapter 6 illustrates the results of the scientific collaborations with other members of the research group. A brief summary of the researches completed (Dominech et al., 2020, submitted; Ebrahimi et al., 2022, under review; Somma et al., 2021) is reported and, for each collaboration, details on the contribution given are proposed.

References

Albanese, S., 2008. Evaluation of the bioavailability of potentially harmful elements in urban soils through ammonium acetate–EDTA extraction: a case study in southern Italy. Geochem.: Explor. Environ. Anal. 8, 49-57.

Albanese, S., Breward, N., 2011. Sources of Anthropogenic Contaminants in the Urban Environment, in: Johnson, C.C. (Eds.), Mapping the chemical environment of urban areas. Wiley, pp. 116-127.

Albanese, S., De Vivo, B., Lima, A., Cicchella, D., 2007. Background and baseline values of toxic elements in stream sediments of Campania region (Italy). J. Geochem. Explor. 93, 21-34.

Albanese, S., Guarino, A., Pizzolante, A., Nicodemo, F., Ragone, G., Iorio, R., D'Antonio, A., Ferraro, A., 2022. The use of natural geochemical background values for the definition of local environmental guidelines: the case study of the Vesuvian plain. In: Baldi, D., and Uricchio, F. (Eds.), Le bonifiche ambientali nell'ambito della transizione ecologica, Società Italiana di Geologia Ambientale (SIGEA) and Consiglio Nazionale delle Ricerche (CNR).

Albanese, S., Guarino, A., Zuzolo, D., Aruta, A., Cicchella, D., Iannone, A., Melito, R., Verrilli, F., Fedele Gianvito, A., 2020. Extending the concept of background to soil gas: natural radon concentrations in soils of Campania region. European Geosciences Union General Assembly 2020, Vienna.

Antoniadis, V., Shaheen, S.M., Levizou, E., Shahid, M., Niazi, N.K., Vithanage, M., Ok, Y.S., Bolan, N., Rinklebe, J., 2019. A critical prospective analysis of the potential toxicity of trace element regulation limits in soils worldwide: Are they protective concerning health risk assessment? - A review. Environ. Int. 127, 819-847. https://doi.org/10.1016/j.envint.2019.03.039.

Aruta, A., Guarino, A., 2020. The European and Italian experience in the global geochemical baseline mapping and some related activities: soils, waters and sediments. GIS DAY 2018, pp 79-100. ISBN: 978-88-255-2952-4.

Cicchella, D., De Vivo, B., Lima, A., 2005. Background and baseline concentration values of harmful elements in the volcanic soils of metropolitan and Provincial areas of Napoli (Italy). Geochem.: Explor. Environ. Anal 5, 1-12.

Cicchella, D., Giaccio, L., Lima, A., Albanese, S., Cosenza, A., Civitillo, D., De Vivo, B, 2014. Assessment of the topsoil heavy metals pollution in the Sarno River basin, south Italy. Environ. Earth Sci. 71(12), 5129-5143.

Darnley, A.G., Bjorklund, A., Bolkiven, B., Gustavsson, N., Koval, P.V., Plant, J.A., Steenfelt, A., Tauchid, M., Xie, X., 1995. A global geochemical database for environmental and resource management. Recommendation for international geochemical mapping. Final Report of IGCP Project 259, Earth Sciences 19, UNESCO, Paris.

De Vivo, B., Albanese, S., Lima, A., Qu, C., Fortelli, A., Guarino, A., Zuzolo, D., Esposito, M., Pizzolante, A., Cerino, P., Hope, D., Pond, P., Cicchella, D., 2021a. Monitoraggio Geochimico-Ambientale dei suoli della Regione Campania – Volume 2 (Composti Organici Persistenti: Idrocarburi Policiclici Aromatici, Policlorobifenili, Pesticidi). Aracne Editrice, Roma. ISBN: 978-88-255-4107-6.

De Vivo, B., Cicchella, D., Albanese, S., Qu, C., Guarino, A., Fortelli, A., Esposito, M, Cerino, P., Pizzolante, A., Hope, D., Pond, P., Lima, A., 2022a. Monitoraggio geochimico-ambientale della matrice aria della Regione Campania. Il Piano Campania Trasparente. Volume 3. Idrocarburi Policiclici Aromatici (IPA, Policlorobifenili (PCB), Pesticidi (OCP), Eteri di Polibromobifenili (PBDE), Elementi Potenzialmente Tossici (EPT). Aracne Editrice, Roma. ISBN: 979-12-5994-733-8, 676 pag.

De Vivo B., Cicchella D., Lima, A., Fortelli A., Guarino A., Zuzolo D., Esposito M., Cerino P., Pizzolante A., Albanese S., 2021b. Monitoraggio Geochimico-Ambientale dei suoli della Regione Campania – Volume 1 (Elementi Potenzialmente Tossici e loro Biodisponibilità, Elementi Maggiori e in Traccia; distribuzione in suoli superficiali e profondi). Aracne Editrice, Roma. ISBN: 978-88-255-4036-9.

De Vivo, B., Cicchella, D., Lima, A., Guarino, A., Qu, C., Fortelli, A., Esposito, M, Cerino, P., Pizzolante, A., Albanese, S., 2022b. Sintesi del monitoraggio dei suoli e dell'aria della regione Campania, a scala regionale e locale. Piano Campania Trasparente. Volume 4: Elementi potenzialmente tossici (EPT) e loro biodisponibilità elementi maggiori e in traccia, Idrocarburi Policiclici Aromatici (IPA), Policlorobifenili (PCB), Pesticidi (OCP), Eteri di Polibromobifenili (PBDE). Aracne Editrice, Roma. ISBN: 979-12-5994-735-2, 240 pag.

De Vivo, B., Lima, A., Albanese, S., Cicchella, D., 2006. Atlante geochimico-ambientale dei suoli dell'area urbana e della provincia di Napoli. Aracne editrice, pp 216.

De Vivo, B., Lima, A., Albanese, S., Cicchella, D., Rezza, C., Civitillo, D., Minolfi, G., Zuzolo, D., 2016. Atlante Geochimico- ambientale dei suoli della Campania. Aracne editrice, Roma, pp 359.

De Vos, W., Tarvainen, T., 2006. Geochemical atlas of Europe. Part 2, Geochemistry of elements. Geological Survey of Finland Otamedia Oy Espoo.

Dominech, S., Albanese, S., Guarino, A., Yang, S., submitted. Using compositional data analysis and multivariate statistics to indicate the enrichments of potentially toxic elements (PTEs) in sediments from the Changjiang (Yangtze) River. Geochemical Transactions

Dominech, S., Guarino, A., Aruta, A., Ebrahimi, P., Yang, S., Albanese, S., 2020. Potentally toxic elements (PTEs) distribution and main geochemical processes in Sabato River Catchment Basin (southern Italy): a focus on cadmium. Conference proceedings, Proscience vol. 7. ISSN: 2283-5954.

Ebrahimi, P., Guarino, A., Allocca, V., Caliro, S., Cicchella, D., Albanese, S., under review. The dissolved radon and carbon dioxide contents in Phlegraean Fields volcanic aquifer: a follow-up study. Chemosphere

Ebrahimi, P., Guarino, A., Allocca, V., Caliro, S., Avino, R., Bagnato, E., Capecchiacci, F., Carandente, A., Minopoli, C., Santi, A., Albanese, S., 2022. Hierarchical clustering and compositional data analysis for interpreting groundwater hydrogeochemistry: The application to Campi Flegrei volcanic aquifer (south Italy). J. Geochem. Explor. 233. https://doi.org/10.1016/j.gexplo.2021.106922

Guarino, A., Albanese, S., Cicchella, D., Ebrahimi, P., Dominech, S., Allocca, C., Romano, N., De Vivo, B., Lima, A., submitted. Selected major and potentially toxic elements bioavailability in agricultural soils of Campania region (Italy): spatial patterns and influencing factors. J. Geochem. Explor.

Guarino, A., Aruta, A., Ebrahimi, P., Dominech, S., Albanese, S., 2020a. The "Triangle of Death": a case study from Campania region (Italy). Goldschmidt Virtual 2020, Honolulu. DOI: 10.46427/gold2020.897.

Guarino, A., Aruta, A., Ebrahimi, P., Dominech, S., Lima, A., Cicchella, D., Albanese, S., 2021a. Radon fluxes estimate from geochemical data and gamma radiation in Campania region (Italy). BeGeo scientists 2021, Naples. https://doi.org/10.3301/ABSGI.2021.04

Guarino, A., Aruta, A., Ebrahimi, P., Dominech, S., Lima, A., De Vivo, B., Qi, S., Albanese, S., 2020b. Potentially Harmful Elements and Polycyclic Aromatic Hydrocarbons in the soils of Acerra, southern Italy. Conference proceedings, Proscience vol. 7. ISSN: 2283-5954.

Guarino, A., Aruta, A., Ebrahimi, P., Dominech, S., Lima, A., De Vivo, B., Qi, S., Albanese, S., 2020c. Potentially Harmful Elements and Polycyclic Aromatic Hydrocarbons in the soils of Acerra, southern Italy. GEOHEALTH 2020 - INTERNATIONAL MEETING OF GEOHEALTH SCIENTISTS, Bari. Scientific Research Abstracts Vol. 10, p. 25. ISSN 2464-9147.

Guarino, A., Aruta, A., Ebrahimi, P., Dominech, S., Lima, A., De Vivo, B., Qi, S., Albanese, S., 2021b. Organochlorine pesticides in the soils of the Acerra plain: concentration and distribution of DDT isomers and metabolites. European Geosciences Union General Assembly 2021, Vienna. DOI: 10.5194/egusphere-egu21-5739

Guarino, A., Aruta, A., Ebrahimi, P., Dominech, S., Zuzolo, D., Lima, A., Cicchella, D., Albanese, S., 2020d. Pedogenic radon fluxes predictions from geochemical data and gamma ray: the Campania region experiment. GEOHEALTH 2020 - INTERNATIONAL MEETING OF GEOHEALTH SCIENTISTS, Bari. Scientific Research Abstracts Vol. 10, p. 26. ISSN 2464-9147.

Guarino, A., Lima, A., Cicchella, D., Albanese, S., 2022. Radon flux estimates, from both gamma radiation and geochemical data, to determine sources, migration pathways, and related health risk: The Campania region (Italy) case study. Chemosphere 287(1), 132233. https://doi.org/10.1016/j.chemosphere.2021.132233

Guarino, A., Pizzolante, A., Nicodemo, F., Ragone, G., D'Antonio, A., Ferraro, A., Albanese, S., 2021c. The definition of geochemical background values at local scale as a key procedure to set reliable guidelines for contaminated land management. Goldschmidt Virtual 2021, Lyon. DOI: 10.7185/gold2021.3810

Petruzzelli, G., Pedron, F., Rosellini, I., 2020. Bioavailability and bioaccessibility in soil: a short review and a case study. AIMS Environ. Sci. 7(2), 208-225.

Plant, J., Smith, D., Smith, B., Williams, L., 2001. Environmental geochemistry at the global scale. J. Appl. Geochem. 16, 1291-1308.

Reimann, C., Birke, M., Demetriades, A., Filzmoser, P., O'Connor, P., (Eds.) 2014a. Chemistry of Europe's Agricultural Soils. Part A: Methodology and Interpolation of the GEOMAS Data Set. Geol. Jb., Hannover, 528 pp.

Reimann, C., Birke, M., Demetriades, A., Filzmoser, P., O'Connor, P., (Eds.) 2014b. Chemistry of Europe's Agricultural Soils. Part B: Genera Background Information and Further Analysis of the GEMAS Data Set – Geol. Jb., Hannover, 352 pp.

Ryu, H., Chung, J.S., Nam, T., Moon, H.S., Nam, K., 2010. Incorporation of heavy metals bioavailability into risk characterisation. Clean (Weinh) 38(9), 812–815.

Salminen, R., Batista, M.J., Bidovec, M., Demetriades, A., De Vivo, B., De Vos, W., Duris, M., Gilucis, A., Gregorauskiene, V., Halamic, J., Heitzmann, P., Lima, A., Jordan, G., Klaver, G., Klein, P., Lis, J., Locutura, J., Marsina, K., Mazreku, A., O'Connor, P.J., Olsson, S.A., Ottesen, R.T., Petersell, V., Plant, J.A., Reeder, S., Salpeteur, I., Sandström, H., Siewers, U., Steenfelt, A., Tarvainen, T., 2005. FOREGS Geochemical Atlas of Europe. Part 1 – Background Information. Methodology, and Maps. Geological Survey of Finland, Espoo, 526 pp.; http://weppi.gtk.fi/publ/foregsatlas/

Salminen, R., Gregorauskiene, V., 2000. Considerations regarding the definition of a geochemical baseline of elements in the surficial materials in areas differing in basic geology. Appl. Geochem. 15, 647-653.

Somma, R., Ebrahimi, P., Troise, C., De Natale, G., Guarino, A., Cicchella, D., Albanese, S., 2021. The first application of compositional data analysis (CoDA) in a multivariate perspective for detection of pollution source in sea sediments: The Pozzuoli Bay (Italy) case study. Chemosphere 274. DOI: 10.1016/j.chemosphere.2021.129955

Thiombane, M., Martín-Fernández, J.-A., Albanese, S., Lima, A., Doherty, A., De Vivo, B., 2018a. Exploratory analysis of multi-element geochemical patterns in soil from the Sarno River Basin (Campania region, southern Italy) through compositional data analysis (CODA). J. Geochem. Explor. 195, 110-120,

Thiombane, M., Zuzolo, D., Cicchella, D., Albanese, S., Lima, A., Cavaliere, M., De Vivo, B., 2018b. Soil geochemical follow-up in the Cilento World Heritage Park (Campania, Italy) through exploratory compositional data analysis and C-A fractal model. J. Geochem. Explor. 189, 85-99.

CHAPTER 1 – Geochemical atlases of Campania region

The results of this activity were published/presented in:

De Vivo, B., Albanese, S., Lima, A., Qu, C., Fortelli, A., Guarino, A., Zuzolo, D., Esposito, M., Pizzolante, A., Cerino, P., Hope, D., Pond, P., Cicchella, D., 2021a. Monitoraggio Geochimico-Ambientale dei suoli della Regione Campania – Volume 2 (Composti Organici Persistenti: Idrocarburi Policiclici Aromatici, Policlorobifenili, Pesticidi). Aracne Editrice. ISBN: 978-88-255-4107-6.

De Vivo, B., Cicchella, D., Albanese, S., Qu, C., Guarino, A., Fortelli, A., Esposito, M, Cerino, P., Pizzolante, A., Hope, D., Pond, P., Lima, A., 2022a. Monitoraggio geochimico-ambientale della matrice aria della Regione Campania. Il Piano Campania Trasparente. Volume 3. Idrocarburi Policiclici Aromatici (IPA, Policlorobifenili (PCB), Pesticidi (OCP), Eteri di Polibromobifenili (PBDE), Elementi Potenzialmente Tossici (EPT). Aracne Editrice, Roma. ISBN: 979-12-5994-733-8, 676 pag.

De Vivo, B., Cicchella, D., Lima, A., Fortelli, A., Guarino, A., Zuzolo, D., Esposito, M., Cerino, P., Pizzolante, A., Albanese, S., 2021b. Monitoraggio Geochimico-Ambientale dei suoli della Regione Campania – Volume 1 (Elementi Potenzialmente Tossici e loro Biodisponibilità, Elementi Maggiori e in Traccia; distribuzione in suoli superficiali e profondi). Aracne Editrice. ISBN: 978-88-255-4036-9.

De Vivo, B., Cicchella, D., Lima, A., Guarino, A., Qu, C., Fortelli, A., Esposito, M, Cerino, P., Pizzolante, A., Albanese, S., 2022b. Sintesi del monitoraggio dei suoli e dell'aria della regione Campania, a scala regionale e locale. Piano Campania Trasparente. Volume 4: Elementi potenzialmente tossici (EPT) e loro biodisponibilità elementi maggiori e in traccia, Idrocarburi Policiclici Aromatici (IPA), Policlorobifenili (PCB), Pesticidi (OCP), Eteri di Polibromobifenili (PBDE). Aracne Editrice, Roma. ISBN: 979-12-5994-735-2, 240 pag.

Figure 1.0 Covers of the published volumes.

1.1 Introduction

In recent years, Campania has been the subject of media attention for the alleged degradation of the agricultural territories which mainly concerned an area notoriously known as "Terra dei Fuochi", which comprehends 90 municipalities belonging to the provinces of Naples and Caserta. According to media, the practices of illegal waste disposals severely damaged the local environment affecting the health of local population (Flora, 2015). The lack of coverage of geochemical data collected at high spatial density, certifying the actual presence of contaminants in the various environmental media of the area, has favoured the diffusion of alarms relating to environmental emergencies no better defined in terms of territorial extension and health impact. The acquisition of scientific knowledge of a geochemical, medical and nutritional nature is essential to carry out studies aiming at potentially defining the cause-effect relationship between environmental exposure to contaminants and the onset of specific pathologies in living beings (De Vivo, 1995; Filippelli et al., 2012; Belkin et al., 2013; Valera et al., 2014).

The Environmental Geochemistry Working Group (EGWG) of the Department of Earth, Environment and Resources Sciences (DiSTAR) of the University of Naples Federico II, formerly chaired by Prof. Benedetto De Vivo and now by prof. Stefano Albanese, has repeatedly intervened on the problem that arose for the Campania region, proposing that it should be treated on a scientific basis, to try to determine, where possible, the potential migration paths followed by pollutants from the geological-environmental sector towards the biological one and, from the latter, along the food chain towards the apex, represented by man, but also to scientifically demonstrate the traceability of agri-food products that reach consumers, with the aim of characterising and certifying the quality of typical products of different types.

The problem was acknowledged and adopted by the “Campania Trasparente” project, financed by the Campania Region through the Experimental Zooprophylactic Institute of Southern Italy (IZSM), in which the Environmental Geochemistry Research Group of the University actively participated. The project, which began in September 2015 and ended in 2018, provided for the collection of tens of thousands of samples, including soils, groundwater, agricultural products, animal and human biological media, in order to guarantee the health of consumers of Campania products and evaluate the phenomena of human exposure landed by the biomonitoring Study of Exposure in the Susceptible Population (SPES).

The research aimed at carrying out investigations to characterise the geochemical composition of agricultural soil and groundwater on a regional and local basis, define the level of bioavailability of toxic elements and compounds, determine the absorption rates, by the various types of vegetable

crops, of the various potential chemical contaminants present in soils and groundwater and try to demonstrate a direct relationship between the presence of contaminants in soils, in air, in water, in agricultural products and finally in human media (hair, urine, blood) through innovative methodologies.

The enrichment or depletion of metal elements in soils, as well as the extent of contamination, depends on their relative mobility, in the chemical-physical conditions that regulate the environment of surface alteration and other factors. The known sources of anthropogenic contamination must be monitored and evaluated over time and the developed cartography, contained in the various geochemical-environmental atlases produced, constitutes one of the essential tools for achieving this goal.

In the framework of this thesis, only the databases related to the concentration of elements and organic compounds in the soil and air media have been treated to produce the basic geochemical mapping. This chapter briefly illustrates the sampling and analytical methods and the methodologies used to produce the geochemical maps and the statistical set of graphs are dealt with in detail.

1.2 Study area

Campania region has an extension of 13'670.60 km^2, divided into 5 provinces (Naples, Salerno, Caserta, Avellino and Benevento) and 550 municipalities (Fig. 1.1). With a population of about 5'624'260 persons and a population density of about 415 pop./km^2, it is the second most densely populated region of Italy, even if some city (e.g., Portici, Casavatore, San Giorgio a Cremano) have a population density of more than 10k pop./km^2, the highest in Italy. The distribution of the population is very uneven, with very large urban agglomerations along the coast, which often merge with the neighbouring ones, while in the mountainous areas of the Campania hinterland, such as those of Matese to the north and Cilento to the south, we find a scarce presence of inhabitants, no longer concentrated in macro urban systems but in traditional agricultural towns.

The region is bordered to the west by the Tyrrhenian Sea, to the north it borders with Lazio and Molise, to the east with Puglia and to the south with Basilicata. Its territory comprehends four important volcanic centres: to the north, in the Caserta province, is located the Mt. Roccamonfina, further south, in the central sector of the region, we found the Phlegrean Fields and Mt. Somma-Vesuvius, which surround the city of Naples to the north and south respectively, and the volcanic complex of the island of Ischia, the Mt. Epomeo (Fig. 1.2).

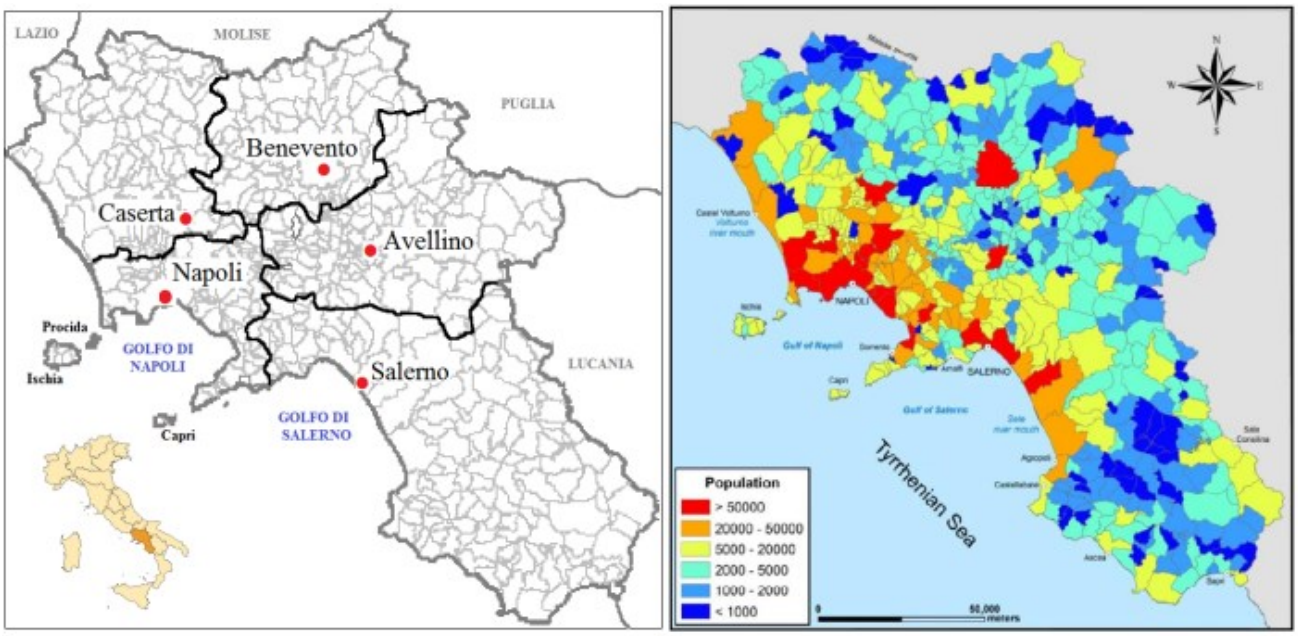

Figure 1.1 Provinces of the Campania Region, municipalities, and distribution of the resident population (De Vivo et al., 2021b).

Figure 1.2 Simplified geological map.

The geological-structural setting of the Campania region is very complex as it is the product of a considerable variety of geological processes (Vitale and Ciarcia, 2018). The geochemical variations recorded in the soils are due to a large number of variables, but a certainly greater weight is given by the lithologies on which the pedogenetic process is based. In the internal part of the region we find the Apennine reliefs, made up of carbonate and siliciclastic sedimentary successions, while in the external part we find the river plains (from north to south, Volturno, Sarno and Sele) and the volcanic reliefs and deposits (Fig. 1.2).

1.3 Soil

The primary objective has been the geostatistical and cartographic processing of the geochemical data relating to the soil media produced by the IZSM, as part of the "Campania Trasparente" project, and by the EGWG in previous activities. The geochemical data were validated and combined in order to produce an integrated and geo-referenced database aimed at the production of a set of basic geochemical maps, and derivative products, that could support the design of an integrated action aimed, at regional scale, to the evaluation of the intervention priorities for which to foresee follow-up and monitoring activities.

The produced databases contain the results of the analytical reports relating to samples of topsoils and bottom soils, analysed to determine the total and bioavailable concentrations of PTEs and other elements and the total concentrations of organic compounds of the families of polycyclic aromatic hydrocarbons (PAHs), polychlorinated biphenyls (PCBs) and organo-chlorine pesticides (OCPs).

Before cartographic processing, for each of the considered analytes, a univariate statistical analysis was carried out, alongside the graphical representation of the data (Fig. 1.3 and 1.4). Using an Excel worksheet, tables containing the main statistical indices (maximum, minimum, mean, median, mode, standard deviation, percentiles, kurtosis, asymmetry, mean absolute deviation, coefficient of variation) useful for the characterisation of the datasets were drawn up. The graphical representation of the statistical distribution of the data, including boxplots, cumulative histograms, and cumulative frequency curves, was generated using the KaleidaGraph software (Figs. 1.3 and 1.4).

All the data relating to the concentrations of the analytes in the soils were then processed in a GIS environment to produce the dot and raster basic cartography. Specifically, 241 dot maps with discrete distribution and 199 interpolated maps with spatially continuous distribution were produced.

Given the large number of materials developed, just some of the maps produced are shown here.

Litio (Li)

Distribuzione puntuale delle concentrazioni
Dot map

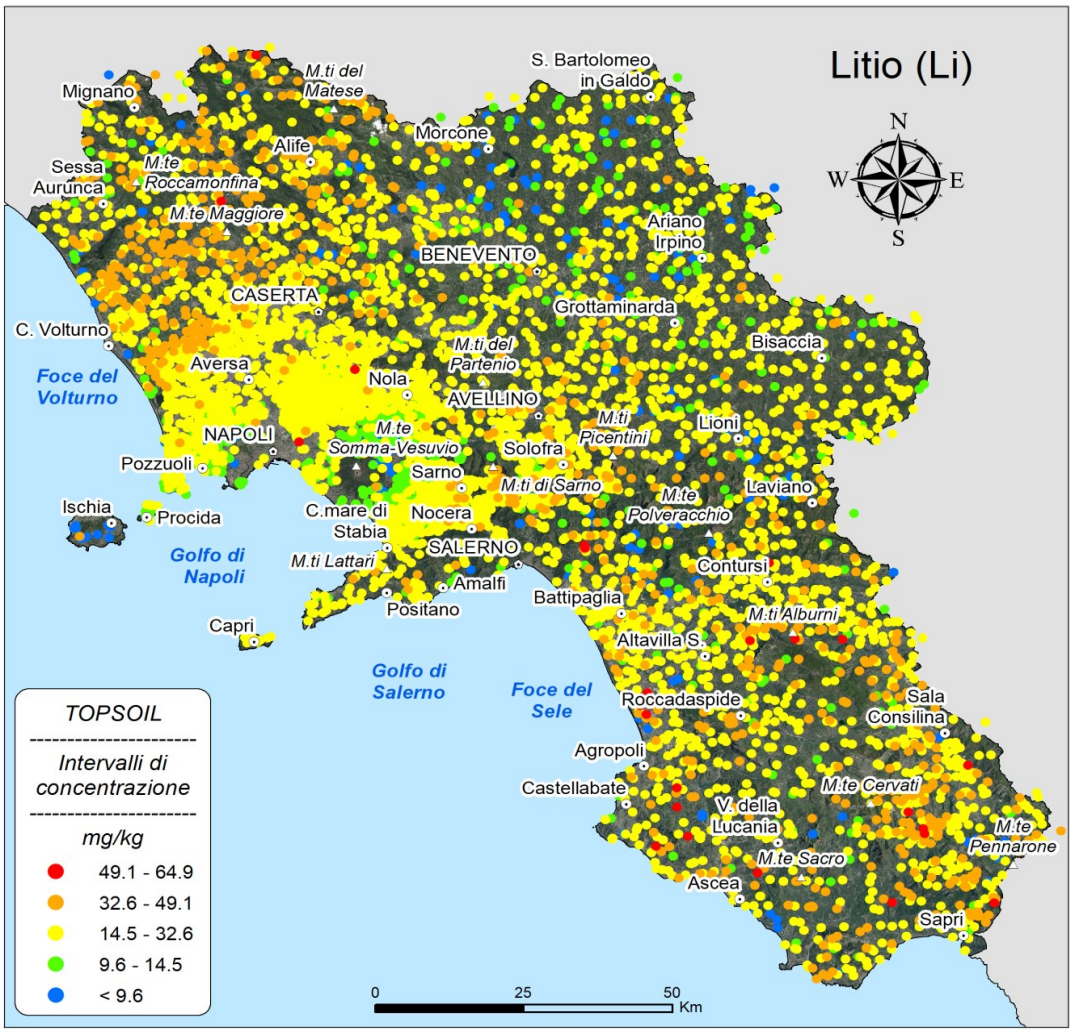

Elemento	Li
Unità di misura	mg/kg
N. campioni	5531
LRS	0,1
Accuratezza	4,3
Precisione	5,2
Minimo	0,9
25° percentile	17,35
Media	23,4
Mediana	22,8
75° percentile	28,5
95° percentile	38,8
Max	64,9

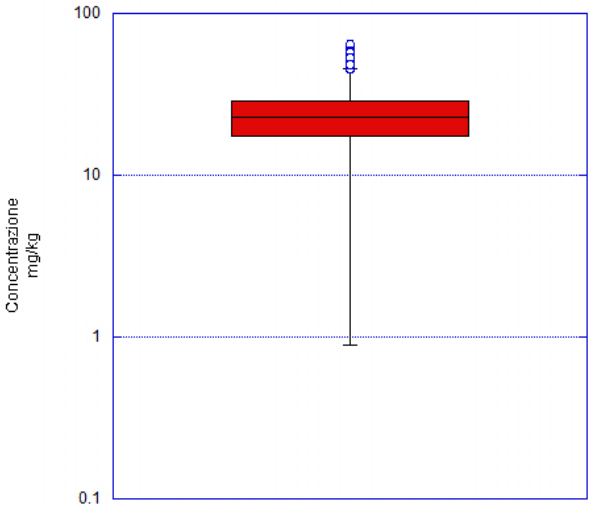

Figure 1.3 Example of a dot map with associated statistical graphs published in De Vivo et al. (2021b).

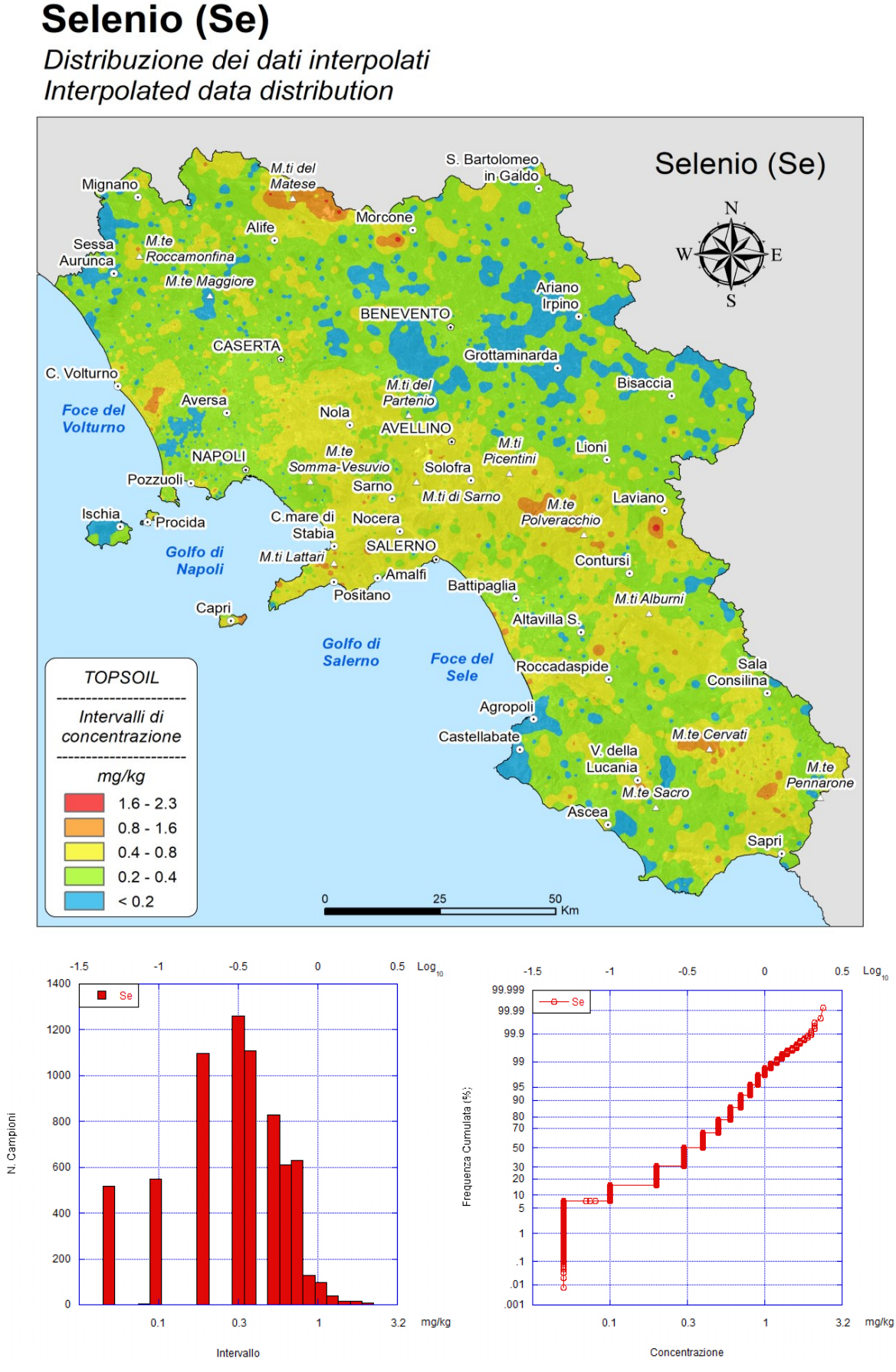

Figure 1.4 Example of a interpolated data map with associated statistical graphs published in De Vivo et al. (2021b).

1.3.1 Maps of the distribution of PTEs and other elements in topsoils and bottom soils

Until 2017, 7300 topsoil samples were collected, within a depth of 0.10 to 0.15 m below ground level, according the FOREGS procedures (Salminen et al., 1998), with a higher sampling density near urban centers and lower in rural areas (nominal average density is of ca. 1 sample per sqkm). In addition, 500 bottom soil samples were collected, within a depth of 0.80 to 1.20 m below ground level, in correspondence of the main river courses.

An aliquot of about 15 grams of the sample fraction <2 mm has been digested in an Aqua Regia modified solution (2 volumes of HCl + 2 volumes of HNO_3 + 2 parts of distilled water). The solutions were then analysed combining the ICP-MS (Inductively Coupled Plasma Mass Spectrometry) and ICP-ES (Inductively Coupled Plasma Emission Spectrometry) analytical methods, at the Bureau Veritas (formerly Acme) Analytical Laboratories Ltd. (Vancouver, Canada), to determine the concentration of 53 elements (Ag, Al, As, Au, B, Ba, Be, Bi, Ca, Cd, Ce, Co, Cr, Cs, Cu, Fe, Ga, Ge, Hf, Hg, K, In, La, Li, Mg, Mn, Mo, Na, Nb, Ni, P, Pb, Pd, Pt, Rb, Re, S, Sb, Sc, Se, Sn, Sr, Ta, Te, Th, Ti, Tl, U, V, Y, W, Zn, Zr). Further details on the sampling, analytical and quality control procedures can be found in De Vivo et al. (2021b).

The classification and definition of the concentration intervals for the dot maps of top and bottom soils took place through the analysis of the cumulative frequency curves of the data, normalised by logarithmic conversion (Log_{10}): where the distribution showed a normal distribution, for the classification were considered the values resulting from the addition formula between the arithmetic mean and standard deviation ($\dot{x} \pm n\sigma$, with n [0; 3], $\dot{x}$ = mean and σ = St.dev) (Siegel, 2002); instead, where the distribution was found to be multimodal (i.e., characterised by the presence of multiple data populations) the categorisation was performed on the basis of the values corresponding to the inflection points identified on the cumulative curve (which represent, approximately, the transition between different statistical populations) (Albanese et al., 2007b; De Vivo et al., 2006; Lima et al., 2007). Low frequency colours (shades of blue and green) were assigned to the lowest concentration ranges and colours with increasing frequency (from yellow to red) to those with higher concentrations (Fig. 1.5). Due to the high number of samples with concentrations below the instrumental detection limit (bdl), the maps of Ta, Re, Pd and Pt were not produced.

Given the strong characteristics of anisotropy and clustering of the sampling points, the data of the concentrations in the bottom soil have not been interpolated. The raster maps of the concentrations in topsoils were produced by mean of the Multifractal Inverse Distance Weighting (MIDW) interpolation algorithm, implemented with the GeoDAS software (Cheng et al., 2001). The method consists of an approach that uses the principles of fractal and multifractal geometry (Cheng, 1994,

1999; Cheng et al., 1994, 1996, 1999, 2000, 2001; Lima et al., 2003; Cicchella et al., 2005; Albanese et al., 2007a) to define, in a probabilistic way, the spatial distribution patterns of the input geochemical variables while preserving the high frequency information. In fact, it allows to preserve the existing spatial associations and singularities of the input data, which are to be considered as interruptions of the normal distribution of data and therefore as potential points of enrichments, or depletions, of the concentrations (characterised by limited extensions) to be intended as geochemical anomalies.

The pixels constituting the interpolated grids, produced for each analyte, were classified in intervals established by using a classification method called Concentration-Area (C-A) plot (Fig. 1.6). This method allows to divide the MIDW grids into various intervals (or populations) to each of which is assigned a colour to represent, on the maps, the different geochemical processes present in the investigation area. The subdivision is performed on the C-A diagram, which is obtained by plotting the concentration values (ρ), associated with each pixel, on the abscissa and the cumulative areas A(ρ), with concentration value ρ, on the ordinates (Cheng, 1999), in order to associate the spatial and geometric properties with the frequency distribution of the pixel values. From the projection on the abscissa of the slope breaking points (inflections) of the curve, the corresponding concentration values are obtained which are then used for the separation of the data into representative intervals to be proposed in the legend of the maps (Xu and Cheng, 2001).

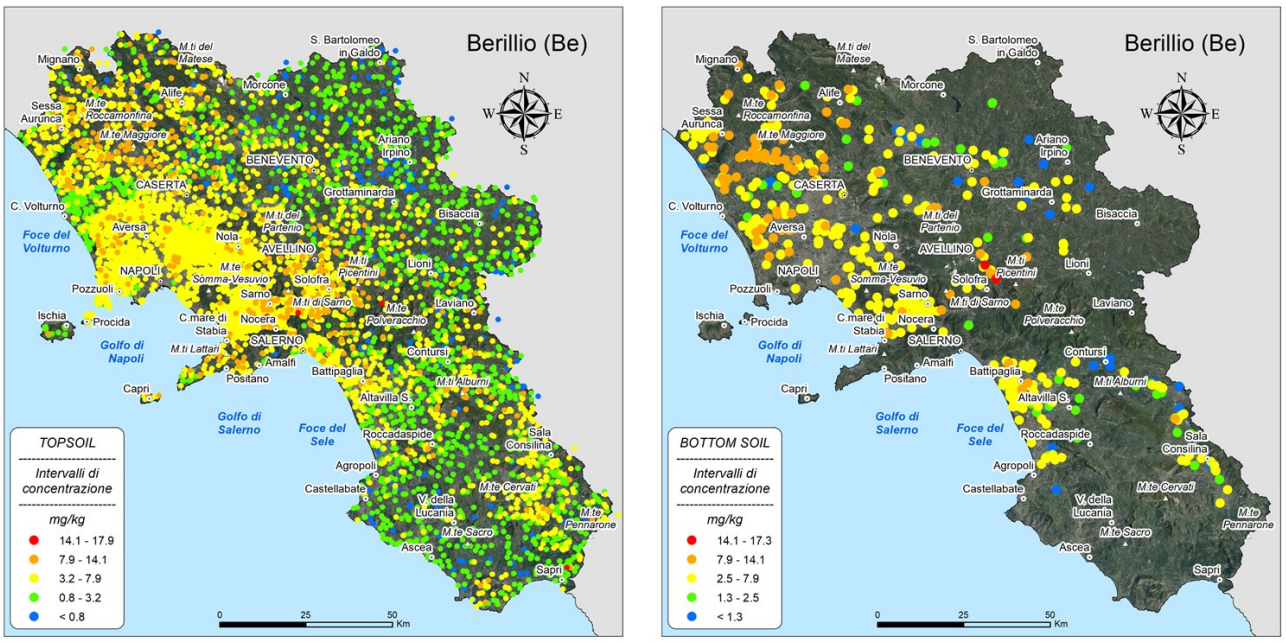

Figure 1.5 Examples of dot maps produced for the concentrations of elements in top and bottom soils (De Vivo et al., 2021b).

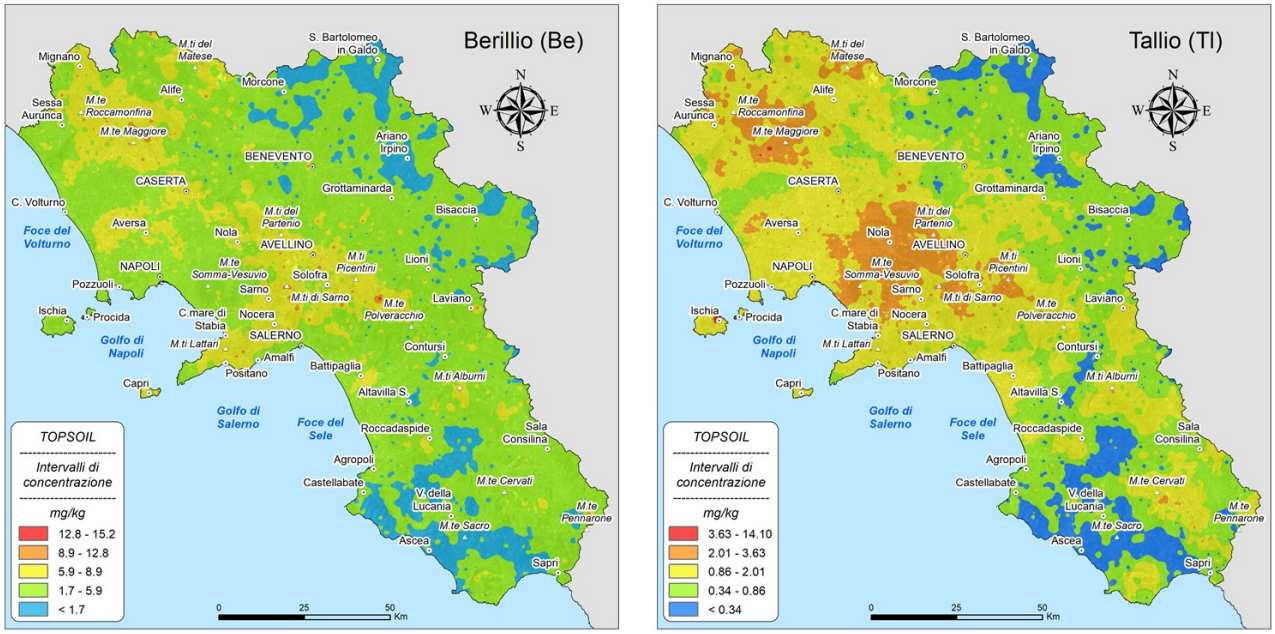

Figure 1.6 Examples of raster maps produced for the concentrations of elements in topsoils (De Vivo et al., 2021b).

1.3.2 Maps of the distribution of organic compounds in topsoils

In specific areas of Campania, characterised by a greater anthropic impact, 802 topsoil samples were collected, according the same FOREGS procedures (Salminen et al., 1998), within a depth of 0.10 to 0.40 m below ground level and with a nominal average density of ca. 1 sample per 17 sqkm. An aliquot of 15 g of the sample fraction <2 mm has been analysed, at the Pacific Rim Laboratories (Vancouver, Canada), by High Resolution Gas Chromatography for the determination of the concentrations of 20 PAHs [Acenaphthene, Acenaphthlyene, Anthracene, Benz(a)anthracene, Benzo(a)pyrene, Benzo(b)fluoranthene, Benzo(ghi)perylene, Benzo(k)fluoranthene, Chrysene, Dibenz(a,h)anthracene, Dibenzo(a,e)pyrene, Dibenzo(a,h)pyrene, Dibenzo(a,i)pyrene, Dibenzo(a,l)pyrene, Fluoranthene, Fluorene, Indeno(1,2,3-cd)pyrene, Naphthalene, Phenanthrene, Pyrene], 24 OCPs (α-HCH, β-HCH, γ-HCH, δ-HCH, Hexachlorobenzene, Heptachlor, Aldrin, α-Chlordane, γ-Chlordane, cis-Nonachlor, trans-Nonachlor, op'-DDE, pp-DDE, op'-DDD, pp-DDD, op'-DDT, pp-DDT, Dieldrin, Endrin, Mirex, Methoxychlor, Endosulphan I, Endosulphan II, Endosulphan sulphate) and 29 PCBs (81, 77, 123, 118, 114, 105, 123, 167, 156, 157, 169, 189, 28, 52, 101, 153, 138, 180, Monochlorobiphenyls, Dichlorobiphenyls, Trichlorobiphenyls, Tetrachlorobiphenyls, Pentachlorobiphenyls, Hexachlorobiphenyls, Heptachlorobiphenyls, Octachlorobiphenyls, Nonachlorobiphenyls, Decachlorobiphenyl, Total PCBs). Further details on the sampling, analytical and quality control procedures can be found in De Vivo et al. (2021a).

For the classification and definition of the concentration intervals for the dot maps, given that most of the analytes had many samples with concentrations bdl, a methodological criterion was adopted: the number of intervals in which to discretise the data was choose depending on the percentage of samples with concentrations bdl (i.e., from 2 to 5 intervals according the percentage < bdl was > 90, > 70, >50, > 20 or ≤ 20) (Fig. 1.7).

Also for the organic compounds, the raster maps were produced by mean of the MIDW interpolation algorithm and the classification of the maps in interval was performed by applying the C-A plot method (Fig. 1.7).

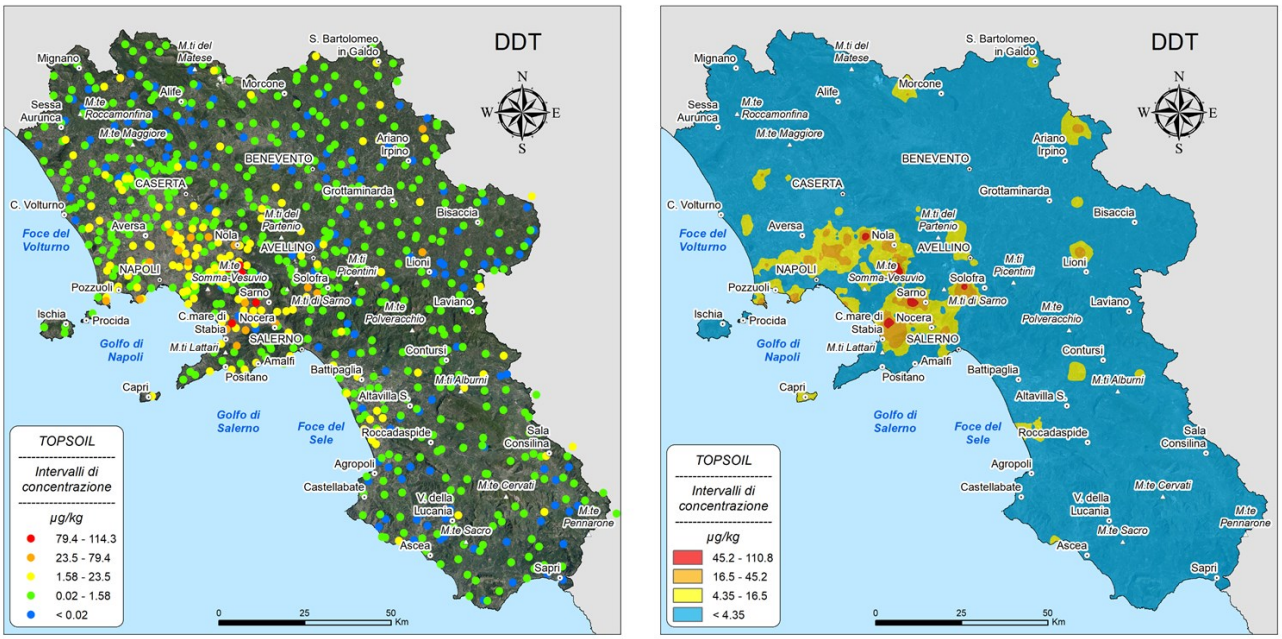

Figure 1.7 Examples of dot and raster maps produced for the concentrations of organic compound in topsoils (De Vivo et al., 2021a).

1.3.3 Maps of the distribution of the potential hazard of PTEs and organic compounds

The annex 5 of the Italian Legislative Decree 152/2006 (D.Lgs. 152/06) and the annex 2 of the Italian Ministerial Decree 46/2019 (D.M. 46/19) indicate 15 elements (As, Be, Cd, Co, Cr, Cu, Hg, Ni, Pb, Sb, Se, Sn, Tl, V, Zn), 13 PAHs [Benz(a)anthracene, Benzo(a)pyrene, Benzo(b)fluoranthene, Benzo(ghi)perylene, Benzo(k)fluoranthene, Chrysene, Dibenz(a,h)anthracene, Dibenzo(a,e)pyrene, Dibenzo(a,h)pyrene, Dibenzo(a,i)pyrene, Dibenzo(a,l)pyrene, Indeno(1,2,3-cd)pyrene, Pyrene], 14 OCPs (α-HCH, β-HCH, γ-HCH, Aldrin, Chlordane (as sum of α-Chlordane and γ-Chlordane) and DDTs (as sum of op'-DDE, pp-DDE, op'-DDD, pp-DDD, op'-DDT and pp-DDT) Dieldrin, Endrin) and the Total PCB (as sum of Monochlorobiphenyls, Dichlorobiphenyls, Trichlorobiphenyls,

Tetrachlorobiphenyls, Pentachlorobiphenyls, Hexachlorobiphenyls, Heptachlorobiphenyls, Octachlorobiphenyls, Nonachlorobiphenyls, Decachlorobiphenyl) as potentially toxic substances.

For these PTEs in the top and bottom soils (Fig. 1.8) and for the potentially toxic organic compounds in the topsoils (Fig. 1.9), the maps of the distribution of the potential hazard were produced reclassifying the dot maps according to the guideline values (defined CSC) established for the residential and commercial/industrial land use by the D.Lgs 152/06 and the ones established for agricultural land use by the D.M 46/19.

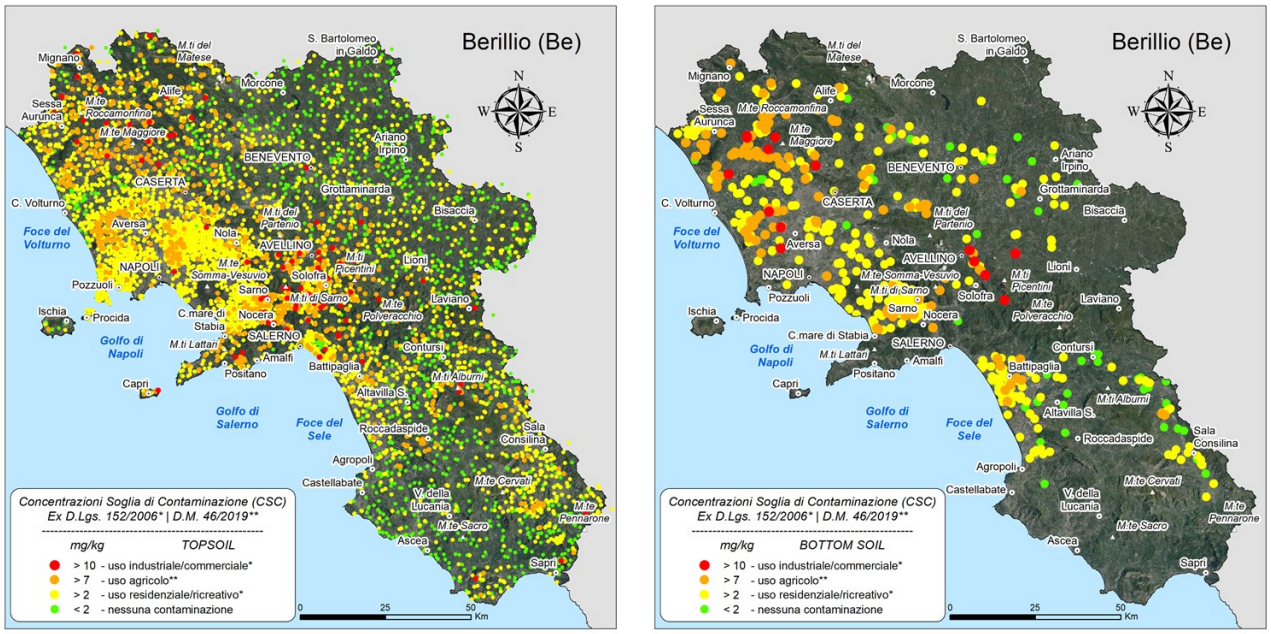

Figure 1.8 Examples of potential hazard maps produced for the concentrations of elements in top and bottom soils (De Vivo et al., 2021b).

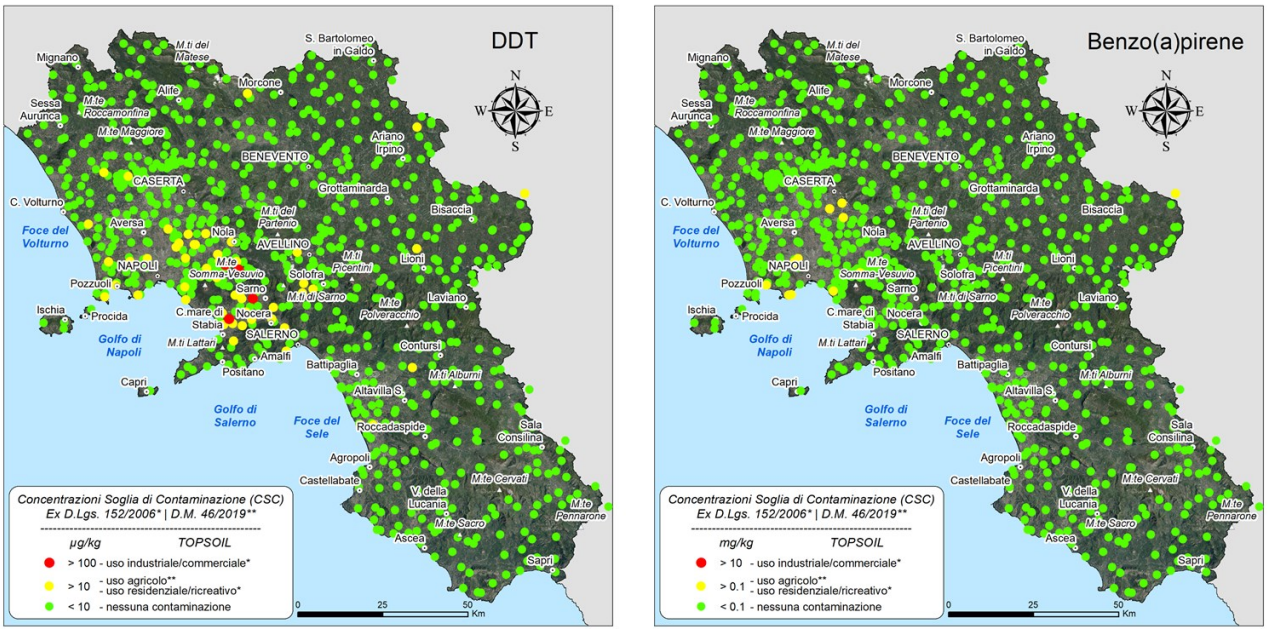

Figure 1.9 Examples of potential hazard maps produced for the concentrations of organic compound in topsoils (De Vivo et al., 2021a).

1.3.4 Maps of the bioavailability of PTEs

From the total 7300 topsoils collected for the analysis of the total concentration of PTEs and other elements, 1993 samples were selected and an aliquot of 15 grams was treated with Ammonium Nitrate (NH_4NO_3). The solutions were then analysed combining ICP-MS and ICP-ES, at the Bureau Veritas (formerly Acme) Analytical Laboratories Ltd. (Vancouver, Canada), to determine the bioavailable concentrations of 59 elements (Ag, Al, As, Au, Ba, Be, Bi, Ca, Cd, Ce, Co, Cs, Cu, Dy, Er, Eu, Fe, Ga, Gd, Ge, Hf, Hg, Ho, In, K, La, Li, Lu, Mg, Mn, Mo, Nb, Nd, Ni, P, Pb, Pr, Rb, Re, Sb, Sc, Se, Sm, Sn, Sr, Ta, Tb, Te, Th, Ti, Tl, Tm, U, V, W, Y, Yb, Zn, Zr). Further details on the sampling, analytical and quality control procedures can be found in De Vivo et al. (2021b).

The maps were produced only for the bioavailable concentrations of the 15 elements indicated as PTEs in the Annex 5 of the D.Lgs. 152/06 and the Annex 2 of the D.M. 46/19 (As, Be, Cd, Co, Cr, Cu, Hg, Ni, Pb, Sb, Se, Sn, Tl, V and Zn), excluding the Total Cr and Cr VI species for which there were no useful analytical determinations. For the classification and definition of the concentration intervals for the dot maps representing the bioavailability, we adopted the same criteria indicated for the concentration of organic compounds in topsoils (Fig. 1.10).

Also for the bioavailable concentration, the raster maps were produced by mean of the MIDW interpolation algorithm and the classification of the maps in interval was performed by applying the C-A plot method.

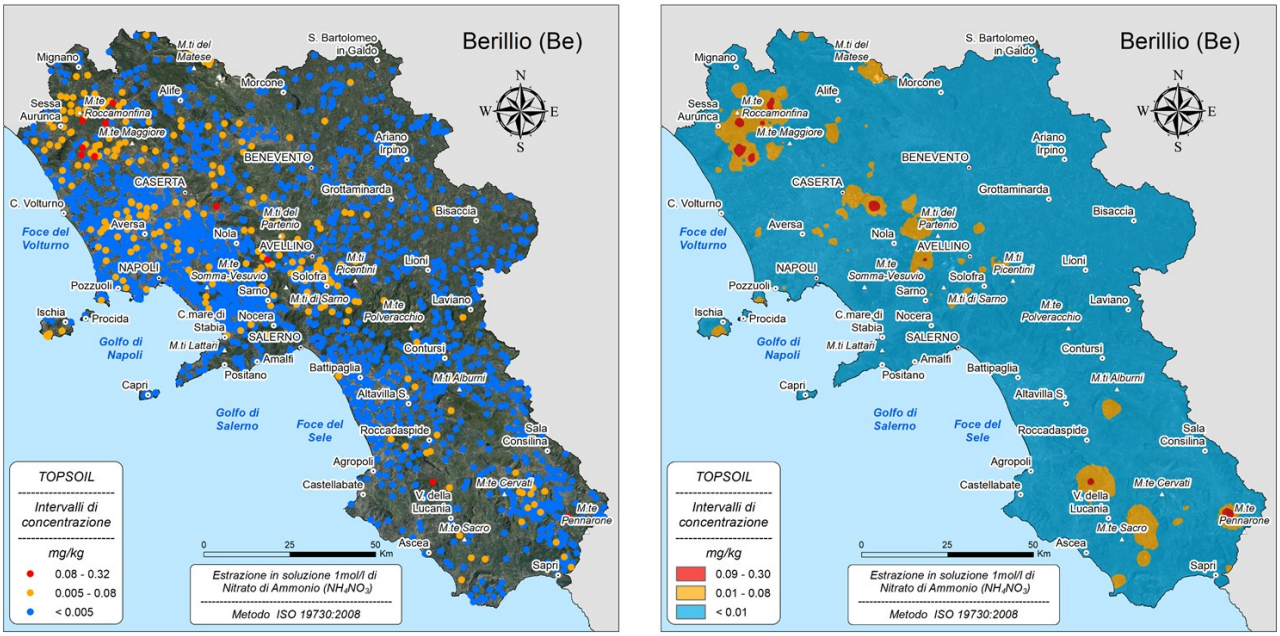

Figure 1.10 Examples of dot and raster maps produced for the bioavailable concentrations of PTEs in topsoils (De Vivo et al., 2021b).

1.3.5 Baseline maps of PTEs and other elements

For the determination of the background (baseline) values a fractal filtering technique was applied to the MIDW raster grids produced for the concentrations of PTEs and other elements in the topsoils. The used filtering technique is defined Separation-Analysis (S-A), applied by mean of the GeoDAS software (Cheng et al., 2001), and has the function of separating the values of the background contents from the anomalies.

The basic assumption of the S-A method is that a geochemical field or image, generated by specific geochemical processes, can be described in terms of its fractal (scale invariant) properties which, in turn, can be defined in both the frequency and the spatial domain (Turcotte, 1997). In the spatial domain the scaling properties are related to the geometric patterns, to the frequency of the values distribution and to the variation of shapes (corresponding to variation in values), as occurs in the MIDW method. In the frequency domain these properties are represented by a power spectrum (Lewis et al., 1999; Cheng et al., 1999, 2000) on whose characteristics the fractal filter to be used is defined, to separate the components characterised by similar scale properties.

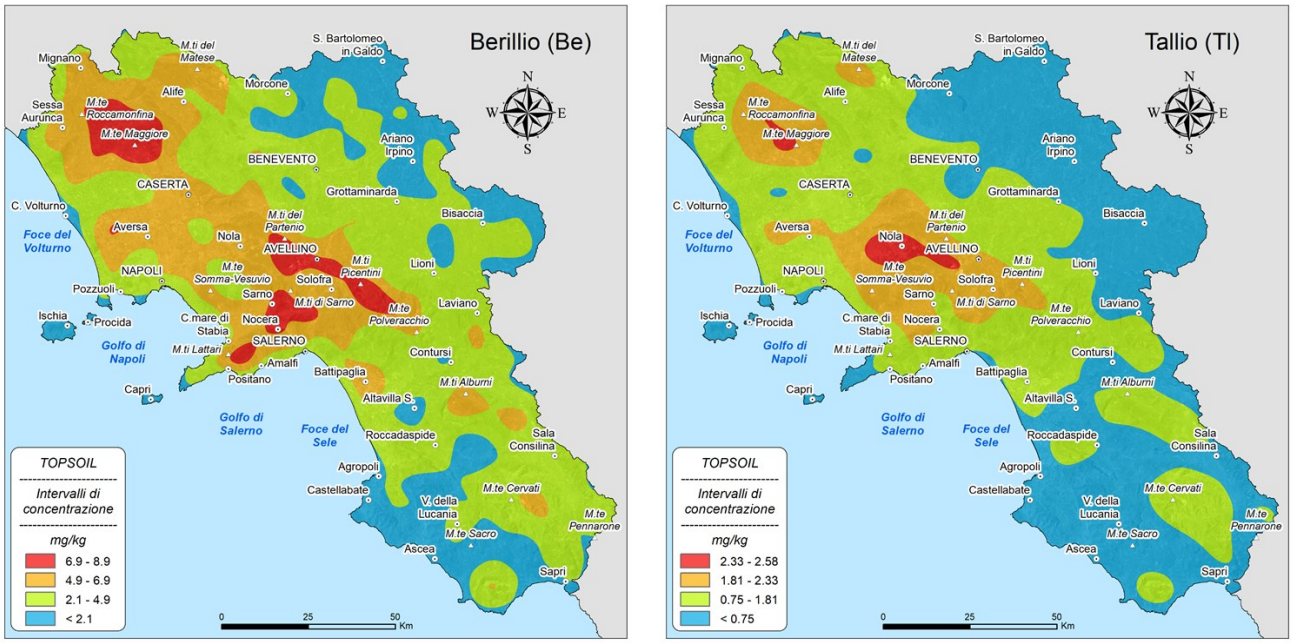

Figure 1.11 Examples of baseline maps produced for the concentrations of elements in topsoils (De Vivo et al., 2021b).

This type of filter is an irregular shaped one, due to the inherently anisotropic and complex structure of the geochemical data and can be used to extract anomalies from background values or other significant patterns from the original map. The S-A method uses the S-G filter (Spector and

Grant, 1970), well known to geophysicists for its applications. This filter is based on the relationships between the power spectrum E(f) and the relative frequency f. Fractal filters are defined in the Fourier space with the application of the C-A model, already discussed, to the power spectrum obtained from the processed geochemical data. The Fourier transform and the inverse Fourier transform are the basis for the conversion of the distributions of geochemical values (pixels) from the spatial to the frequency domain and vice versa. In fact, the Fourier transform can convert geochemical data into a frequency domain in which the different characteristics of the frequencies can be identified; the signals filtered, with certain frequency ranges depending on the geochemical properties of the considered elements, are then backconverted into the spatial domain through the inverse Fourier transform to create the background values grids.

The new created grids were then classified according to the C-A method to generate the background values maps (Fig. 1.11).

1.4 Air

With the aim of recording spatial and temporal variations of the transport of organic and inorganic contaminants in the atmosphere at a local and regional scale, an active sampling activity was carried out over several seasons, from summer 2015 to winter 2016, on the whole regional territory.

The installation of about 150 polyurethane foam-based passive air samplers (PUF-PAS) and 50 wet and dry sampler bulk deposimeters (W&D), allowed to characterise the dusts present in the air, measuring the presence of potentially toxic persistent organic pollutants (POPs), such as OCPs, PCBs, Polybromodiphenyl ethers (PBDEs), PAHs, and metals.

Data relating to the concentrations of the considered analytes in air samples were processed in a GIS environment to produce the dot maps. Specifically, 909 dot maps were produced (537 for PUF-PAS samplers, 312 for W&D samplers and 60 for the wet deposition of PTEs).

Details on the sampling, analytical and quality control procedures can be found in De Vivo et al. (2022a).

1.4.1 Polyurethane foam-based passive air samplers (PUF-PAS)

In the passive air samplers (PAS) the active material is composed of polyurethane foam (PUF), which has the ability to adsorb organic compounds in the vapor state, and is capable of concentrating numerous types of molecules, that differ in terms of both molecular weight and chemical-physical characteristics.

For PUF-PAS samplers, 537 dot maps were generated: 225 relating to the seasons from summer 2015 to spring 2015 (named seasons A, B and C) for the province of Naples (Fig 1.12) and 312 for the seasons from spring 2016 to winter 2016 (named seasons D, E, F and G) for the whole Campania region (Fig. 1.13).

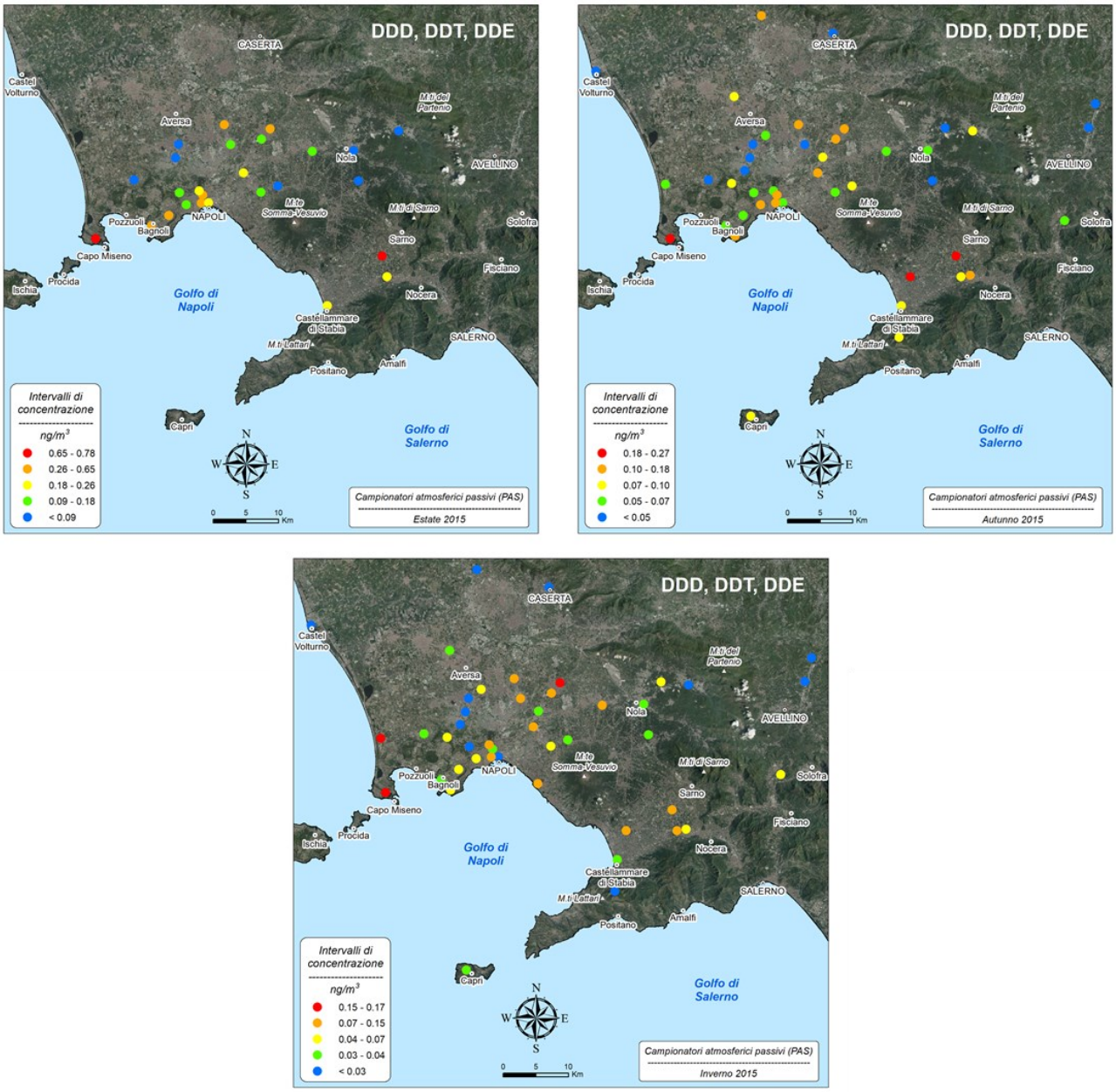

Figure 1.12 Examples of dot maps produced for the concentration of organics compound in the atmosphere detected with PUF-PAS samplers in seasons A, B and C in the Napoli province (De Vivo et al., 2022a).

A total of 75 maps were generated for each of the seven seasons reporting the concentration of 21 PAHs [Acenaphthene, Acenaphthlyene, Anthracene, Benz(a)anthracene, Benzo(a)pyrene, Benzo(b)fluoranthene, Benzo(ghi)perylene, Benzo(k)fluoranthene, Chrysene,

Dibenz(a,h)anthracene, Dibenzo(a,e)pyrene, Dibenzo(a,h)pyrene, Dibenzo(a,i)pyrene, Dibenzo(a,l)pyrene, Fluoranthene, Fluorene, Indeno(1,2,3-cd)pyrene, Naphthalene, Phenanthrene, Pyrene, Total PAHs], 25 OCPs (α-HCH, β-HCH, γ-HCH, δ-HCH, Hexachlorobenzene, Heptachlor, Aldrin, α-Chlordane, γ-Chlordane, cis-Nonachlor, trans-Nonachlor, op'-DDE, pp-DDE, op'-DDD, pp-DDD, op'-DDT, pp-DDT, Dieldrin, Endrin, Mirex, Methoxychlor, Endosulphan I, Endosulphan II, Endosulphan sulphate, Total OCPs) and 29 PCBs (81, 77, 123, 118, 114, 105, 123, 167, 156, 157, 169, 189, 28, 52, 101, 153, 138, 180, Monochlorobiphenyls, Dichlorobiphenyls, Trichlorobiphenyls, Tetrachlorobiphenyls, Pentachlorobiphenyls, Hexachlorobiphenyls, Heptachlorobiphenyls, Octachlorobiphenyls, Nonachlorobiphenyls, Decachlorobiphenyl, Total PCBs).

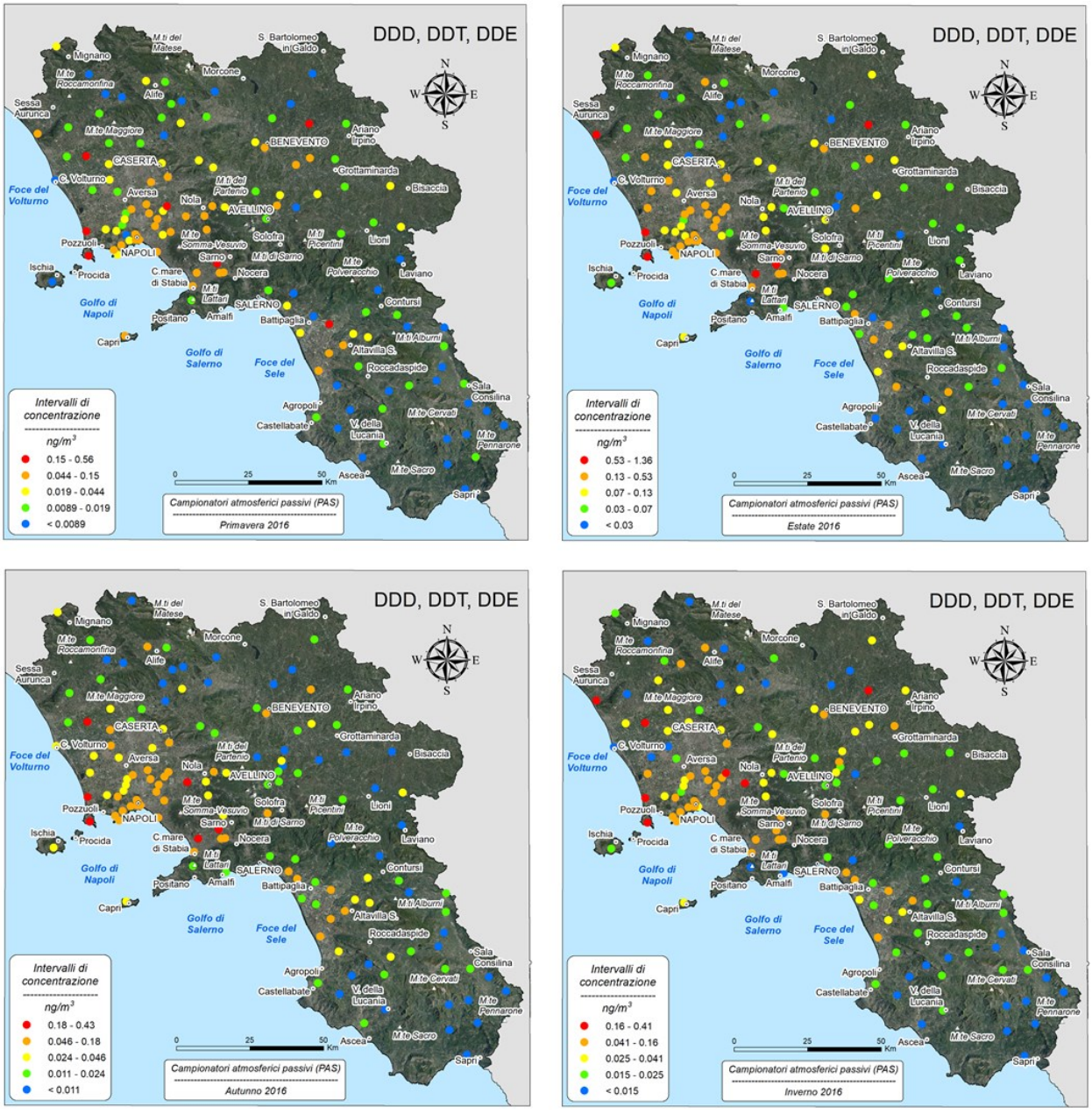

Figure 1.13 Examples of dot maps produced for the concentration of organics compound in the atmosphere detected with PUF-PAS samplers in seasons D, E, F and G in Campania region (De Vivo et al., 2022a).

In addition, for the seasons D, E, F and G, reporting the concentrations of the analytes in the whole region, also the 3 maps of the concentration of PBDEs (47, 99, 100) were generated.

The classification and definition of the concentration interval in the maps was made according specific percentiles, specifically the 25th, 50th, 70th and 95th, so as to obtain five classes. Low frequency colours (shades of blue and green) were assigned to the lowest concentration ranges and colours with increasing frequency (from yellow to red) to those with higher concentrations (Fig. 1.12 and 1.13).

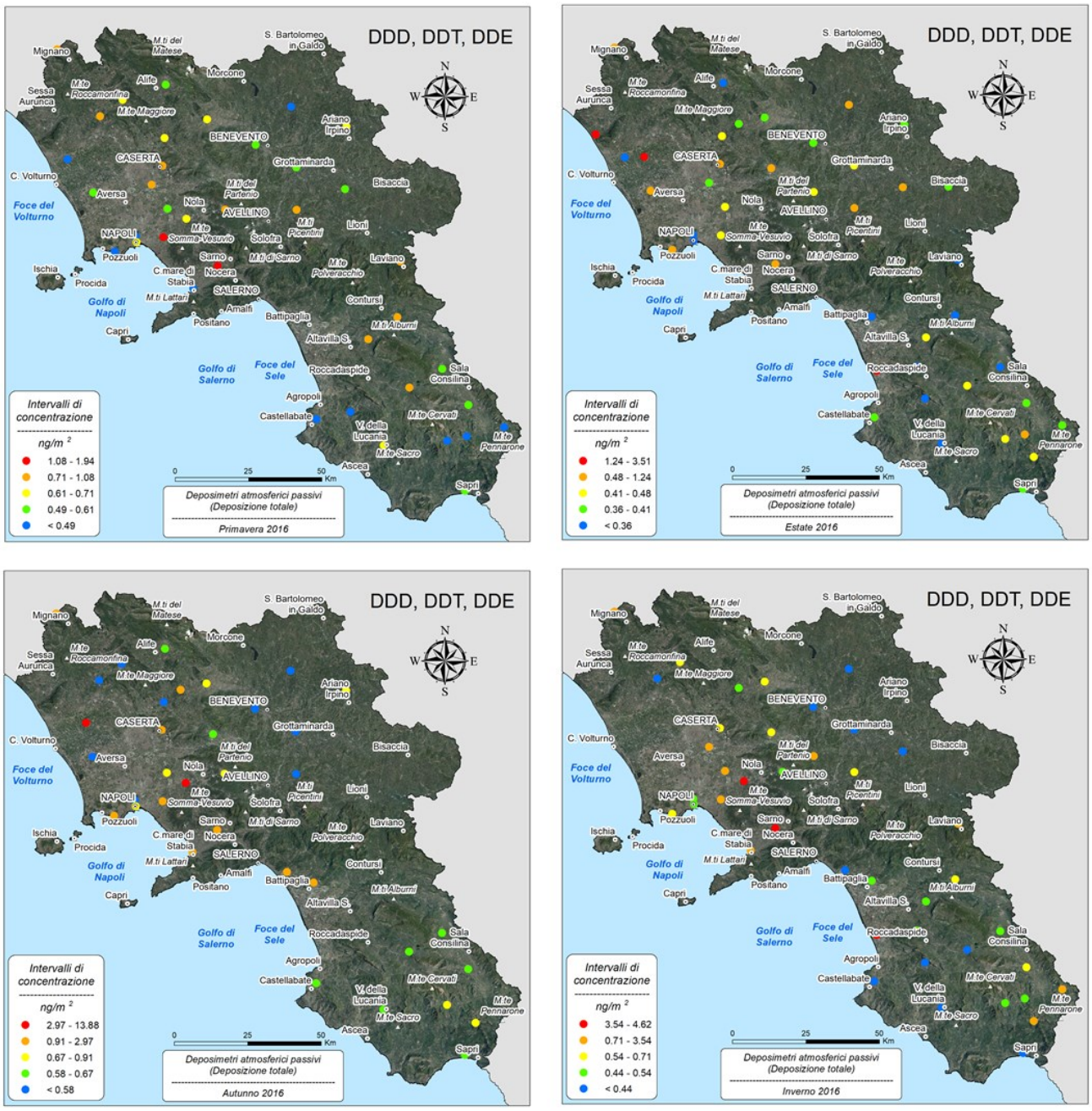

Figure 1.14 Examples of dot maps produced for the concentration of organics compound in the atmosphere detected with W&D samplers in seasons D, E, F and G in Campania region (De Vivo et al., 2022a).

Piombo

Deposimetri atmosferici passivi (deposizione umida)

Distribuzione puntuale delle concentrazioni medie giornaliere
Dot map - Daily average concentrations

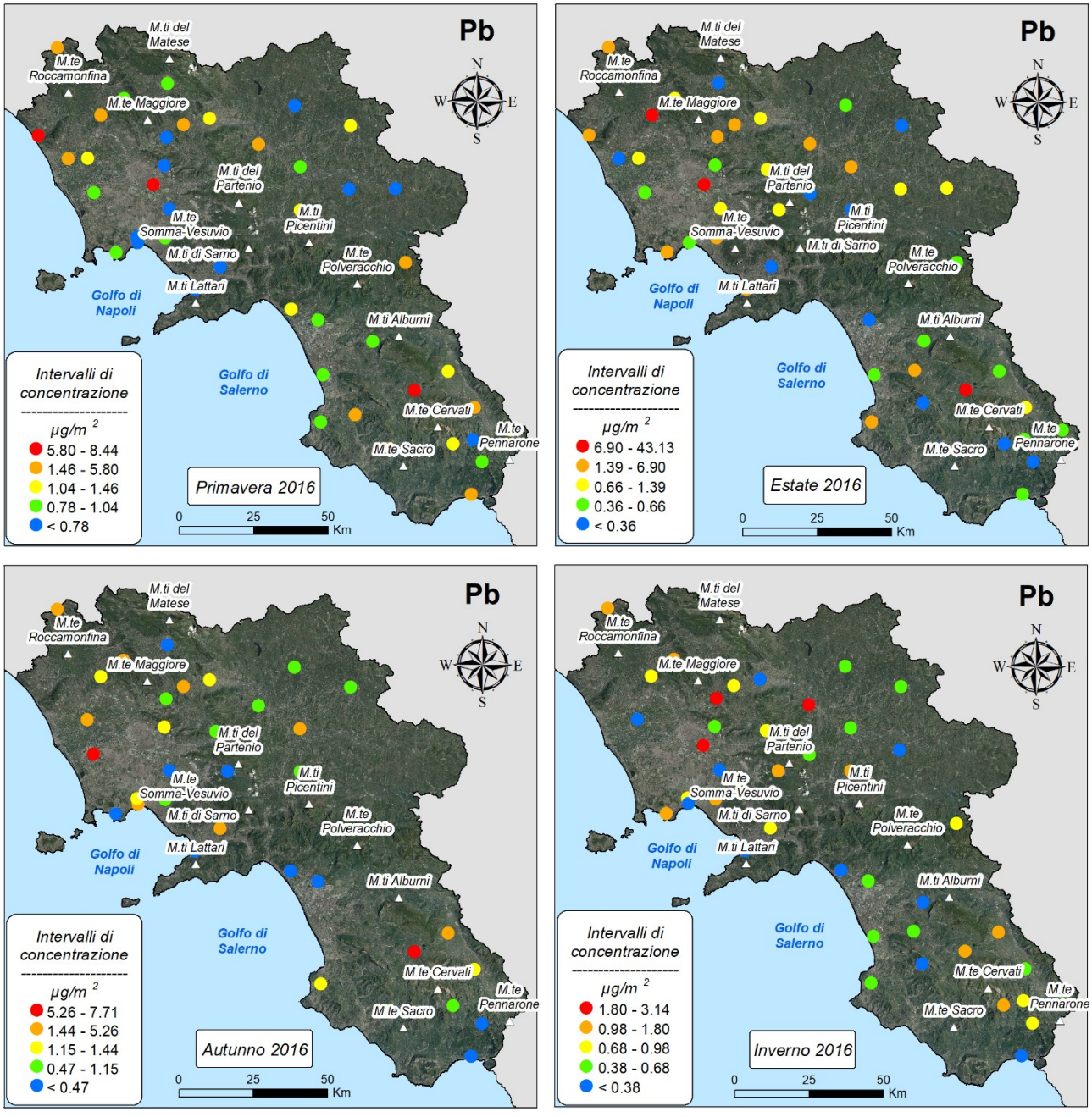

Figure 1.15 Examples of dot maps produced for the concentration of PTEs in the atmosphere detected with W&D samplers (wet deposition) in seasons D, E, F and G in Campania region (De Vivo et al., 2022a).

1.4.2 Wet and dry sampler bulk deposimeters (W&D)

The W&D deposimeters consist of a rainwater collection bottle and an overlying funnel with a cylindrical wall, that allows the collection of the liquid deposition and the separation from it of the particulate deposited during the entire exposition time.

For W&D samplers, 372 dot maps were generated relating to the seasons from spring 2016 to winter 2016 (named seasons D, E, F and G) for the whole Campania region. As regards the data relating to the concentration values of the seasons from summer 2015 to spring 2015 (named seasons A, B and C) for the province of Naples, due to the small number of samples, the maps were not produced.

78 maps were generated for each of the four seasons reporting the concentration of 21 PAHs, 25 OCPs, 29 PCBs and 3 PDBEs (Fig. 1.14). In addition, for the same seasons, 15 maps for each were produced, reporting the concentrations of PTEs (As, Be, Cd, Co, Cr, Cu, Hg, Ni, Pb, Sb, Se, Sn, Tl, V, Zn) detected considering only the wet deposition (Fig. 1.15).

For the classification and definition of the concentration interval in the maps we used the same abovementioned methods.

1.5 Conclusions

The work produced gave a complete picture of the chemism and the environmental conditions of the Campania regional soils that has no equal in Italy.

The cartography produced has made it possible to highlight how the distribution of PTEs and other elements and POPs in Campania soils is influenced by both the local geology and the presence of anthropic activities which have various impacts on the environmental context.

The results obtained with this study confirm the results already obtained in previous research activities carried out on the soil and air media of the entire Campania region by the EGWG (Buccianti et al., 2015; Cicchella et al., 2020; De Vivo et al., 2016; Minolfi et al., 2018, 2019; Petrik et al., 2018a, 2018b, 2018c, 2018d, 2018e; Qu et al, 2016; 2017; 2018a; 2018b; 2018c; Rezza et al., 2018a, 2018b; Thiombane et al., 2018a, 2018b, 2019; Zuzolo et al., 2017, 2018a, 2018b).

The analysis of the distribution of the various substances analysed made it possible to demonstrate how the areas mainly characterised by a significant anthropic pressure, and a consequent relative accumulation of contaminants, are not generically located in the municipalities belonging to the area identified as “Terra dei Fuochi” (of which appear to be affected only the Aversano district and the

eastern municipal areas falling within the Metropolitan Area of Naples), but rather mainly in the territories of the provincial and metropolitan area of Naples and the Sarno River Basin.

The study also highlighted that the current regulatory tools for controlling the level of soil contamination (guideline values of D.Lgs. 152/2006 and D.M. 46/2019) are not adequate for the geo-pedological variability of the soils of Campania and the baseline cartography produced could be used at sub-regional scale to establish reference values to be used as a guideline for starting the health risk assessment and remediation procedures at a site-specific scale.

In addition, the study highlighted how the bioavailability of PTEs and other elements does not follow a linear relationship with respect to the analysed total concentrations. The analysis of the distribution of the values makes it clear that bioavailability is not only a function of the geochemical characteristics of the elements and their total concentrations but that there are physico-chemical variables, not verified in this study, that probably have a significant and substantial influence on the characteristics of mobility and availability of the elements so as to produce a great local variability.

References

Albanese, S., De Vivo, B., Lima, A., Cicchella D., 2007a. Background and baseline values of toxic elements in stream sediments of Campania region (Italy). J. Geochem. Explor. 93, 21-34.

Albanese, S., Lima, A., De Vivo, B., Cicchella, D., 2007b. Atlante geochimico-ambientale dei suoli del territorio comunale di Avellino. Aracne Editrice, Roma.

Belkin, H.E., De Vivo, B., Manno, M., 2013. Medical geology perspective on the risks associated with volcanism and brownfield. Preface of Editors to the Special Issue (Medical geology perspective on the risks associated with volcanism and brownfield). J. Geochem. Explor. 131, vii-viii.

Buccianti, A., Lima, A., Albanese, S., Cannatelli, C., Esposito, R., De Vivo, B., 2015. Exploring topsoil geochemistry from the CoDA (Compositional Data Analysis) perspective: the multi-element data archive of the Campania Region (Southern Italy). J. Geochem. Explor. 159, 302-316.

Cheng, Q., 1994. Multifractal modelling and spatial analysis with GIS: Gold potential estimation in the Mitchell-Sulphurets area. Northwestern British Columbia - Unpublished PhD thesis. University of Ottawa, Ottawa, 268 pp.

Cheng, Q., Agteberg, F.P., Ballantyne, S.B., 1994. The separation of geochemical anomalies from background by fractal methods. J. Geochem. Explor. 51, 109-130.

Cheng, Q., 1999. Spatial and scaling modelling for geochemical anomaly separation. J. Geochem. Explor. 65, 175–194.

Cheng, Q., Agteberg, F.P., Bonham-Carter, G.F., 1996. A spatial analysis method for geochemical anomaly separation. J. Geochem. Explor. 56, 183-195.

Cheng, Q., Xu, Y., Grunsky, E., 2000. Integrated spatial and spectrum method for geochemical anomaly separation. Nat. Resour. Res. 9, 43 -56.

Cheng, Q., Xu, Y., Grunsky, E., 1999. Integrated spatial and spectrum analysis for geochemical anomaly separation. In: Lippard S.J., Naess A. & Sinding-Larsen R. (Eds), Proceedings of the International Association for Mathematical Geology Meeting, Trondheim, Norway, 1, 87-92.

Cheng, Q., Bonham-Carter, G.F., Raines, G.L., 2001. GeoDAS: A new GIS system for spatial analysis of geochemical data sets for mineral exploration and environmental assessment. The 20th Intern. Geochem. Explor. Symposium (IGES). Santiago de Chile, 6/5-10/5, 2001, 42-43.

Cicchella, D., De Vivo, B., Lima, A., 2005. Background and baseline concentration values of harmful elements in the volcanic soils of metropolitan and Provincial areas of Napoli (Italy). Geochem.: Explor. Environ. Anal 5, 1-12.

Cicchella, D., Zuzolo, D., Albanese, S., Fedele, L., Di Tota, I., Guagliardi, I., Thiombane, M., De Vivo, B., Lima, A., 2020. Urban soil contamination in Salerno (Italy): Concentrations and patterns of major, minor, trace and ultra-trace elements in soils. J. Geochem. Explor. 213.

De Vivo, B., 1995. Elementi e metodi di geochimica ambientale. Liguori Editore, Napoli, pp 493.

De Vivo, B., Albanese, S., Lima, A., Qu, C., Fortelli, A., Guarino, A., Zuzolo, D., Esposito, M., Pizzolante, A., Cerino, P., Hope, D., Pond, P., Cicchella, D., 2021a. Monitoraggio Geochimico-Ambientale dei suoli della Regione Campania – Volume 2 (Composti Organici Persistenti: Idrocarburi Policiclici Aromatici, Policlorobifenili, Pesticidi). Aracne Editrice, Roma, Italia.

De Vivo, B., Cicchella, D., Albanese, S., Qu, C., Guarino, A., Fortelli, A., Esposito, M, Cerino, P., Pizzolante, A., Hope, D., Pond, P., Lima, A., 2022a. Monitoraggio geochimico-ambientale della matrice aria della Regione Campania. Il Piano Campania Trasparente. Volume 3. Idrocarburi Policiclici Aromatici (IPA, Policlorobifenili (PCB), Pesticidi (OCP), Eteri di Polibromobifenili (PBDE), Elementi Potenzialmente Tossici (EPT). Aracne Editrice, Roma. ISBN: 979-12-5994-733-8, 676 pag**.**

De Vivo, B., Cicchella, D., Lima, A., Albanese, S., 2006. Atlante geochimico-ambientale dei suoli dell'area urbana e della Provincia di Napoli. Aracne Editrice, Roma.

De Vivo, B., Cicchella, D., Lima, A., Fortelli, A., Guarino, A., Zuzolo, D., Esposito, M., Cerino, P., Pizzolante, A., Albanese, S., 2021b. Monitoraggio Geochimico-Ambientale dei suoli della Regione Campania – Volume 1 (Elementi Potenzialmente Tossici e loro Biodisponibilità, Elementi Maggiori e in Traccia; distribuzione in suoli superficiali e profondi). Aracne Editrice, Roma, Italia.

De Vivo, B., Cicchella, D., Lima, A., Guarino, A., Qu, C., Fortelli, A., Esposito, M, Cerino, P., Pizzolante, A., Albanese, S., 2022b. Sintesi del monitoraggio dei suoli e dell'aria della regione Campania, a scala regionale e locale. Piano Campania Trasparente. Volume 4: Elementi potenzialmente tossici (EPT) e loro biodisponibilità elementi maggiori e in traccia, Idrocarburi Policiclici Aromatici (IPA), Policlorobifenili (PCB), Pesticidi (OCP), Eteri di Polibromobifenili (PBDE). Aracne Editrice, Roma. ISBN: 979-12-5994-735-2, 240 pag.

De Vivo, B., Lima, A., Albanese, S., Cicchella, D., Rezza, C., Civitillo, D., Minolfi, G., Zuzolo D., 2016. Atlante geochimico-ambientale dei suoli della Campania. Aracne Editrice, Roma, pp. 364.

Filippelli, G.M., Morrison, D., Cicchella, D., 2012. Urban Geochemistry and Human Health. Elements 8(6), 439-444.

Flora, A., 2015. La Terra dei Fuochi: ambiente e politica industriale nel Mezzogiorno. Rivista economica del Mezzogiorno, Trimestrale della Svimez 1-2, 89-122.

Lewis, G.M., Lovejoy, S., Schertzer, D., Pecknold, S., 1999. The scale invariant generator technique for quantifying anisotropic scale invariance. Comput. Geosci. 25, 963–978.

Lima, A., De Vivo, B., Cicchella, D., Cortini, M., Albanese, S., 2003. Multifractal IDW interpolation and fractal filtering method in environmental studies: an application on regional stream sediments of Campania Region (Italy). Appl. Geochem. 18, 1853-1865.

Lima, A., De Vivo, B., Grezzi, G., Albanese, S., Cicchella, D., 2007. Atlante geochimico-ambientale dei suoli del territorio comunale di Caserta. Aracne Editrice, Roma.

Minolfi, G., Albanese, S., Lima, A., Tarvainen, T., Rezza, C., De Vivo, B., 2018. Human health risk assessment in Avellino-Salerno metropolitan areas, Campania Region, Italy. Sp. Issue (De Vivo et al., Eds). J. Geochem. Explor. 195, 97-110.

Minolfi, G., Petrik, A., Albanese, S., Lima, A., Cannatelli, C., Rezza, C., De Vivo, B., 2019. The distribution of Pb, Cu and Zn in topsoil of the Campanian Region, Italy. Geochem.: Explor. Environ. Anal 19(3), 205-215.

Petrik, A., Albanese, S., Lima, A., De Vivo, B., 2018a. The spatial pattern of beryllium and its possible origin using compositional data analysis on a high-density topsoil data set from the Campania Region (Italy). Appl. Geochem. 91, 162-173.

Petrik, A., Thiombane, M., Albanese, S., Lima, A., De Vivo, B., 2018b. Source patterns of Zn, Pb, Cr and Ni potentially toxic elements (PTEs) through a compositional discrimination analysis: A case study on the Campanian topsoil data. Geoderma 331, 87-99.

Petrik, A., Albanese, S., Lima, A., Jordan, G., Rolandi, R., Rezza, C., De Vivo, B., 2018c. Spatial pattern recognition of arsenic in topsoil using high-density regional data. Thematic Issue (De Vivo et al., Eds), Geochem.: Explor. Environ. Anal 18, 319-330.

Petrik, A., Albanese, S., Lima, A., Jordan, G., Rolandi, R., De Vivo, B., 2018d. Spatial pattern analysis of Ni and its concentrations in topsoils in the Campania region (Italy). Sp. Issue (De Vivo et al., Eds). J. Geochem. Explor. 195, 130-142.

Petrik, A., Thiombane, M., Lima, A., Albanese, S., Buscher, T.J., De Vivo, B., 2018e. Soil Contamination Compositional Index: a new approach to quantify contamination demonstrated by assessing compositional source patterns of potentially toxic elements in the Campania Region (Italy). Appl. Geochem. 96, 264-276.

Qu, C., Albanese, S., Chen, W., Lima, A., Doherty, A.L., Piccolo, A., Arienzo, M., Qi, S., De Vivo, B., 2016. The status of organochlorine pesticide contamination in the soils of Campanian Plain, southern Italy, and correlations with soil properties and cancer risk. Environ. Pollut. 216, 500-511.

Qu, C., Albanese, S., Lima, A., Doherty, A.L., Li, J., Qi, S., De Vivo, B., 2017. Residues of hexachlorobenzene and chlorinated cyclodiene pesticides in the soils of the Campanian Plain, southern Italy. Environ. Pollut. 231P2, 1497-1506.

Qu, C, Doherty, A.L., Xing, X., Sun, W., Albanese, A., Lima, A., Qi, S., De Vivo, B., 2018a. Polyurethane foam-based passive air samplersin monitoring persistent organic pollutants: Theory and application, in: De Vivo, B., Belkin, H.E, Lima, A, (Eds.) Environmental Geochemistry - Site Characterization, Data Analysis and Case Histories, Elsevier, pp 521-542.

Qu, C., Albanese, S., Lima, A., Wang, M., Sacchi, M., Molisso, F., De Vivo, B., 2018b. Polycyclic aromatic hydrocarbons in the sediments of the Gulfs of Naples and Salerno, Southern Italy: status, sources and ecological risk. Ecotoxicol. Environ. Saf. 161, 156-163.

Qu, C., Sun, Y., Albanese, S., Lima, A., Sun, W., Di Bonito, M., Qi, S., De Vivo, B., 2018c. Organochlorine pesticides in sediments from Gulfs of Naples and Salerno, Southern Italy. Sp. Issue (De Vivo et al., Eds). J. Geochem. Explor., 195, 87-96.

Rezza, C., Albanese, S., Ayuso, R., Lima, A., Sorvari, J., De Vivo, B., 2018a. Geochemical and Pb isotopic characterization of soil, groundwater, human hair, and corn samples from the Domizio Flegreo and Agro Aversano area (Campania region, Italy). Sp. Issue (Bech J. et al., Eds), J. Geochem. Explor. 184(Part B), 318-332.

Rezza, C., Petrik, A., Albanese, S., Lima, A., Minolfi, G., De Vivo, B., 2018b. Molybdenum, Sn and W patterns in topsoils of the Campania Region, Italy. Thematic Issue (De Vivo et al., Eds) Geochem.: Explor. Environ. Anal 18, 331-342.

Salminen, R., Tarvainen, T., Demetriades, A., Duris, M., Fordyce, F.M., Gregorauskiene, V., Kahelin, H., Kivisilla, J., Klaver, G., Klein, H., Larson, J.O., Lis, J., Locutura, J., Marsina, K., Mjartanova, H., Mouvet, C., O'Connor, P., Odor, L., Ottonello, G., Paukola, T., Plant, J.A., Reimann, C., Schermann, O., Siewers, U., Steenfelt, A., Van der Sluys, J., De Vivo, B., Williams, L., 1998. FOREGS Geochemical Mapping Field Manual. Geological Survey of Finland, Espoo Guide 47. http://www.gtk.fi/foregs/34eochem/fieldmanan.pdf

Siegel, F.R., 2002. Environmental Geochemistry of Potentially Toxic Elements. Springer, Verlag, Berlin.

Spector, A., Grant, F.S., 1970. Statistical models for interpreting aeromagnetic data. Geophysics 35, 293–302.

Thiombane, M., Zuzolo, D., Cavaliere, M., Cicchella, D., Albanese, S., Lima, A., De Vivo, B., 2018. Soil geochemical follow-up in the Cilento World Heritage Park) (Campania, Italy) through exploratory compositional data analysis and C-A fractal model. Sp. Issue (Agteberg F. & Cheng Q. Eds.), J. Geochem Explor. 189, 85-99.

Thiombane, M., Martín-Fernández, J.A., Albanese, S., Lima, A., Doherty, A., De Vivo, B., 2018. Exploratory analysis of multielement geochemical patterns in soil from the Sarno River Basin (Campania region, southern Italy) through Compositional Data Analysis (CODA). Sp. Issue (De Vivo et al., Eds). J. Geochem. Explor. 195, 110-120.

Thiombane, M., Di Bonito, M., Albanese, S., Zuzolo, D., Lima, A., De Vivo, B. 2019. Geogenic versus anthropogenic behaviour and geochemical footprint of Al, Na, K and P in the Campania region (Southern Italy) soils through compositional data analysis and enrichment factor. Geoderma 335, 12-26.

Turcotte, D.L., 1997. Fractals in Geology and Geophysics, second ed. Cambridge University Press, New York.

Valera, P., Zavattari, P., Albanese, S., Cicchella, D., Dinelli, E., Lima, A., De Vivo, B., 2014. A correlation study between Multiple Sclerosis and Type 1 Diabetes incidences and geochemical data in Europe. Env. Geochem & Health 36(1), 79-98.

Vitale, S., Ciarcia, S., 2018. Tectono-stratigraphic setting of the Campania region (southern Italy). J. Maps 14(2), 9-21. https://doi.org/10.1080/17445647.2018.1424655

Xu, Y., Cheng, Q., 2001. A fractal filtering technique for processing regional geochemical maps for mineral exploration. Geochem.: Explor. Environ. Anal. 1, 147-156.

Zuzolo, D., Cicchella, D., Catani, V., Giaccio, L., Guagliardi, I., Esposito, L., De Vivo, B., 2017. Assessment of potentially harmful elements pollution in the Calore River basin (Southern Italy). Environ. Geochem. Health 39(3), 531–548.

Zuzolo, D., Cicchella, D., Albanese, S., Lima, A., Zuo, R., De Vivo, B., 2018a. Exploring uni-element geochemical data under a compositional perspective. Applied Geochemistry, 91, 174-184.

Zuzolo, D., Cicchella, D., Doherty, A.L., Albanese, S., Lima, A., De Vivo, B., 2018b. The distribution of precious metals (Au, Ag, Pt, and Pd) in the soils of the Campania Region (Italy). J. Geochem. Explor. 192, 33-44.

CHAPTER 2 – Comparing methods for the determination of the background values of some PTEs to set local environmental guidelines in the south-eastern sector of the Campania plain

The results of this activity were published/presented in:

Albanese, S., Guarino, A., Pizzolante, A., Nicodemo, F., Ragone, G., Iorio, R., D'Antonio, A., Ferraro, A., 2022. The use of natural geochemical background values for the definition of local environmental guidelines: the case study of the Vesuvian plain. In: Baldi, D., and Uricchio, F. (Eds.), Le bonifiche ambientali nell'ambito della transizione ecologica, Società Italiana di Geologia Ambientale (SIGEA) and Consiglio Nazionale delle Ricerche (CNR).

Guarino, A., Pizzolante, A., Nicodemo, F., Ragone, G., D'Antonio, A, Ferraro, A., Albanese, S., 2021. The definition of geochemical background values at local scale as a key procedure to set reliable guidelines for contaminated land management. Goldschmidt Virtual 2021, Lyon. DOI: 10.7185/gold2021.3810

2.1 Introduction

The genesis and mobility of contaminants in an environmental media depend on various factors, both natural or anthropogenic, such as the geological characteristics of the territory, the nature of the human activities present, the chemical reactivity, the accumulation rate and the transformation operated by the biotic component (Antoniadis et al., 2019).

Waters, soils, sediments, air, vegetation and agricultural products are the main media affected by the contamination by PTEs and POPs, such as PCBs, OCPs and PAHs.

To better understand the nature of the geochemical anomalies found in the various environmental media, it is of fundamental importance to identify the concentration ranges that represent the natural background values (Albanese et a., 2007). The definition of the latter is a key step in the process of estimating the levels of environmental contamination, which is mainly based on the discrimination of the geogenic component from the anthropogenic one.

The evaluation and interpretation of the concentration increases of contaminants in the environmental media is also an indispensable process for assessing the ecological and health risks and for the arrangement of monitoring networks aimed at controlling and conserving the natural heritage of a specific territorial context.

The art. 240, paragraph 1, letter b, of the Italian Environmental Law (D.Lgs. 152/06) defines the Contamination Threshold Concentration (CSC) values as "the contamination levels of the environmental media that constitute the values above which site characterization and site-specific risk assessment are required, as identified in the annex 5 to the fourth part of this decree. If the potentially contaminated site is in an area affected by anthropogenic or natural phenomena that have led to the exceeding of one or more CSC, the latter are assumed to be equal to the existing background value for all the exceeded parameters".

According to art. 252, paragraph 1, of the same code "the Sites of National Interest (SIN), for the reclamation purposes, are identifiable in relation to the characteristics of the site, the quantity and danger of the pollutants present, the impact on the surrounding environment in terms of health and ecological risks, as well as the damage to the cultural and environmental heritage". In such areas it is therefore of fundamental importance to define the geochemical background values (concentrations) to be used, at the site scale, to distinguish the values due to the geogenic component from those influenced by the anthropogenic component, and which can be adopted as a reference values for the preliminary remediation objectives.

This work reports the results of a study whose purpose has been the determination of the background values for arsenic (As), beryllium (Be), copper (Cu), thallium (Tl), vanadium (V) and

zinc (Zn) in the soils of an area occupying the south-eastern sector of the Campanian Plain which includes two former SIN, now under regional jurisdiction: the "Areas of the Vesuvian Coast" (Aree del Litorale Vesuviano), to the west, and, only partially, the "hydrographic Basin of the Sarno river" (Bacino idrografico del fiume Sarno), to the east.

Data come from the geochemical-environmental prospecting work conducted in the framework of the “Campania Trasparente” project (www.campaniatrasparente.it), financed by the Resolution Regional Council no. 497/2013, Fund for Anti-cyclical Measures and Occupational Safeguard - Action B4 "Mapping of the Territory", approved with the Executive Decree DG "Economic Development" no. 585/2015, and coordinated by the Zooprophylactic Institute of Southern Italy (IZSM) with the support of the Environmental Geochemistry Working Group (EGWG) of the Department of Earth, Environmental and Resources Sciences of the University of Naples Federico II.

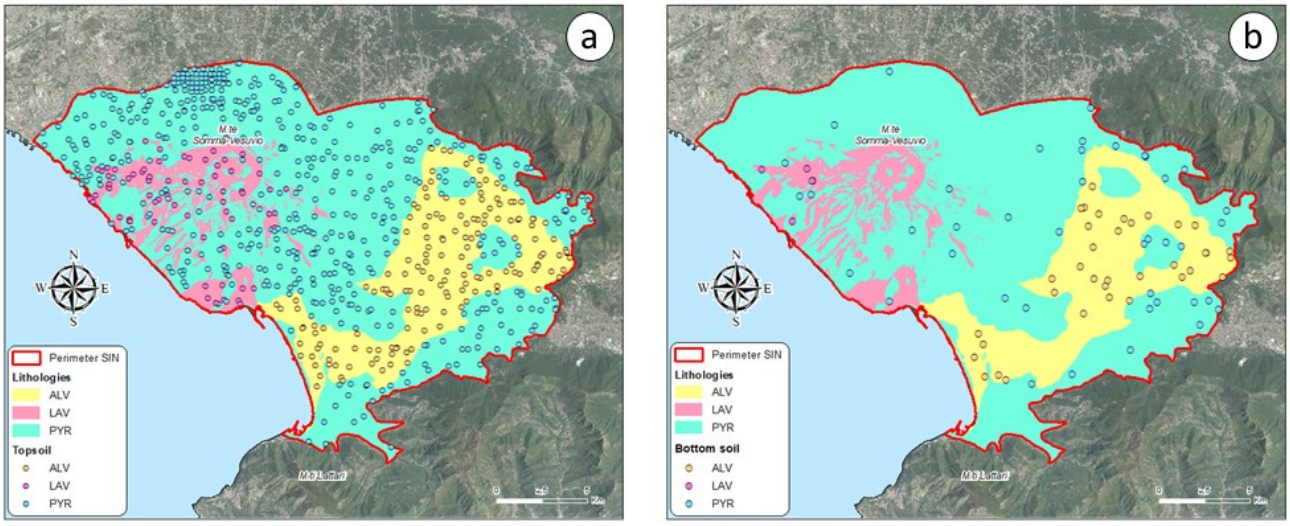

Figure 2.1 Geographical location and lithological subdivision of the topsoil (a) and bottom soil (b) samples in the study area.

2.2 Geological setting

The current geological setting of Campania is the result of various deformational processes that have led the regional territory to be distinguished in an internal hilly sector, mainly occupied by the Apennine chain, and in a western coastal sector, washed by the Tyrrhenian Sea, mainly occupied by large alluvial plains and volcanic complexes characterized by an intricated evolutionary history (Buccianti et al., 2015; Minolfi et al., 2018). In the coastal territory of the central-northern sector of the region we find the Campania Plain, result of the filling of a Plio-Pleistocene graben by sediments of various origins (Vitale and Ciarcia, 2018). The central sector of the Plain has been the site, for

about one million years, of a substantial volcanic activity, mainly explosive, whose products make up the majority of the filling of the Plain itself (De Vivo et al., 2010).

The study area (Fig. 2.1) is located in the southern portion of the Campania Plain, specifically in the area between the Sarno River Plain and the Mount Somma-Vesuvius. This latter is a strato-volcano, which rests on a Mesozoic carbonatic basement, whose structure is composed of a summit caldera, formed following the collapse of the ancient Somma apparatus, within which it was formed, starting from the eruption of 79 AD, the most recent structure of Vesuvius (Scarpati and Perrotta, 2018). The Sarno River Plain, which occupies the southernmost area of the Campania Plain, is a plain of aggradation formed as a result of the deposition of large volumes of pyroclastic fall material remodelled by the fluvial action.

2.3 Materials and methods

The geochemical data used for the purposes of this study include the analytical results relating to natural residual soil samples, collected by the ISZM, as part of the "Campania Trasparente" project, and by the EGWG. Samples include both topsoils (collected within a depth range between 10-30 cm) and bottom soils (collected in a range of 80-120 cm), analysed combining the inductively coupled plasma mass spectrometry (ICP-MS) and emission spectrometry (ICP-ES) techniques used on the samples digested in a modified aqua regia solution (De Vivo et al., 2021).

From the original database, made up of data relating to about 7300 topsoil and 500 bottom soil samples, the records relating to 720 topsoil and 83 bottom soil samples falling within the area of interest were extracted. With the aid of a simplified geo-lithological map, each of the extracted samples was associated with one of the predominant lithology found in the study area: alluvial products (ALV), lavas (LAV) and pyroclastic products (PYR) (Fig. 2.1).

Six chemical elements (As, Be, V, Tl, Cu, Zn), considered PTEs according to the D.Lgs. 152/06, were selected for the purposes of the study. Table 2.1 shows the basic statistical parameters (minimum, median, maximum, mean, mode and percentiles) representative of the distribution of the single analytes, in the top and bottom soil, and the CSC extracted from Annex 5 of the D.Lgs. 152/06 for public and residential land use (col. A) and for commercial and industrial land use (col. B). Within the extracted sub-set of data, the values reported as non-detected (ND), because showed concentrations below the instrumental detection limit (bdl), have been replaced by the value corresponding to 50% of the bdl itself (Reimann et al., 2008).

The concentration values relating to the various statistical indicators reported in Table 2.1, in many cases, significantly exceed the CSC reported, suggesting the need to investigate the applicability of

the national established CSC to the reference context if an anthropogenic origin of the high concentrations found is not verified. Indeed, considering the boxplots produced to represent the statistical distribution of the data in the different soil layers (Fig. 2.2), it is relevant that As, Be, V, and, partially, Tl have similar concentration ranges values between top and bottom soil. This condition suggests a preponderance of the geological contribution to the concentration values of these elements in the soils of the study area, not excluding, on the contrary, an anthropic contribution relevant for Cu and Zn given the concomitant mismatch of the concentration ranges and the presence of numerous positive outliers found in the topsoil.

Table 2.1 Univariate statistics of the chemical elements under study, divided by sampling depth, with indication of the CSCs pursuant to Legislative Decree 152/2006.

Element	As		Be		V		Tl		Cu		Zn	
Media	top	btm	top	btm	top	btm	top	btm	top	btm	top	btm
Unit	mg/kg		mg/kg		mg/kg		mg/kg		mg/kg		mg/kg	
Min	1	5,8	2	1,8	36	37	0,56	0,72	10,07	24,94	35,8	17,3
Median	11,9	12,4	5,4	5,7	107	107	2,0	2,1	166,3	84,8	114,6	68,1
75° %ile	13,8	13,3	6,3	6,5	118	115,5	2,3	2,5	251,7	116,03	160,6	81,7
90° %ile	16	14,5	7,4	7,4	128	126,0	2,5	2,7	434,9	158,6	242,7	98,8
Max	44	22,1	14,2	9,9	175	148	3,46	3,21	1873	365,23	1115,5	150,3
Mean	12,02	12,41	5,60	5,65	105,23	106,10	2,00	2,14	237,84	100,77	142,59	72,36
Mode	13	12,9	5,5	6,7	108	107	2,13	2,03	198	-	84	61,3
CSC col.A	20		2		90		1		120		150	
CSC col.B	50		10		250		10		600		1500	

Regarding the topsoil only, the analysis of the distribution of the geochemical data, divided according the considered lithologies, reported in the form of boxplots (Fig. 2.3), further confirms how reasonable it is to think, especially for Be, Tl, and V, that there is a substantial contribution to their compositional variability due to the different geo-lithological units involved in the analysis.

The observations resulting from the analysis of the statistical distribution of the data, the presence of anomalous values (outliers) in the dataset, the physiological uncertainty accompanying the geochemical data, led to the need to define the reference ranges values for the geochemical background for the study area, which was realised using four different methodological approaches:

- EF-MAX and EF-95P;
- Median + 2MAD;
- Fractal filtering;
- Guidelines SNPA.

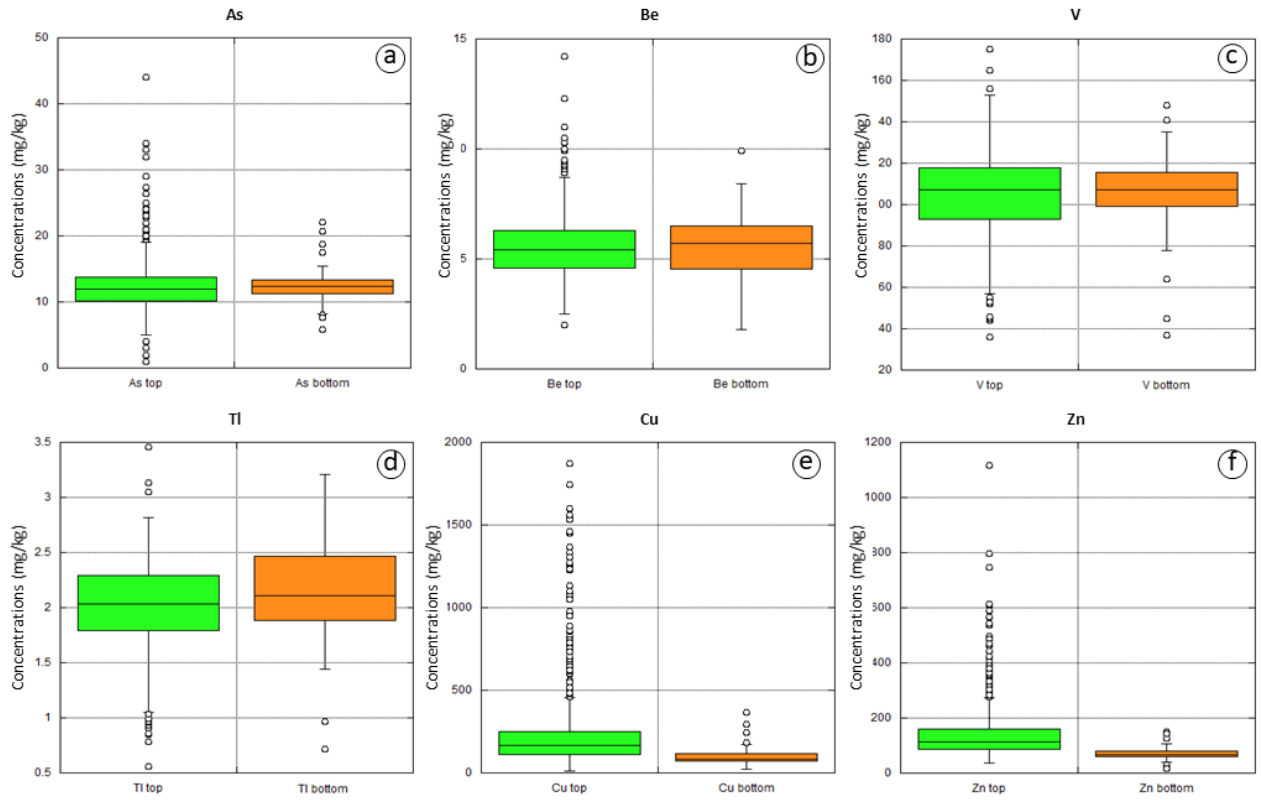

Figure 2.2 Boxplots of As, Be, V, Tl, Cu and Zn in the top and bottom soil of the study area.

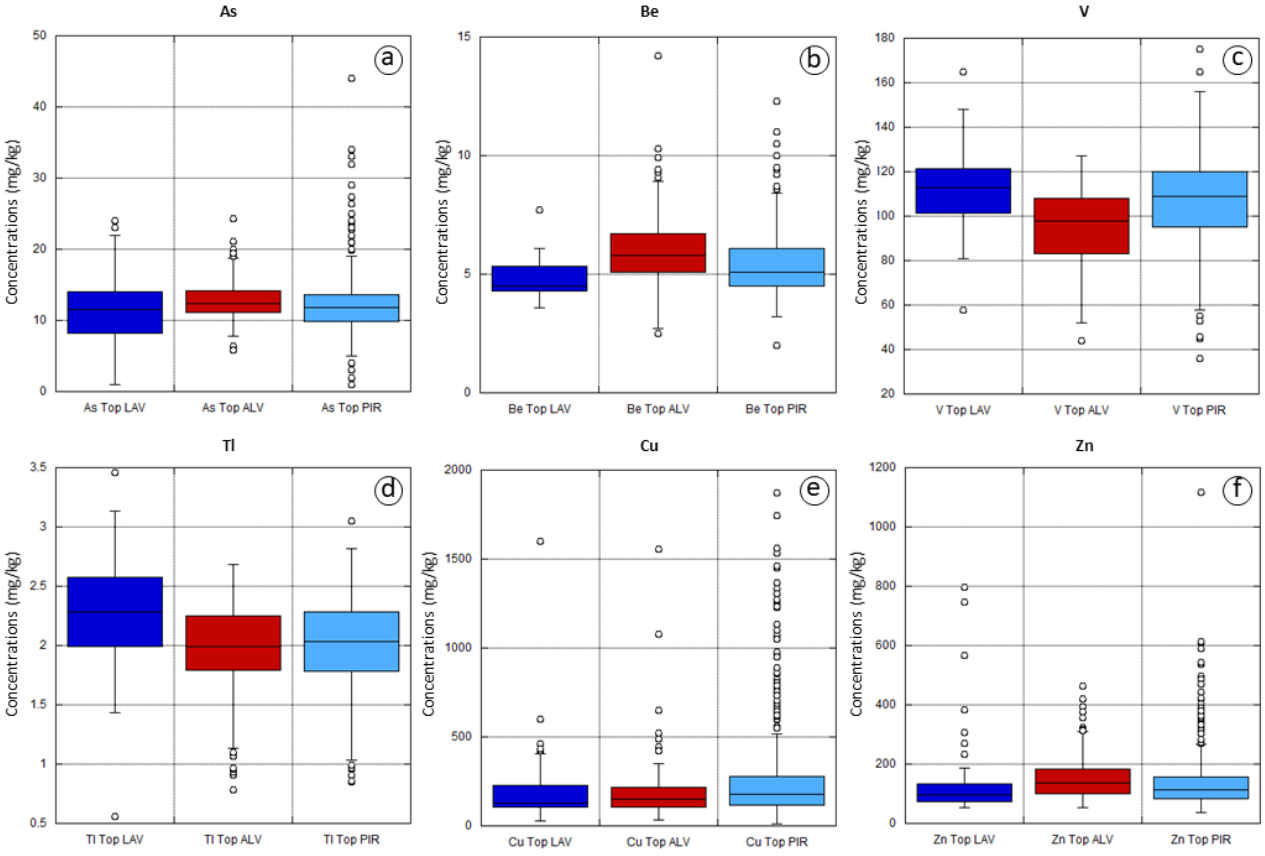

Figure 2.3 Boxplots of As, Be, V, Tl, Cu and Zn in the top and bottom soil of the study area divided on a lithological basis (LAV = Lavas; ALV = Alluvial material; PYR = Pyroclastic material).

The comparison and synthesis of the results resulting from the application of the different methods were used to estimate local reference values to be officially used, replacing the national CSC, in the procedures for assessing the state of contamination of the sites falling within the reference study area.

2.3.1 EF-MAX and EF-95P

The enrichment factors (EFs) are indices used to represent the degree of contamination of an environmental media in relation to what is considered to be the natural concentration of a specific chemical element present in it. The EFs of an anthropogenic contaminant is determined by normalizing its concentration in the considered media with respect to the concentration, in the same environmental media, of an element taken as a reference (Loska et al., 1997).

As a reference element the choice must be on a stable element in the soil, that is characterized by weak vertical mobility, not affected by weathering processes, not involved in anthropogenic contamination phenomena and naturally impoverished in the biosphere (Barbieri, 2016). Among all the 53 variables present in the original database (Ag, Al, As, Au, B, Ba, Be, Bi, Ca, Cd, Ce, Co, Cr, Cs, Cu, Fe, Ga, Ge, Hf, Hg, K, In, La, Li, Mg, Mn, Mo, Na, Nb, Ni, P, Pb, Pd, Pt, Rb, Re, S, Sb, Sc, Se, Sn, Sr, Ta, Te, Th, Ti, Tl, U, V, Y, W, Zn, Zr), cerium (Ce) was chosen as normalizing element as it was found to be characterized by the lowest values of the coefficient of variation (CV), calculated for all elements, both in the top and the bottom soil. As the reference concentration to determine the EFs of the analytes we used the concentration in the bottom soil (Sutherland et al., 2000). Thus, the equations used for the calculation of the CVs and EFs were the following (Eqq. 2.1 and 2.2):

$$CV_{[Element]} = \frac{Standard\ deviation\ of\ concentrations}{|Mean\ of\ concentrations|} * 100 \quad Eq.\ 2.1$$

$$EF_{[Element]} = \frac{Conc.\ element_{[topsoil]} / Conc.\ Ce_{[topsoil]}}{Conc.\ element_{[bottom\ soil]} / Conc.\ Ce_{[bottom\ soil]}} \quad Eq.\ 2.2$$

Since there was no precise correspondence between the sampling points of the topsoil and those of the bottom soil (Fig. 2.1), to estimate the EFs a pre-processing of the data in a GIS environment was applied.

In detail, the geochemical data relating to the concentrations in topsoils were processed by mean of a multifractal interpolation method (Multifractal Inverse Distance Weighted - MIDW) (Cheng et al., 2001), widely used in the environmental sciences (Lima et al. al., 2003, 2008; Albanese et al., 2007), to produce the raster maps of the spatial distribution of As, Be, V, Tl, Cu, Zn for the study area (Fig. 2.4).

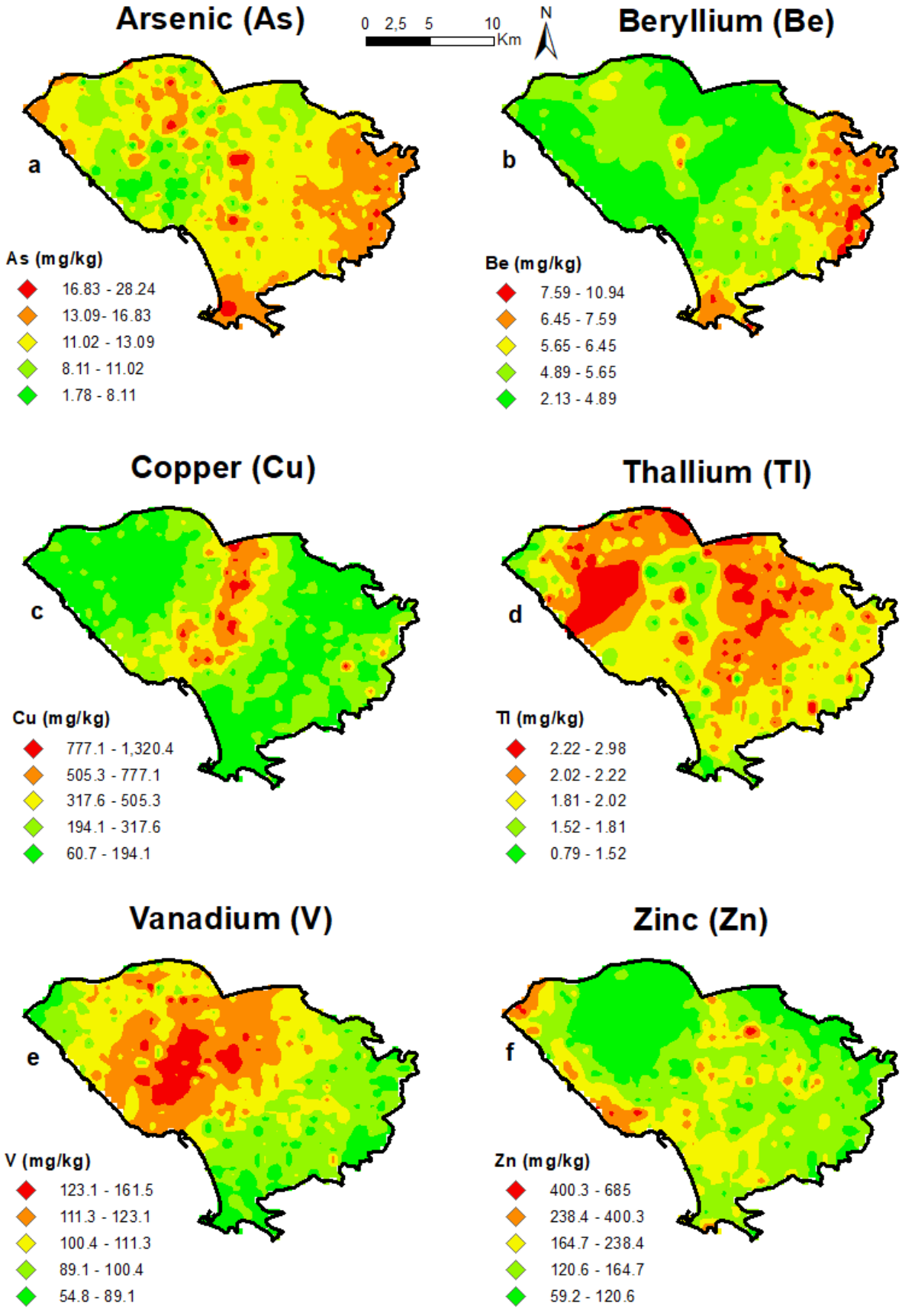

Figure 2.4 Maps of the spatial distribution of the concentrations of the elements of interest produced with the multifractal interpolation method (MIDW).

The MIDW method, based on the principles that fractal and / or multifractal geometry can be used to describe the spatial patterns of geochemical variables in a probabilistic way, is able to represent the regional variability of the data while preserving high frequency informations (anomalies) (Cheng et al., 2001).

The coordinates of the bottom soil samples were then used to extract the concentration values of the elements in the topsoils from the MIDW raster files at the same geographical point. These topsoils concentration values extracted were, finally, used in equation 2.2 for the determination of the EFs in each soil sampling point.

The reference intervals of the background contents were then determined considering only the samples with enrichment factors lower than 2. Specifically, for each element and for each lithology, the background interval was defined considering the minimum value as the lower background limit (LBL) and the maximum concentration value available (EF-MAX) or, alternatively, the value corresponding to the 95th percentile (EF-95P) as the upper background limit (UBL) (Table 2.1).

2.3.2 Median + 2MAD

The second estimation method used is based on the determination of a robust statistical index, defined as such as it is not very sensitive to the effects of the presence of any outliers in the dataset.

Specifically, it was used the approach for calculating the UBLs suggested by Reimann et al. (2008), which involve the median value and the mean absolute deviation (MAD) of the data by means of equation 2.3:

$$UBL = median + 2MAD \qquad Eq.\ 2.3$$

$$MAD = 1.4826 * median\ (|median - x_i|) \qquad Eq.\ 2.4$$

Since the use of robust statistical estimators require a Gaussian (or normal) distribution of the data for at least 50% of the same, the dataset was prior normalised by log-transformation (Log_{10}) before the calculations required by the method. Subsequently, for each analyte and each single lithology considered, the MAD and UBLs were calculated only for the topsoil samples. The final values were then back transformed to obtain the UBLs values (Table 2.2).

2.3.3 Fractal filtering

Using as input the MIDW maps of the interpolated distribution produced for As, Be, V, Tl, Cu, Zn in the topsoils, the raster cartography of the distribution of the background values of the study area

was produced using the software GeoDAS (Cheng et al., 2001), applying a fractal filtering technique on the MIDW raster files (See § 2.3.1).

The filtering technique applied to determine the background values is defined Separation-Analysis (S-A) and allows, through the application of a Spector-Grant (S-G) type filter (Spector and Grant, 1970) to the intepolated data, the separation of the background values from the anomalies present in the raster grids (Cheng et al., 1996). This filter is based on the principle of the Fourier transform and the inverse Fourier transform, which are the keys for the conversion of geochemical data from the spatial domain to that of frequencies and vice versa. In the frequency domain it is possible to identify the different frequency characteristics of the geochemical data and isolate the background values, characterized by a specific frequency (Fig. 2.5).

For the purpose of the methodological comparison aim of this study, the maximum value extracted for each element and for each lithology, acquired as the reference UBLs value, were calculated by mean of an algorithm of zonal statistic applied to the rasters representing the distribution of the background concentrations obtained from fractal filtering. This aimed at extracting the minimum and maximum value assumed by the pixels falling in the areas pertaining to a specific lithology (Table 2.2).

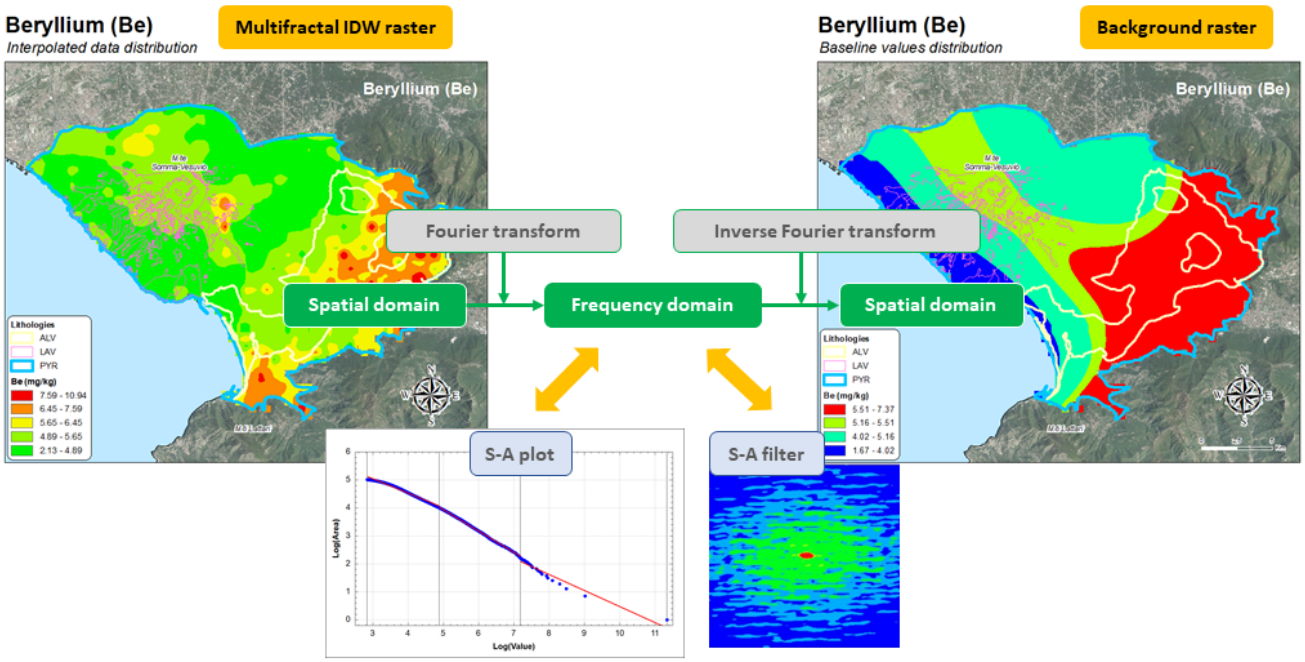

Figure 2.5 Scheme of the extraction process of the background values of the Be starting from the interpolated raster map (MIDW) of the element in the topsoils of the study area. The limits of the lithological units used for the classification of the individual soil samples are show superimposed on the rasters.

2.3.4 Guidelines SNPA

The "Guidelines for the determination of the background values for soils and groundwater" (Resolution of the SNPA Council; Meeting of 14.11.2017. Doc. N.20 / 17) (ISPRA, 2019) provides methodological indications for the estimation of the background values through the application of rigorous statistical procedures with reference to contaminated sites and groundwater bodies.

In general, the application of the method involves several operational steps which include: preliminary analysis of the dataset and treatment of outlier and non-detect values; statistical tests for the definition of the data distribution type; representation of the dataset with the use of numerical and graphical descriptors; determination of the representative values of the background contents (UBLs).

In the specific case, since the differences found between the elemental concentrations in the top and the bottom soil turned out to be, in general, not very marked, the geochemical data relating to the 720 topsoil samples were combined with those of the 83 bottom soil ones available for the study area, forming a single dataset. Assuming, then, that the distribution of concentrations in the residual soils in the study area was influenced mainly by the compositional characteristics of the geological materials of origin, the dataset produced was classified exclusively on a lithological basis with reference to alluvial products (ALV), lavas (LAV) and pyroclastic products (PYR) (Fig. 2.1).

To identify and manage potential outlier values, which generally produce a "tail" to the right in the distribution, the ProUCL software (version 5.1) was used. Specifically, the Dixon's Outlier Test (Dixon, 1950) and Rosner's Outlier Test (Rosner, 1970) were applied to the dataset. These tests require an assumption of normality of the distribution once the outliers have been excluded from the statistical analysis. In any case, once the potential outlier values have been identified, the normality of the data distribution was evaluated with the "Goodness-of-Fit Test" considering both the data deprived of the outliers and those inclusive of the same. Specifically, the distribution type(s) was associated with the samples falling in the different lithologies considered: normal (N), log-normal (LN), gamma (G) or non-parametric (NP).

Finally, the determination of the UBLs, for the elements considered, was made using two approaches: the estimate of the 95 % Upper Tolerance Limit with 95% coverage (95UTL95) and the estimate of the 95% Upper Prediction Limit (95UPL). Specifically, the first (i.e., 95UTL95) represents the value below which the 95% of the population is expected to fall within a 95% confidence interval, while the second (i.e., 95UPL) represents the upper limit of the range within which, with a given confidence level (95%), one or more observations, sampled simultaneously from the same population from which the sample was taken, and on which the interval was calculated, are expected to fall (Edwards, 2015) (Table 2.2).

Table 2.2 Summary of the parameters estimated with the different methodologies for the definition of the geochemical background values.

Lithology	UBLs								CV (%)	MEDIAN UBL
	EF-95P	EF-Max	MEDIAN + 2MAD	SA-MIDW	95UTL95 TOT	95UTL95 NO OUT	95 UPL TOT	95 UPL NO OUT		
Be mg/kg										
ALV	8.0	9.9	8.2	7.2	9.1	9.3	8.7	8.8	9.7	8.75
LAV	5.6	5.9	6.0	5.4	7.1	6.3	6.4	5.9	8.7	5.95
PYR	7.5	8.4	7.2	7.3	8.2	8.2	8.0	7.9	5.7	7.95
Tl mg/kg										
ALV	2.89	3.05	2.60	2.17	2.64	-	2.61	-	11.3	2.63
LAV	2.50	2.52	3.14	2.30	3.38	3.26	3.14	3.05	14	3.09
PYR	2.83	3.21	2.79	2.31	2.70	-	2.64	-	10.7	2.74
V mg/kg										
ALV	131	148	131	109	126	-	125	-	9.8	128.5
LAV	122	126	143	124	148	-	143	-	8.6	134.5
PYR	126	141	145	124	142	141	139	139	5.6	140
As mg/kg										
ALV	19.3	22.1	16.2	15	19	19	18	18	11.6	18.5
LAV	12.9	13.3	18.7	13	23	-	21	-	26.5	16
PYR	15.3	17.5	17.4	15	20	19.9	19	19.0	10.9	18.2
Cu mg/kg										
ALV	160	161	301	317	390	321	351	346	29.4	319
LAV	153	155	224	460	600	464	443	428	45.4	435.5
PYR	290	365	395	461	918	889	786	782	42.6	621.5
Zn mg/kg										
ALV	129	150	252	159	314	308	286	281	32.5	266.5
LAV	73	73	170	157	659	547	439	334	73	252
PYR	100	143	209	183	362	359	332	330	41.8	269.5

2.4 Results and discussions

Table 2.2 shows a summary of the estimates of the UBLs obtained from the different methods used and, in the second-last column of the table, the coefficient of variability (CV) of the same UBLs values is reported for each element and lithology.

In general, Be, Tl, As and V show a low variability of the values, as can be verified empirically by observing the data. On the contrary, Cu and Zn show a marked variability which highlights how the different methods used probably have a different sensitivity to the outliers and, therefore, a different statistical robustness.

The last column of table 2.2 shows the median values, for each element and lithology, of the various estimated UBLs. The median is, generally, a robust operator that is not very sensitive to outliers and, therefore, was chosen as the optimal tool to definitively determine the reference UBLs values for the different lithologies present in the territorial context involved in this study.

In any case, regardless of the lithologies, the comparison of the median values of the UBLs, determined for Be, Tl, V, Cu and Zn, with the national CSCs envisaged for sites intended for private and residential land use has shown, for the study area, a substantial dissimilarity between them; in

detail, in fact, all elements (with the exception of As) are characterized by geochemical background values and, consequently, by UBLs higher than the national guidelines. As, on the other hand, in contrast to the trend, is the only one in the category of the considered analytes that has median values of the UBLs substantially overlapping with the national guidelines and, in some cases (i.e., for LAV litology), even significantly lower than the latter.

Due to the evidence produced by the comparison between median values of the UBLs and the national guidelines (CSCs), the former, relating to Be, Tl, V, Cu and Zn, approximated to unity for simplification and applicability, have been proposed as substitutes for the latter for the soils falling within the Vesuvian and Sarno River Plain areas (Tab. 2.3).

Table 2.3 Suggested reference values for the upper background limits (UBLs) of beryllium, thallium, vanadium, copper and zinc for the area of the ex-SIN areas in relation to the main lithologies identified.

Lithology	Suggested CSC	CSC Annex 5 Col. A	CSC Annex 5 Col. B
Be mg/kg			
ALV	9	2	10
LAV	6		
PYR	8		
Tl mg/kg			
ALV	3	1	10
LAV	3		
PYR	3		
V mg/kg			
ALV	129	90	250
LAV	135		
PYR	140		
Cu mg/kg			
ALV	319	120	600
LAV	436		
PYR	622		
Zn mg/kg			
ALV	267	150	1500
LAV	252		
PYR	270		

To quantify the effects of the possible application of the replacement values proposed in Table 2.3 for the reclassification of the topsoils, used for the estimation of the UBLs, it was calculated the reduction, in percentage terms, of the number of samples that would be potentially contaminated compared to the simple use of the national CSCs. The results are shown in Table 2.4. It is evident that, for each of the five chemical elements selected, the application of reference values estimated

based on the compositional characteristics of the local soils produces a significant reduction in the number of samples to be considered potentially contaminated. Obviously, the numerical reduction relating to the samples corresponds to a substantial reduction in the portions of the Vesuvian and Sarno territories to be considered "outlawed" according to national legislation. In the case of Tl, Be and V, the percentage decrease reaches values that clearly show the total and absolute inadequacy of the reference values proposed by the national D.Lgs. 152/06, especially when dealing with territories characterized by a complex geological history and a highly articulated pedological variety such as those of the study area.

Table 2.4 Evaluation of the number of samples to be considered potentially contaminated based on the application of both the CSCs for residential land use established by the D.Lgs. 152/2006 and the replacement values proposed for the study area. The table also reports in the last column the percentage decrease of topsoil samples to be considered potentially contaminated recorded applying the replacement values presented in table 2.3 instead of the application of the national CSCs.

Element	N° topsoil samples	N° samples C > CSC D.Lgs. 152/06	N° samples C > suggested CSC		Total decrease
			Lithology	Total	
Be	421	420	ALV 7 LAV 2 PYR 14	23	94.5 %
Tl	542	529	ALV 0 LAV 2 PYR 1	3	99.4 %
V	720	563	ALV 0 LAV 8 PYR 16	24	95.2 %
Cu	720	511	ALV 9 LAV 3 PYR 43	55	89.2 %
Zn	720	211	ALV 17 LAV 7 PYR 38	62	71.6 %

In the case of Cu and Zn, for which the concrete possibility of a contribution deriving from human activities notoriously exists in anthropized contexts, the smaller percentage decrease recorded, which remains, however, rather significant, seems to further confirm the effectiveness of the replacement values determined: the latter, in fact, made it possible to discriminate, within the entire dataset used, those samples (specifically 55 for Cu and 66 for Zn) which are likely to be subject of potential contamination by anthropogenic activities as highlighted by their spatial location within the study area (Fig. 5.6). In fact, as far as Cu is concerned, most of the samples that show concentrations higher than the proposed replacement values (Table 3) are concentrated in a strip of land, oriented SW-NE, which laps the eastern slopes of the Mt. Somma-Vesuvius notoriously characterised by the presence

of vineyards, for whose treatment cupric fungicides are historically used; as regards Zn, the samples exceeding the replacement values (Table 3) are mainly concentrated in correspondence with the Tyrrhenian coast, characterized by the presence of arterial roads, and in internal areas associated with significant volumes of motor vehicle traffic for which elements such as Zn (together with Pb and other PTEs) are notoriously geochemical markers.

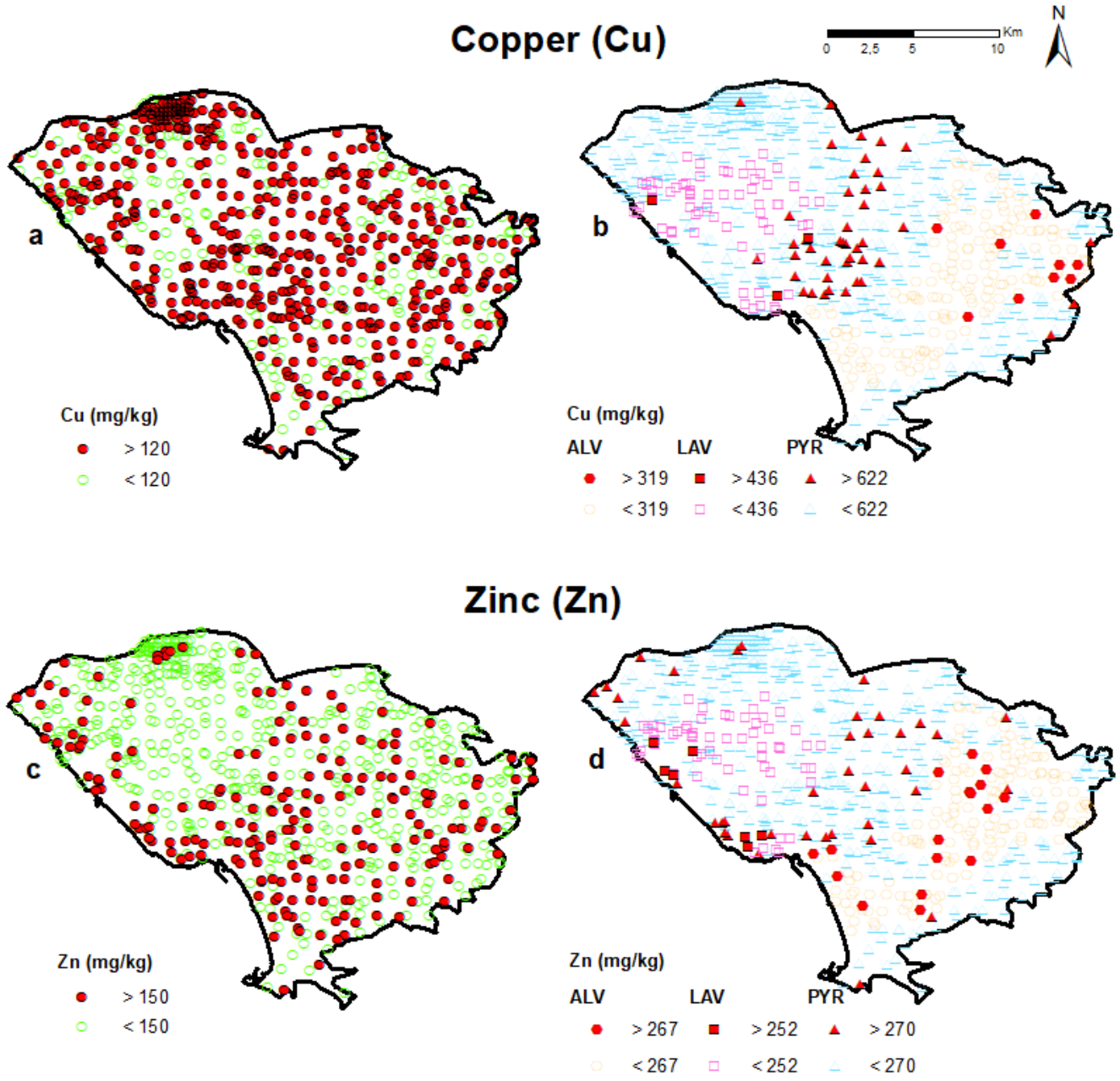

Figure 2.6 Potential hazard maps considering both the national CSC values (for residential land use), respectively, for Cu (a) and Zn (c) and the proposed UBLs values (b, d) determined for the different lithologies present in the study area.

2.5 Conclusions

The work made it possible to highlight how the distribution of high concentrations of some elements in the soils of the Campania region is heavily influenced by the local geology, rather than the presence of a marked anthropogenic contamination.

With this in mind, we wanted to demonstrate that the use of unique national reference values, for the identification of potentially contaminated sites to be subjected, possibly, to expensive risk analysis procedures, is a potentially deleterious practice in economic and environmental protection terms.

Specifically, the results obtained in this work have the presumption of assuming a double positive relevance: on the one hand, we wanted to provide a complex territory with a valid operational tool for the correct discrimination and the right sizing of the environmental emergencies present and, on the other hand, it was intended to develop an operational protocol that could be applicable to other areas of the regional or even national territory for which there should be the need to reach, through an open methodological comparison rather than through the application of a single predetermined procedure, to the estimate of the natural background values and to the definition of reference values to be used locally, also at site-specific scale, in the environmental characterization assessments.

References

Albanese, S., De Vivo, B., Lima, A., Cicchella, D., 2007. Geochemical background and baseline values of toxic elements in stream sediments of Campania region (Italy). J. Geochem. Explor. 93(1), 21-34.

Antoniadis, V., Shaheen, S.M., Levizou, E., Shahid, M., Niazi, N.K., Vithanage, M., Ok, Y.S., Bolan, N., Rinklebe, J., 2019. A critical prospective analysis of the potential toxicity of trace element regulation limits in soils worldwide: Are they protective concerning health risk assessment? - A review. Environ. Int. 127, 819-847. https://doi.org/10.1016/j.envint.2019.03.039.

Barbieri, M., 2016. The Importance of Enrichment Factor (EF) and Geoaccumulation Index (Igeo) to Evaluate the Soil Contamination. J Geol Geophys 5(1), 1000237-

Buccianti, A., Lima, A., Albanese, S., Cannatelli, C., Esposito, R., De Vivo, B., 2015. Exploring topsoil geochemistry from the CoDA (Compositional Data Analysis) perspective: the multi-element data archive of the Campania Region (Southern Italy). J. Geochem. Explor. 159, 302-316.

Cheng, Q., Agterberg, F.P., Bonham-Carter, G.F., 1996. A spatial analysis method for geochemical anomaly separation. J. Geochem. Explor. 56(3), 183-195.

Cheng, Q., Bonham-Carter, G.F., Raines, G.L., 2001. GeoDAS: A new GIS system for spatial analysis of geochemical data sets for mineral exploration and environmental assessment. The 20th International Geochemical Exploration Symposium (IGES). Santiago de Chile, 6/5-10/5, 42-43.

De Vivo, B., Cicchella, D., Lima, A., Fortelli, A., Guarino, A., Zuzolo, D., Esposito, M., Cerino, P., Pizzolante, A., Albanese, S., 2021. Monitoraggio Geochimico-Ambientale dei suoli della Regione Campania – Volume 1 (Elementi Potenzialmente Tossici e loro Biodisponibilità, Elementi Maggiori e in Traccia; distribuzione in suoli superficiali e profondi). Aracne Editrice, Roma, Italia.

De Vivo, B., Petrosino, P., Lima, A., Rolandi, Belkin, H.E., 2010. Research progress in volcanology in Neapolitan area, southern Italy: a review and alternative views. Mineral. Petrol. 99, 1–28.

Dixon, W.J., 1950. Analysis of extreme values. Ann. Math. Stat. 21(4), 488-506.

Edwards, T.S., 2015. Probability of Future Observations Exceeding the One-Sided, Normal, Upper Tolerance Limits. J Spacecr Rockets 52(2), 622-624.

ISPRA, 2019. Linee guida per la determinazione dei valori di fondo per i suoli e per le acque sotterranee: Delibera del Consiglio SNPA. Manuali e Linee Guida 174/2018

Lima, A., De Vivo, B., Cicchella, D., Cortini, M., Albanese, S., 2003. Multifractal IDW interpolation and fractal filtering method in environmental studies: an application on regional stream sediments of (Italy), Campania region. Appl. Geochem. 18(12), 1853-1865.

Lima, A., Plant, J.A., De Vivo, B., Tarvainen, T., Albanese, S., Cicchella, D., 2008. Interpolation methods for geochemical maps: a comparative study using arsenic data from European stream waters. Geochem.: Explor. Environ. Anal 8(1), 41-48.

Loska, K., Cebula, J., Pelczar, J., Wiechuła, D., Kwapuliński, J., 1997. Use of enrichment, and contamination factors together with geoaccumulation indexes to evaluate the content of Cd, Cu, and Ni in the Rybnik water reservoir in Poland. Water Air Soil Pollut 93, 347–365.

Minolfi, G., Albanese, S., Lima, A., Tarvainen, T., Fortelli, A., De Vivo, B., 2018. A regional approach to the environmental risk assessment - human health risk assessment case study in the Campania region. J. Geochem. Explor. 184 (B), 400-416.

Reimann, C., Filzmoser, P., Garrett, R.G., Dutter, R., 2008. Statistical Data Analysis Explained: Applied Environmental Statistics with R. Wiley, Chichester, UK.

Rosner, B., 1975. On the Detection of many outliers. Technometrics 17(2), 221-227.

Scarpati, C., Perrotta, A., 2018. Vesuvius, in: Bagnall, R.S., Brodersen, K., Champion, C.B., Erskine, A., Hollander, D. (Eds.) The Encyclopedia of Ancient History, John Wiley & Sons, Hoboken, New Jersey.

Spector, A., Grant, F.S., 1970. Statistical models for interpreting aeromagnetic data. Geophysics 35(2), 293-302.

Sutherland, R.A., Tolosa, C.A., Tack, F.M.G., Verloo, M.G., 2000. Characterization of selected element concentrations and enrichment ratios in background and anthropogenically impacted roadside areas. Arch Environ Contam Toxicol 38, 428-438.

Vitale, S., Ciarcia, S., 2018. Tectono-stratigraphic setting of the Campania region (southern Italy). J. Maps 14(2), 9-21. https://doi.org/10.1080/17445647.2018.1424655

CHAPTER 3 – Spatial patterns and factors influencing the bioavailable and pseudo-total content of some major and potentially toxic elements in soils of Campania region (Italy)

The results of this activity were published/presented in:

Guarino, A., Albanese, S., Cicchella, D., Ebrahimi, P., Dominech, S., Allocca, C., Romano, N., De Vivo, B., Lima, A., submitted. Selected major and potentially toxic elements bioavailability in agricultural soils of Campania region (Italy): spatial patterns and influencing factors. Journal of Geochemical Exploration.

.

3.1 Introduction

The distribution patterns and concentration of chemical elements in the surface environment of the earth depend on both the compositional characteristics and geochemical processes featuring and affecting, respectively, the geological substrate (and its weathered materials), and the degree of interference of anthropogenic activities with natural processes (Albanese, 2008).

Defining the origin of anomalous concentrations of potentially toxic elements in soils is of fundamental importance since, generally, the elemental fractions of geogenic origin have strong bonds with the crystalline lattices of minerals while those of anthropogenic origin are more mobile and can be removed easier from the matrix. This latter condition, on one hand, is a key factor influencing the effectiveness of the remediation procedures of contaminated soils, and, on the other hand, can favour the uptake of both essential and non-essential toxic metals to plants and vegetables which represent the base of the food chain, as well (Albanese, 2008).

Under standard environmental conditions, the amount of a chemical that can be transferred from the natural environment to the biological context can be defined as the bioavailable fraction of the total content (Petruzzelli et al., 2020; Ryu et al., 2010). Specifically, bioavailability can be seen as a process made up of three phases: one related to the "environmental availability" (also known as "External bioavailability") of an element mostly associated with its desorption from the media and accumulation in pore waters, one related to the "environmental bioavailability" which is the fraction of element which can be transferred from the media to the plant roots, one related to "toxicological bioavailability", which is associated to the accumulation of the element into the plant tissues (Kim et al., 2015). In general, bioavailability depends on both soil characteristics (i.e., pH, clays percentage, organic matter, cation exchange capacity, redox potential, presence of oxides and hydroxides) and physiology of the life forms involved (NRC, 2002). We should not consider the total (or pseudo-total) concentration (even if it is remarkably high) of a potentially toxic element in soils when willing to assess the possible adverse effect of contaminated soil on living beings, from plants to human beings, unless you want to assume a 100% contaminant bioavailability, which is by no means a realistic condition.

Currently, no regulation unambiguously establishes which analytical method is best suited to assess bioavailability in soil, since this parameter is influenced by several factors that should be assessed on a case-by-case basis before carrying out the proper analysis (Naidu et al., 2008). The used techniques normally consist in some single, or even sequential, extraction methods based on weak acids such as calcium chloride, sodium nitrate, acetic acid, ammonium nitrate, ethylenediaminetetraacetic acid (EDTA), diethylenetriaminepentaacetic acid (DTPA) (Dean, 2010),

in some cases, joint with some chelant agents (i.e., EDTA, DTPA) to mimic the action of roots on soil (Albanese, 2008; Tarvainen and Kallio, 2002).

The term bioavailability can be also referred to as the fraction of chemicals in the soil that could reach higher organisms' blood after being directly ingested and absorbed in the gastrointestinal tract following the action of dissolution operated by gastric juices (Ruby et al., 1999). In the latter case, bioavailability is usually termed bioaccessibility and can be assessed in the laboratory through in vitro assays simulating the leaching of metals from soil in a fluid media, which replicates the gastrointestinal tract of a 2–3-year-old infant (Ruby et al., 1996). Anyhow, the ISO standard 19730:2008 "Soil quality - Extraction of trace elements from soil using ammonium nitrate solution" specifies a method of extracting trace elements from soil using a 1 mol/l NH4NO3 solution. This method can be considered suitable for measuring the actual available content of metals in pore waters since it reproduces pH values commensurate to the ones of the soil solutions (Gryschko et al., 2005). It is a weak partial extraction method, that can be applied to a range of different soils, and is capable to determine the "readily available" concentrations of several substances that can be involved in plant uptake processes.

This study aims primarily at comparing the distribution patterns of the bioavailable concentrations (determined employing ammonium nitrate leaching) of some major and potentially toxic elements in the agricultural soils in the region of Campania (southern Italy) with their total concentrations. These total concentrations were determined using a modified Aqua Regia digestion which is, in reality, a pseudo-total extraction method capable to dissolve clay minerals, carbonates, most sulphide minerals, salts, hydroxides, and some silicates (Salminen, 1995). We also explore the potential influence that some physical and chemical properties of soils, such as grain size and organic matter content, can have on the spatial variability of the bioavailable concentrations of the individual elements.

3.2 Study area

Campania is an administrative region located along the Tyrrhenian margin of southern Italy. This territory is mainly made-up of volcanic lithotypes, carbonate rocks and sediments. The geological-structural setting of the region is very complex as it is the result of a variety of geological processes. The eastern portion of the territory is characterized by the presence of a sector of the Apennines mountains, a fold and thrust belt system that was formed during the Miocene (Steckler et al., 2008; Pierantoni et al., 2020). The rocks that characterize Apennines are part of Mesozoic sedimentary units made up of dolostone, limestone, siliceous schists, and terrigenous sediments. The western sector of the region is occupied by a Plio-Pleistocene graben, formed as a result of the intense extensional

forces (developed starting from Miocene) associated with the formation of the Apennine chain (Vitale and Ciarcia, 2018). The graben was filled by sediments of silico-clastic, carbonatic, and evaporitic origins, and it corresponds to the actual Campania and Sele plains (Fig. 3.1a).

The volcanism in Campania, which is related to the Roman Comagmatic Province, ranges from about 600 ka BP to the present (De Vivo et al., 2010; Peccerillo, 2005, 2020) and it is witnessed by the presence of four important volcanic complexes across the regional territory: Mt. Roccamonfina on the north-western sector, and Mt Somma-Vesuvius, Phlegrean Fields, and Ischia Island (i.e., Mt. Epomeo) along the western Tyrrhenian margin of the region. Potassic to ultrapotassic rocks and pyroclastic deposits represent the main products of the volcanic activity. Pyroclastics, as loose materials, mantle large portions of the region and form cover beds on most of carbonate reliefs and some siliciclastic formations (Fig. 3.1a).

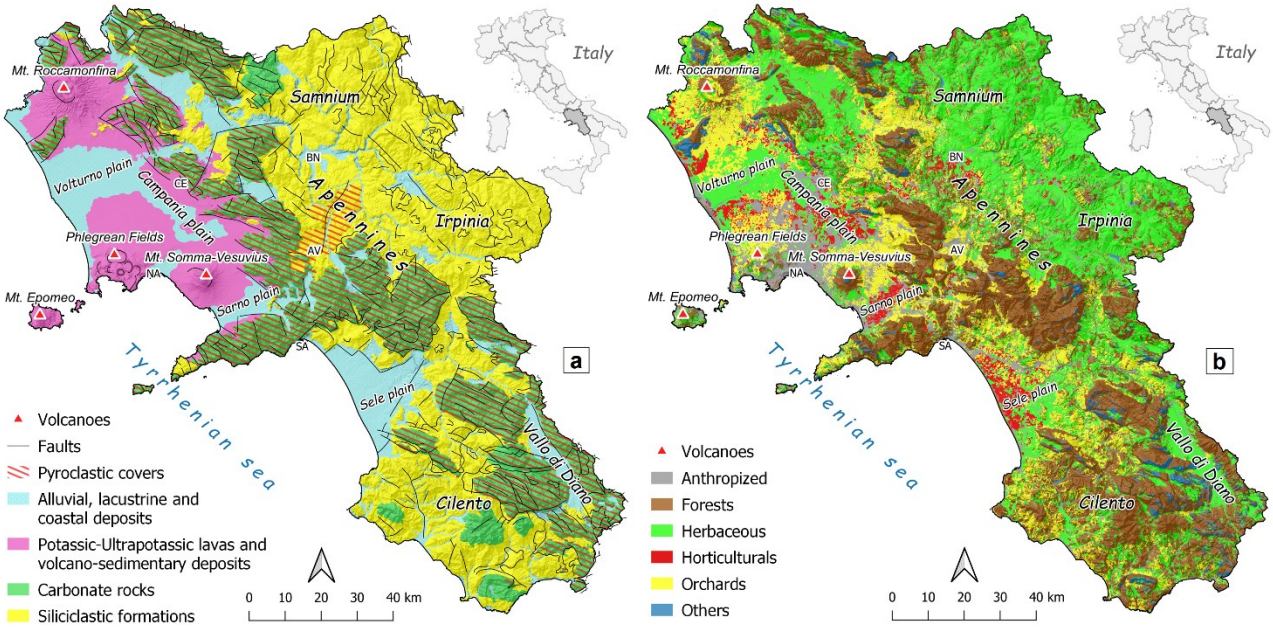

Figure 3.1 Simplified geological map (a) and agricultural land use map (b).

Thanks to their prevalent volcanic origin and the favourable climate, the soils of Campania, in particular those belonging to the coastal plains characterized by a higher abundance of water, have an exceptional agricultural yield. In fact, Campania is one of the Italian regions where agriculture is most flourishing, both in terms of quantity and quality of products, and most of the territory is occupied by herbaceous crops (e.g., wheat, cereals, weeds, pasture areas, ornamental plants, industrial crops), horticultural crops (e.g., potatoes, tomatoes) and orchards combining chestnut groves, olive groves, vineyards, citrus groves, and other minor fruit trees. Forests are mostly characterized by the

presence of coniferous, broad-leaved, sclerophyllous, bushes and shrubs and they are concentrated in correspondence with the Apennines relieves (Fig. 3.1b).

Many of the main urban areas, including the metropolitan area of Naples, are distributed along the northern and central coastal sector of the region facing the Tyrrhenian Sea; in the internal territories the cities of Benevento, Caserta and Avellino are the capitals of the homonymous provinces.

The historical industrial areas of Campania are usually located close to the main cities; those most recent are concentrated in polygons which have often been placed in easily accessible flat areas surrounded by territories with a major agricultural use.

3.3 Materials and methods

3.3.1 Sampling procedures and analytical methods

Until 2017, across the whole regional territory, 7300 topsoil samples were collected, within a depth ranging from 0.10 to 0.15 m below ground level-with a higher sampling density in correspondence with urbanizes areas and a lower one over rural areas (nominal density is of ca. 1 sample per sq/km).

More the half of these samples were collected and analysed within the frame of the research activities carried out over the years by the Environmental Geochemistry Working Group at the Department of Earth, Environmental and Resource Sciences (DiSTAR) of the University of Naples Federico II (Buccianti et al., 2015; De Vivo et al 2016; Minolfi et al., 2018; Petrick et al., 2018a, 2018b, 2018c, 2018d; Thiombane et al., 2019; Guarino et al., 2022), while the remaining part was collected and analyzed in the framework of the "Campania Trasparente" project (funded by the regional government) in collaboration with the Experimental Zooprophylactic Institute of Southern Italy (IZSM) (Guagliardi et al., 2020; Zuzolo et al., 2020; De Vivo et al 2021).

Despite the fact that the soil samples were collected over a period of about five years, sample preparation procedures and analytical methods applied were kept consistent along the time.

Specifically, after an appropriate preparation at laboratory of Environmental Geochemistry (DiSTAR), including soil drying at a temperature below 37 °C to avoid massive Hg volatilization, an aliquot of each of the 7300 samples of about 30 grams at a fraction <2 mm was sent to the Bureau Veritas (formerly Acme) Analytical Laboratories Ltd. (Vancouver, Canada), to undergo a digestion in an Aqua Regia modified solution (2 volumes of HCl + 2 volumes of HNO_3 + 2 parts of distilled water) and to be analysed combining ICP-MS (Inductively Coupled Plasma Mass Spectrometry) and ICP-ES (Inductively Coupled Plasma Emission Spectrometry). The concentration of 53 elements was

determined. A 50 g duplicate of each sample was also stored at the sample storage room of DiSTAR for possible future analyses.

It is worth specifying that the digestion with aqua regia can be considered total for all those metals which are, in the sample, found as soluble salts, bound to clay particles (cation exchange sites), in organic chelates, amorphous oxides and hydroxides of Fe and Mn, in carbonates, sulphides and some sulphates. The metals contained in the silicates (generally the ferromagnesic ones) and in some crystalline oxides of Fe, Ti and Cr are partially solubilized. The refractory minerals of Ta, Hf, Zr, Nb, and the sulphates of Ba are very resistant to this extraction method (De Vivo et al., 2021). For this, now on, we referred to the concentrations measured following aqua regia digestion as "pseudo-total".

Subsequently, based on the observation of analytical result obtained from the application of Aqua Regia leaching, 1993 samples were selected and an aliquot of 15 g was collected from duplicates and treated with Ammonium Nitrate (NH_4NO_3) to determine the bioavailable fraction of 59 elements.

In addition, among the samples collected within the framework of "Campania Trasparente" blueprint, on 418 samples, the organic carbon (OC) content was determined at the same laboratory.

Subsequently, the amount of OC was converted to the respective organic matter (OM) using a factor of 2 (Eq. 3.1), based on the assumption that organic matter is made of about 50% of carbon, which is deemed more accurate than the conventional "van Bemmelen factor" of 1.724 (Pribyl, 2010):

$$OM\ (\%) = OC\ (\%) * 2 \qquad \text{Eq. 3.1}$$

Besides, within the planned activities of "Campania Trasparente", disturbed samples and undisturbed cores were collected from the topsoil of 3,316 locations in the entire region. All of these samples were subjected to several tests at the Laboratory of Soil Hydrology (Department of Agricultural Sciences, University of Naples Federico II) to determine physico-chemical and hydraulic properties and, in particular, the grain size distributions (Nasta et al., 2020). Oven-dry bulk density values were obtained by inserting the undisturbed soil cores in a ventilated oven for at least 24 hours (depending on the soil textural class) and measuring the mass of dry soil per unit of volume. Instead, the disturbed soil samples were employed to measure the soil textural characteristics. Specifically, a standard laboratory protocol was employed to determine the soil grain-size distribution for soil material fractions < 2 mm (Gee and Or, 2002). Our protocol was carried out according to the USDA (United States Department of Agriculture) classification and entailed the measurement of the mass fraction of the sand particles (SN, in the range 2.0 mm – 0.050 mm) by a sieving procedure, whereas the mass fraction of the clay particles (CL, less than 0.0020 mm) was obtained by the hydrometer method. The mass fraction of the silt particles (SL, in the range 0.050 mm – 0.0020 mm) is obtained by difference.

3.3.2 Statistics and geochemical mapping

3.3.2.1 Geochemical variables

The geochemical datasets, as stated, contain the values of the pseudo-total concentration of 53 elements and the bioavailable fraction of 59 elements. Before being treated to handle values below the detection limits and missing values, respectively, some considerations were made for the choice of elements to be treated.

First of all, of course, we only handled the samples (i.e., 1993) and variables for which chemical data referring to both ammonium nitrate and Aqua Regia leaching were available. As for the analytes, only 15 elements, out of the whole set of variables, presented a percentage of values below the detection limit < 25%. Among them for the aims of this paper we decided to elaborate and focus our discussion on aluminium (Al), calcium (Ca), potassium (K), magnesium (Mg), copper (Cu), and thallium (Tl).

The choice was made since each of these analytes, albeit for different reasons, is linked to agricultural processes. Aluminium is phytotoxic; it limits plant growth and renders soils unproductive (Rout et al., 2001). Calcium is important for regulating plant growth and balances the absorption of the other cations (Thor, 2019). Potassium is an element that should never be lacking because it increases the resistance of crops to both cold periods and water shortage (Prajapati and Modi, 2012; Sardans and Peñuelas, 2021). Magnesium is also a nutrient, and it takes part in the formation of chlorophyll, and it is essential for the development of chloroplasts which are organelles responsible for the photosynthesis process (Yan and Hou, 2018). Copper is a nutrient for plants but can also limit their growth when in excess (Yruela, 2005); it is a component of the cupric fungicides, very used in agriculture. Thallium, like Cu, is a potentially toxic element (PTE) and is an element naturally present in the minerals of volcanic origin, but it is also a component of pesticides and rodenticides (in the form of thallium sulfate) and it can inhibit plant seed development (Horn, 1934; Rader et al., 2019).
In addition to Cu and Tl, the Italian Environmental Law (D.lgs. 152/2006) defines as PTEs other 13 elements (i.e., As, Be, Cd, Co, Cr, Hg, Ni, Pb, Sb, Se, Sn, V and Zn) and fixes thresholds to be respected for their concentration in soils depending on the residential or industrial land use, as well as the D.M. 46/2019 does for agricultural land use (Table 3.3). These thresholds are defined for the total concentrations of these chemical elements, that is considering their 100% bioavailability. Since the bioavailable fraction of Cr was not analyzed while most of the other elements, for the same concentrations, had a number of samples with values below the instrumental detection limit >> 50% (Table 3.3), these others PTEs were not taken into consideration for the study of the influencing

factors because of the poor statistical significance. However, we decided to show their spatial pattern distribution to demonstrate the scarce bioavailability of these elements in regional soils with respect to the measured pseudo-total concentrations.

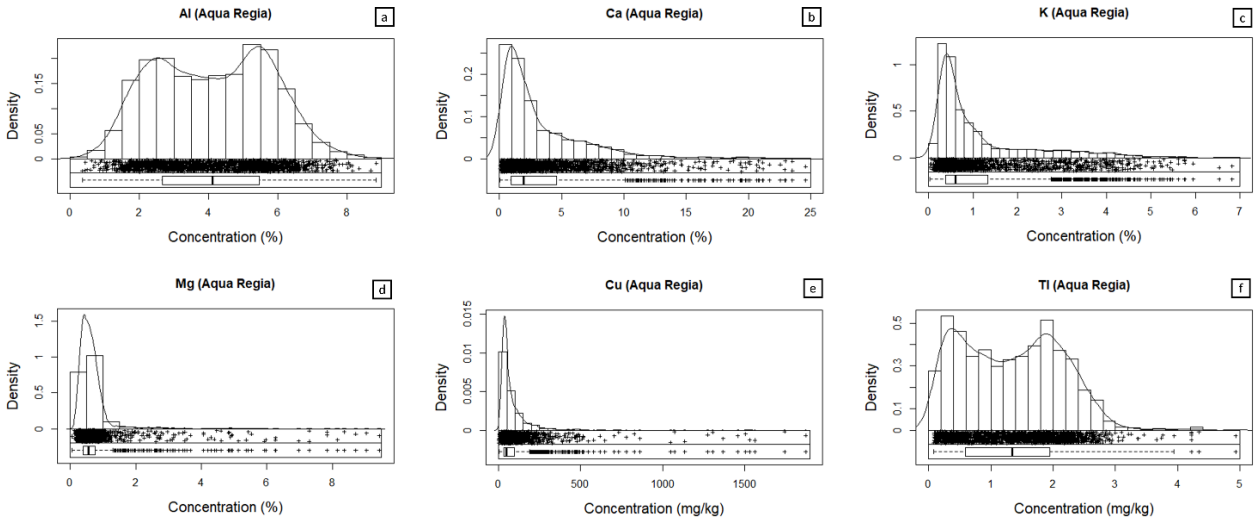

Figure 3.2 Edaplots of the pseudo-total concentrations of Al (a), Ca (b), K (c), Mg (d), Cu (e) and Tl (f).

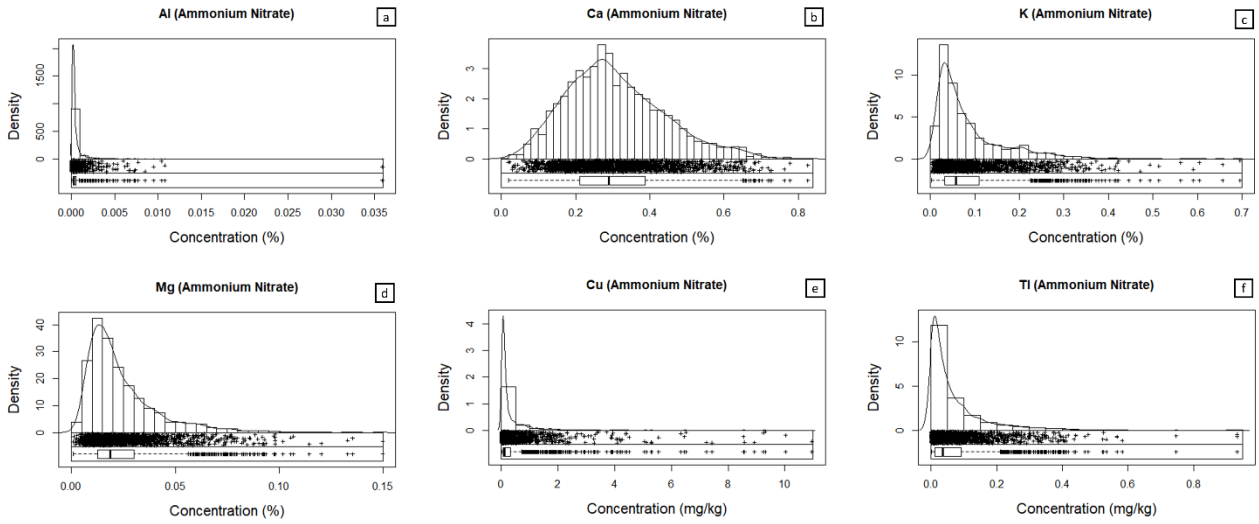

Figure 3.3 Edaplots of the bioavailable concentrations of Al (a), Ca (b), K (c), Mg (d), Cu (e) and Tl (f).

3.3.2.2 Data preparation

Values below the detection limit were replaced by a value equal to half of the limit itself (Reimann et al., 2008). Besides, regarding the missing values, there are various types of these that can be present in a dataset, classified based on the reason why they are missing and whether they can be predicted from the know variables or not: all the observations (i.e., the samples) that presented, for a given

analyte, even a single value which was found to be missing for spatial clustering were eliminated, while we proceeded with the estimate of those values absent because some variables (i.e., chemicals) were not considered in the analytic suite at the time of the firsts analyses.

Before applying the algorithm for the imputation of missing values, the goodness of fit test was run at the 1% and the 5% level of significance. Since data did not appear to follow any discernible distribution, at neither of the two levels of significance, we proceeded to normalize the data according to the Box-Cox transformation (Box and Cox, 1964). The algorithm for the Box-Cox transformation is a method for identifying which data transformation can best convert their distribution, estimating the power lambda (λ) thatresults in the best approximation of a normal distribution curve.

Table 3.1 Summary statistics of data.

	Aqua Regia digestion					
Element	**Al**	**Ca**	**Cu**	**K**	**Mg**	**Tl**
Unit	%	%	mg kg-1	%	%	mg kg-1
DL	0.01	0.01	0.01	0.01	0.01	0.02
N° of samples	1973	1973	1973	1973	1973	1904
Min	0.36	0.07	2.51	0.03	0.06	0.08
First quartile	2.66	0.94	33.58	0.39	0.41	0.59
Median	4.12	1.97	49.58	0.61	0.57	1.34
Third quartile	5.47	4.61	95.89	1.34	0.77	1.95
Max	8.85	24.57	1873	6.82	9.43	4.93
MAD	2.08	1.88	32.04	0.43	0.25	1.01
CVR %	50.38	95.58	64.62	70.48	44.22	75.24
Skewness	0.05	2.23	6.98	1.77	6.10	0.29
Kurtosis	-0.95	6.17	66.06	2.53	46.09	-0.48
	Ammonium Nitrate extraction					
Element	**Al**	**Ca**	**Cu**	**K**	**Mg**	**Tl**
Unit	%	%	mg kg-1	%	%	mg kg-1
DL	0.0001	0.0005	0.01	0.0005	0.0001	0.001
N° of samples	1973	1973	1973	1973	1973	1904
Min	0.00005	0.019	0.01	0.0032	0.001	0.001
First quartile	0.0002	0.21	0.056	0.032	0.013	0.012
Median	0.0003	0.29	0.11	0.057	0.019	0.036
Third quartile	0.0005	0.39	0.33	0.11	0.030	0.092
Max	0.036	0.83	10.95	0.70	0.15	0.93
MAD	0.00015	0.13	0.11	0.044	0.012	0.043
CVR %	49.42	44.47	98.39	76.99	61.51	119.43
Skewness	16.42	0.59	6.12	2.18	2.01	2.90
Kurtosis	438.77	0.16	49.46	6.76	5.67	13.41
%Bio	0.0073	14.71	0.22	9.34	3.30	2.69
R^2	0.047	0.049	0.710	0.047	0.067	0.33
p-value	< 2.2e-16	< 2.2e-16	< 2.2e-16	< 2.2e-16	< 2.2e-16	< 2.2e-16

The imputation of missing values was then performed applying the Expectation-Maximization algorithm (EM), which preserves the relationship with other variables better than mean imputations, whose purpose is to maximize the likelihood of the parameters of a model (Dempster et al., 1977). The EM is an iterative algorithm in which each iteration consists of an Expectation step (E-step), that creates a function to impute the missing variable, and a Maximization step (M-step), which optimizes the parameters of the model. These two steps are applied until convergence is reached and when it no longer increases the likelihood.

Following the estimate of missing values, a univariate statistical analysis was carried out for each variable in the dataset determining the main statistical parameters: minimum, maximum, median, quartiles, median absolute deviation (MAD) (Reimann et al., 2008), robust coefficient of variation (CVR) (Reimann et al., 2008), kurtosis and, skewness (Table 3.1). For each variable a graphical representation of data distribution was generated, as well (Figs. 3.2 and 3.3).

In addition, to have clear evidence of the bioavailable fraction (C_{AN}) compared to the pseudo-total (C_{AR}) one, the percent bioavailability was calculated as a ratio between the bioavailable concentration and the pseudo-total one at each sample location as follow (Albanese, 2008):

$$\%\ Bioavailability = \frac{C_{AN}}{C_{AR}} * 100 \qquad \text{Eq. 2.2}$$

Where:

- C_{AN} is the concentration analyzed after Ammonium Nitrate extraction
- C_{AR} is the concentration analyzed after Aqua Regia digestion.

For each element, Table 3.1 also reports the median value of the percent bioavailability.

3.3.2.3 Geospatial analysis

Data of all the considered variables (i.e., C_{AR}, C_{AN}, percent bioavailability, OM, and grain size) were processed in a GIS environment and they were interpolated by Multifractal Inverse Distance Weighted (MIDW) method (Cheng, 1999) (Figs. 3.2, 3.3, 3.4 and 3.5). The method uses the principles of fractal and multifractal geometry to define, in a probabilistic way, the spatial distribution patterns of the input variables while preserving the high-frequency information (i.e., the anomalies), that are generally lost in conventional interpolation methods; it also takes into account both the spatial association and the local singularity of the data.

To perform the separation of the pixels of the raster grids into discrete intervals (i.e., to assign a value range and a specific colour to each class) and to represent on each map the different

geochemical characteristics of the investigated area, the Concentration-Area (C-A) method was used (Cheng et al., 1994; Zuo and Wang, 2020; Albanese et al, 2007). Specifically, the separation was obtained locating the more marked inflection points on a log-log plot (the C-A plot) putting the total area of all pixels with values above a specific concentration (A(ρ)) against the concentration value itself (ρ).

As there was no correspondence between the samples collected for the determination of the CAN (and CAR, of course) and the samples for which the OM values were available, for the implementation of subsequent statistical analysis, we extracted the cell values of the raster grids of OM, previously generated, using as input the locations of the 1993 samples selected from the regional geochemical database for the aim of the present study.

3.3.2.4 Regression analysis

A simple linear regression model was applied to data to assess the relationship between C_{AN} and C_{AR}. A linear function was fitted considering C_{AR} as the independent variable and C_{AN} as the dependent one. The R-squared (R^2) or the coefficient of determination, which is an index representing the proportion of the variance between the variables explained by the model, is reported, for each element, in Table 3.1. Likewise, in Table 3.1 it is also reported the p-value, which is a measure of the probability of rejecting the null hypothesis that a correlation exists among involved variables: a small p-value (< 0.05) means that variables are significantly correlated.

Having available data referring to other parameters on soil samples (i.e., OM and grain size), to better understand the spatial features of bioavailable concentrations in soils, a multiple regression model was also applied to the data.

Finally, C_{AN} was again set as the dependent (or response) variable and C_{AR} together with OM and the grain size distribution (i.e., clay - CL, silt - SL, sand - SN) were used as independent (or explanatory) variables.

The method used was the standard stepwise regression, which is a combination of the stepwise forward and the stepwise backward procedures (Draper and Smith, 1998; Hocking, 1976). It essentially consists of a series of iterations in which, step-by-step, the explanatory variables are included in or excluded from the model, according to a statistical criterion (i.e., F-test statistical significance), to achieve an optimal model (Reimann et al, 2008). In Table 3.2 the adjusted R^2, the p-values of the models, and the regression equations are reported in the form of:

$$y = \beta_0 + \beta_1 x_1 + \beta_2 x_2 + \cdots + \beta_n x_n + \varepsilon \qquad \text{Eq. 2.3}$$

Where:

- y is the dependent variables;
- x_i is the i-esim independent variables;
- β_i is i-esim regression coefficients;
- ε is the error.

*Table 3.2 Equations, adjusted R^2 and p-values of the multiple regression models. Significance codes of the coefficients: *** = p-values range [0, 0.001]; ** = (0.001, 0.01]; * = (0.01, 0.05]; ° °= (0.05, 0.1]; ° = (0.1, 1]. OM = organic matter; SN = sand; CL = clay; SL = silt.*

Regression equations	R^2	p-values
$\mathbf{Al_{AN}} \simeq$ - 1.204e-04°° + 1.534e-04*** $\mathbf{Al_{AR}}$	0.0468	< 2.2e-16
$\mathbf{Ca_{AN}} \simeq$ 1.575e-01*** + 4.858e-03*** $\mathbf{Ca_{AR}}$ + 8.943e-06** **OM** + 5.572e-03*** **CL**	0.4126	< 2.2e-16
$\mathbf{Cu_{AN}} \simeq$ - 2.702e-01*** + 5.192e-03*** $\mathbf{Cu_{AR}}$ + 5.243e-03*** **SN**	0.7146	< 2.2e-16
$\mathbf{K_{AN}} \simeq$ 1.966e-01*** + 7.579e-03*** $\mathbf{K_{AR}}$ - 5.651e-06* **OM** - 1.246e-03*** **SN** - 2.928e-03*** **CL**	0.1403	< 2.2e-16
$\mathbf{Mg_{AN}} \simeq$ 4.829e-02*** + 5.946e-03*** $\mathbf{Mg_{AR}}$ - 4.434e-04*** **SN** - 3.015e-04*** **SL**	0.2054	< 2.2e-16
$\mathbf{Tl_{AN}} \simeq$ - 9.14714e-02*** + 6.68643e-02*** $\mathbf{Tl_{AR}}$ + 1.7554e-03*** **SL** + 2.122e-04° **CL**	0.3576	< 2.2e-16

3.4 Results and discussion

3.4.1 Aluminium

Aluminium (Al) is one of the most abundant lithophilic elements in the earth's crust. It is the major constituent of many igneous minerals, such as feldspar, micas, amphiboles, pyroxenes, and garnets (De Vos and Tarvainen, 2006).

In general, the highest values of pseudo-total concentrations of Al (Al_{AR}) (> 3.24%) feature the regional soils developed on pyroclastic covers of the carbonate relieves, and on potassic-ultrapotassic lava and volcano-sedimentary deposits in correspondence with the volcanic centres of Mt. Somma-Vesuvius and Mt. Roccamonfina (Fig. 3.4a). Lower values of Al_{AR} are mostly found where siliciclastic sediments are present and, partly, in correspondence of some sectors of the alluvial plains of Volturno and Sele rivers, respectively.

The bioavailable fraction of Al (Al_{AN}) ranges from a minimum of 0.00005% to a maximum of 0.036%, with a median value of 0.0003% (Table 3.1). The map of the interpolated distribution (Fig. 3.5a) shows that the highest values (> 0.0004%) clearly mark the soil developed in correspondence of the mountains covered by pyroclastics (Fig. 3.1a) and occupied by forests (Fig. 3.1b). Bioavailability in soils seems to decrease in correspondence with the alluvial plains of the coastal

sector and the siliciclastic sediments of the inner part of the region where it goes from low (< 0.0004%) to very low (< 0.00017%) values, respectively.

The fitted equation of the multiple linear regression model (Table 3.2), even if it explains only <5% (R^2 = 0.0468) of the variability, was found to be statistically significant (p-value < 2.2e-16). Specifically, only Al_{AR}, as an independent variable, results to be a significant predictor for the response variable Al_{AN} (β = 1.534e-04, p-value < 2.2e-16).

The percent bioavailability of this element is, in general, very low with a median value equal to 0.0073 % (Table 3.1 and Fig. 3.6a); however, maximum values, up to 1.56 %, appear roughly related with the distributions of pyroclastic covers (Fig. 3.1a) and forestal areas (Fig. 3.1b) which are probably associated with more acidic conditions of soils compared to the rest of regional territory.

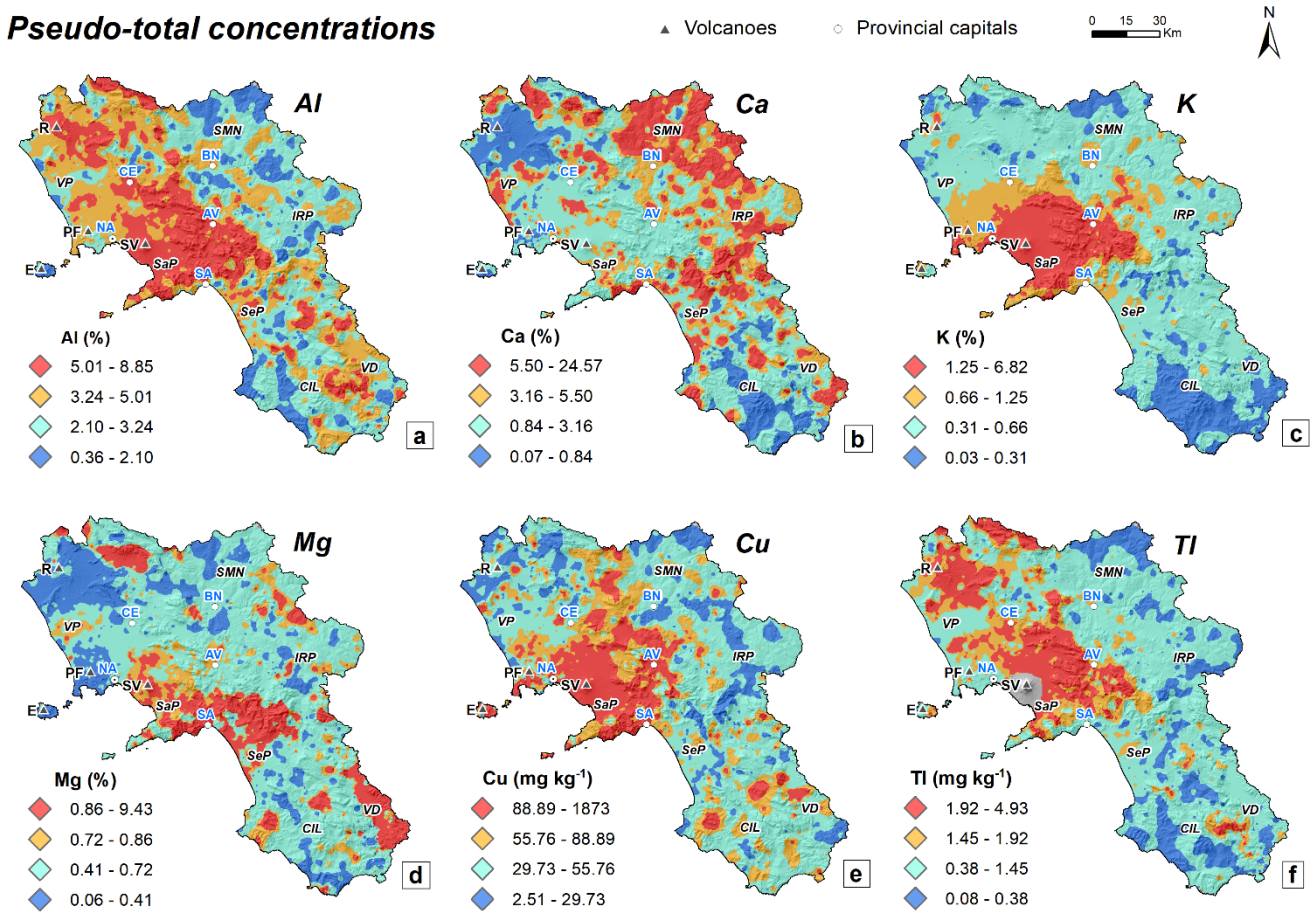

Figure 3.4 Interpolated maps of the distribution of the pseudo-total concentrations of Al (a), Ca (b), K (c), Mg (d), Cu (e) and Tl (f). (Volcanoes: R=Roccamonfina; PF=Phlegrean Fields; SV=Somma-Vesuvius; E=Epomeo. River plains: VP=Volturno; SaP=Sarno; SeP=Sele. Areas: SMN=Samnium; IRP=Irpinia; CIL=Cilento; VD=Vallo di Diano (in black). Provincial capitals: NA=Napoli; CE=Caserta; AV=Avellino; BN=Benevento; SA=Salerno (in blue)).

3.4.2 Calcium

Calcium (Ca) is the fifth for abundance among all elements and constitutes 3.5 wt% of the continental crust. It is a moderately mobile lithophilic element that easily enters the lattices of many silicates and phosphatic minerals (De Vos and Tarvainen, 2006).

The pseudo-total concentrations of Ca (Ca_{AR}) in regional soils range from a minimum of 0.07% to a maximum of 24.57%, with a median value of 1.97% (Table 3.1). The inner part of the region, mostly characterized by the presence of siliciclastic formations, show the highest Ca_{AR} with values > 3.16 %. Scattered areas with limited extension are featured by high Ca_{AR} in correspondence of the alluvial deposits of the Volturno River mouth and the Sele plain, as well. Volcanic areas and their surroundings, including relieves with pyroclastic covers show, instead, the lowest values of Ca_{AR}; soils at Mt. Roccamonfina slopes are the most depleted in Ca (Such as the Cilento soils, on the south) with values <0.84% (Fig. 3.4b).

The minimum bioavailable concentration of Ca (Ca_{AN}) equals to 0.019% while the maximum is 0.83% (Table 3.1). Calcium C_{AN}, in general, show a spatial pattern similar to Ca_{AR}. However, some differences are visible in the southern regional territory where bioavailability seems to be promoted by the presence of pyroclastic coverages (Fig. 3.1a) unlike other parts of the region where lithologies of volcanic origin (regardless of whether they are loose materials or rocks) are marked by the lowest Ca_{AN} (<0.23%) (Fig. 3.5b).

The overall regression (Table 3.2) is statistically significant (p-value < 2.2e-16) and, specifically, Ca_{AN} (β = 4.858e-03, p-value = 6.91e-15), OM (β = 8.943e-06, p-value = 0.00558) and CL (β = 5.572e-03, p-value < 2e-16) were found to be significant predictors of the bioavailable values of Ca explaining, together, a good amount of the model variability (R^2 = 0.4126). The result of regression can be visually verified by observing the distribution pattern of Ca_{AN} (Fig. 3.5b) in relation with the distribution of clay in soils across the whole region (Fig. 3.7b) and, in some spot areas, with the highest values of organic matter (Fig. 3.7a). Furthermore, the influence of both clay and organic matter on the spatial distribution of the bioavailable fraction is also made evident by the change occurred to R^2 value (from 0.049 to 0.4126) when they were included in the model in addition to Ca_{AR}.

The patterns of the distribution of the percent bioavailability of Ca appear to be strongly different from those of both pseudo-total and bioavailable concentrations; the highest values (up to 95 %) (Fig. 3.6b), in facts, are found on the south-eastern sector of Mt. Roccamonfina, and in correspondence with Matese Mts. (at the northern regional border) and the Cilento area (on the south). It is probable that, to some extent, the highest percent bioavailability values could correspond to agricultural areas

(e.g., south-eastern sector of Mt. Roccamonfina) where amendments (such as calcium hydroxide and oxide, raw product, etc.) are used to regulate the pH of soils as well as to increase the ion exchanges.

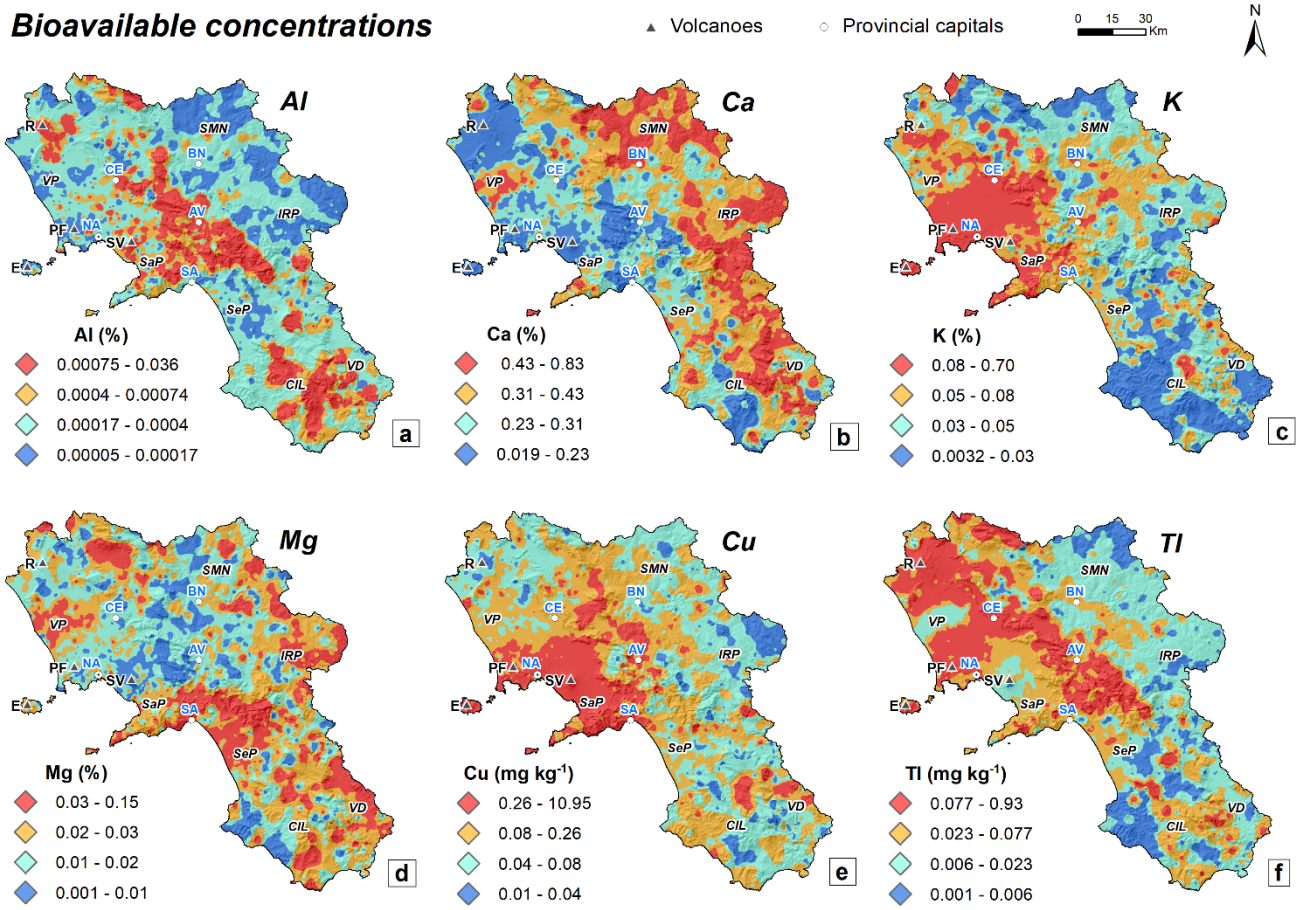

Figure 3.5 Interpolated maps of the distribution of the bioavailable concentrations of Al (a), Ca (b), K (c), Mg (d), Cu (e) and Tl (f). (Volcanoes: R=Roccamonfina; PF=Phlegrean Fields; SV=Somma-Vesuvius; E=Epomeo. River plains: VP=Volturno; SaP=Sarno; SeP=Sele. Areas: SMN=Samnium; IRP=Irpinia; CIL=Cilento; VD=Vallo di Diano (in black). Provincial capitals: NA=Napoli; CE=Caserta; AV=Avellino; BN=Benevento; SA=Salerno (in blue)).

3.4.3 Potassium

Potassium (K) is an alkaline metallic element, lithophilic and biophilic. It is one of the major constituents of many minerals, mainly K-feldspar and micas (De Vos and Tarvainen, 2006).

The pseudo-total concentrations of K (K_{AR}) are between a minimum of 0.03 % and a maximum of 6.82 % (Table 3.1). The areas characterized by the highest values of K_{AR} (0.66 % to 6.82 %) covers most of the southern sector of Campania Plain (excluding the Volturno River plain) and includes the soils developed on the pyroclastic covers of the carbonate relieves in the mid-central sector of the region (Fig. 3.4c). In general, a direct influence of the geochemical characteristics of the erupted

products of Mt. Somma-Vesuvius and Phlegrean Fields on the composition of corresponding soil can be said with certainty by considering their potassic and ultrapotassic nature (Guagliardi et al., 2020).

The bioavailable concentrations of K (K_{AN}) are, in general, noticeably low compared to the K_{AR} and they range from 0.0032 % and 0.70 %, with a median value of 0.057 %. The highest values (from 0.08 to 0.70 %) are mainly recorded in the western portion of the region (Fig. 3.5c) and they can be roughly superimposed to K_{AR} spatial patterns with some exceptions. In fact, unlike K_{AR}, the highest K_{AN} also marks the soils developed on the volcanic deposits located on the northern side of the Campania Plain toward the Roccamonfina complex. Further, average values of K_{AN} (between 0.05 and 0.08 %) feature the coastal sector of the Sele plain and the inner part of the central territory of the region (between Samnium and Irpinia) where the presence of horticultural crops and orchards is reported.

The overall multiple regression (Table 3.2) was found to be statistically significant (p-value < 2.2e-16) although it has a low predictive ability ($R^2 = 0.1403$). As a matter of the fact, K_{AR} seems to be a good predictor for K_{AN} ($\beta = 7.579e-03$, p-value = 0.00015), together with OM ($\beta = -5.651e-06$, p-value = 0.01943), SN ($\beta = -1.246e-03$, p-value = 2.92e-10) and CL ($\beta = -2.928e-03$, p-value < 2e-16); in facts, the introduction of these latter variables in the model has brought the R^2 to grow from 0.047 (Table 1) to 0.1403. It is important to point out that, excluding K_{AR}, the β coefficients of the independent variables are all negative, which means that there is, according to this model, an inverse proportionality with the bioavailability of K in soil.

The percent bioavailability reaches maximum values (up to 58 %) (Fig. 3.6c) in correspondence with the volcanic areas of the Phlegrean Fields, Mt. Roccamonfina and its surroundings, and several small spots across the whole region.

The partial differences in distribution patterns of percent bioavailability compared to KAN is probably due not only to the different composition and degree of alteration of minerals of the volcanic soils of Phlegrean Fields and Mt. Roccamonfina, compared to those of the Vesuvian area, but also the use of potassium-based soil improvers in the cultivated areas present in this portion of the region. The plain surrounding the Mt. Somma-Vesuvius, characterized by a sandy texture of the loose volcanic products, appears to be the area with the lowest percent bioavailability, possibly indicating that K is firmly bounded in the crystalline structure of soil minerals. In addition, it is also worth considering that the soils of the Phlegraean area and those on the slopes of the Mt. Roccamonfina are classified by di Gennaro et al. (2002) as neutral and as slightly acidic, respectively; this would further justify the greater extractability of K determined for these areas.

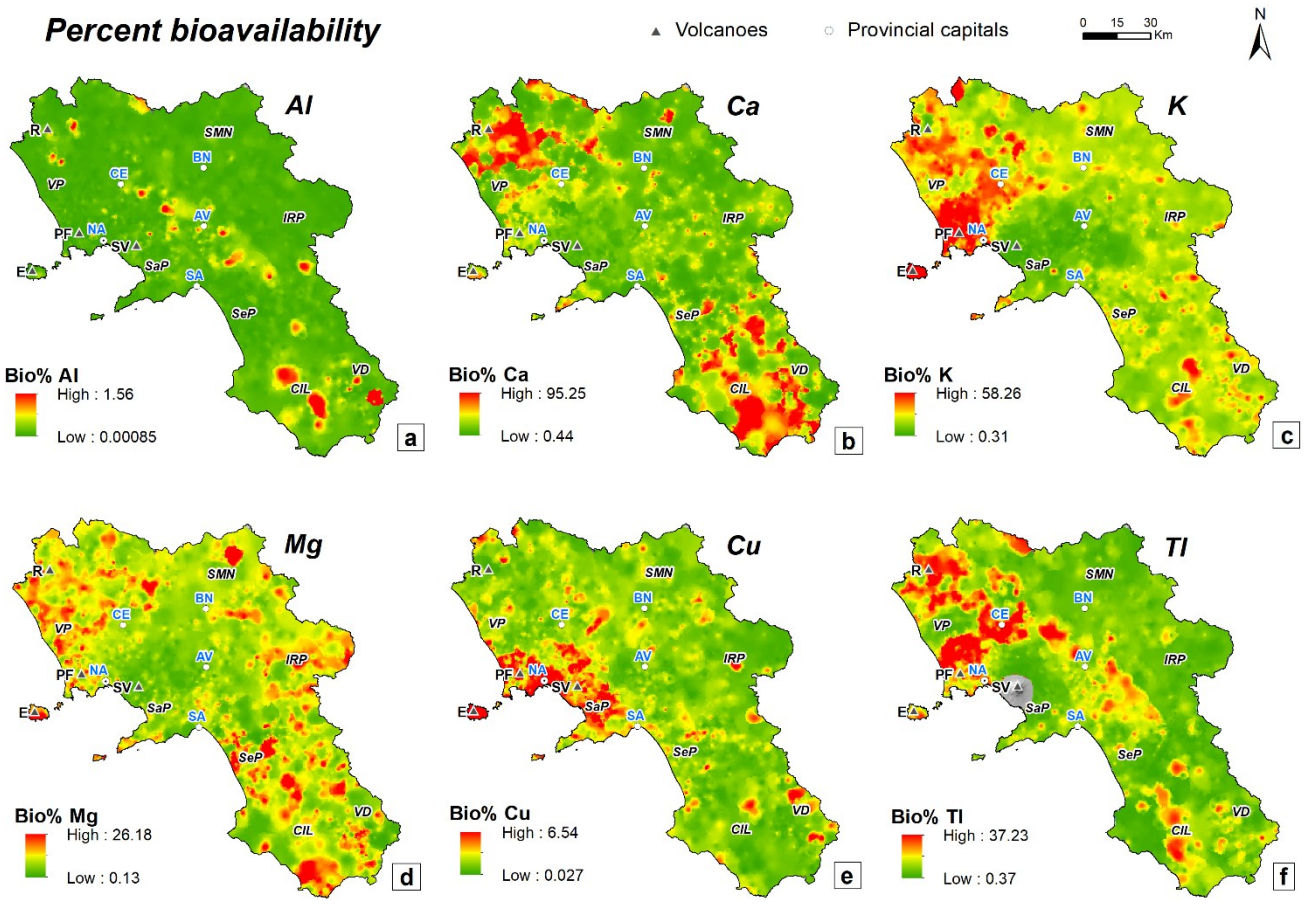

Figure 3.6 Interpolated maps of the distribution of the percent bioavailability of Al (a), Ca (b), K (c), Mg (d), Cu (e) and Tl (f). (Volcanoes: R=Roccamonfina; PF=Phlegrean Fields; SV=Somma-Vesuvius; E=Epomeo. River plains: VP=Volturno; SaP=Sarno; SeP=Sele. Areas: SMN=Samnium; IRP=Irpinia; CIL=Cilento; VD=Vallo di Diano (in black). Provincial capitals: NA=Napoli; CE=Caserta; AV=Avellino; BN=Benevento; SA=Salerno (in blue)).

3.4.4 Magnesium

Magnesium (Mg) is a major metal, lithophilic, and moderately mobile. It is found in association with Fe, Cr, Ni, Co, and Ti in mafic and ultramafic igneous rocks (De Vos and Tarvainen, 2006).

The pseudo-total concentrations of Mg (Mg_{AR}) range from 0.06 to 9.43% (Table 3.1). The areas with the highest values (0.86 to 9.43%) (Fig. 3.4d) roughly correspond with the surroundings of the Mt. Somma-Vesuvius including the Sarno river plain, and most of the Sele plain. High concentrations of Mg_{AR} also are present on the south-western slopes of Mts. Matese, in the morphological depression of Vallo di Diano and in some spots of Cilento, Irpinia and Samnium. In general, most of the soils with markedly high Mg_{AR} corresponds to lowlands collecting sediments from the carbonatic massives featured by dolomitic lithotypes which are located in the middle and inner sectors of the region, from north to south (Vitale and Ciarcia, 2018).

The Mg bioavailable concentrations (Mg_{AN}) range from 0.001 % to 0.15 %. The patterns of highest Mg_{AN} concentrations (>0.03 %) mostly resemble the patterns of the highest Mg_{AR} values (i.e., Sele River plain, slopes of Mts. Matese, Vallo di Diano) and include the Volturno River mouth and a number of small areas scattered across Samnium, Irpinia and Cilento (Fig. 3.5d). In general, the lowest Mg_{AN} concentrations (<0.02 %) feature the plain surrounding Mt. Somma-Vesuvius and a wide belt connecting this latter with Samnium, along an SW-NE direction.

The equation of the multiple linear regression model (Table 3.2) was found to be statistically significant (p-value < 2.2e-16) although with a limited representativity (R^2 = 0.2054). Starting from the assumption that Mg_{AR}, as an independent variable, can explain a very limited amount of Mg_{AN} variability (R^2= 0.067) (Table 3.1), the introduction of SN (β = -4.434e-04, p-value < 2e-16) and SL (β = -3.015e-04, p-value = 4.92e-11) in the model brought the overall value of R^2 to 0.2054, showing, anyway, a favorable impact of these variables on its predictive ability. Furthermore, the negative signs of the coefficients of these two latter elements imply that they have an inverse relationship with the changes occurring to the bioavailable concentrations of Mg in soils.

The highest percent bioavailability is equal to 26.18 % (Fig. 3.6d) although the median regional value is 3.3 % (Table 3.1). The areas with the highest percent of bioavailability, with individual limited extensions, are irregularly scattered across the whole regional territory with a major density in correspondence with the northern sector of the Campania Plain and the siliciclastic lithologies featuring the inner and the southern sectors of the region, respectively. In general, a rough correspondence of the highest percent of bioavailability with clayey soils can be inferred (Fig. 3.7b).

3.4.5 Copper

Copper (Cu) is a strong chalcophile element, it forms various minerals such as chalcopyrite, covellite, malachite but is also found dispersed in others such as biotite, pyroxene, and amphibole (De Vos and Tarvainen, 2006).

The pseudo-total concentrations of Cu (Cu_{AR}) range from 2.51 mg/kg to 1,873 mg/kg, with a median of 49.58 mg/kg (Table 3.1). The highest concentration of Cu_{AR} (from 55.76 mg/kg up to 1,873 mg/kg) features a huge territory including the Vesuvian plain, the Sarno river catchment basin, the western sector of the Irpinia territory and a wide belt that goes from the Vesuvian area to the northern border of the region, including part of the Samnium territory. This element is mostly characterized by values between 55.76 mg/kg and 88.89 mg/kg while the rest of the region is generally featured by medium to low values of Cu_{AR} (< 55.76 mg/kg) (Fig. 3.4e).

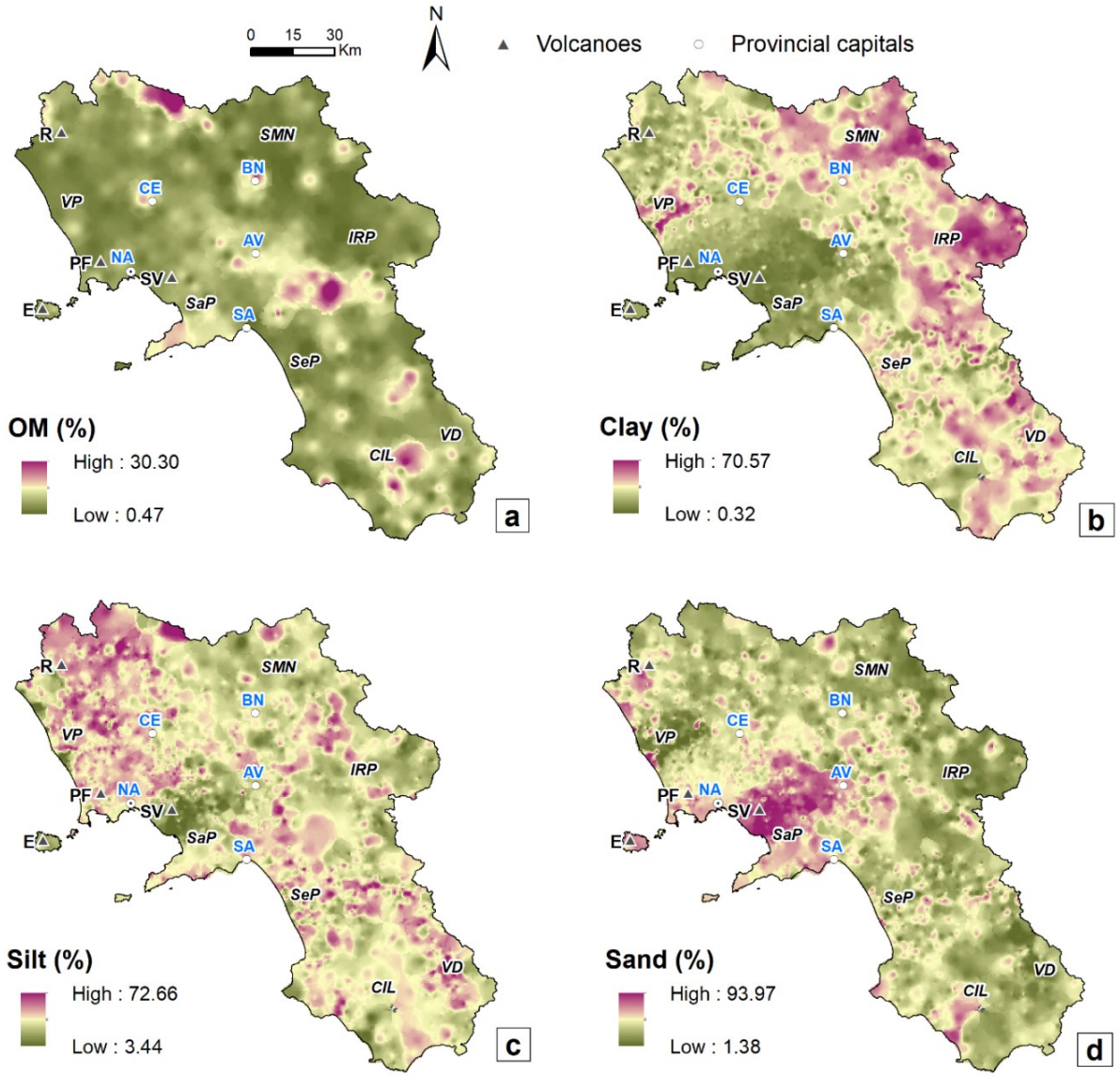

Figure 3.7 Interpolated maps of the distribution of some parameters analysed in the soils of the region: soil organic matter (a), clay fraction (b), silt fraction (c) and sand fraction (d). (Volcanoes: R=Roccamonfina; PF=Phlegrean Fields; SV=Somma-Vesuvius; E=Epomeo. River plains: VP=Volturno; SaP=Sarno; SeP=Sele. Areas: SMN=Samnium; IRP=Irpinia; CIL=Cilento; VD=Vallo di Diano (in black). Provincial capitals: NA=Napoli; CE=Caserta; AV=Avellino; BN=Benevento; SA=Salerno (in blue)).

Referring to Cu_{AR}, it is noteworthy that about 8 % of the regional territory overcomes the national guideline values (200 mg/kg) established for agricultural use of soil (D.M. 46/2019). More in detail, concentrations exceed guidelines in correspondence with the slopes of Mt. Somma-Vesuvius and the surrounding plain, partly the Phlegrean Fields and some areas within the Sarno river catchment basin (Fig. 3.8a) all characterized by a huge presence of vineyards which are commonly associated with the use of copper-based fungicides (Fig. 3.1b).

The bioavailable Cu concentrations (Cu_{AN}) in the analyzed samples vary from a minimum of 0.01 mg/kg to a maximum of 10.95 mg/kg (Table 3.1). Observing the map of the interpolated distribution (Fig. 3.5e), one can easily note that the highest Cu_{AN} (> 0.26 mg/kg) roughly follows the spatial

pattern of the highest concentration intervals determined for Cu_{AR}. Though the percentage bioavailability is quite low (the median is equal to 0.22 %) (Table 3.1), the similarity existing among the distribution patterns of both Cu_{AR} and Cu_{AN} suggests that a significant correlation between the two variables can be inferred.

As a matter of the fact, the overall multiple regression model (Table 3.2) was found to be statistically significant (p-value < 2.2e-16) and it explains more than 70% of the variability of Cu_{AN} (R^2 = 0.7146); more specifically, Cu_{AR} significantly predicts the response variable Cu_{AN} (β = 5.192e-03, p-value < 2.2e-16), as also can be seen from the individual R^2 (0.710) reported in table 1, but, in addition, also SN (β = 5.243e-03, p-value = 1.3e-15) exerts a role on the explanation of its changes. While observing the spatial distribution of Cu_{AN} (Fig. 3.5e) and SN (Fig. 3.7b) it can be seen that in correspondence with the central-western part of the region (Vesuvian area and its surroundings) the highest values of both variables overlap.

As a matter of fact, also the percent bioavailability of Cu, despite it is generally low across the whole region, show relatively more marked values (up to 6.54%) in correspondence with the Vesuvian and Phlegrean territories (Fig. 3.6e) where soils are featured by a more sandy texture (Fig. 3.7d); this latter condition, also highlighted by the multiple regression model, suggests to relate the higher extractability of the metal to the low binding strength of the coarser fractions of the soils (Rieuwerts et al., 1998) and, possibly, to the agricultural use of cupric fungicides in the care of orchards (which includes vineyards) and horticultural which are widely spread across the southern sector of the Campania plain (Fig. 3.1b).

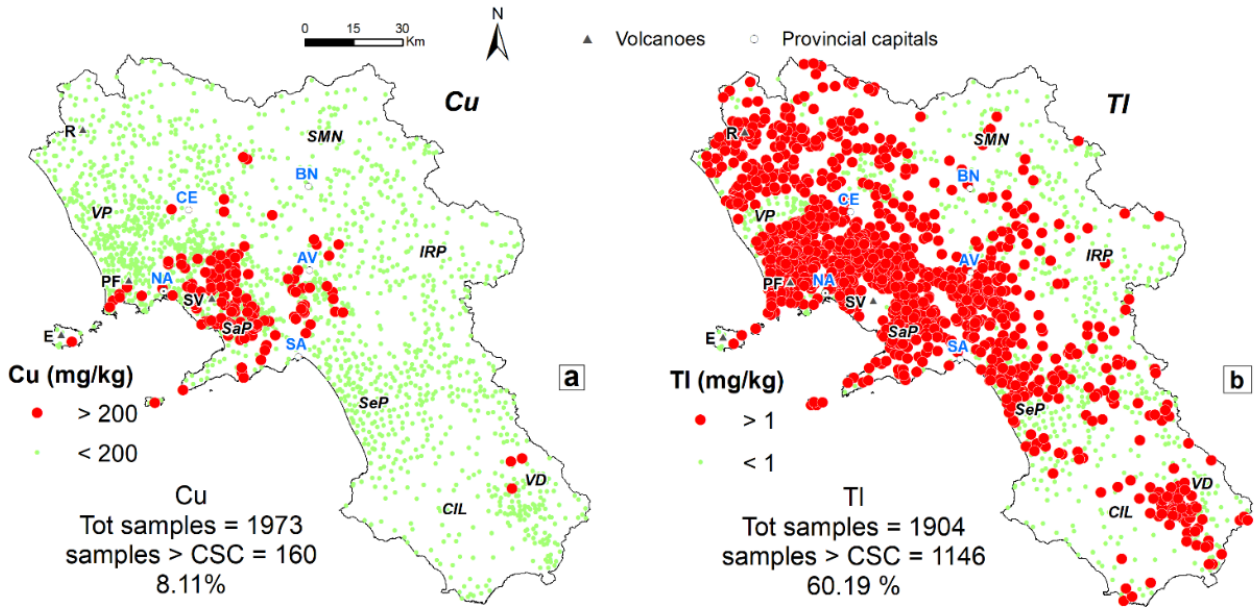

Figure 3.8 Potential hazard maps of Cu (a) and Tl (b). (Volcanoes: R=Roccamonfina; PF=Phlegrean Fields; SV=Somma-Vesuvius; E=Epomeo. River plains: VP=Volturno; SaP=Sarno; SeP=Sele. Areas: SMN=Samnium; IRP=Irpinia; CIL=Cilento; VD=Vallo di Diano (in black). Provincial capitals: NA=Napoli; CE=Caserta; AV=Avellino; BN=Benevento; SA=Salerno (in blue)).

3.4.6 Thallium

Thallium (Tl) is an element with chalcophilic and lithophilic properties. The minerals of igneous and magmatic rocks that have the highest Tl contents are plagioclase, K-feldspar, micas such as phlogopite, biotite, and muscovite (De Vos and Tarvainen, 2006).

The pseudo-total concentrations of Tl (Tl_{AR}) range from 0.08 to 4.93 mg/kg (Table 3.1). The areas with the highest values (from 1.45 to 4.93 mg / kg) (Fig. 3.3f) roughly correspond with the regional soils developed on the pyroclastic covers of the carbonate relieves in the central and northern sectors of the region, respectively, and on lavas and volcano-sedimentary deposits located in the surroundings of both Mt. Somma-Vesuvius and Mt. Roccamonfina (Fig. 3.1a).

Soils belonging to the inner and the southern parts of the regions, respectively, show the lowest Tl_{AR} values (< 1.45 mg/kg); low Tl_{AR} concentrations features the Phlegrean Fields, as well.

More than 60% of the collected samples (namely 1146 over a total of 1904 considered in the framework of this study) overcome the national guideline values (1 mg/kg) established for soil destined to an agricultural use (D.M. 46/2019) (Fig. 3.8b). The samples overcoming the reference values are mostly located in correspondence with areas characterized by the presence of rocks and loose materials of volcanic origin related with Mt. Roccamonfina and Mt. Somma-Vesuvius; the latter condition suggests that for these concentrations an anthropogenic origin cannot be inferred but rather there is good evidence that the elemental enrichment could depend on the compositional nature of the substrate (Calderoli et al., 1983).

The bioavailable concentrations of Tl (Tl_{AN}) vary from 0.001 mg/kg to a maximum of 0.93 mg/kg (Table 3.1). The highest Tl_{AN} concentrations (from 0.023 to 0.93 mg/kg) mark the carbonate missives covered by volcanic soils, the Mt. Roccamonfina domain and the Phelegrean Fields, although this latters showed a low pseudo-total content of the element (Fig. 3.3f). Medium to low values (from 0.001 to 0.023 mg/kg) of bioavailable concentrations characterize the alluvial plain of Volturno River, the volcanic area of Mt. Somma-Vesuvius (for which Tl_{AR} concentrations are missing) and the rest of the regional territory mostly covered by soils developed on siliciclastic materials.

The fitted equation of the multiple linear regression model for Tl (Table 3.2) was found to be statistically significant (p-value < 2.2e-16) although it is representative of a limited amount of the overall variability ($R^2 = 0.3576$). It was found that Tl_{AR}, as an independent variable, significantly can predict the variations of Tl_{AN} ($\beta = 6.68643e-02$, p-value < 2e-16). In addition, SL ($\beta = 1.7554e-03$, p-value < 2e-16) and CL ($\beta = 2.122e-04$, p-value = 0.11) resulted to be predictors of Tl_{AN}, as well, although CL shows a minor evidence of his predictive capability.

The median percent bioavailability of Tl is equal to 2.69 % (Table 3.1) which is well below the maximum that reaches about the 37 %. The percent bioavailability distribution map (Fig. 3.6f) of Tl shows a spatial pattern of values variations like those of the Tl_{AR} and Tl_{AN} maps (Figs. 3.2f and 3.3f); in facts, the areas reaching the highest values of percent bioavailability roughly corresponding to the distributions of the pyroclastic covers (Fig. 3.1a). A moderately extended area intensely dedicated to horticulture and orchard, between the Volturno plain and the volcanic area of the Phlegrean Fields, is characterized by high values of percent bioavailability, as well.

Table 3.3 Summary statistic of the pseudo-total and the bioavailable concentrations of PTEs in the topsoils of Campania region. We reported also the threshold limits (CSC) fixed by the D.Lgs. 152/2006 for residential (colA) and industrial (colB) land use and by the D.M. 46/2019 for agricultural (agr) land use.

Element	As	Be	Cd	Co	Cu	Hg	Ni	Pb	Sb	Se	Sn	Tl	V	Zn
Unit	mg/kg	mg/kg	mg/kg	mg/kg	mg/kg	µg/kg	mg/kg	mg/kg	mg/kg	mg/kg	mg/kg	mg/kg	mg/kg	mg/kg
Aqua Regia														
DL	0.1	0.1	0.01	0.1	0.01	5	0.1	0.01	0.02	0.1	0.1	0.02	2	0.1
N. of samples	1973	1783	1958	1973	1973	1897	1973	1973	1910	1897	1783	1904	1973	1973
Min	0.8	0.2	0.01	1.0	2.51	2.5	0.4	3.40	0.06	0.1	0.2	0.08	7	3.9
Max	117.6	17.9	6.62	88.0	1873.0	2738	155.6	1035.5	21	1.8	100	4.93	234	947.5
Mean	12.4	4.6	0.45	13.0	88.63	65.3	23.0	49.53	0.65	0.4	3.5	1.33	70	94.7
Median	11.7	4.6	0.30	12.5	49.58	39.0	18.0	43.49	0.47	0.4	2.7	1.34	67	83.9
St.Dev	8.3	2.5	0.51	5.9	135.8	125.7	14.7	45.94	0.96	0.3	5.0	0.80	29	56.6
Ammonium Nitrate														
DL	0.025	0.005	0.005	0.005	0.01	5	0.025	0.02	0.005	0.05	0.005	0.001	0.05	0.025
N. of samples	1993	1993	1993	1993	1973	1993	1993	1993	1993	1993	1993	1904	1993	1993
N. samples < DL	1882	1693	1662	1083	0	1992	739	1593	1697	1985	1989	0	1849	942
% samples < DL	94.4	84.9	83.4	54.3	0.0	99.9	37.1	79.9	85.1	99.6	99.8	0.0	92.8	47.3
Min	0.013	0.0025	0.0025	0.0025	0.010	2.5	0.013	0.01	0.003	0.025	0.003	0.001	0.025	0.013
Max	0.194	0.322	0.172	1.483	10.95	8	1.174	2.45	0.104	0.12	0.068	0.93	0.36	18.22
Mean	0.015	0.005	0.004	0.009	0.398	2.5	0.048	0.02	0.004	0.03	0.003	0.068	0.03	0.229
Median	0.013	0.003	0.003	0.003	0.11	2.5	0.035	0.01	0.003	0.03	0.003	0.036	0.03	0.029
St.Dev	0.009	0.015	0.007	0.038	0.885	0.1	0.057	0.06	0.006	0.00	0.002	0.091	0.02	0.928
Median %Bio	0.11	0.05	0.83	0.02	0.22	6.41	0.19	0.02	0.53	6.25	0.09	2.69	0.04	0.03
CSC colA	20	2	2	20	120	1000	120	100	10	3	1	1	90	150
CSC colB	50	10	15	250	600	5000	500	1000	30	15	350	10	250	1500
CSC agr	30	7	5	30	200	1000	120	100	10	3	-	1	90	300

3.4.7 Other PTEs

In addition to Cu and Tl, for the other PTEs (i.e., As, Be, Cd, Co, Hg, Ni, Pb, Sb, Se, Sn, V, Zn), their distribution reflects both a geogenic and anthropogenic source. A geogenic source control is found, e.g., for the suites Zn-Co-Ni, Be-As, and V: the suite Zn-Co-Ni is due to the presence of Mn and Fe oxides and hydroxides which determine the Zn, Co and Ni co-precipitation, immobilizing them in the soils, whereas the suites Be-As (together with Sn-Tl as well) and V are strictly related to

soils formed on alkaline volcanic rocks (Roccamonfina, Vesuvius, Campi Flegrei and Ignimbrites). For Zn, Hg, Sb, and Pb an anthropogenic source is evident, considering that the distribution of their high values is found mostly in urbanized areas (i.e., Napoli, Caserta, Benevento, Salerno).

3.5 Conclusions

Referring to the considered elements, we have observed how the soils of the Campania region behave in a varied way in terms of bioavailability; elements show both different levels of dispersion and a spatial variability that seems to be only partially dependent on the compositional characteristics of source geology.

As a matter of fact, in this study, we selected as predictive variables of the bioavailable fraction the grain size, and the organic matter content of soils together with the pseudo-total concentration of elements.

The pseudo-total concentrations of Al, Ca, K, and Mg resulted to be poorly able to predict the variability of the bioavailable fraction whereas Tl and, above all, Cu resulted to be more capable to forecast the patterns of the bioavailable concentrations based on Aqua Regia. Furthermore, the addition of the grain size distribution and organic matter content to regression models was able to substantially expand their predictive capability only for Ca, K, and Mg whereas it gave a very marginally contribution to the explanation of the bioavailability of Al, Cu, and Tl suggesting that other variables (not considered here) probably exert a major influence on their mobility.

In general, for soils of the Campania region the bioavailable concentrations of elements showed a sensible reduction if compared with the results obtained by applying the Aqua Regia leaching to the same samples; the median value of the percent bioavailability, which is a measure of the extractability of elements from the media, follows the order Ca>K>>Mg≃Tl>>Cu>>Al which seems to be a positive finding in terms of both agricultural productivity and environmental quality.

In fact, as regards Tl and Cu, and in general all the PTEs, the results obtained suggest that probably the use of total or pseudo-total concentrations when dealing with the assessment of risks deriving from consumption of agricultural products, should be considered of limited significance since, as stated above, it was demonstrated that a few variables related with physical-chemical characteristics of soils could influence the real amount of an element which is finally transferred from soil to plants. Being evident that, as already widely stated in scientific literature, more factors (with their influence changing according to the chemical element and the reference environment) could affect the transfer process, further researches will be conducted to include in the predictive models more phisical-chemical variables such as soil pH, redox potential, content in Iron and manganese oxides, etc.

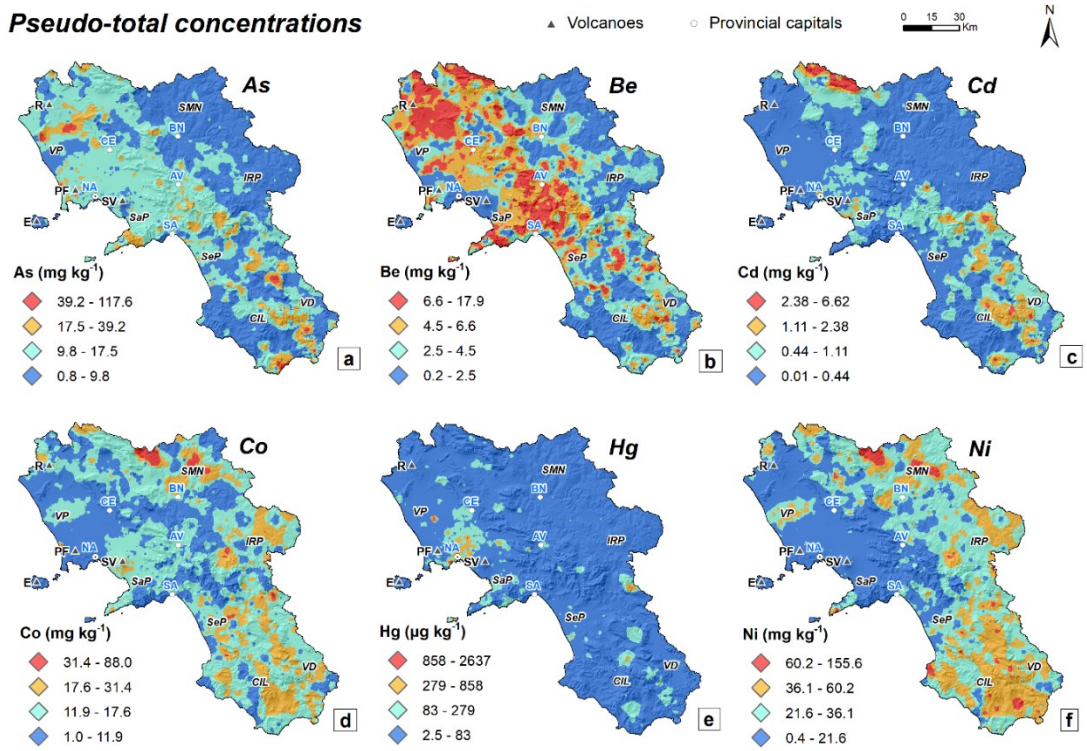

Figure 3.9 Interpolated maps of the distribution of the pseudo-total concentrations of As (a), Be (b), Cd (c), Co (d), Hg (e) and Ni (f). (Volcanoes: R=Roccamonfina; PF=Phlegrean Fields; SV=Somma-Vesuvius; E=Epomeo. River plains: VP=Volturno; SaP=Sarno; SeP=Sele. Areas: SMN=Samnium; IRP=Irpinia; CIL=Cilento; VD=Vallo di Diano (in black). Provincial capitals: NA=Napoli; CE=Caserta; AV=Avellino; BN=Benevento; SA=Salerno (in blue)).

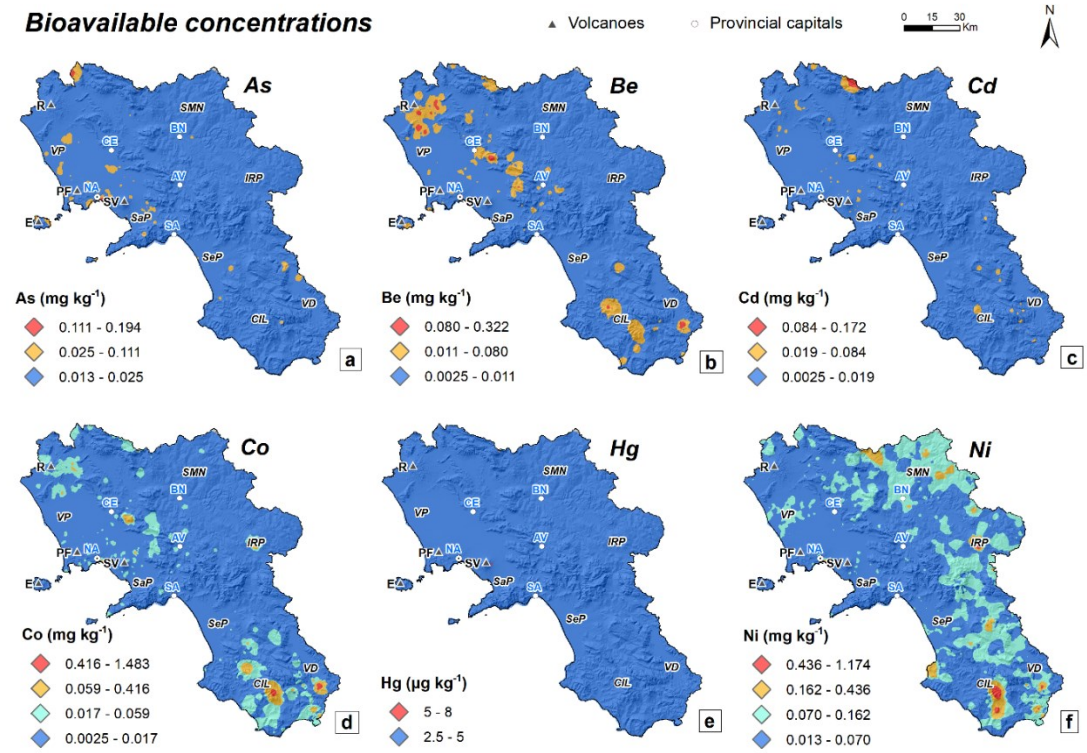

Figure 3.10 Interpolated maps of the distribution of the bioavailable concentrations of As (a), Be (b), Cd (c), Co (d), Hg (e) and Ni (f). (Volcanoes: R=Roccamonfina; PF=Phlegrean Fields; SV=Somma-Vesuvius; E=Epomeo. River plains: VP=Volturno; SaP=Sarno; SeP=Sele. Areas: SMN=Samnium; IRP=Irpinia; CIL=Cilento; VD=Vallo di Diano (in black). Provincial capitals: NA=Napoli; CE=Caserta; AV=Avellino; BN=Benevento; SA=Salerno (in blue)).

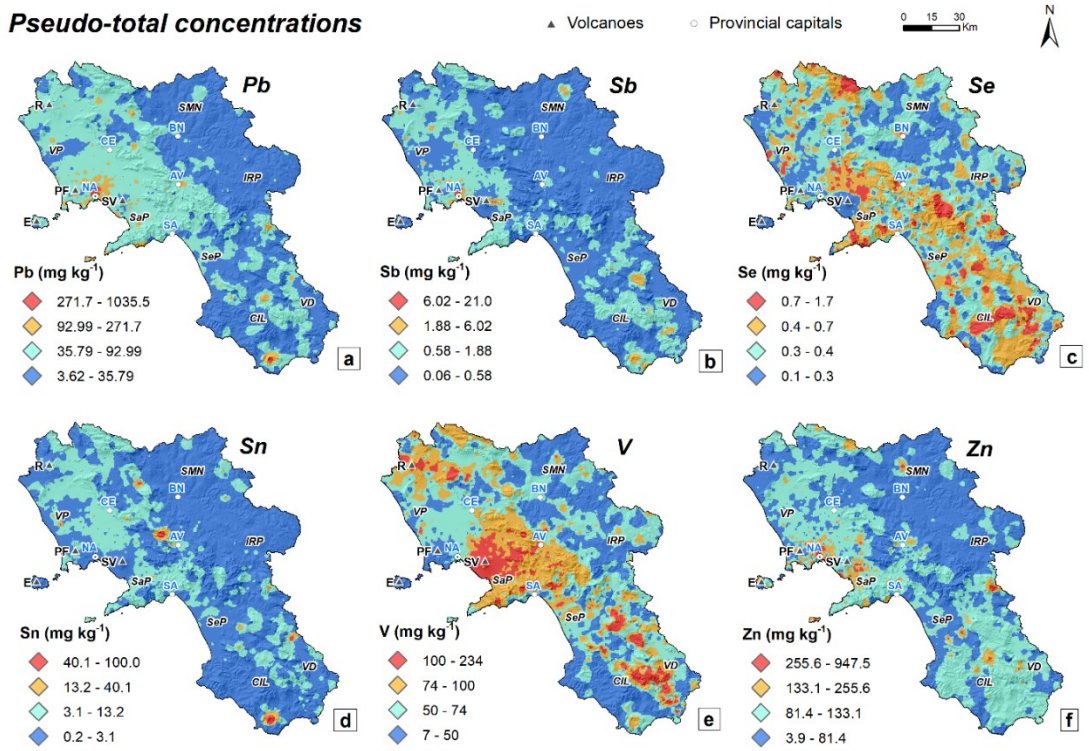

Figure 3.11 Interpolated maps of the distribution of the pseudo-total concentrations of Pb (a), Sb (b), Se (c), Sn (d), V (e) and Zn (f). (Volcanoes: R=Roccamonfina; PF=Phlegrean Fields; SV=Somma-Vesuvius; E=Epomeo. River plains: VP=Volturno; SaP=Sarno; SeP=Sele. Areas: SMN=Samnium; IRP=Irpinia; CIL=Cilento; VD=Vallo di Diano (in black). Provincial capitals: NA=Napoli; CE=Caserta; AV=Avellino; BN=Benevento; SA=Salerno (in blue)).

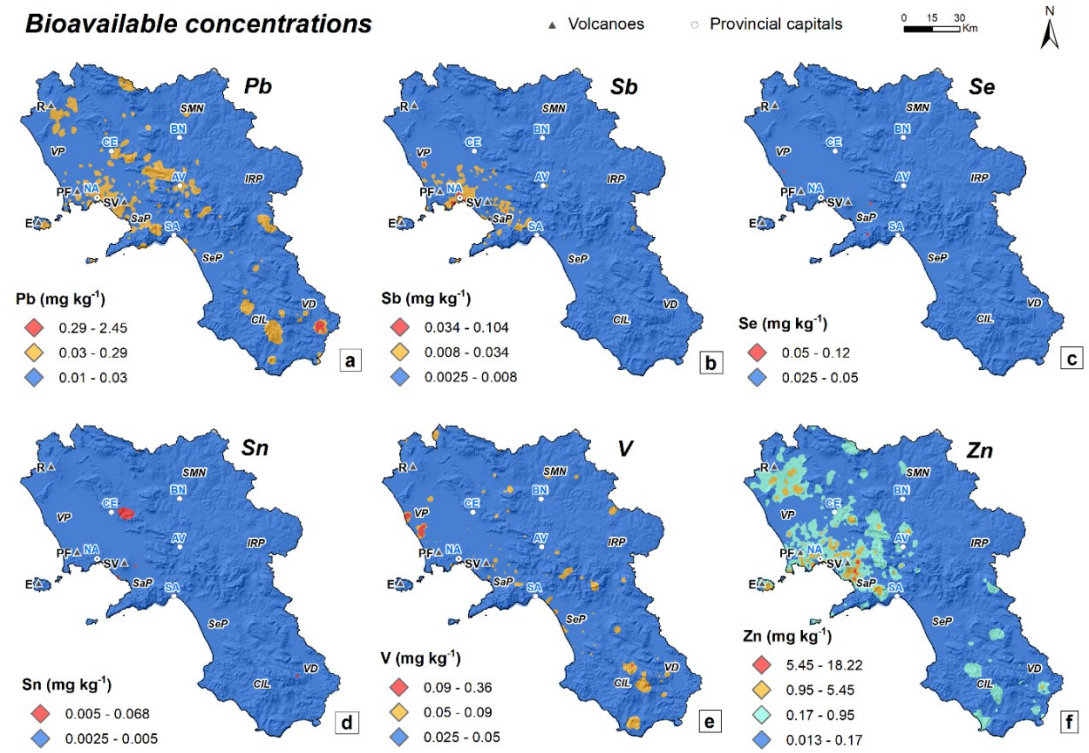

Figure 3.12 Interpolated maps of the distribution of the bioavailable concentrations of Pb (a), Sb (b), Se (c), Sn (d), V (e) and Zn (f). (Volcanoes: R=Roccamonfina; PF=Phlegrean Fields; SV=Somma-Vesuvius; E=Epomeo. River plains: VP=Volturno; SaP=Sarno; SeP=Sele. Areas: SMN=Samnium; IRP=Irpinia; CIL=Cilento; VD=Vallo di Diano (in black). Provincial capitals: NA=Napoli; CE=Caserta; AV=Avellino; BN=Benevento; SA=Salerno (in blue)).

References

Albanese, S., 2008. Evaluation of the bioavailability of potentially harmful elements in urban soils through ammonium acetate–EDTA extraction: a case study in southern Italy. Geochem.: Explor. Environ. Anal. 8, 49-57.

Albanese S., De Vivo B., Lima A., Cicchella D., 2007. Geochemical background and baseline values of toxic elements in stream sediments of Campania region (Italy). J. Geochem. Explor. 93(1), 21–34.

Box, G.E.P., Cox, D.R., 1964. An Analysis of Transformations. J R Stat Soc Series B Stat Methodol 26(2), 211-252

Buccianti, A., Lima, A., Albanese, S., Cannatelli, C., Esposito, R., De Vivo, B., 2015. Exploring topsoil geochemistry from the CoDA (Compositional Data Analysis) perspective: the multi-element data archive of the Campania Region (Southern Italy). J. Geochem. Explor. 159, 302–316.

Calderoni, G., Giannetti, B., Masi, U., 1983. Abundance and behavior of thallium in the K-alkaline rocks from the Roccamonfina Volcano (Campania, southern Italy). Chem. Geol. 38(3-4), 239–253. https://doi.org/10.1016/0009-2541(83)90057-8

Cheng, Q., 1999. Spatial and scaling modelling for geochemical anomaly separation. J. Geochem. Explor. 65, 175–194.

Cheng, Q., Agterberg, F.P., Ballantyne, S.B., 1994. The separation of geochemical anomalies from background by fractal methods. J. Geochem. Explor. 51(2), 109-130.

De Vivo, B., Cicchella, D., Lima, A., Fortelli, A., Guarino, A., Zuzolo, D., Esposito, M., Cerino, P., Pizzolante, A., Albanese S., 2021. Monitoraggio Geochimico-Ambientale dei suoli della Regione Campania – Volume 1 (Elementi Potenzialmente Tossici e loro Biodisponibilità; Elementi Maggiori e in Traccia; distribuzione in suoli superficiali e profondi). Aracne Editrice, pp 586. ISBN: 978-88-255-4036-9.

De Vivo, B., Lima, A., Albanese, S., Cicchella, D., Rezza, C., Civitillo, D., Minolfi, G., Zuzolo D., 2016. Atlante geochimico-ambientale dei suoli della Campania. Aracne Editrice, Roma, pp. 364.

De Vivo, B., Petrosino, P., Lima, A., Rolandi, Belkin, H.E., 2010. Research progress in volcanology in Neapolitan area, southern Italy: a review and alternative views. Mineral. Petrol. 99, 1–28.

De Vos, W., Tarvainen, T., 2006. Geochemical atlas of Europe. Part 2, Geochemistry of elements. Geological Survey of Finland Otamedia Oy Espoo.

Dean, J.R., 2010. Heavy metal bioavailability and bioaccessibility in soil. Methods Mol Biol. 599, 15-36.

Dempster, A.P., Laird, N.M., Rubin, D.B., 1977. Maximum likelihood from incomplete data via the EM algorithm (with discussion). J R Stat Soc Series B Stat Methodol 39, 1–38.

di Gennaro, A., Aronne, G., De Mascellis, R., Vingiani, S., Sarnataro, M., Abalsamo, P., Cona, F., Vitelli, L., Arpaia, G., 2002. I sistemi di terre della Campania. Monografia e carta 1:250.000, con legenda. SELCA, Firenze, pp 63.

Draper, N.R., Smith, H., 1998. Applied Regression Analysis. John Wiley & Sons, Inc., New York, 3 rd edition, 706 pp.

Guagliardi, I., Zuzolo, D., Albanese, S., Lima, A., Cerino, P., Pizzolante, A., Thiombane, M., De Vivo, B., Cicchella, D., 2020. Uranium, thorium and potassium insights on Campania region (Italy) soils: Sources patterns based on compositional data analysis and fractal model. J. Geochem. Explor. 212, 106508. https://doi.org/10.1016/j.gexplo.2020.106508

Guarino, A., Lima, A., Cicchella, D., Albanese, S., 2022. Radon flux estimates, from both gamma radiation and geochemical data, to determine sources, migration pathways, and related health risk: The Campania region (Italy) case study. Chemosphere 287(1), 132233. https://doi.org/10.1016/j.chemosphere.2021.132233

Gee, G.W., Or, D., 2002. Particle-size analysis. In: Dane, J.H., Topp, G.C., Eds., Methods of Soil Analysis, Part 4, Physical Methods. SSSA, Book Series 5, Madison, USA, pp. 255-293.

Gryschko, R., Kuhnle, R., Terytze, K., Breuer, J., Stahr, K., 2005. Soil extraction of readily soluble heavy metals and As with 1 M NH4NO3-solution evaluation of DIN 19730. J. Soils Sediments 5, 101–106.

Hocking, R.R., 1976. The analysis and selection of variables in linear regression. Biometrics 32, 1-49.

Horn, E.E., 1934. The effect of thallium on plant growth. Circular N.409, United States Department of Agriculture.

ISO 19730:2008, Soil quality - Extraction of trace elements from soil using ammonium nitrate solution.

Kim, R-Y., Yoon, J-K., Kim, T-S., Yang, J. E., Owens, G., Kim, K-R., 2015. Bioavailability of heavy metals in soils: definitions and practical implementation—a critical review. Environ. Geochem. Health, 37, 1041–1061. https://doi.org/10.1007/s10653-015-9695-y

Minolfi, G., Albanese, S., Lima, A., Tarvainen, T., Fortelli, A., De Vivo, B., 2018. A regional approach to the environmental risk assessment - human health risk assessment case study in the Campania region. J. Geochem. Explor. 184(B), 400-416.

Migaszewski, Z. M., Gałuszka A., 2021. Abundance and fate of thallium and its stable isotopes in the environment. Reviews in Environmental Science and Bio/Technology, 20, 5–30. https://doi.org/10.1007/s11157-020-09564-8

Naidu, R., Semple, K.T., Megharaj, M., Juhasz, A.L., Bolan, N.S., Gupta, S.K., Clothier, B.E., Schulin, R., 2008. Bioavailability: definition, assessment and implications for risk assessment. In Hartemink, A.E., McBratney, A.B., Naidu, R. (Eds.), Chemical Bioavailability in Terrestrial Environment. 32 ed. Vol. 32. London: Elsevier. p. 39-51. (Developments in Soil Science).

Nasta, P., Palladino, M., Sica, B., Pizzolante, A., Trifuoggi, M., Toscanesi, M., Giarra, A., D'Auria, J., Nicodemo, F., Mazzitelli, C., Lazzaro, U., Di Fiore, P., Romano, N., 2020. Evaluating pedotransfer functions for predicting soil bulk density using hierarchical mapping information in Campania, Italy. Geoderma Reg. 21, e00267.

NRC, 2002. Bioavailability of contaminants in soils and sediments: processes, tools and applications. National Research Council (NRC). National Academies: Washington, DC.

Peccerillo, A., 2005. Plio-quaternary Volcanism in Italy. Petrology, Geochemistry, Geodynamics. Springer-Verlag, Berlin Heidelberg. ISBN 978-3-540-29,092-6

Peccerillo, A., 2020. Campania volcanoes: petrology, geochemistry, and geodynamic significance. In: De Vivo, B., Belkin, H.E., Rolandi, G., Edts, Vesuvius, Campi Flegrei, and Campanian volcanism, Elsevier, p. 79-120. ISBN 9780-12-816454-9.

Petrik, A., Albanese, S., Lima, A., De Vivo, B., 2018a. The spatial pattern of beryllium and its possible origin using compositional data analysis on a high-density topsoil data set from the Campania Region (Italy). Appl. Geochem. 91, 162-173.

Petrik, A., Thiombane, M., Albanese, S., Lima, A., De Vivo, B., 2018b. Source patterns of Zn, Pb, Cr and Ni potentially toxic elements (PTEs) through a compositional discrimination analysis: A case study on the Campanian topsoil data. Geoderma 331, 87-99.

Petrik, A., Albanese, S., Lima, A., Jordan, G., Rolandi, R., Rezza, C., De Vivo, B., 2018c. Spatial pattern recognition of arsenic in topsoil using high-density regional data. Thematic Issue (De Vivo et al., Eds), Geochem.: Explor. Environ. Anal 18, 319-330.

Petrik, A., Albanese, S., Lima, A., Jordan, G., Rolandi, R., De Vivo, B., 2018d. Spatial pattern analysis of Ni and its concentrations in topsoils in the Campania region (Italy). Sp. Issue (De Vivo et al., Eds). J. Geochem. Explor. 195, 130-142.

Petruzzelli, G., Pedron, F., Rosellini, I., 2020. Bioavailability and bioaccessibility in soil: a short review and a case study. *AIMS Environ. Sci.* 7(2), 208-225.

Pierantoni, P.P., Penza, G.,Macchiavelli., C., Schettino, A., Turco, E., 2020. Kinematics of the Tyrrhenian-Apennine system and implications for the origin of the Campanian magmatism. In: De Vivo, B., Belkin, H.E., Rolandi, G., Edts, Vesuvius, Campi Flegrei, and Campanian volcanism, Elsevier, p. 33-56. ISBN 9780-12-816454-9.

Prajapati, K., Modi, H.A., 2012. The importance of potassium in plant growth–a review. Indian Journal of Plant Sciences, 1(02-03), 177-186.

Pribyl, D.W., 2010. A critical review of the conventional SOC to SOM conversion factor. Geoderma 156(3–4), 75–83.

Rader, S. T., Maier, R. M., Barton, M. D., Mazdab, F. K., 2019. Uptake and Fractionation of Thallium by Brassica juncea in a Geogenic Thallium-Amended Substrate. Environ. Sci. Technol. 53(5), 2441-2449. https://doi.org/10.1021/acs.est.8b06222

Reimann, C., Filzmoser, P., Garrett, R., Dutter, R., 2008. Statistical Data Analysis Explained: Applied Environmental Statistics with R. Wiley. ISBN: 978-0-470-98581-6

Rieuwerts, J.S., Thornton, I., Farago, M.E., Ashmore, M.R., 1998. Factors influencing metal bioavailability in soils: preliminary investigations for the development of a critical loads approach for metals. Chemical Speciation and Bioavailability, 10 (2), 61-75. https://doi.org/10.3184/095422998782775835

Rout, G., Samantaray, S., Das, P., 2001. Aluminium toxicity in plants: a review. Agronomie, 21 (1), 3-21. https://doi.org/10.1051/agro:2001105

Ruby, M.V., Davis, A., Schoof, R., Eberle, S., Sellstone, C.M., 1996. Estimation of lead and arsenic bioavailability using a physiologically based extraction test. Environ. Sci. Technol. 30, 422–430.

Ruby, M.V., Schoof, R., Brattin, W., Goldade, M., Post, G., Harnois, M., Mosby, D. E., Casteel, S.W., Berti, W., Carpenter, M., Edwards, D., Cragin, D., Chappell, W. 1999. Advances in evaluating the oral bioavailability of inorganics in soil for use in human health risk assessment. Environ. Sci. Technol. 33, 3697–3705.

Ryu, H., Chung, J.S., Nam, T., Moon, H.S., Nam, K., 2010. Incorporation of heavy metals bioavailability into risk characterization. Clean (Weinh) 38(9), 812–815.

Salminen, R., 1995. Alueellinen geokemiallinen kartoitus suomessa vuosina, 1994. English summary: regional geochemical mapping in Finland in 1982–1994. Report of Investigation, 130. Geological Survey of Finland, Espoo.

Sardans, J., Peñuelas, J., 2021. Potassium Control of Plant Functions: Ecological and Agricultural Implications. Plants, 10, 419. https://doi.org/10.3390/ plants10020419

Steckler, M.S., Agostinetti, N.P., Wilson, C.K., Roselli, P., Seeber, L., Amato, A., Lemer-Lam, A., 2008. Crustal structure in the Southern Apennines from teleseismic receiver functions. Geology 2, 155–158.

Tarvainen, T., Kallio, E., 2002. Baselines of certain bioavailable and total heavy metal concentrations in Finland. Appl. Geochem. 17(8), 975-980.

Thiombane, M., Di Bonito, M., Albanese, S., Zuzolo, D., Lima, A., De Vivo, B. 2019. Geogenic versus anthropogenic behaviour and geochemical footprint of Al, Na, K and P in the Campania region (Southern Italy) soils through compositional data analysis and enrichment factor. Geoderma 335, 12-26.

Thor, K., 2019. Calcium-Nutrient and Messenger. Frontier in Plant Sciences, 10: 440. https://doi.org/10.3389/fpls.2019.00440

Vitale, S., Ciarcia, S., 2018. Tectono-stratigraphic setting of the Campania region (southern Italy). J. Maps 14(2), 9-21. https://doi.org/10.1080/17445647.2018.1424655

Yan, B., Hou, Y., 2018. Effect of Soil Magnesium on Plants: a Review. IOP Conference Series: Earth and Environmental Science, 170(2), 022168. https://doi.org/10.1088/1755-1315/170/2/022168

Yruela, I., 2005. Copper in plants. Brazilian Journal of Plant Physiology, 17, 145-156. https://doi.org/10.1590/S1677-04202005000100012

Zuo, R., Wang, J., 2020. ArcFractal: An ArcGIS Add-In for Processing Geoscience Data Using Fractal/Multifractal Models. Nat. Resour. Res. 29, 3-12.

Zuzolo, D., Cicchella, D., Lima, A., Guagliardi, I., Cerino, P., Pizzolante, A., Thiombane, M. De Vivo, B., Albanese, S., 2020. Potentially toxic elements in soils of Campania region (southern Italy): combining raw and compositional data. J. Geochem. Explor., 213, 10652.

.

CHAPTER 4 – Potentially Toxic Elements (PTEs), Polycyclic Aromatic Hydrocarbons (PAHs) and Organochlorine Pesticides (OCPs) in the soils of the Acerra plain

The results of this activity were published/presented in:

Guarino, A., Aruta, A., Ebrahimi, P., Dominech, S., Lima, A., De Vivo, B., Qi, S., Albanese, S., 2020. Potentially Harmful Elements and Polycyclic Aromatic Hydrocarbons in the soils of Acerra, southern Italy. Conference proceedings, Proscience vol. 7. ISSN: 2283-5954.

Guarino, A., Aruta, A., Ebrahimi, P., Dominech ,S., Lima, A., De Vivo, B., Qi, S., Albanese, S., 2021. Organochlorine pesticides in the soils of the Acerra plain: concentration and distribution of DDT isomers and metabolites. European Geosciences Union General Assembly 2021, Vienna. DOI: 10.5194/egusphere-egu21-5739

Guarino, A., Aruta, A., Ebrahimi, P., Dominech, S., Lima, A., De Vivo, B., Qi, S., Albanese, S., 2020. Potentially Harmful Elements and Polycyclic Aromatic Hydrocarbons in the soils of Acerra, southern Italy. GEOHEALTH 2020 - INTERNATIONAL MEETING OF GEOHEALTH SCIENTISTS, Bari. Scientific Research Abstracts Vol. 10, p. 25. ISSN 2464-9147.

Guarino, A., Aruta, A., Ebrahimi, P., Dominech, S., Albanese, S., 2020. The "Triangle of Death": a case study from Campania region (Italy). Goldschmidt Virtual 2020, Honolulu. DOI: 10.46427/gold2020.897

4.1 Introduction

In recent years, Campania has been the subject of media attention for the alleged degradation of the agricultural territories of an area sadly known as "Land of Fires". In October 2004, the British medical journal The Lancet Oncology published a work by the researchers Senior and Mazza in which the inhabited centers of Marigliano, Nola and Acerra were indicated as vertices of what was called "the triangle of death" where the resident population, heavily exposed to toxic and carcinogenic substances, resulted affected by an incidence rate of tumour pathologies higher than the regional average. The increase in the mortality rate was associated by Senior and Mazza with the presence of many toxic wastes illegally buried in agricultural areas, close to urban centers, that had contaminated the soils and groundwaters for decades.

The purpose of this work has been the evaluation of the geochemical-environmental conditions, trough the determination of the distribution patterns and the analysis of the contamination sources of some PTEs, PAHs and OCPs in topsoil, of the north-eastern sector of the metropolitan city of Naples, which is one of the areas with the highest population density in Italy and represents an area of great socio-economic interest not only for the urban settlements present, but also for the production activities, infrastructures and existing natural resources.

4.1.1 PTEs

The origin of PTEs in an environmental media can depend on both the geo-lithological characteristics of the reference context and the nature of the human activities that insist on it, and the dynamics of the same depend on innumerable factors that range from the chemical reactivity of the elements to the ability of accumulation and transformation of the same by living organisms.

The source of metals (mainly Cu, Pb, Zn, Cd, Hg, Sn, Ni, V and Cr) and metalloids (such as As, Sb and Se) in the urban environment can depend on a wide range of different anthropogenic agents and processes, such as mining, smelting, industrial manufacturing, domestic activities, residential heating, incinerators, power plants, industrial boilers, petrol and diesel vehicles, cigarette smoke and the spreading of fertilizers and anti-cryptogams on the agricultural soils, as well as natural causes (Albanese and Breward, 2011).

The distribution of chemical elements in the environment is a cause for concern because, although many of them are essential for life, some natural elements are potentially harmful to plants and animals in high doses (WHO, 2006). The hazard to environmental or human health that these elements cause depend on many factors, which include: their degree of sorption, chemical form, concentration,

mobility, bioavailability, the properties of the media (such as the acidity of waters or soils, the soil texture and mineral composition), the level of exposure and the dose received (Albanese and Breward, 2011). Once metals and metalloids have entered the food chain, they tend to accumulate in the human body, causing damage to the organs and the nervous and immune systems, and, some of them, they are also carcinogenic and/or teratogenic (Liu et al., 2007).

National governments and international agencies developed, in the years, policies to limit the amount and the impacts of PTEs in the environment. The purpose was also to establish concentration limit thresholds for intervention procedures, and the assessment of the background and bioavailable concentrations values as key concepts for the definition of the related risks. The criteria adopted for the regulations by the various Countries worldwide are not univocal: some set threshold limits based on the land use (e.g., residential, industrial, agricultural, etc.), some based on the soil properties, groundwaters uses, and others (Antoniadis et al., 2019). Also the number and types of PTEs regulated are not homogeneous among the different Countries.

In Italy, the Legislative Decree 152/2006 (D.Lgs. 152/06), also called the "Environmental Code", establishes all environmental regulations and identifies 15 elements, that is As, Be, Cd, Co, Cr, Cu, Hg, Ni, Pb, Sb, Se, Sn, Tl, V and Zn, as PTEs and defines the concentrations guideline values for residential and industrial land use, as well as the guideline values for other elements and compounds in the other natural media. In addition, the Ministerial Decree 46/2019 (D.M. 46/19) defines the guideline values (for PTEs as well other compounds) for the agricultural land use.

4.1.2 PAHs

Polycyclic aromatic hydrocarbons (PAHs) are ubiquitous environmental organic pollutants, formed by two or more benzene rings fused together through pairs of carbon atoms shared, with covalent bond, between adjacent rings. In particular, the name refers to compounds containing only carbon and hydrogen atoms. They can be classified, based on their molecular weight, in low molecular weight (LMW) PAHs (consisting of 2 or 3 rings) and high molecular weight (HMW) PAHs (from 4 to 7 rings).

They are carcinogenic and mutagenic substances, toxic for all organisms, considered the most carcinogenic contaminants present in the environment (ATSDR, 2009). In 1980, the U.S. Environmental Protection Agency (USEPA) included sixteen PAHs in the list of priority pollutants. These include 10 high molecular weight PAHs, i.e. fluoranthene, pyrene, benzo(a)anthracene, chrysene, benzo(b)fluoranthene, benzo(k)fluoranthene, benzo(a)pyrene, indeno(1,2,3-cd)pyrene, dibenzo(a,h)anthracene, benzo(g,h,i)perylene (consisting of 4, 5 or 6 rings), and 6 low molecular

weight PAHs, naphthalene, acenaphthylene, acenaphthene, fluorene, phenanthrene and anthracene (consisting of 2 or 3 rings) (USEPA, 1980).

These substances can derive from natural phenomena, such as volcanic eruptions and the maturation of the organic substance however, particularly in highly urbanized or industrialized regions, most of them have an anthropogenic origin and their formation is mostly associated with incomplete combustion processes of organic matter (pyrolysis).

PAHs are emitted as complex mixtures, containing over a hundred different compounds, and the related molecular concentration ratios are considered characteristic of a given emission source (Manoli et al., 2004). Generally, low molecular weight compounds derive from petrogenic processes, i.e. produced by slow processes at low temperatures, while high molecular weight compounds from pyrogenic processes, formed when the organic matter is in anoxic conditions and subjected to high temperatures.

Due to the high lipophilicity, which increases with the molecular weight, PAHs can be easily adsorbed by plants, and therefore potentially transferred to animals and humans through the food chain and have a great aptitude to bioconcentrate and bioaccumulate in organisms, predominantly in the adipose tissues (Eisler, 2000).

Given the size of molecules, PAHs adsorbed on the atmospheric particulate can easily penetrate the lungs by breathing and be inhaled or even ingested. In mammals, they are rapidly absorbed both from the gastro-intestinal tract and from the pulmonary epithelium and thus distributed in various tissues, including fetal ones, and especially the adipose tissues, as they are lipophilic, and are widely metabolized by different tissues and organs (lung, skin, esophagus, colon, liver, placenta, etc.).

Because of its toxicity, benzo(a)pyrene is the most studied and most frequently determined compound in the various media, both environmental and food, and is often used as an indicator of the class of PAHs as regards both the levels of contamination and the carcinogenic risk.

4.1.3 OCPs

Organic chlorides are a vast category of chlorinated aromatic hydrocarbons, that is, molecules consisting of organic structures containing at least one aromatic ring and one covalently bonded chlorine atom. Organochlorine pesticides (OCPs) are a group of synthetic molecules widely used for decades mainly in the agricultural field as insecticides and fungicides (Sparling, 2016b) and, subordinately, in the medical field (Schaefer et al., 2015).

There are different types of OCPs, grouped into families based on their structural characteristics, which can have different origins and paths in the environment. Some compounds have stereoisomers,

i.e. molecules having the same brute formula but different spatial orientation of the atoms, which can differ significantly in their chemical and biological properties (ISPRA, 2015).

The best-known compound is certainly the dichloro-diphenyl-trichloroethane (DDT), synthesized since 1873 but used as an insecticide and pesticide since the 1940s. DDT has been and still is used to combat malaria in some sensitive areas such as Africa, India and South America. Its use in Italy has been banned since 1978.

Most OCPs are hydrophobic and lipophilic, i.e., slightly soluble in water and easily soluble in oils and fats. Compared to other synthetic organic pesticides on the market, OCPs show greater environmental persistence and are generally characterized by a marked tendency towards bioaccumulation and biomagnification along the food chain due to their lipophilic character. Some types of OCPs, such as dichloro-diphenyl-trichloroethane (DDT), hexachlorobenzene (HCB), dieldrin, hexachlorocyclohexane (HCH α and β) and lindane (HCH γ), are currently banned from the market due to the attitude they have to accumulate in the chain food and their non-selective toxicity towards different living species including mammals, without excluding humans. The main toxic action of these substances towards insects concerns the nervous system, both central and peripheral: they act on the sodium channels along the neuronal axons causing the interruption of the functions related to the control of the muscles, including those used for breathing, leading to death by asphyxiation (Sparling, 2016a).

Soil is the environmental media that contains the highest concentrations of OCP, while in water and in the atmosphere (in which they are released following volatilization from the soil) these compounds are generally present in lower concentrations.

Since 2001, following the Stockholm Convention, whose main objectives are the elimination or decrease of use of some harmful substances, determined OCPs, specifically aldrin, chlordane, DDT, HCB, HCH (α, β and γ), dieldrin, endrin, heptachlor, endosulfan (α and β), endosulfan sulfate and mirex, have been included among the substances defined as Persistent Organic Pollutants (POPs).

The International Agency for Research on Cancer (IARC) in 2015 has classified DDT and its derivatives DDD and DDE (dichloro-diphenyl-dichloroethane and dichloro-diphenyl-dichloroethylene, respectively) as probably carcinogenic substances for humans (class 2A), also responsible for damage to the liver, reproductive system and nervous system.

4.2 Study area

The study area, corresponding to the Acerra-Marigliano conurbation, is located in the central sector of the Campania Plain, a wide coastal belt roughly extending from the Garigliano River plain,

in the northwest of the region (at the border with the Latium region), to the Sarno River Basin, southward of the volcanic complex of Mt. Somma-Vesuvius. The conurbation covers a total area of about 100 km^2 and includes 6 municipalities (Acerra, Pomigliano D'Arco, Castello di Cisterna, Brusciano, Mariglianella and Marigliano).

Local geology reflects the geological history of the Campania Plain which has been generated by the surface levelling of a huge graben generated during the Pleistocene and filled by volcanic products (De Vivo et al., 2001) and by alluvial deposits, mainly consisting in reworked pyroclastic deposits and weathered carbonatic material proceeding from the surrounding mountains, belonging to the Apennine chain.

According to the underlying geology, in the flat areas, soil developed on pyroclastic deposits is characterized by a coarse texture and a good availability of oxygen; soil developed on alluvial sediments has a medium texture at the surface and they become finer with the depth increase (di Gennaro, 2002).

In the municipal area of Acerra, two hydrogeological systems can be distinguished: a superficial unconfined aquifer and a deeper aquifer (ca. 5 m below ground level), both located in the pyroclastic complexes and confined by the Campanian Ignimbrite (Corniello and Ducci, 2009). The tuffaceous complex shows, in the north-western and south-eastern sectors of the Acerra area, a significant reduction in the thickness and the degree of cementation, so the complex itself does not guarantee the net confinement of the deep aquifer, allowing vertical drainage and creating mixtures between the two water bodies. This condition is also facilitated by the fact that in these areas there are numerous wells without adequate conditioning necessary for the separation between the two aquifers. Due to the interconnections between the aquifers, the state of the groundwater of the area appears to be strongly compromised, both due to diffuse agricultural pollution phenomena and for industrial pollution phenomena.

The total population is about 160,000 and the most populous municipality is Acerra with more than 50,000 inhabitants. The average population density is about 1600 inhabitants/sqkm, if considering the total surface of the conurbation, which could be corrected to 6-7000 inhabitants /sqkm if we consider only the effective extension of the urbanised areas (18-20 km^2).

Non urbanized areas are mostly occupied by agricultural activities (Crops, orchards and vineyard) and, subordinately, by industrial settlements (Fig. 4.1a). Three principal industrial settlements can be distinguished in the area: 1) a branch of the italian automotive industries FIAT, where car models of the Alfa Romeo brand have been mostly assembled since the beginning, which came into activity in the early 70's and nowadays counts about 6000 employees, is present between the town of Acerra and Pomigliano D'Arco; 2) in the middle of the plain north to Acerra, in the ASI consortium, (that

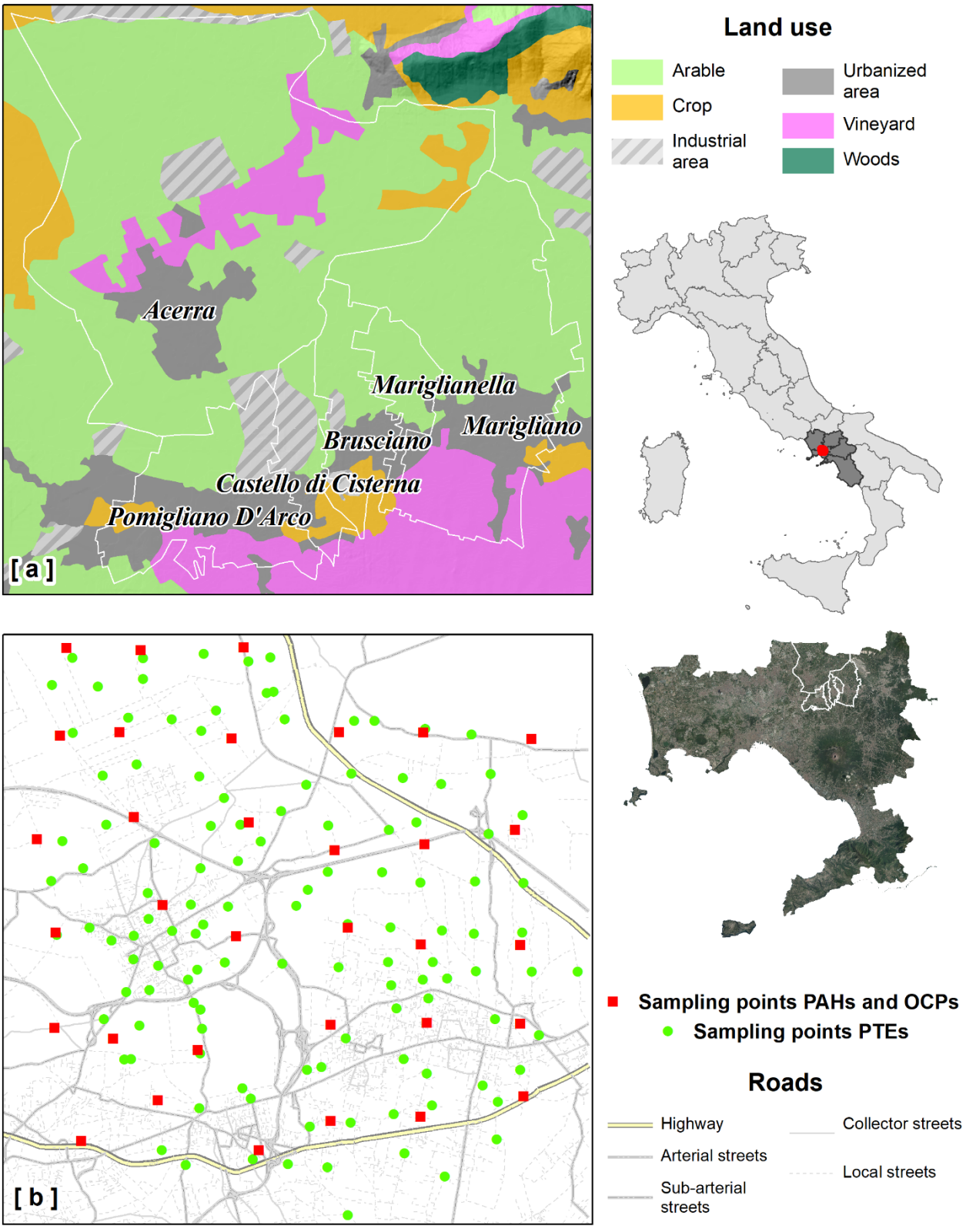

Figure 4.1 Setting of the study area: land use map (a) and location of the sampling points (b).

covers an area of 2.6 km^2), we find the the Montefibre factory, which, since the beginning of 80's, produces polyester fibres and it is accused of being one of the main culprits of pollution of soil and

groundwater in the area, and a thermoelectric power plant, equipped with diesel engines and fuelled with palm oil operating since 2008 with an annual output of about 600.000 MWh; 3) in 2009 an incinerator for urban waste treatment has been inaugurated, close to the ASI-Montefibre area, and started to burn non-differentiated waste, coming from every part of the Napoli metropolitan area, accumulated during the Campania region worldwide notorious waste crises (2004, 2008-2009).

Epidemiological and environmental studies demonstrated that the rate of cancer mortality in the Acerra area (better known as "Triangle of death") (Senior and Mazza, 2004) and, more in general, in the Napoli metropolitan territory (Albanese et al., 2008) are higher than the regional average value. In the "Triangle of death" the higher rate of mortality has been mostly related to the presence of many toxic wastes illegally buried in agricultural areas which have been contaminating soils and groundwaters for decades.

4.3 Soil sampling, sample preparation and analyses

A total of 121 surficial composite soil samples were collected across the study area, at an average sampling density of 3 samples/km^2 in urbanized areas and 1 sample/km^2 in suburban and agricultural/uncultivated areas, to analyse the content in PTEs (Fig. 4.1b). In addition, a total of 33 surficial composite soil samples were collected, during the spring period of 2011, across the study area to be analysed for their PAHs and OCPs content, with an average density of 1 sample/4 km^2(Fig. 4.1b).

The samples were collected following the FOREGS procedures (Salminen et al., 1998). At each sampling location, the composite sample was made up by mixing five soil aliquots collected at the corners and the centre of a 10 x 10 m virtual square. The single aliquots were collected within a depth interval between 0 and 15 cm from the surface by using a scoop and they were enveloped in an aluminium foil and stored in plastic bags, avoiding any contact between the soil sample and the plastic bag itself. Each sampling site was regularly described for spatial coordinates, soil and air temperature, local geology, type and main properties of soils, land use, and any additional detail related to anthropic activities in the surroundings.

In addition, the samples for PAHs and OCPs analysis were kept at a temperature of 4° C by means of a portable cooler during the transport from the collection site to the Environmental Geochemistry Laboratory (LGA) at University of Naples Federico II. The 33 samples boxed together with dry ice pellets (to keep temperature of samples conveniently low) were then sent to the Key Laboratory of Biogeology and Environmental Geology of Ministry of Education at China University of Geosciences in Wuhan for analyses.

4.3.1 PTEs analyses

After being dried by means of infra-red lamps at a controlled temperature below 35 °C, to avoid Hg volatilization, the samples were sieved to retain the 100 mesh (~150 μm) fraction. The obtained pulps were stored in small plastic bags containing at least 30 g of samples, and then sent to the ACME Analytical Laboratories Ltd (now Bureau Veritas) (Vancouver, Canada), accredited under ISO 9002, to be analyzed for the concentrations of 53 elements (Ag, Al, As, Au, B, Ba, Be, Bi, Ca, Cd, Ce, Co, Cr, Cs, Cu, Fe, Ga, Ge, Hf, Hg, In, K, La, Li, Mg, Mn,Mo, Na, Nb, Ni, P, Pb, Pd, Pt, Rb, Re, S, Sb, Sc, Se, Sn, Sr, Ta, Te, Th, Ti, Tl, U, V,W, Y, Zn, and Zr).

Each sample was digested in 90 ml of aqua regia and leached for 1 h in a hot (95 C°) water bath. After cooling, the solution was made up to a final volume of 300 ml with 5 % HCl. The sample weight to solution volume ratio is 1 g per 20 ml. The solutions were analyzed combining a Spectro Ciros Vision emission spectrometer for ICP-AES (inductively coupled plasma atomic emission) and a Perkin Elmer Elan 6,000/9,000 for ICP-MS (inductively coupled plasma mass spectrometry).

The quality of all data was assessed by estimations of accuracy and precision which resulted to be always in the range of 10–15%.

4.3.2 PAHs analyses

At the Key Laboratory of Biogeology and Environmental Geology, 10 g of homogenized and freeze-dried soils from each sample were spiked with 1000 ng (5μl of 200 mg l-1) of recovery surrogates (naphthalene-D8; acenaphthene-D10; phenanthrene-D10; chrysene-D12 and perylene-D12) and were Soxhlet-extracted (4-6 cycles/h) with dichloromethane for 24 h. Elemental sulfur was removed by adding activated copper granules to the collection flasks.

The sample extract was concentrated and solvent-exchanged to hexane and further reduced to 2-3 ml by a rotary evaporator (Heidolph 4000). A 1:2 (v/v) alumina/silica gel column (both 3% deactivated with H2O) was used to clean up the extract and PAHs were eluted with 30 ml of dichloromethane/hexane (3:7). The eluate was then concentrated to 0.2 ml under a gentle nitrogen stream and 1000 ng (5 μl of 200 mg l-1) of hexamethylbenzene were added as an internal standard prior to gas chromatography- mass spectrometry (GC- MS) analysis.

A HP6890N gas chromatograph equipped with a mass selective detector (5975MSD) operating in the electron impact mode (EI mode, 70 eV) and a DB-5MS (30.0 m×250 mm×0.25 mm film thickness) capillary column were used for detecting the concentrations of fluoranthene, pyrene, benzo(a)anthracene, chrysene, benzo(b)fluoranthene, benzo(k)fluoranthene, benzo(a)pyrene,

indeno(1,2,3-cd)pyrene, dibenzo(a,h)anthracene, benzo(g,h,i)perylene, naphthalene, acenaphthylene, acenaphthene, fluorene, phenanthrene and anthracene in collected soils. The chromatographic conditions were as follows: injector and detector temperatures were of 270 °C and 280 °C, respectively; oven temperature program started at 60 °C for 5 min and increased to 290 °C at a rate of 3 °C min−1 and then was kept at 290 °C for 40 min. The carrier gas was highly pure helium at a constant flow rate of 1.5 ml min^{-1}. The mass spectrometer operated in the selected ion monitoring (SIM) mode and was tuned with perfluorotributylamine (PFTBA) according to the manufacturer criteria. Mass range between 50 and 500 m/z was used for quantitative determinations. Data acquisition and processing were made by a HP Chemstation data system. Chromatographic peaks of samples were identified by mass spectra and by comparison with the standards. An aliquot of 1 μl of the purified sample was injected into the GC-MSD for the analysis, conducted in splitless mode with a solvent delay of 5 min. A six-point response factor calibration was established to quantify the target analyses.

4.3.3 OCPs analyses

The analytical method for OCPs was carried out based on the method of US-EPA 8080A. At the Key Laboratory of Biogeology and Environmental Geology, 10 g of dried soil from each sample, after being homogenized and freeze-dried, were spiked with 20 ng (4μl of 5mg l-1) of TCmX and PCB209 as recovery surrogates and were Soxhlet-extracted with dichloromethane for 24 h. Elemental sulfur was removed by adding activated copper granules to the collection flasks.

The sample extract was concentrated and solvent-exchanged to hexane and further reduced to 2-3 ml by a rotary evaporator (Heidolph4000). A 1:2 (v/v) alumina/silica gel column (both 3% deactivated with H2O) was used to cleanup the extract and OCPs were eluted with 30 ml of dichloromethane/hexane (2:3). The eluate was then concentrated to 0.2 ml under a gentle nitrogen stream. 20ng (4μl of 5mg l-1) PCNB was added as an internal standard prior to gas chromatography-electron capture detector (GC-ECD) analysis.

An HP7890A gas chromatograph equipped with a 63Ni electron capture detector (GC-ECD) was used for detecting the concentrations of p,p'-DDT, o,p'-DDT, p,p'-DDD, o,p'-DDD, p,p'-DDE, o,p'-DDE, α-HCH, β-HCH, γ-HCH, δ-HCH, HCB, aldrin, dieldrin, endrin, α-endosulfan, β-endosulfan, trans-chlordane, cis-chlordane, endosulfan sulfate, endrin aldehyde, endrin ketone, heptachlor, heptachlor epoxide, trans-Nonachlor, cis-Nonachlor and methoxychlor in the soil samples. The capillary column used for the analysis was a HP-5 (30.0 m×320 μm×0.25 μm film thickness). Nitrogen was used as the carrier gas at 2.5 ml/min under the constant flow mode. Injector and detector

temperatures were maintained at 290°C and 300°C, respectively. The temperature program is used as follows: the oven temperature began at 100°C (equilibrium time 1 min), rose to 200°C at 4°C/min, then to 230°C at 2°C/min, and at last reached 280°C at a rate of 8°C/min, held for 15 min. A 2 µl sample was injected into the GC-ECD for analysis. A six-point response factor calibration was established to quantify the target analyses.

4.4 Data processing

For the purposes of this work, the geochemical data of the 15 PTEs defined by the D.Lgs. 152/06, the 16 PAHs defined as priority pollutant by the USEPA and the OCPs defined as POPs by the Stockholm convention were considered.

With the aim of characterizing the geochemical conditions of the area, cartographic elaborations were created for each of these analytes, useful for having a clear vision of the spatial distribution of the same. Before being mapped, a univariate statistical analysis was carried out on data, aimed at identifying the main statistical indices useful for the characterization of the data, alongside the graphical representation (box plots, histograms, cumulative frequency curves) (Tables 1, 2 and 3).

The interpolated maps were produced with the Inverse Distance Weight (IDW) spatial interpolation method, associated with a methodology that uses the fractal geometry (Multifractal - IDW) (Cheng, 1999) implemented with an add-in of the software ArcMap (Zuo and Wang, 2019).

For each analyte (PTEs, PAHs, OCPs) were produced both the raster maps of the simple concentrations' distribution and the ones of the potential hazard, where applicable. The raster maps were classified by mean of the Concentration-Area (C-A) plot method (Cheng et al., 1994; Zuo and Wang, 2019) based on the use of a logarithmic plot reporting in the abscissa the concentration values of the pixels and in the ordinate the cumulative values of the areas occupied by specific concentration pixels. The classification is made by identifying the inflection points along the C-A plot curve and taking the corresponding concentration values on the abscissa to be used as interval ranges, which allows to create maps whose pattern reflect the geochemical variability of the territory (Albanese et al., 2007).

The potential hazard maps were obtained by using, where applicable, the contamination threshold concentration values (CSC) established by the Italian D.Lgs. 152/06 for residential and industrial land use and the one established by the Italian D.M. 46/19 for agricultural land use to classify the pixels of the previously developed interpolated maps.

Subsequently, an analysis was carried out to establish the emission source of the analysed contaminants, following three different routes for each one of the family of analytes considered.

A factor analysis was performed on the 15 PTEs with, given the close relationship between these due to the use in agricultural procedures, in addition Fe and P. The main goal of factor analysis, a method of multivariate statistics, is to find associations of elements, or chemical compounds, that are correlated in terms of spatial distribution, suggesting the existence of latent sources (or processes) that influence their behaviour (Albanese et al., 2007; Field 2009). The factor analysis, conducted with the SPSS software, was carried out on the data log-normalized (Log_{10}), using the "varimax" as a rotation method with Kaiser normalization and principal component analysis (PCA) as an extraction method (Field 2009). Elements that showed communalities <0.5 have been eliminated from the data matrix. Following the factor analysis in R-mode, form the observation of the scree plot (Cattell, 1966), the 3-component factor model was chosen, responsible for 82.1% of the total data variability. For the determination of the 3 associations of elements (F1, F2 and F3), constituting the chosen factorial model, the elements with a weight (eigenvalue) > $\left|0.7\right|$ were considered (Jolliffe, 1972; 1986). Once the sets of elemental associations were defined, a score based on the relevance of each factor/component was assigned to each sample in the dataset.

As regard PAHs, in order to discriminate the emission sources, as suggested by Tobiszewski and Namiesnik 2011, diagnostic ratios were taken into consideration. The use of these ratios is based on the thermodynamic stability of the PAHs molecules, since during low temperature (petrogenic) processes (e.g., wood burning) LMW PAHs are usually formed, while high temperature (pyrogenic) processes (e.g., combustion of fuels in engines) emit HMW compounds (Mostert et al., 2010). For the determination of the source of origins of PAHs, we used several diagnostic ratios: ΣLMW/ΣHMW (Zhang et al., 2008); anthracene/(anthracene + phenanthrene) (Pies et al., 2008); fluoranthene/(fluoranthene + pyrene) (De La Torre-Roche et al., 2009); benzo(a)anthracene/(benzo(a)anthracene + chrysene) (Akyüz and Çabuk, 2010); indeno(1,2,3-cd)pyrene/(indeno(1,2,3-cd)pyrene + benzo(ghi)perylene) (Yunker et al., 2002); benzo(a)pyrene/ benzo(ghi)perylene (Katsoyiannis et al., 2007).

For OCPs the ratios between the parent compound and its metabolites have been used, where possible, as pollution sources indicators (Jiang et al., 2009). Because some OCPs tend to degrade over time in other metabolites and since the technical pesticides (i.e., DDT, HCH, chlordane, endosulfan) used, mainly in agricultural practices, are composed by a precise percentage of the different molecules, the ratio between the parent compound and its metabolites can help identify whether the concentrations found in soil are attributable to fresh or historical use of these substances. The ratio used were: o,p'-DDT/p,p'-DDT (Qiu et al., 2005); p,p'-DDT/(p,p'-DDE + p,p'-DDD) (Jiang et al., 2009); α-HCH/γ-HCH (Iwata et al., 1995; Zang et al., 2004); α-HCH/β-HCH (Zang et al., 2011); cis-

chlordane/trans-chlordane (Bidleman et al., 2000); α-endosulfan /β-endosulfan (WHO 1984; Jiang et al., 2009).

All the variables resulting from the analyses conducted (i.e., factor scores, PAHs and OCPs ratios) were interpolated, again with the MIDW method, to generate a set of maps.

4.5 Results and discussion

Table 4.1 Summary statistics of PTEs and legislative guideline values.

			Statisthical parameters					D.M. 46/19	D.Lgs. 152/06	
Element	**Unit**	**DL**	**Min**	**Max**	**Mean**	**St.Dev**	**Median**	**Agr.**	**Res.**	**Ind.**
As	mg/kg	0.1	6.4	60.9	13.8	6.1	13.2	30	20	50
Be	mg/kg	0.1	1.9	12.2	4.7	1.3	4.6	7	2	10
Cd	mg/kg	0	0.18	1.38	0.51	0.16	0.51	5	2	15
Co	mg/kg	0.1	5.3	17.4	12.0	2.9	12.5	30	20	250
Cr	mg/kg	0.5	4.0	177.8	19.5	19.4	15.8	150	150	800
Cu	mg/kg	0.01	17.90	329.58	144.87	52.53	140.21	200	120	600
Fe	%	0.01	1.08	3.42	2.62	0.59	2.78			
Hg	µg/kg	5	28	563	136	100	109	1000	1000	5000
Ni	mg/kg	0.1	5.6	25.4	15.5	2.9	15.8	120	120	500
P	%	0.001	0.033	0.507	0.280	0.072	0.286			
Pb	mg/kg	0.01	35.94	1099.09	85.95	133.83	64.22	100	100	1000
Sb	mg/kg	0.02	0.38	5.41	0.88	0.58	0.73	10	10	30
Se	mg/kg	0.1	0.2	1.6	0.7	0.2	0.6	3	3	15
Sn	mg/kg	0.1	2.4	18.9	4.9	2.6	4.1		1	350
Tl	mg/kg	0.02	0.87	2.91	2.12	0.50	2.21	1	1	10
V	mg/kg	2	36	117	85	21	89	90	90	250
Zn	mg/kg	0.1	42.8	627.9	119.2	66.1	109.6	300	150	1500

4.5.1 PTEs distribution and sources

Table 4.1 shows the statistic of PTEs. Cd, Co, Hg, Ni, Sb and Se did not show concentration values exceeding the guideline values established by the D.Lgs. 152/06, neither for the residential land use nor for the industrial use, and by the D.M. 46/19 for agricultural land use (Table 4.1).

Cr overcomes both the guidelines for residential and agricultural land use of 150 mg/kg just in one sample in the northernmost area of the municipality of Acerra (Table 4.1).

Sn overcomes the guidelines set for residential land use of 1 mg/kg in all the analysed samples (there are no guidelines set for agricultural land use for this element) (Table 4.1).

Tl, except for two sample in the northern area of the municipality of Acerra, overcomes both the guidelines for residential and agricultural land use of 1 mg/kg in all the analysed samples (Table 4.1).

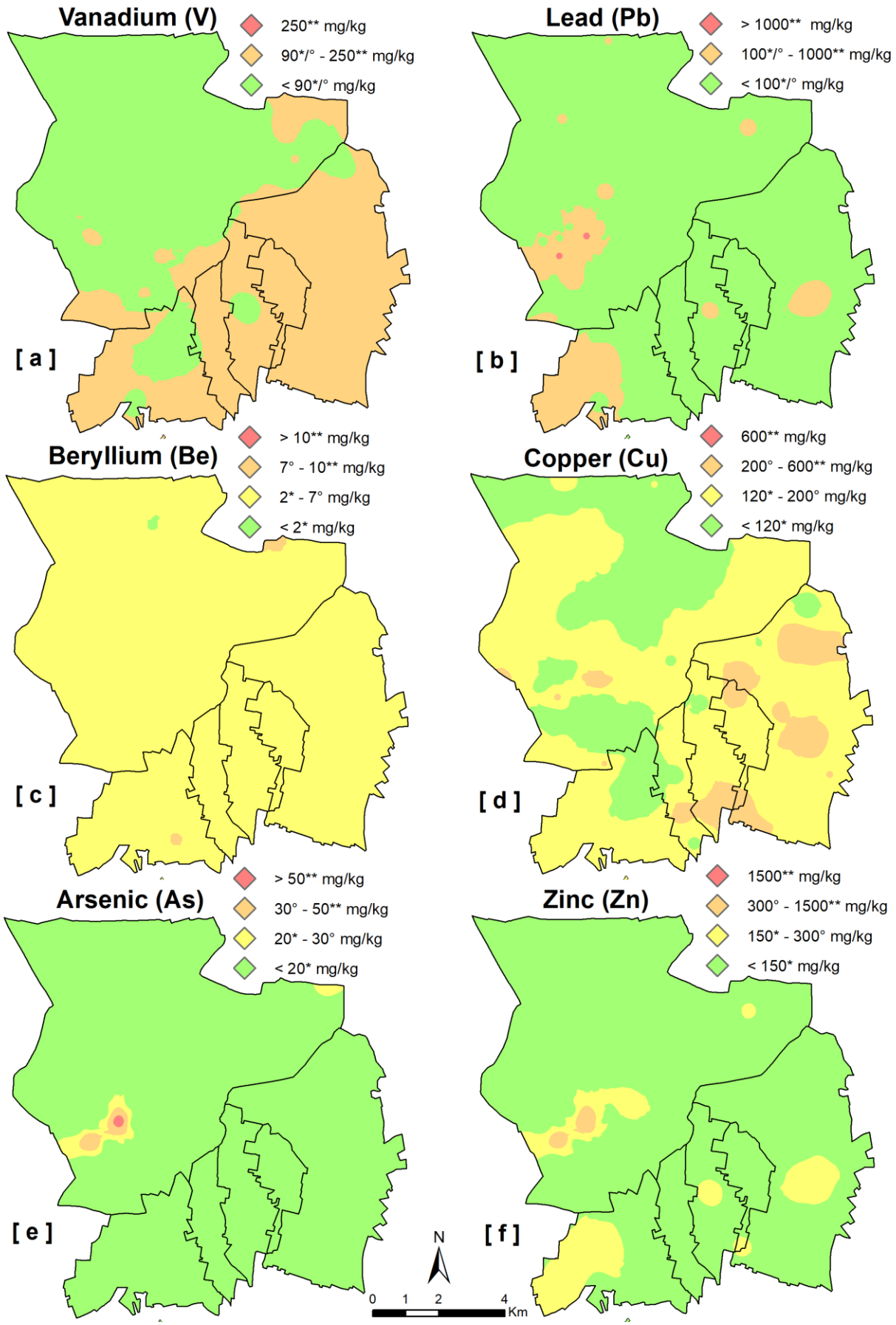

Figure 4.2 Potential hazard maps of PTEs. (and ** are the guideline values established by the D.Lgs. 152/06 for residential and industrial land use, respectively; ° are the ones established by the D.M 46/19).*

V overcomes the guidelines values for residential and agricultural land use of 90 mg/kg in almost all the samples located in the southern and the eastern sectors of the study area, except around the town of Brusciano and in the north-eastern area of the municipality of Pomigliano (Fig. 4.2a).

As (Fig. 4.2e), Zn (Fig. 4.2f) and Pb (Fig. 4.2b) have some samples that overcome both the guidelines for residential and agricultural land use (respectively of 20 and 30 mg/kg for As, 150 and 300 mg/kg for Zn and both of 100 mg/kg for Pb) around the urban centre of Acerra, and as for As and Pb even exceeding the ones for industrial land use (of 50 mg/kg and 1000 mg/kg, respectively); also near the urban centres of Pomigliano, Brusciano and Marigliano Pb exceed both the guideline values set for residential and agricultural land use (both equal to 100 mg/kg) and Zn the ones set for residential land use (150 mg/kg).

Be shows concentrations exceeding the guideline values established for residential land use of 2 mg/kg in the whole study area, except in one sample in the north of the municipality of Acerra for which there are no exceedances and two samples, one in the municipality of Pomigliano and one in the municipality of Acerra, in which it shows values overcoming the guidelines for agricultural use of soil of 7 mg/kg (Fig. 4.2c).

Cu overcomes the guidelines values for residential land use of 120 mg/kg, and, for some ones, even the guideline set for agricultural land use of 200 mg/kg, in almost all the samples located in the southern and the eastern sectors of the study area, except in the area between the towns of Pomigliano and Acerra and in the northern area of the municipality of Acerra (Fig. 4.2d).

The results of the factor analysis led to the identification of three factorial association (F1, F2 and F3) responsible for the 82.1% of the total variability of data.

F1, composed by Co, Fe, V, Tl and Be, is responsible for the 36.1% of the total variability of the data. From the map of the distribution of the factor scores (Fig. 4.3a) it is clear that, the samples taken in the area north-west of the municipality of Acerra have negative values, indicating an impoverishment of the elements that form this association. Positive values are recorded throughout the area east of the study area and near the urban centers of Acerra and Pomigliano. F1 was associated to the geochemical composition of the volcanic soils. In the area north of Acerra these elements are probably impoverished in the soils due to the superficiality of the water table, which causes the leaching from the soils.

F2, composed by Pb, Zn, Sb and Sn, is responsible for the 28.13% of the total data variability, and has been associated with urbanized areas. In fact, Pb derives mainly from the heritage of gasoline, and Zn from the decay of tires, as it is used in the vulcanization process of rubbers, together with zinc oxides (Albanese and Breward, 2011); both these elements are therefore linked to vehicular traffic. Sn and Sb are also linked to urban areas, but due to anthropogenic residential activities. The map of

the distribution of the scores (Fig. 4.3b) denotes, in fact, a correspondence between urban areas and the ones with intense vehicular traffic with the areas characterized by the higher scores.

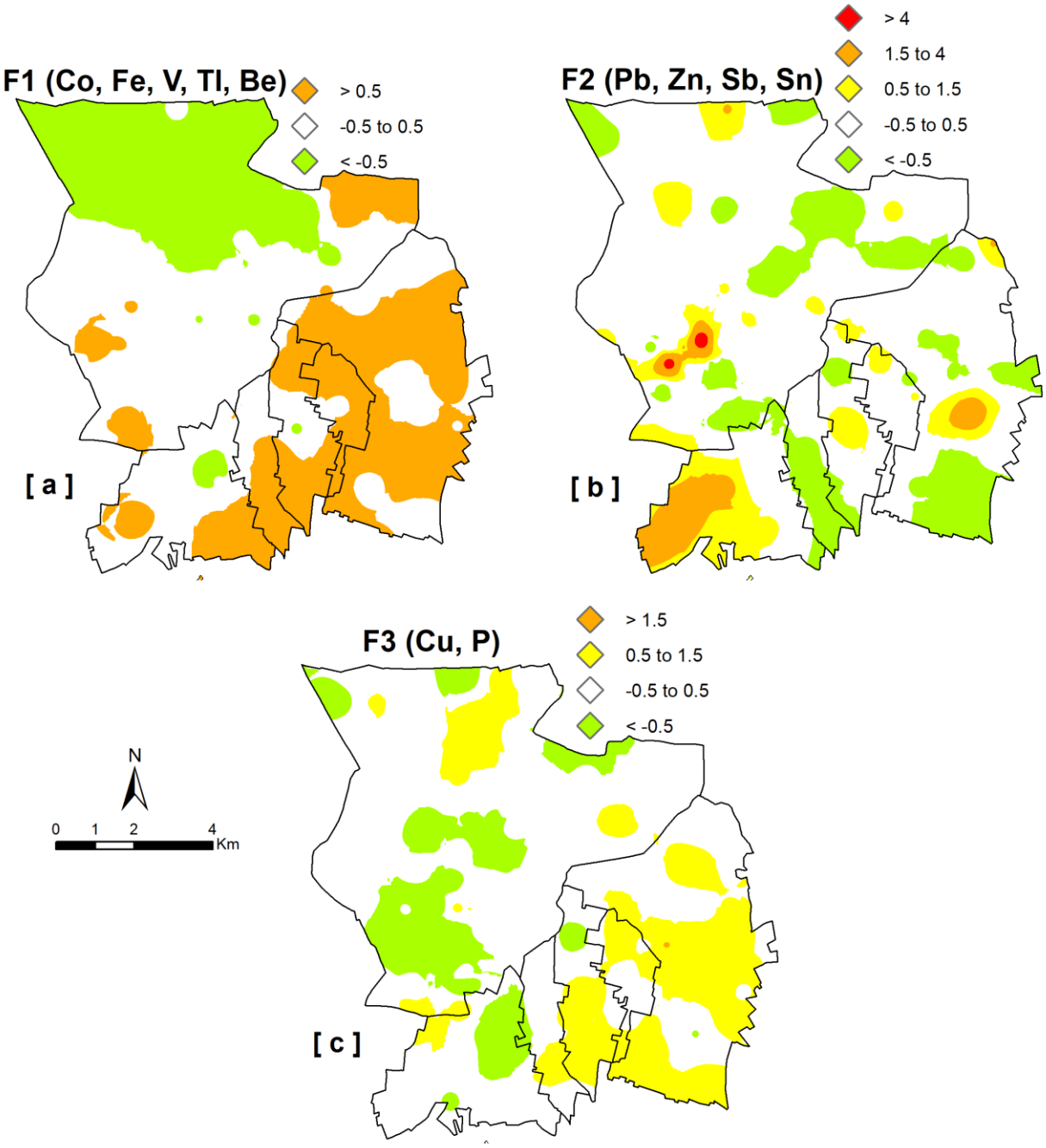

Figure 4.3 Maps of the factorial association of PTEs.

F3, responsible for 17.87% of the total variability of the model, is characterized by Cu and P. As already mentioned, P was added due to the high use of this element in agricultural practices. Positive score factors are found concentrated in the south-eastern area, close to the Vesuvius slopes, while negative factors are linked to urban centers (Fig. 4.3c). Since Cu is a component of fungicides,

precisely defined as cupric, and P is present in soil improvers (fertilizers) and phosphate fertilizers, this association was attributed to the predominantly agricultural use of the soil.

Table 4.2 Summary statistics of PAHs and legislative guideline values.

		Statisthical parameters						D.M. 46/19	D.Lgs. 152/06	
Compound	**Unit**	**MDL**	**Min**	**Max**	**Mean**	**St.Dev**	**Median**	**Agr.**	**Res.**	**Ind.**
Naphthalene	ng/g	0.04	2.55	25.26	9.50	5.68	8.50			
Fluorene	ng/g	0.05	0.03	7.54	2.21	1.62	1.75			
Acenaphthylene	ng/g	0.10	0.05	33.14	8.42	8.17	5.45			
Acenaphthene	ng/g	0.04	0.02	4.94	0.93	1.17	0.64			
Phenanthrene	ng/g	0.27	3.44	111.40	33.55	27.43	22.50			
Anthracene	ng/g	0.16	0.53	27.30	6.79	6.04	4.72			
Fluoranthene	ng/g	0.14	4.20	410.30	86.38	82.49	57.99			
Pyrene	ng/g	0.10	4.02	396.7	79.88	77.83	55.21		5000	50000
Benzo[a]anthracene	ng/g	0.20	3.34	424.9	70.58	79.66	51.26	1000	1000	10000
Chrysene	ng/g	0.16	19.74	780.6	234.1	181.4	174.2	1000	5000	50000
Benzo[b]fluoranthene	ng/g	0.16	15.76	878.8	224.1	205.5	172.0	1000	500	10000
Benzo[k]fluoranthene	ng/g	0.08	6.48	381.8	108.1	93.3	73.7	1000	1000	10000
Benzo[a]pyrene	ng/g	0.16	18.98	1131.6	302.5	263.7	234.6	100	100	10000
Dibenzo[a,h]anthracene	ng/g	0.04	0.02	181.1	40.68	40.92	28.01	100	100	10000
Indeno[1,2,3-cd]pyrene	ng/g	0.14	13.85	1078.7	254.6	244.3	171.0	1000	100	5000
Benzo[g,h,i]perylene	ng/g	0.17	8.37	615.4	162.2	146.5	108.5	5000	100	10000

4.5.2 PAHs distribution and sources

Table 4.2 shows the statistic of PAHs. Benzo(a)anthracene, benzo(k)fluoranthene, chrysene and pyrene did not show concentration exceeding neither the guideline values established by the D.Lgs. 152/06, for residential and industrial land use, nor the ones established by the D.M. 46/16 for agricultural land use (Table 4.2).

Dibenzo(a,h)anthracene (Fig. 4.4b) and benzo(b)fluoranthene (Fig. 4.4d) overcome the guidelines values for residential land use of 100 ng/g (which for dibenzo(a,h)anthracene corresponds also to the guideline established by the D.M. 46/19 for agricultural land use) and 500 ng/g, respectively, in correspondence of the industrial area between the town of Acerra and Brusciano.

Benzo(a)pyrene (Fig. 4.4a) and indeno(1,2,3-cd)pyrene (Fig. 4.4e) show values exceeding the guidelines for residential land use of 100 ng/g for both (which for benzo(a)pyrene corresponds also to the guideline established by the D.M. 46/19 for agricultural land use) almost in all the study area, except for two small portion in the municipality of Acerra and Marigliano. Indeno(1,2,3-cd)pyrene also shows a sample with values exceeding the guideline for agricultural land use of 1000 ng/g near the town of Brusciano.

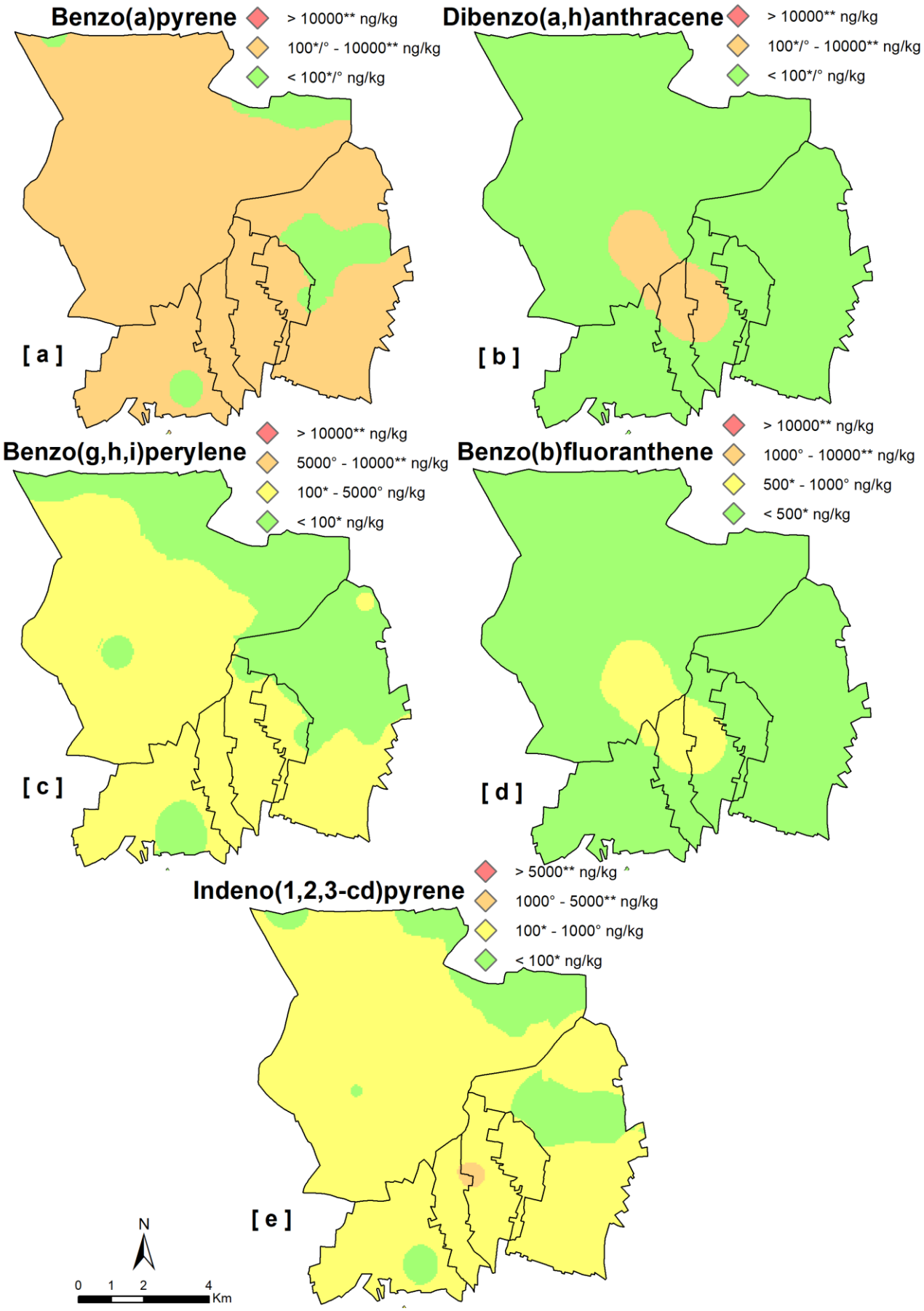

Figure 4.4 Potential hazard maps of PAHs. (and ** are the guideline values established by the D.Lgs. 152/06 for residential and industrial land use, respectively; ° are the ones established by the D.M 46/19).*

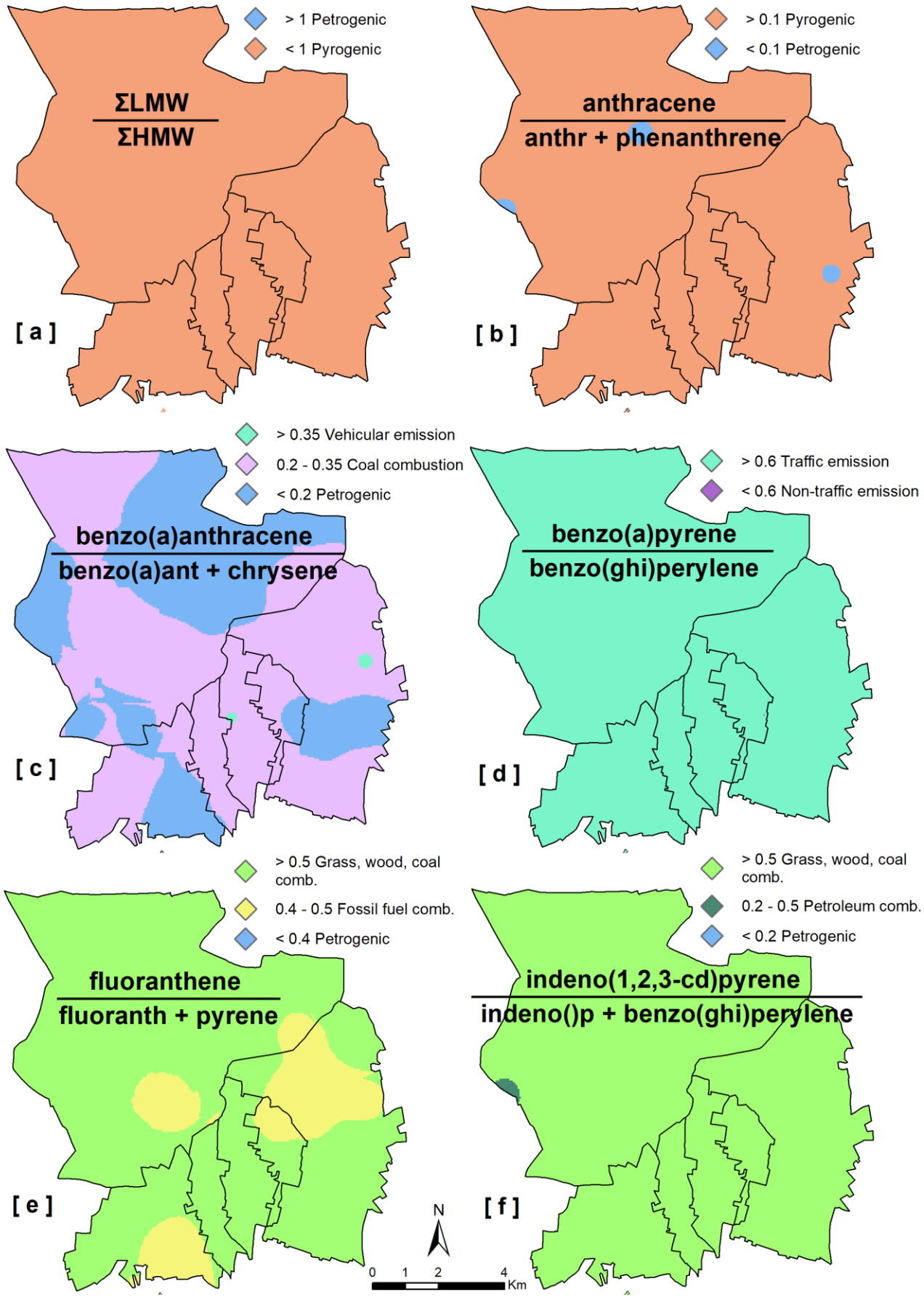

Figure 4.5 Maps of the diagnostic ratios of PAHs.

Benzo(g,h,i)perylene has values not exceeding the guidelines for residential land use of 100 ng/g around the towns of Acerra and Pomigliano and in the north-eastern sector of the study area, while it overcomes it in the remaining portions (Fig. 4.4c).

As for naphthalene, fluorene, acenaphthylene, acenaphthene, phenanthrene, anthracene and fluoranthene the D.lgs. 152/06 and the D.M. 46/19 do not provide guideline values.

The ratio between low and high molecular weight PAHs suggests an origin pyrogenic of these compounds, since in all the area values are < 1 (Zhang et al., 2008) (Fig. 4.5a). This is confirmed also from the ratio between anthracene and phenanthrene, which, almost in the whole area except for three sample, assumes values > 0.1 (Pies et al., 2008) (Fig. 4.5b).

Both the ratios between fluoranthene and pyrene (Fig. 4.5e) and the one of indeno(1,2,3-cd)pyrene and benzo(ghi)perylene (Fig. 4.5f) also show that the origins are linked to pyrogenic processes. In fact, in almost the whole area the values are, for both, > 0.5 suggesting that the origin of these PAHs is attributable to the combustion of biomasses (De La Torre-Roche et al., 2009; Yunker et al., 2002) and, only in small portions of the area, to the pyrolysis of fossil fuels.

The ratio between benzo(a)anthracene and chrysene shows that in almost the half of the study area the origin of these compound is attributed to petrogenic processes (values < 0.2) while the rest to coal combustion (values from 0.2 to 0.35) (Akyüz and Çabuk, 2010) (Fig. 4.5c).

The ratio between benzo(a)pyrene and benzo(ghi)perylene assumes values > 0.5 in the whole study are, which means that the origin of these compounds is linked to traffic emission (Katsoyiannis et al., 2007) (Fig. 4.5d).

4.5.3 OCPs distribution and sources

Table 4.3 shows the statistic of OCPs. For all the OCPs for which exist guideline values established by the D.Lgs. 152/06 and by the D.M. 46/19 (i.e., p,p'-DDT, o,p'-DDT, p,p'-DDD, o,p'-DDD, p,p'-DDE, o,p'-DDE, α-HCH, β-HCH, γ-HCH, aldrin, dieldrin, endrin, trans-chlordane, cis-chlordane), the values for residential land use correspond to the ones set for agricultural land use, which is equal to 10 ng/g for all of them.

Trans-chlordane, cis-chlordane, o,p'-DDD, o,p'-DDE, α-HCH, γ-HCH, aldrin and endrin did not show concentration values exceeding the guideline values established by the D.Lgs. 152/06, neither for the residential land use nor for the industrial use, and by the D.M. 46/19 for agricultural land use.

Dieldrin (Fig. 4.6f) and β-HCH (Fig. 4.6e) overcome the guideline of 10 ng/g just in one sample, in the municipality of Acerra β-HCH and in the one of Marigliano dieldrin.

O,p'-DDT (Fig. 4.6b) and p,p'-DDD (Fig. 4.6c) overcome the guideline of 10 ng/g around the urban centres of Marigliano and Brusciano and in some samples in the municipality of Acerra.

P,p'-DDT (Fig. 4.6a) and p,p'-DDE (Fig. 4.6d) overcome the guidelines in almost all the study area, except for a few scattered samples, and show even values exceeding the guideline set for industrial land use of 100 ng/g in the municipality of Acerra and Marigliano both, and in the area between the urban centres of Castello and Mariglianella p,p'-DDE.

Table 4.3 Summary statistics of PAHs and legislative guideline values.

		Statisthical parameters						D.M. 46/19	D.Lgs. 152/06	
Compound	**Unit**	**MDL**	**Min**	**Max**	**Mean**	**St.Dev**	**Median**	**Agr.**	**Res.**	**Ind.**
HCB	ng/g	0.063	0.358	0.78	0.60	0.11	0.61			
α-HCH	ng/g	0.070	0.035	0.91	0.16	0.19	0.10	10	10	100
β-HCH	ng/g	0.067	0.034	15.40	1.74	3.16	0.65	10	10	500
γ-HCH	ng/g	0.105	0.053	3.17	0.41	0.62	0.19	10	10	500
o,p'-DDT	ng/g	0.075	0.038	36.73	5.67	7.91	2.04			
p,p'-DDT	ng/g	0.162	0.081	492.7	70.37	100.1	25.53			
o,p'-DDE	ng/g	0.055	0.028	3.89	0.75	0.96	0.33	10	10	100
p,p'-DDE	ng/g	0.079	0.040	337.9	75.94	92.08	31.02			
o,p'-DDD	ng/g	0.063	0.059	4.39	1.44	1.25	1.21			
p,p'-DDD	ng/g	0.065	0.033	21.19	6.24	5.95	3.66			
Dieldrin	ng/g	0.207	0.104	14.45	1.67	3.57	0.25	10	10	100
Aldrin	ng/g	0.092	0.046	1.52	0.54	0.39	0.45	10	10	100
Endrin	ng/g	0.183	0.092	2.43	0.49	0.63	0.09	10	10	2000
Heptachlor	ng/g	0.164	0.082	7.11	1.61	1.47	1.20			
Trans-Chlordane	ng/g	0.061	0.031	0.44	0.06	0.08	0.03	10	10	100
cis-Chlordane	ng/g	0.036	0.018	0.55	0.05	0.10	0.02			
α-Endosulfan	ng/g	0.066	0.033	1.71	0.41	0.41	0.26			
β-Endosulfan	ng/g	0.066	0.033	2.22	0.42	0.58	0.10			

The ratio o,p'-DDT/p,p'-DDT was used to discriminate between technical DDT and dicofol contamination, since high values (> 1.3) indicates dicofol sources while small values (< 0.3) technical DDT (Qiu et al., 2005). The values have a median of 0.06, suggesting that more of the half of the values found are attributable to the use of technical DDT, while, just in a small area west to the town of Acerra, is linked to dicofol use (Fig. 4.7a).

Since DDE and DDD are the main degradation products of DDT dechlorination (ATSDR, 2002), the ratio between p,p'-DDT, p,p'-DDE and p,p'-DDD can be used as indicator of the input of this compound in the environment because high values (> 1) indicates fresh application while small values (< 1) historical DDT (Jiang et al., 2009). The ratio assumed a median value of 0.77, in fact, less of the half of the area is attributable to a fresh input of DDT (Fig. 4.7b).

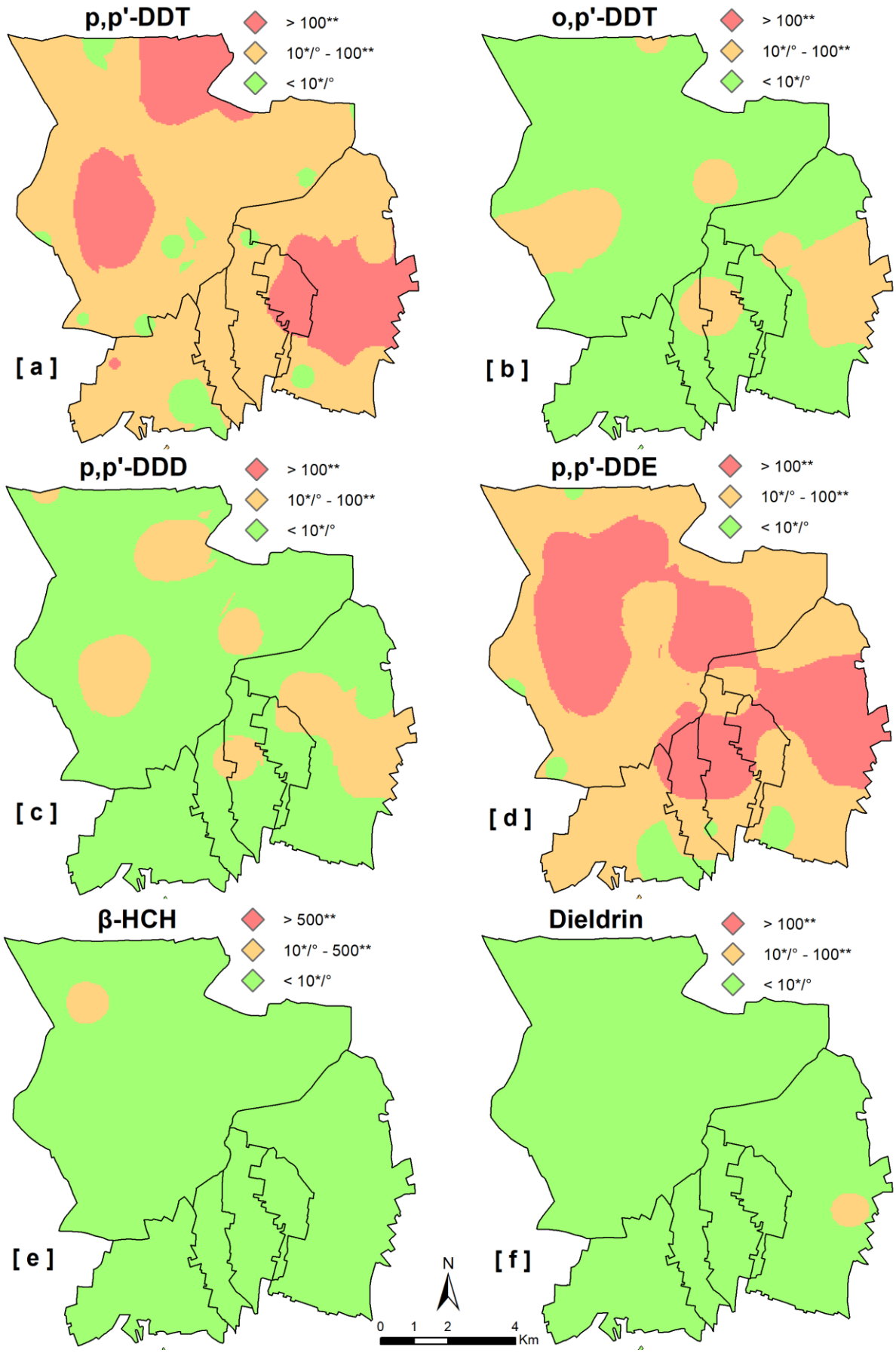

Figure 4.6 Potential hazard maps of OCPs. (and ** are the guideline values established by the D.Lgs. 152/06 for residential and industrial land use, respectively; ° are the ones established by the D.M 46/19).*

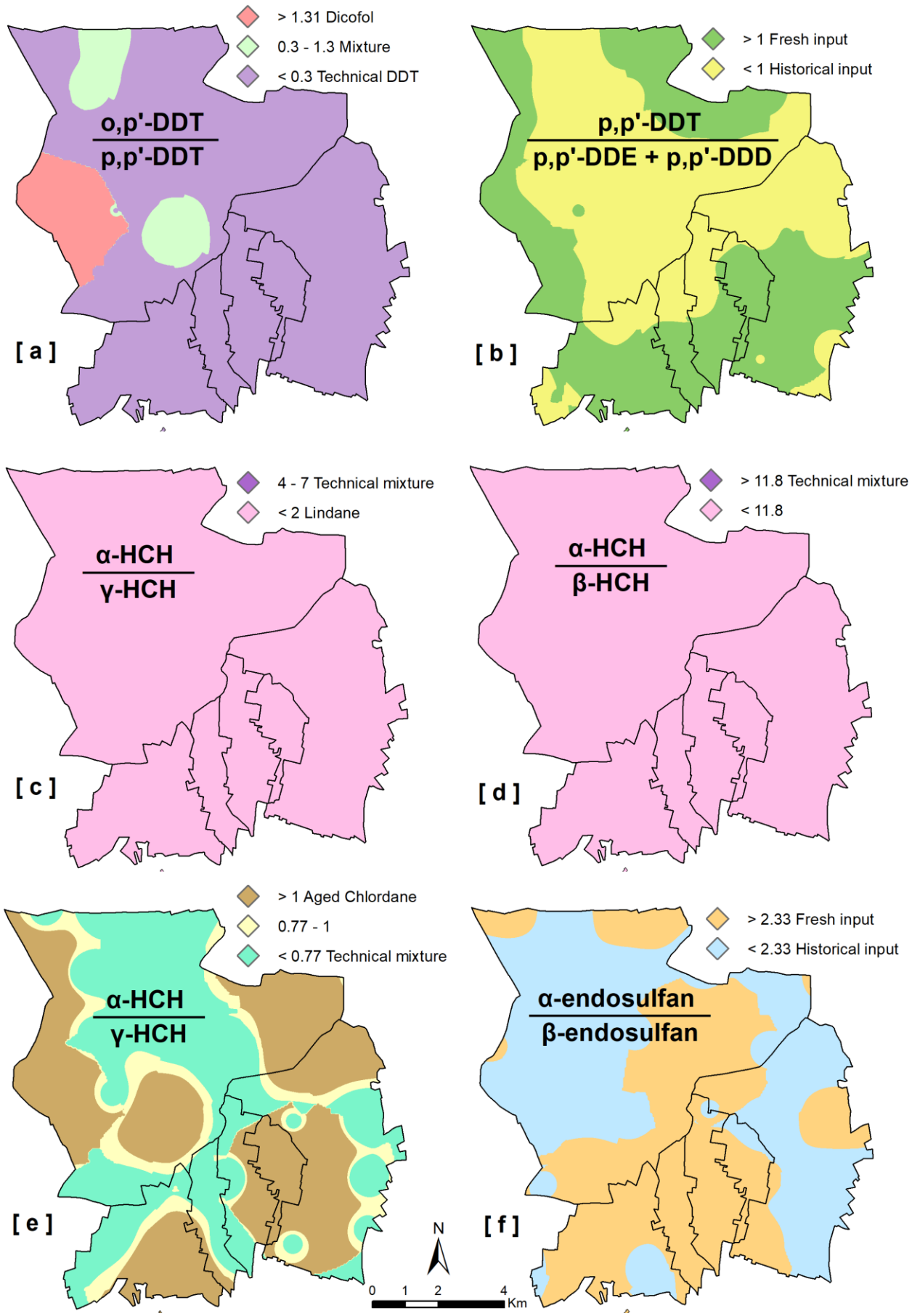

Figure 4.7 Maps of the isomeric ratios of OCPs.

The sequence of degradation of HCHs is α-HCH > γ-HCH > δ-HCH > β-HCH. Both the ratio α-HCH/γ-HCH (Fig. 4.7c) and α-HCH/β-HCH (Fig. 4.7d) indicate that the contamination is not linked to the use of technical mixture, since values for α-HCH/γ-HCH are <2, hence not included in the range of 4-7 indicated for that use (Iwata et al., 1995; Zang et al., 2004), ant the ones for α-HCH/β-HCH are < 11.8 (Zang et al., 2011).

Trans-chlordane degrades more easily than cis-chlordane, and, values of the ratio cis-chlordane/trans-chlordane > 1 indicate aged chlordane (Bidleman et al., 2000). In the area around the city centers and in the north-eastern sector of the study area values are < 0.77 indicating the use of technical mixtures, while in the areas roughly corresponding to the cultivated areas the values are indicative of aged chlordane (Fig. 4.7e).

The ratio α-endosulfan/β-endosulfan, because α-endosulfan degrades more easily than β-endosulfan, is used to define the age of the mixture. The ratio in technical mixtures of the two isomers is about 2.33 (WHO 1984; Jiang et al., 2009). Values range from 0.25 to 28.8 indicating that there have been recent applications of technical endosulfan, most in the central sector of the investigated area (Fig. 4.7f).

4.6 Conclusions

From the analyses carried out it emerged that several PTEs, PAHs and OCPs have concentrations in the urban area of Acerra and neighbouring municipalities exceeding the guideline values set by the D.Lgs. 152/06 and the D.M. 46/19.

Specifically, over the entire investigated area Tl, Be, Sn and, limited to the south-eastern sector, V show exceedances of the guideline values even if the reasons are attributable to the volcanic origin of the pedological media. In the south-eastern sector, the surplus of Cu can be associated with the use of copper-based pesticides in agricultural practices set on volcanic soils destined for the cultivation of vines and, near urban centers, the high concentrations of Zn and Pb can mainly refer to motor vehicle traffic (current and past).

Benzo(a)pyrene, benzo(ghi)perylene and indeno(123-cd)pyrene showed high concentration values, above the guideline limits, in the whole study area, with the exception of the north-eastern portion of the territory analysed, free from industrial activities. Dibenzo(a,h)anthracene and benzo(b)fluoranthene were found to be characterized by high values, higher than the CSCs for residential use, in the industrial area between the municipalities of Acerra and Brusciano.

The results obtained from the analysis of the contamination sources of PAHs showed that, in almost the entire area, most of the hydrocarbons derive from combustion processes, mostly biomass,

and this is in line with the intense agricultural activity and the presence of plants that produce electricity (Fri-el palm oil power station) in the area.

The OCPs that showed the highest concentration, higher than the guidelines established by the D.Lgs. 152/06 and the D.M. 46/19, were p,p'-DDT, o,p'-DDT, p,p'-DDD and p,p'-DDE. The highest values were found mainly in the urban and industrial areas around urban centres of Acerra, Brusciano and Marigliano.

The analysed ratios showed that, despite the use of most OCPs is banned, there still is a present contribution to the high concentrations in soil due to fresh application of mixtures of pesticides in some portions of the study area.

Given the huge number of people residing in the area, and the presence of numerous productive activities, the results obtained are not surprising. It is clear, however, that it is necessary to implement new studies aimed above all at assessing health risk in probabilistic terms. A detailed analysis could help better identify the areas to which address the highest priority for intervention, and the use of more advanced multivariate statistical techniques could help to discriminate the causes of pollutant emissions with greater precision.

References

ATSDR, 2002. Toxicological Profile for DDT, DDE, and DDD. Dept Health Human Services. Agency for Toxic Substances and Disease Registry (ATSDR), Atlanta GA.

ATSDR, 2009. Toxicity of Polycyclic Aromatic Hydrocarbons (PAHs). Agency for Toxic Substances and Disease Registry (ATSDR), Atlanta GA.

Akyüz, M., Çabuk, H., 2010. Gas e particle partitioning and seasonal variation of polycyclic aromatic hydrocarbons in the atmosphere of Zonguldak, Turkey. Sci. Total Environ. 408, 5550-5558.

Albanese, S., Breward, N., 2011. Sources of Anthropogenic Contaminants in the Urban Environment, in: Johnson, C.C. (Eds.), Mapping the chemical environment of urban areas. Wiley, pp. 116-127.

Albanese, S., De Luca, M.L., De Vivo, B., Lima, A., Grezzi, G., 2008. Relationships between heavy metals distribution and cancer mortality rates in the Campania Region, Italy, in: De Vivo, B., Belkin, H.E., Lima, A. (Eds.), Environmental Geochemistry: Site Characterization, Data Analysis and Case Histories. Elsevier, Amsterdam, pp. 391–404.

Albanese, S., De Vivo, B., Lima, A., Cicchella, D., 2007. Geochemical background and baseline values of toxic elements in stream sediments of Campania region (Italy). J. Geochem. Explor. 93 (1), 21-34. https://doi.org/10.1016/j.gexplo.2006.07.006.

Antoniadis, V., Shaheen, S.M., Levizou, E., Shahid, M., Niazi, N.K., Vithanage, M., Ok, Y.S., Bolan, N., Rinklebe, J., 2019. A critical prospective analysis of the potential toxicity of trace element regulation limits in

soils worldwide: Are they protective concerning health risk assessment? - A review. Environ. Int. 127, 819-847. https://doi.org/10.1016/j.envint.2019.03.039.

Bidleman, T.F., Jantunen, L.L.M., Helm, P.A., Brorström-Lundén, E., Juntto, S., 2000. Chlordane enantiomers and temporal trends of chlordane isomers in Arctic air, Environ. Sci. Technol. 36, 539–544.

Cattell, R.B. (1966). The scree test for the number of factors. Multivar. Behav. Res. 1, 245–276.

Cheng, Q., 1999. Spatial and scaling modelling for geochemical anomaly separation. J. Geochem. Explor. 65, 175–194.

Cheng, Q., Agterberg, F.P., Ballantyne, S.B., 1994. The separation of geochemical anomalies from background by fractal methods. J. Geochem. Explor. 51 (2), 109-130. https://doi.org/10.1016/0375-6742(94)90013-2.

Corniello, A., Ducci, D., 2009. Origine dell'inquinamento da nitrati nelle falde dell'area di Acerra (Piana Campana). EngHydroEnv Geology 12, 155-164.

De La Torre-Roche, R.J., Lee, W.-Y., Campos-Díaz, S.I., 2009. Soil-borne polycyclic aromatic hydrocarbons in El Paso, Texas: analysis of a potential problem in the United States/Mexico border region. J. Hazard. Mater. 163, 946-958.

De Vivo, B., Rolandi, G., Gans, P. B., Calvert, A., Bohrson, W. A., Spera, F. J., Belkin, H. E., 2001. New constraints on the pyroclastic eruptive history of the Campanian volcanic Plain (Italy). Mineral Petrol 73(1–3), 47–65.

di Gennaro, A., 2002. I sistemi di terre della Campania. Risorsa srl. Selca, Firenze.

Eisler, R., 2000. Handbook of Chemical Risk Assessment: Health Hazards to Humans, Plants and Animals, vol 2. Organics. Lewis Publishers, Boca Raton.

Field, A., 2009. Discovering Statistics Using SPSS. 3rd Edition, Sage Publications Ltd., London.

IARC, 2015. Monographs evaluate DDT, lindane, and 2,4-D. Press Release Number 236. International Agency for Research on Cancer (IARC)

ISPRA, 2015. Impatto sugli ecosistemi e sugli esseri viventi delle sostanze sintetiche utilizzate nella profilassi anti-zanzara. Istituto Superiore per la Protezione e la Ricerca Ambientale (ISPRA).

Iwata, H., Tanabe, S., Ueda, K., Tatsukawa, R., 1995. Persistent organochlorine residues in Air, Water, Sediments, and Soils from the Lake Baikai Region, Russia. Environ. Sci. Technol. 29, 792-801.

Jiang, Y.-F., Wang, X.-T., Jia, Y., Wang, F., Wu, M.-H., Sheng, G.-Y., Fu, J.M., 2009. Occurrence, distribution and possible sources of organochlorine pesticides in agricultural soil of Shanghai, China. J. Hazard. Mater. 170 (2–3), 989-997.

Jolliffe, I.T., 1972. Discarding variables in a principal component analysis, I: Artificial data. J R Stat Soc Ser C Appl Stat 21, 160–173.

Jolliffe, I.T., 1986. Principal component analysis. Springer, New York.

Katsoyiannis, A., Terzi, E., Cai, Q.-Y., 2007. On the use of PAH molecular diagnostic ratios in sewage sludge for the understanding of the PAH sources. Is this use appropriate? Chemosphere 69, 1337-1339.

Liu, J., Goyer, R.A., Waalkes, M.P., 2007. Toxic effects of metals, in: Klaassen, C.D. (Eds.), Casarett and Doull's Toxicology: The Basic Science of Poisons, 7th edn. McGraw-Hill Professional, New York, pp. 931–980.

Manoli, E., Kouras, A., Samara, C., 2004. Profile analysis of ambient and source emitted particle-bound polycyclic aromatic hydrocarbons from three sites in northern Greece. Chemosphere 56, 867-878.

Mostert, M.M.R., Ayoko, G.A., Kokot, S., 2010. Application of chemometrics to analysis of soil pollutants. Trends Analyt Chem 29, 430-435.

Pies, C., Hoffmann, B., Petrowsky, J., Yang, Y., Ternes, T.A., Hofmann, T., 2008. Characterization and source identification of polycyclic aromatic hydrocarbons (PAHs) in river bank soils. Chemosphere 72, 1594-1601.

Qiu, X., Zhu, T., Yao, B., Hu, J., Hu, S., 2005. Contribution of dicofol to the current DDT pollution in China. Environ. Sci. Technol. 39, 4385–4390.

Salminen, R., Tarvainen, T., Demetriades, A., Duris, M., Fordyce, F.M., Gregorauskiene, V., Kahelin, H., Kivisilla, J., Klaver, G., Klein, H., Larson, J.O., Lis, J., Locutura, J., Marsina, K., Mjartanova, H., Mouvet, C., O'Connor, P., Odor, L., Ottonello, G., Paukola, T., Plant, J.A., Reimann, C., Schermann, O., Siewers, U., Steenfelt, A., Van der Sluys, J., De Vivo, B., Williams, L., 1998. FOREGS Geochemical Mapping Field Manual. Geological Survey of Finland, Espoo Guide 47. http://www.gtk.fi/foregs/ eochem/fieldmanan.pdf

Schaefer, C., Peters, P., Miller, R.K., 2015. Drugs During Pregnancy and Lactation. Third ed. Elsevier, Amsterdam.

Senior, K., Mazza, A., 2004. Italian "Triangle of death" linked to waste crisis. Lancet Oncol, 5 (9): 525–527.

Sparling, D.W., 2016a. Ecotoxicology Essentials. Organochlorine Pesticides. First ed. Elsevier, Amsterdam, pp. 69-107.

Sparling, D.W., 2016b. Ecotoxicology Essentials. Polycyclic Aromatic Hydrocarbons. First ed. Elsevier, Amsterdam, pp. 193-221.

Tobiszewski, M., Namiesnik, J., 2011. PAH diagnostic ratios for the identification of pollution emission sources. Environ. Pollut. 162, 110-119.

USEPA, 1980. Ambient water quality criteria for polynuclear aromatic hydrocarbons. Rep. 440/5-80-069. United States Environmental Protection Agency (USEPA), Washington, DC.

WHO, 2006. Air quality guidelines for particulate matter, ozone, nitrogen dioxide and sulphur dioxide – Global update 2005 – Summary of risk assessment. World Health Organization (WHO), Geneva, Switzerland.

World Health Organization, 1984. Environmental Health Criteria 40: Endosulfan. World Health Organization (WHO), Geneva.

Yunker, M.B., Macdonald, R.W., Vingarzan, R., Mitchell, R.H., Goyette, D., Sylvestre, S., 2002. PAHs in the Fraser River basin: a critical appraisal of PAH ratios as indicators of PAH source and composition. Org. Geochem. 33, 489-515.

Zhang, A., Liu, W., Yuan, H., Zhou, S., Su, Y., Li, Y.F., 2011. Spatial distribution of hexachlorocyclohexanes in agricultural soils in Zhejiang province, China, and correlations with elevation and temperature. Environ. Sci. Technol. 45, 6303-6308.

Zhang, W., Zhang, S., Wan, C., Yue, D., Ye, Y., Wang, X., 2008. Source diagnostics of polycyclic aromatic hydrocarbons in urban road runoff, dust, rain and canopy throughfall. Environ. Pollut. 153, 594 e 601.

Zhang, Z.L., Huang, J., Yu, G., Hong, H.S., 2004. Occurrence of PAHs, PCBs and organochlorine pesticides in Tonghui River of Beijing, China. Environ. Pollut. 130, 249–261.

Zuo, R., Wang, J., 2020. ArcFractal: An ArcGIS Add-In for Processing Geoscience Data Using Fractal/Multifractal Models. Nat. Resour. Res. 29, 3-12. https://doi.org/10.1007/s11053-019-09513-5.

CHAPTER 5 – Estimating radon fluxes through different datasets to discriminate sources and assess health risks in Campania region (Italy).

The results of this activity were published/presented in:

Guarino A., Lima A., Cicchella D., Albanese S., 2021. Radon flux estimates, from both gamma radiation and geochemical data, to determine sources, migration pathways, and related health risk: The Campania region (Italy) case study. Chemosphere 287(1):132233 https://doi.org/10.1016/j.chemosphere.2021.132233

Guarino A., Aruta A., Ebrahimi P., Dominech S., Lima A., Cicchella D., Albanese S., 2021. Estimating radon fluxes through different datasets to discriminate sources and assess health risks in Campania region (Italy). Environmental Geochemistry and Health 2021

Guarino A., Aruta A., Ebrahimi P., Dominech S., Lima A., Cicchella D., Albanese S., 2021. Radon fluxes estimate from geochemical data and gamma radiation in Campania region (Italy). BeGeo scientists 2021, Naples. https://doi.org/10.3301/ABSGI.2021.04

Guarino A., Aruta A., Ebrahimi P., Dominech S., Zuzolo D., Lima A., Cicchella D., Albanese S., 2020. Pedogenic radon fluxes predictions from geochemical data and gamma ray: the Campania region experiment. GEOHEALTH 2020 - INTERNATIONAL MEETING OF GEOHEALTH SCIENTISTS, Bari. Scientific Research Abstracts Vol. 10, p. 26. ISSN 2464-9147.

Albanese S., Guarino A., Zuzolo D., Aruta A., Cicchella D., Iannone A., Melito R., Verrilli F., Fedele Gianvito A., 2020. Extending the concept of background to soil gas: natural radon concentrations in soils of Campania region. European Geosciences Union General Assembly 2020, Vienna. DOI: 10.5194/egusphere-egu2020-22687

5.1 Introduction

Soil gases mainly consist of carbon dioxide (CO_2), methane (CH_4), hydrogen (H_2), nitrous oxide (N_2O), ammonia (NH_3) and some noble gases such as helium (He), argon (Ar) and radon (Rn) (Nieder et al. 2018; Baubron et al., 1991).

Radon is a radioactive natural gas mostly proceeding from igneous rock and volcano-sedimentary materials (including soils). It is the heaviest among the noble gases, and it is chemically inert, colourless, odourless, and moderately soluble in water. In nature, the total radon amount is contributed by three unstable isotopes: ^{219}Rn (from ^{235}U decay chain), also called actinon, with a half-life of 3.96s; ^{220}Rn (from ^{232}Th decay chain), also called thoron, with a half-life of 55 seconds; ^{222}Rn (from ^{238}U decay chain), to which normally we refer as radon, with a half-life of 3.8 days.

Radon flux density from soils to the atmosphere depends on emanation rate from grains to the interstitial spaces, grain size distribution, soil porosity and permeability, partition ratio between gas and liquid phases in pores, temperature and pressure gradients among soil and atmosphere (IAEA, 2013; Nazaroff et al., 1992). Radon can accumulate indoor, and it represents the main source of natural radiation to which human beings can be exposed during their life. It is a human carcinogen (IARC, 1988), and it is considered the second indirect leading cause of lung cancer after cigarette smoking (Zeeb et al., 2009). Among Rn isotopes, ^{222}Rn represents the most relevant for health risks since its progenitor (i.e., ^{238}U) is ubiquitous in nature and its progeny (including ^{218}Po, ^{214}Po, ^{210}Po, ^{214}Bi, ^{210}Bi,^{214}Pb, ^{210}Pb) is chemically and electrically reactive and decays emitting α particles together with large amounts of energy.

Being an inert gas, Rn is chemically not reactive, and it is easily eliminated from the respiratory system; the progeny, which is not in a gaseous form, once adsorbed by airborne particles and inhaled, can adhere to brachial tissues and, by further decays, can irreversibly damage cellular DNA also developing carcinogenic effects on the long-term (Nazaroff et al., 1992).

Several countries in Europe and around the world have adopted regulations to control and limit exposure to radon in indoor environments. Directive 2013/59/Euratom released by the Council of the European Union requires the Member States of the European Union to adopt at national level a guideline value for ^{222}Rn indoor concentration of 300 Bq m^{-3}. WHO also recommends (Zeeb et al., 2009) to adopt a reference level possibly lower than 100 Bq m^{-3} and, in any case, not higher than 300 Bq m^{-3}, as well.

In Italy, to evaluate the average exposure of the population to ^{222}Rn in buildings, in the 90's the Italian National Institute for Environmental Protection and Research (ISPRA) and the Italian National Institute of Health (ISS) coordinated the first national ^{222}Rn survey. The first results provided an

estimate of the average national value of indoor ^{222}Rn of about 70 Bq m^{-3} and an average value for Campania region (in southern Italy) of 90 Bq m^{-3} (Bochicchio et al., 2005) which are, both, well above the worldwide mean of about 40 Bq m^{-3} (UNSCEAR (2000).

Since the geogenic component plays a key role in the onset of elevated Rn concentration in the indoor environments, national and regional surveys have been launched in some countries (e.g., Miles, 1998; Sarra et al., 2016) to identify the so-called radon prone areas (RPAs), whose selection should be based on both a limited number of indoor ^{222}Rn measurements (distributed across the territory to have a good statistical representativeness) and the geological features (lithologies, coverages, structures, etc.) of the studied territories (ICRP, 2007).

In Italy, the Regional Agency for the Protection of the Environment (ARPA) started a nation-wide project aiming at identifying RPAs, as required by the Italian Legislative Decree 230/95. Currently, only a few regions of central and northern Italy made publicly available RPAs regional maps, and the others only partially completed their indoor measurement campaigns.

As for Campania region, Guida et al. (2013) has proposed a preliminary regional RPAs map based only on geological and lithological features and Sabbarese et al. (2021) has published a ^{222}Rn potential concentration regional map based on the estimate of the indoor radon activity concentration using, as proxies, some literature and publicly available data on geology and faults network (Petrik et al., 2018), soils permeability (Duchi et al., 1995; Minolfi et al., 2018), morphological and climatic parameters (Minolfi et al., 2018), ^{238}U activity distribution (Lima et al., 2005), ^{226}Ra activity concentrations, ^{222}Rn emanation coefficients and exhalation rates from geological materials (Sabbarese et al., 2020), and gamma dose measurement in residential buildings (Quarto et al., 2013).

However, estimating the regional distribution of indoor Rn activity concentrations using a sample of gamma dose measurements from existing dwellings could lead to an overestimate of risks for undeveloped land, especially when the construction materials of the older buildings are made of geological materials of volcanic origin, which are, currently, barely used, as it is in Campania region.

To overcome this potential issue, ^{222}Rn flux density, which corresponds to the amount of ^{222}Rn delivered from the ground to the atmosphere in a given time interval, could be considered as a reliable parameter to assess ^{222}Rn risks in the long term (Stavitskaya et al., 2019) excluding the influence that local housing characteristics (Demoury et al., 2013) could exert on its variability.

In line with the above considerations, the Chinese Ministry of Construction, already in 2001, released the "Code for Indoor Environmental Pollution Control of Civil Building Engineering" (GB 50325-2001), establishing that a ^{222}Rn flux above 50 mBq m^{-2} s^{-1} could be considered as a trigger value to start prevention activities to avoid a potentially dangerous accumulation of indoor ^{222}Rn. Similarly, the Russian Federation released in 2010 the "Basic Sanitary Rules of Radiation Safety"

(OSPORB-99/2010) recommending a ^{222}Rn flux limit of 80 mBq m^{-2} s^{-1} for prospective construction sites (both public and residential buildings).

Measurements of ^{222}Rn flux can be achieved through different well-established methods such as passive closed and flow-through monitors (Zarhorowski and Whittlestone, 1996), activated charcoal Rn flux monitors (Countess, 1976), vented electret ion chamber (EIC) with an electrically conducting Tyvek window (Stieff et al., 1996), real-time Rn monitors (specialized ionization chamber, semiconductor detectors, scintillation cells) associated with an accumulation chamber (e.g. Alphaguard device series by Bertin Instruments SAS).

However, there are a lot of studies in which the ^{222}Rn flux (expressed as mBq m^{-2} s^{-1}) is estimated by equations that consider the physical and chemical properties of soils and rocks, such as the ^{222}Rn emanation coefficient, the ^{222}Rn diffusion coefficient, the radium (^{226}Ra) activity concentration in soil, etc. (Ielsch et al., 2002; UNSCEAR, 2000). In addition, terrestrial gamma radiation, which originates from the topmost layers of soil and depends on the concentration of the primordial radionuclides, is considered a good proxy for the estimation of the ^{222}Rn flux at the surface since its strength is controlled by the same factors that control the exhalation of ^{222}Rn such as bulk density, soil type, moisture content, etc. (UNSCEAR, 2000; Manhoar et al., 2013).

Based on the above considerations, since two huge databases are available for Campania region, including field measurements of the gamma radiation at ground (Lima et al., 2005; De Vivo et al., 2006) and chemical concentrations of some radioelements (U, Th, K) in soils (De Vivo et al., 2016), respectively, an estimate of the ^{222}Rn flux across the whole region was carried out applying an empirical method to both data sources.

The main objective of this work was to compare the radiogenic flux estimates of ^{222}Rn resulting from two sets of data with different characteristics and to analyse and interpret any differences which could arise in a geological perspective, if possible. The work also aimed at providing the Campania region with a tool for the management of the regional building development in consideration of the geogenic component that significantly contributes to the onset of health risks associated with the exposure of the population to terrestrial gamma radiation and ^{222}Rn.

5.2 Geological framework of Campania region

Campania, a region located on the south-western sector of the Italian peninsula, has a territory mostly characterized by the presence of volcanic lithotypes and sediments (Fig. 5.1). The geology of the region is the result of different processes and can be generally distinguished in a western coastal sector, occupied by alluvial plains and volcanic complexes, and a hilly eastern sector, mainly

occupied by the Apennines chain (Minolfi et al., 2018). This latter, NW-SE oriented, represents a fold and thrust belt system with vergence in the N-NE direction, developed during the Miocene. The sedimentary rocks, which characterize this part of the region, belong to Mesozoic Units made up of limestone, dolostone, siliceous schists and terrigenous sediments (clays, siltstone, sandstone, and conglomerate) (Buccianti et al., 2015; Minolfi et al., 2018). Starting from Miocene to present, the intense extensional forces associated with the formation of the Apennine chain generated intense block-faulting and rifting processes in the western area of the region (Vitale and Ciarcia, 2018). This area is occupied by a Plio-Pleistocene graben, filled by silico-clastic, carbonatic and evaporitic sediments originating from the mountain erosion, which constitutes the Sele and Campania plains, respectively.

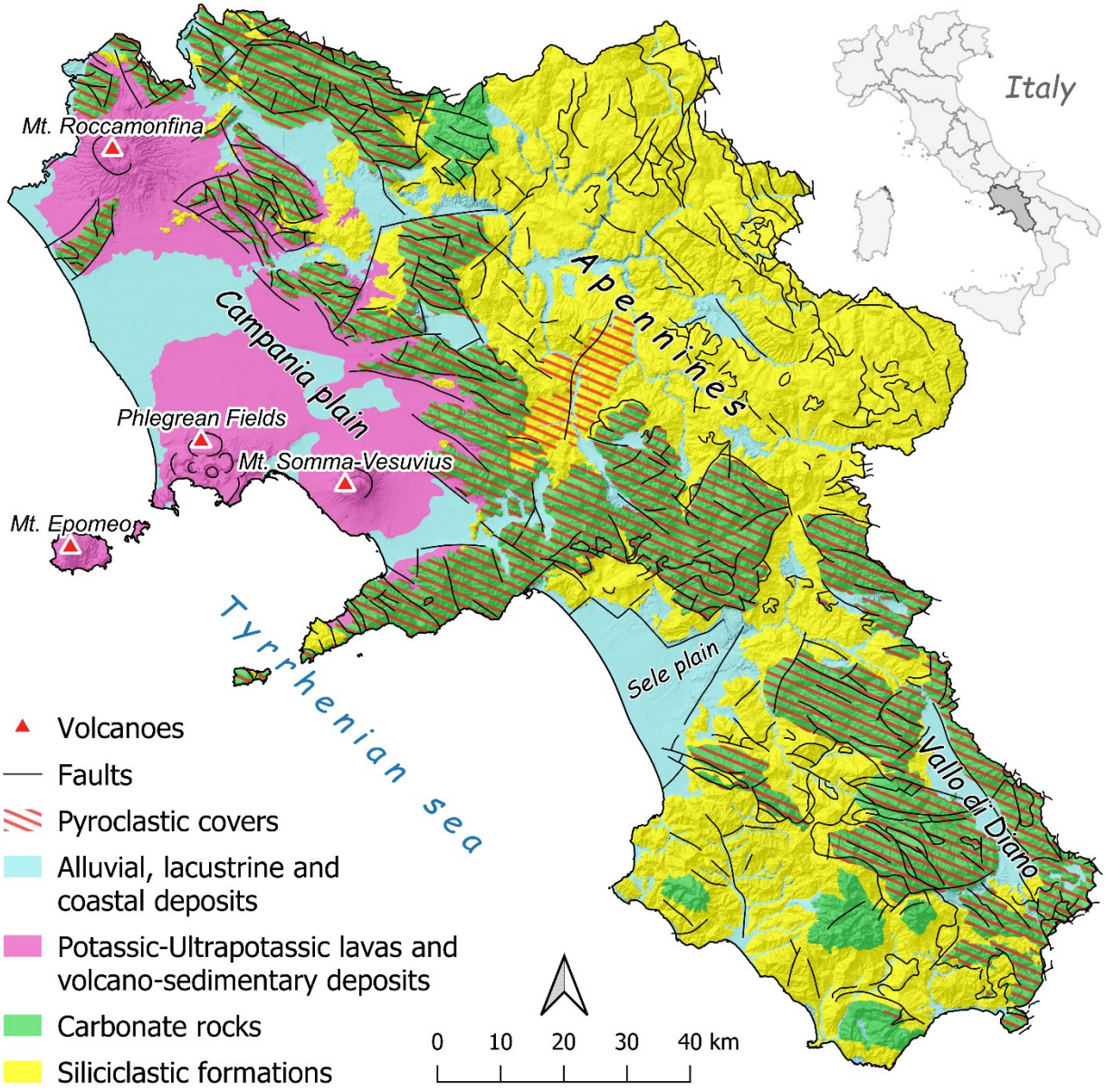

Figure 5.1 Simplified geo-lithological map of Campania region (modified after Zuzolo et al., 2018).

Related to the tectonism, from early Pliocene to present, several K-rich volcanic complexes developed (De Vivo et al., 2010; Peccerillo, 2005). The volcanism in Campania is part of the Roman Comagmatic Province and is characterized by four important volcanic complexes: Mt Somma-Vesuvius, Phlegrean Fields and Mt. Epomeo (i.e., Ischia Island) along the Tyrrhenian margin of the region, Mt. Roccamonfina at the north-western sector. The volcanic activity started about 600 ka BP to present and is represented by potassic to ultrapotassic lavas and pyroclastics (De Vivo et al., 2001). Pyroclastic fall deposits, which form cover beds on overall the carbonate rocks and, to a lesser extent, on the siliciclastic formations, represent the surface materials of a large portion of the region.

5.3 Materials and methods

5.3.1 Data source

5.3.1.1 Geochemical data

During several sampling campaigns, concluded in 2015, a total of 3822 topsoil samples were collected over the whole Campanian territory with an average density of 1 sample per ca. 4 km^2 (Fig. 5.2b). At each sampling point, about 2.5 kg of soil was collected within a depth between 5 and 15 cm, after removing the vegetation cover, according to the international sampling procedures guidelines established by the FOREGS Geochemistry Group (Salminen et al., 1998). To estimate the sampling variability, duplicate field samples were collected every 20 samples during the field activities. At the Environmental Geochemistry Laboratory (LGA) at University of Naples Federico II, all the samples were dried up by means of infra-red lamps, keeping the temperature below 35 °C; samples were, then, disaggregated in a ceramic mortar and sieved, retaining the 2 mm fraction for analysis. A total amount of 30 g of each sample, duly treated, was sent to the Bureau Veritas (formerly Acme Lab) Analytical Laboratories Ltd. (Vancouver, Canada) for chemical analysis by ICP-MS after an aqua regia digestion; duplicates of each sample were stored at the LGA storage room for future investigations.

Geochemical data produced through the different samplings campaigns have been validated and combined to produce a robust and geo-referenced database. Detailed information on analytical methods and statistical treatments applied to these datasets are widely present in literature (Buccianti et al., 2015; Minolfi et al., 2018; Zuzolo et al., 2020).

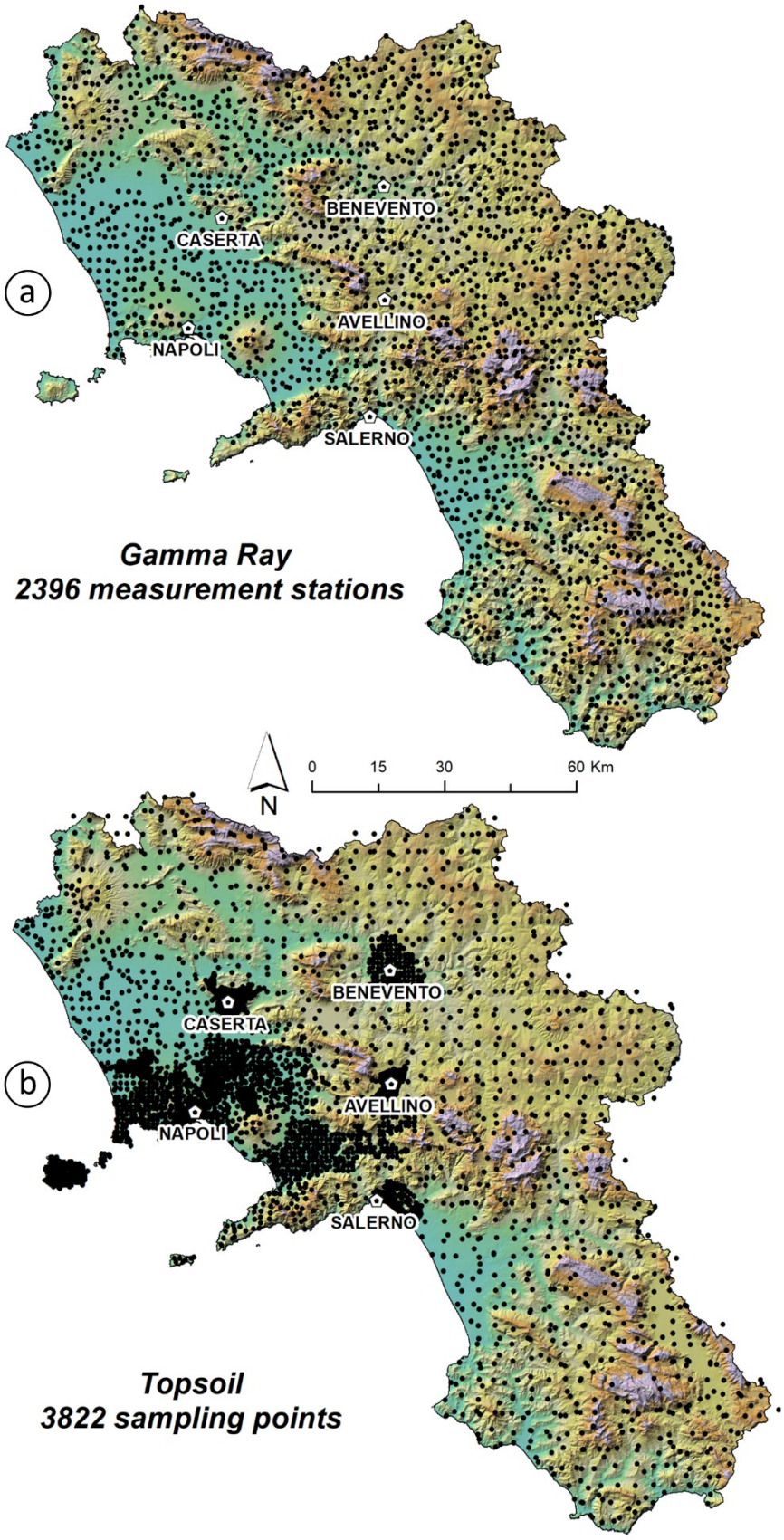

Figure 5.2 Location of the (a) measurement stations for radiometric data and (b) sampling points for geochemical data.

5.3.1.2 Gamma-ray spectrometry

In 2003 a gamma-ray spectrometry survey was completed with a nominal density of 1 station of measurement each 5 km^2, for a total of 2396 measurements, across the entire Campania region (Fig. 5.2a). Radiometric data were acquired by employing a GRS-500 portable scintillometer, produced by Scintrex Ltd (Ontario, Canada). The energy instrument window was suitably selected to measure the total natural gamma radiation emitted by ^{40}K, ^{238}U and ^{232}Th radioisotopes decay. Detailed information about the field measuring methods and the statistical data treatment can be found in Lima et al. (2005) and De Vivo et al. (2006).

5.3.2 Statistics and spatial patterns

Univariate descriptive statistics were generated (Table 5.2 and 5.3) for geochemical and radiometric raw data. For the graphical representation of the statistical distribution of the data, exploratory data analysis plots (in short, Edaplots) were generated in R for each variable. This plot, which combines in one graphical display a scatter plot, a histogram, a density plot and a boxplot, provides a deeper insight into the univariate data distribution and is considered one of the best graphical tools to show and analyse data distribution (Reimann et al., 2008).

Subsequently, both datasets were processed in a GIS environment and the data of each single variable (U, Th, K, ^{232}Th, ^{238}U , ^{40}K) were interpolated by means of the Multifractal Inverse Distance Weighted (MIDW) method (Cheng, 1999); MIDW, based on the principles that fractal and/or multifractal geometry could describe in a probabilistic way the spatial distribution patterns of geochemical variables, is able to depict the regional variability of the data while preserving the high frequency (anomaly) information which can be relevant in the analysis of phenomena related with the earth surface.

Using as input the generated MIDW grids, two colour composite maps (one for geochemical data, one for radiometric data) were produced. Specifically, the colour composite mapping method, which is a technique normally used in remote sensing, consists in combining three monochrome raster images (originally related to different spectral bands) in one, associating each of them to an additive primary colour (i.e. Red, Green, Blue); the technique has been already applied in geochemical mapping (Albanese et al., 2011; Zuzolo et al., 2018; Guagliardi et al., 2020) using as input three geochemical maps in raster format. In general, the ultimate result of the whole procedure is a unique colour composite map in which the value of each pixel is represented by a triplet of numbers (in the range 0-255) which corresponds to a specific colour in the RGB space, which is represented by a

cube. In the specific case of the present work, the final colour of each pixel in the composite map is a synthetic expression of both the value assumed by each variable in relation to its own statistical distribution (split into 256 intervals) and the relationship existing with the distribution of the other two variables involved. The vertices of the RGB cube associated with primary colours correspond, in our case, to the hypothetical condition of a composition made at 100% by one of three geochemical (or radiometric) variables involved while the remaining five vertices and the inner volume of the cube correspond to different compositional ratios among the components.

5.3.3 ^{222}Rn flux estimates

Both datasets have been exploited to estimate, for each sampling site, the fluctuation of ^{222}Rn flux from the ground across the Campania territory. Specifically, the concentrations of U, Th and K (expressed in mg kg^{-1} for U and Th, and in % for K, respectively) in regional topsoils and the activity generated by the decay of ^{238}U, ^{232}Th and ^{40}K (expressed as Bq) were used for the purpose. The method involved the use of different empirical relationships, from literature (Ahmed et al., 2018; Saito and Jacob, 1995; Lemercier et al., 2007; Szegvary et al., 2007b), to convert available data into a prediction of the ^{222}Rn flux, expressed in mBq m^{-2} s^{-1}.

Becquerel (Bq, also referred to as cps – counts per second) is the SI unit to express the activity of a radionuclide and corresponds to the number of atoms required to generate a radioactive decay in a second. It is thus related to the number of constituent atoms (N) and to the radioactive decay constant (λ) of a considered radionuclide (UNSCEAR, 2000; Nazaroff, 1992).

In our case, to estimate ^{222}Rn flux values, the first step consisted in converting all the available data for K, Th and U soil concentrations, on a side, and ^{40}K, ^{238}U and ^{232}Th activity, on the other side, into their own specific activity. Specific activity was, in fact, used as an input to calculate the Terrestrial Gamma Dose Rate (TGDR), expressed as nSv h^{-1}, which is the amount of energy expected to be absorbed by a person in a time unit associated with the gamma radiation emitted by radionuclides naturally occurring in Earth's crust (Manhoar et al., 2013).

For radiometric data, preliminarily, the activity in Bq was converted into the corresponding equivalent concentration values of U and Th (expressed as mg kg^{-1}), and K (expressed as %), using the formulas provided by the GRS-500 operation manual (Scintrex Limited, 1997) as follow (Eq. 5.1, 5.2, 5.3):

$$\text{eTh } [mg\ kg^{-1}] = \frac{1}{S_T}\ (C_T) \qquad \text{[Eq. 5.1]}$$

$$\text{eU } [mg\ kg^{-1}] = \frac{1}{S_U}\ (C_U - \alpha\ C_T) \qquad \text{[Eq. 5.2]}$$

$$eK\,[\%] = \frac{1}{S_K}\,[C_K - \gamma\,(C_U - \alpha\,C_T) - \beta\,C_T) \qquad \text{[Eq. 5.3]}$$

where:

- S_T, S_U, S_K are the sensitivity factors, derived from standard test pads, for the three radionuclides expressed in Bq (or cps) per mg kg^{-1} (for eTh and eU) and in Bq (or cps) per % (for eK), and are 0.054, 0.09 and 1.47, respectively (Scintrex Limited, 1997);
- C_T, C_U, C_K are the count rates for ^{232}Th, ^{238}U, and ^{40}K expressed in Bq (or cps);
- α, β and γ are the dimensionless stripping ratio, also derived from standard test pads, whose function is to eliminate Compton scatter from higher energy photo peaks as well as spectral interference, and are 1.28, 1.41 and 0.81, respectively (Scintrex Limited, 1997).

Subsequently, both U, Th and K concentrations and equivalent values (i.e. eTh, eU and eK), obtained from radiometric data, were used to calculate the specific activity, defined as the activity of a radionuclide per unit mass (in short, activity concentration) expressed as Bq kg^{-1}; more in details, the activity concentration of individual radionuclide was determined by mean of an experimental formula (Eq. 5.4) suggested by Ahmed et al. (2018):

$$A\,\left[\frac{Bq}{kg}\right] \equiv C\,\left[\frac{mg}{kg}\right]\,\varphi = C\,\left[\frac{N_A \ln(2)}{M_w\ T_{1/2}}\right] 10^{-3} \qquad \text{[Eq. 5.4]}$$

where:

- N_A is the Avogadro's constant ($6.02214076 \cdot 10^{23}$ mol^{-1});
- M_w is the molecular weight of the radionuclide in g mol^{-1} (Table 5.1);
- $T_{1/2}$ is the half-life of the radionuclide expressed in second (Table 5.1);
- ϕ is a conversion factor that assumes specific values (12. 36 for U, 4.06 for Th, 259.17 for K).

Table 5.1 Molecular weights and half-lives of the considered radionuclides.

	^{238}U	^{235}Th	^{40}K
M_w (u)	238.05	232.03	39.96
$T_{1/2}$ (year)	$4.5\ 10^9$	$1.405\ 10^{10}$	$1.277\ 10^9$

Known the specific activity concentration of single radionuclides, it was possible to estimate the TGDR from both geochemical ($TGDR_{geoc}$) and radiological ($TGDR_{rad}$) data at 1 m above the ground (expressed in nSv h^{-1}). As already stated, TGDR represents the natural contribution (derived from the crust materials) to the total ambient dose rate affecting an exposed human being (UNSCEAR, 2000; Manhoar et al., 2013). Specifically, by applying some specific dose conversion factors (Saito and Jacob, 1995; Lemercier et al., 2007) to activity concentration data it was possible to calculate TGDR as follows (Eq. 5.5):

$$\text{TGDR}\ [\text{nSv h}^{-1}] = \upsilon\ (^{238}U)\ +\ \tau\ (^{232}Th)\ +\ \kappa\ (^{40}K) \qquad \text{[Eq. 5.5]}$$

where:

- υ, τ, κ are the conversion factors whose values are 0.450, 0.599 and 0.0427 (expressed as nGy h^{-1} per Bq kg^{-1}), respectively. [NB, the Gray (Gy) is the unit used for the absorbed dose, while the Sievert (Sv) is the unit for the effective dose, both defined as one Joule of energy absorbed per kg of matter (J kg^{-1}). In our case 1Gy = 1Sv, because we are considering that the entire human body is exposed to radiation].

Once calculated the TGDR, ^{222}Rn fluxes, both the one related to geochemical data (^{222}Rn $flux_{geoc}$) and the one derived from radiometric data (^{222}Rn $flux_{rad}$), were predicted for the whole regional territory by mean of an empirical regression equation (Eq. 5.6) developed by Szegvary et al. (2007b) on the basis of direct field measurements of both ^{222}Rn flux, carried out with a portable radon monitor (Alphaguard 2000 Pro by Bertin Instruments SAS), and TGDR, obtained through the use of a gamma probe, in different locations of Europe:

$$^{222}Rn\ \text{flux}\ [\text{atoms cm}^{-2}\ \text{s}^{-1}] = \alpha\ \gamma - \text{ɓ} \qquad \text{[Eq. 5.6]}$$

where:

- γ is the gamma-dose rate in μSv h^{-1}
- α and ɓ are dimensionless factors whose values are 11.75 (± 1.27) and 0.15 (± 0.11), respectively.

Once determined, the values of the ^{222}Rn $flux_{geoc}$ and ^{222}Rn $flux_{rad}$ were converted into mBq m^{-2} s^{-1} and, finally, interpolated by means of MIDW. The obtained interpolated grids were classified by means of the concentration-area (C-A) method (Cheng et al., 1994; Zuo and Wang, 2019). The latter is based on the use of a specific logarithmic plot reporting the cumulative values of areas covered by pixels in the ordinate axis and the values of elemental concentrations assigned to pixels in the abscissa. The inflexion points along the C-A plot are representative of the changes occurring in the power laws (represented by linear segments) characterizing the statistical distribution of different subpopulations of pixels within the grid. Using the concentration values corresponding to the inflexion points to set map intervals allow to generate geochemical/compositional maps whose patterns better reflect the geogenic and anthropogenic processes underlying the variability of the datasets (Albanese et al., 2007).

To quantitatively assess the functional relationship among ^{222}Rn $flux_{geoc}$ and ^{222}Rn $flux_{rad}$, a linear regression was also applied to them. For this purpose, about 1500 points, randomly distributed across the regional territory, were generated in GIS and used to extract cell values from both the ^{222}Rn flux

raster maps. Values were, then, used to generate a scatter plot to explore the relationship among the two distributions by fitting a linear function, considering ^{222}Rn flux$_{geoc}$ as the independent variable.

Residuals of ^{222}Rn flux$_{rad}$ with respect to the linear function determined were also estimated, and their absolute values were used to better show their distribution on plot.

Residuals were also used to generate a raster (MIDW) map of their distribution, which was classified through the C-A method, as well. Specifically, since non-negative values are required to generate a C-A plot, equation 5.7 (Somma et al., 2021) was applied to original residual values prior to apply the C-A method:

$$Residuals_{scaled} = (residuals - Min_{residuals}) + 0.1 \quad \text{[Eq. 5.7]}$$

Once the subpopulations of residuals were discriminated on residuals, scaled according to Eq. 5.7, values were back-transformed to set up the intervals in the map.

Furthermore, both ^{222}Rn flux grids were compared between themselves by mean of the Map Comparison Kit (MCK), version 3.3, developed by the Research Institute for Knowledge Systems (RIKS), which is a software for analysis and comparison of raster maps with the same resolution and extend. The comparison method used was the "fuzzy numerical" (RISK, 2013) and it is based on the following formula (Eq. 5.8):

$$s(a,b) = 1 - \frac{|a-b|}{\max(|a|,|b|)} \quad \text{[Eq. 5.8]}$$

Where:

- a and b are the values of pixels from the rasters being compared.

The resulting grid show the variation of the degree of similarity (expressed in %) among the two raster maps across the whole spatial domain of interest (i.e. Campania region), where 100% means that the values are fully identical and 0% that they are fully distinct.

5.4 Results and discussion

5.4.1 Geochemical and radiometric patterns

The summary statistics of U, Th and K concentrations in topsoils and of ^{238}U, ^{232}Th and ^{40}K activity is displayed in Table 5.2. On average, concentrations of U and Th are lightly more abundant than

topsoils European average values (of 2.03 mg kg^{-1} for U, 7.24 mg kg^{-1} for Th and 1.92 % for K) while for K are slightly lower (De Vos and Tarvainen, 2006). Concentrations vary from 0.05 to 23.7 mg kg^{-1} for U, from 0.3 to 59.1 mg kg^{-1} for Th and from 0.03 to 5.97 % for K. As for radioactivity, ^{238}U shows activity values ranging from 0.1 to 4.8 Bq, ^{232}Th from 0 to 2.8 Bq and ^{40}K from 0.5 to 35 Bq.

Table 5.2 Summary statistics of U, Th and K concentrations in topsoils and of ^{238}U, ^{232}Th and ^{40}K activity.

	Concentration in topsoil			***Radioactivity***		
	U	***Th***	***K***	***^{238}U***	***^{232}Th***	***^{40}K***
Unit	***mg kg^{-1}***		***%***		***Bq***	
DL	0.10	0.10	0.01	0.00	0.00	0.00
Min	0.05	0.30	0.03	0.10	0.00	0.50
Q_1	1.70	7.30	0.43	0.70	0.15	1.90
Median	3.00	11.70	0.83	1.00	0.30	2.60
Q_3	4.60	15.70	1.55	1.60	0.50	3.51
Max	23.70	59.10	5.97	4.80	2.80	35.00
Mean	3.33	12.11	1.20	1.20	0.37	3.03
St.Dev.	2.20	6.62	1.05	0.71	0.33	1.80
Skeweness	1.35	1.16	1.46	1.29	2.53	3.48
Kurtosis	4.10	3.52	1.46	1.99	9.65	42.82

The RGB maps, compiled for both geochemical and radiometric data, show a marked dependence of their pattern variability on the main geo-lithological (including pyroclastic coverages) features of the territory (Fig. 5.3). Generally, high values of both U, Th, and K concentrations and ^{238}U, ^{232}Th, and ^{40}K activity (characterized by the brightest colours in maps) correspond well with the volcanic centres in the central-western sector of the region, whereas concurrent low values of the triplets in both maps (represented by greyish/darkish colours) are found in areas characterized by the presence of siliciclastic and carbonate deposits, prevailing in the southern and eastern sectors of the region.

More in detail, we can observe how the ^{238}U-^{40}K association is more marked in correspondence of the Vesuvian territory and of the western sector of Mt. Roccamonfina, whereas the association ^{238}U-^{232}Th is clearly preponderant in the north-eastern part of this latter. As for geochemical data, the soils of Mt. Roccamonfina and of the surrounding areas are clearly marked by a prevalence of Th concentrations while the Vesuvian territory, similarly to what is showed by radiometric data, is featured by a coincident increase of U and K concentrations. Phlegrean Fields, in the case of radiometric values, show, by eye, a similarity with the vesuvian territory; in the case of geochemical data, they are characterized by a darkish green colour which means that there is a general depletion of all three elements with a slightly lesser impoverishment of Th contents.

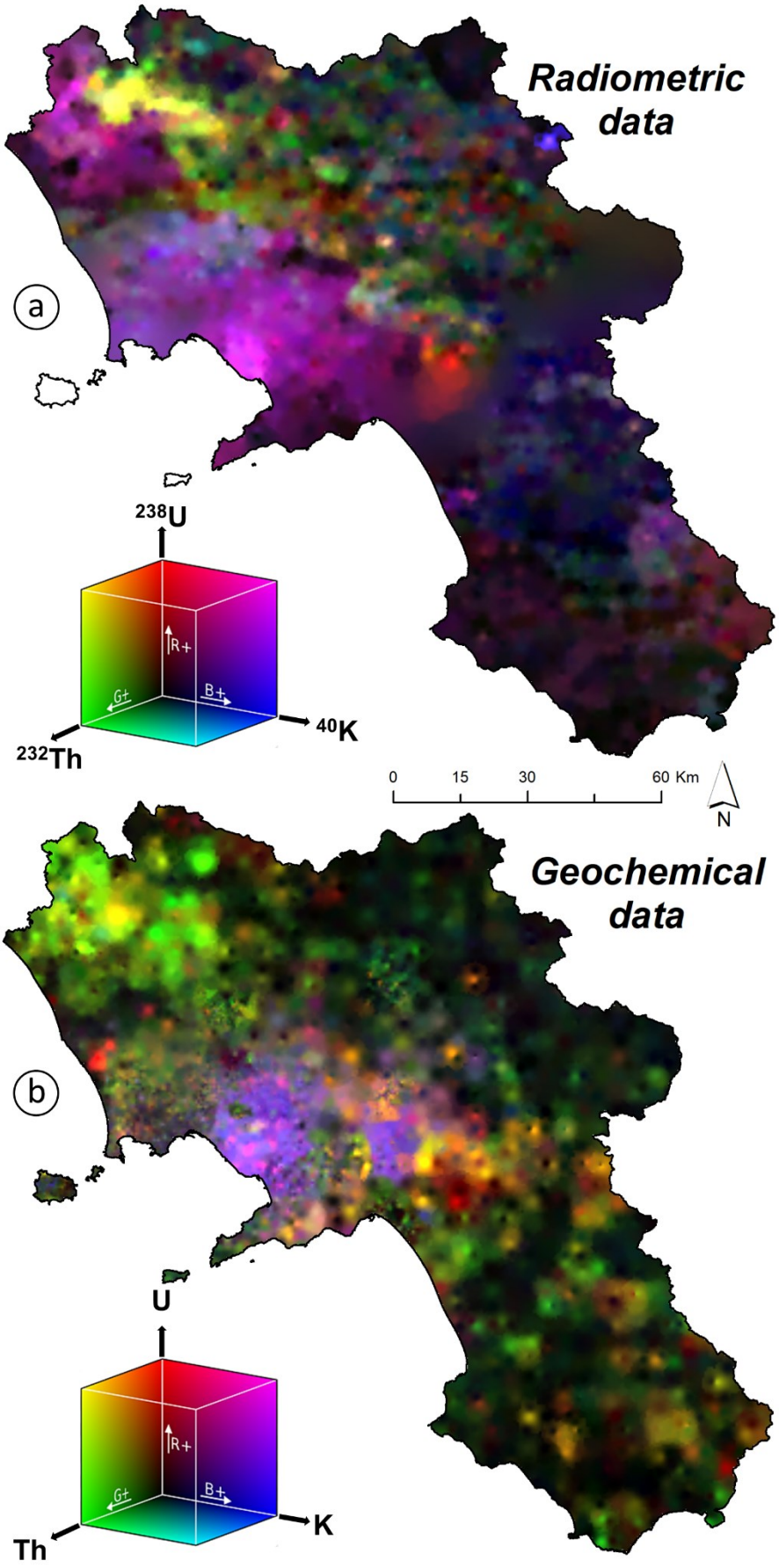

Figure 5.3 RGB map of (a) ^{238}U, ^{232}Th and ^{40}K activity values and (b) U, Th, K concentrations in topsoils.

The preponderance of the ^{238}U-^{40}K association in the radiometric patterns can be explained, in general, by the overall potassic and ultrapotassic nature of the Campanian volcanism, whereas the differences in the colour composite map generated from compositional data are informative with respect to the geochemical mobility and the timing of exposure to weathering processes of soils of the volcanic complexes of Campania (Zuzolo et al., 2018). As a matter of fact, the difference in Th distribution in Campania can be explained by pedogenetic processes, which are more advanced in the areas around Roccamonfina, causing K and U depletion and Th enrichment along with Fe and Mg oxides (Navas et al., 2005; Lima et al., 2005; De Vivo et al., 2016). Mt. Somma-Vesuvius volcanic activity is much more recent (from > 25 ka to date) than that of Roccamonfina (from 600 to 150 ka), and the young soils are more similar to volcanic rock sources.

By comparing the specific activity values obtained from both datasets, it can be seen how the values related to radiometric data are higher than the ones related to geochemical data for both U (mean is 108.22 Bq kg^{-1} and 41.17 Bq kg^{-1}, respectively) and K (mean is 360.29 Bq kg^{-1} vs 309.72 Bq kg^{-1}); the opposite holds true for Th (mean of 24.24 Bq kg^{-1} vs 49.18 Bq kg^{-1}) (Table 5.3).

Table 5.3 Summary statistics of the activity concentration, TGDR and ^{222}Rn flux values related to both geochemical and radiometric datasets.

Variable	U_A	Th_A	K_A	eU_A	eTh_A	eK_A	$TGDR_{geo}$	$TGDR_{rad}$	$^{222}Rn\ flux_{geoc}$	$^{222}Rn\ flux_{rad}$
Unit			**Bq kg^{-1}**				**nSv h^{-1}**		**mBq m^{-2} s^{-1}**	
Min	0.62	1.22	7.78	0.55	0.00	0.48	3.15	11.59	0.0002	0.15
Q_1	21.01	29.64	111.4	54.93	9.77	189.4	35.61	48.48	6.56	7.90
Median	37.08	47.50	215.1	83.50	19.55	312.5	59.58	63.76	12.02	12.08
Q_3	56.86	63.74	401.7	144.9	30.07	464.6	83.45	100.8	18.17	22.29
Max	292.9	239.9	1547	585.7	180.4	5747	253.4	378.8	63.82	98.12
Mean	41.17	49.18	309.7	108.2	24.24	360.3	61.21	78.60	12.69	16.19
St.Dev.	27.15	26.86	272.3	76.14	20.57	261.8	31.79	43.76	8.01	11.91
Skeweness	1.35	1.16	1.46	1.37	2.29	4.89	0.49	1.45	0.61	1.47
Kurtosis	4.10	3.52	1.46	2.16	9.02	83.67	0.20	2.83	0.61	2.87

5.4.2 TGDR and ^{222}Rn fluxes

$TGDR_{geoc}$ values show an almost mesokurtic distribution, with most of the values equally dispersed in the range between the minimum and the third quartile (at 83 nSv h^{-1}). Potential outliers are not particularly numerous, and an anomaly threshold could be set at about 150 nSv h^{-1} in correspondence with the upper Tukey fence of the boxplot. The distribution of $TGDR_{rad}$ data have a more marked leptokurtic distribution, with a peak well in evidence falling between the first quartile (at 35.61 nSv h^{-1}) and the median value (at 63.76 nSv h^{-1}), and a marked asymmetry toward the right

as also highlighted by the value of the skewness and by the considerable difference existing among the mean and the median value. $TGDR_{rad}$ data are characterized by a wider range of the values (maximum is 378.81 nSv h^{-1} compared to the 253.38 nSv h^{-1} of the $TGDR_{geoc}$) and a wider number of observations above the upper Tukey fence which can be classified as potential outliers.

In general, TGDRs obtained from both datasets are roughly in line with those proposed by Szegvary et al. (2007a), which presented the result of a direct monitoring of the gamma-dose rate at a continental scale. In that work, TGDR values for Europe were determined using the data extracted from the EUropean Radiological Data Exchange Platform (EURDEP), which is a network, developed and maintained by the Joint Research Centre (JRC) of the European Commission, for the continuous exchange of radiological monitoring data between European countries.

Besides, seasonal data, in the form of total gamma-dose rate (nSv h^{-1}), also containing the cosmic and the artificial contribution to the gamma-dose as well as the instrument background, were retrieved from the Radioactivity Environmental Monitoring (REMon) for winter and summer 2006, by Cinelli et al. (2019), with the purpose of extracting the natural TGDR contribution for Europe. For Campania region, results showed values ranging between 65 and 80 nSv h^{-1} (with very slight differences between the two seasons) which fit well with the central tendency of TGDR distributions presented in Figs. 5.4a and 5.4b.

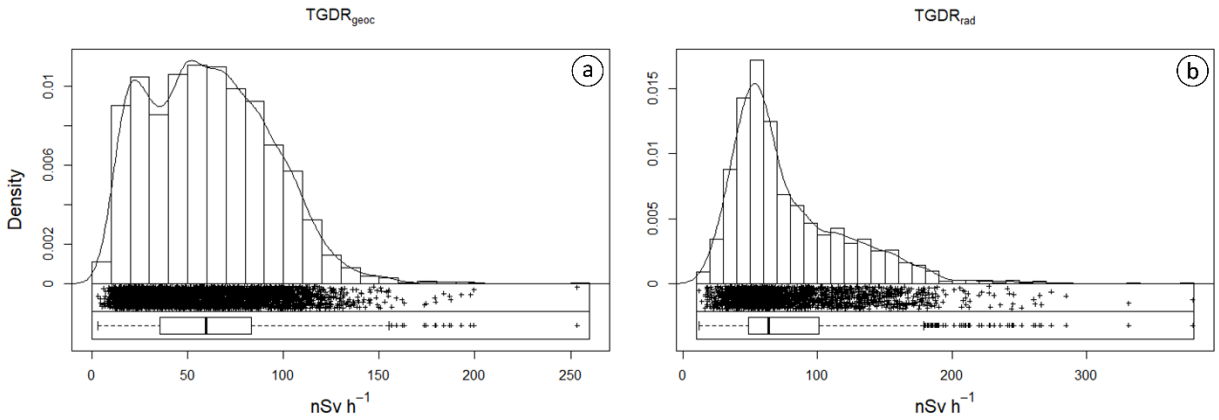

Figure 5.4 Edaplots of (a) TGDRgeoc e (b) TGDRrad.

Maps of both ^{222}Rn $flux_{geoc}$ and ^{222}Rn $flux_{rad}$ are reported in Figure 5.5. The spatial distributions of flux values, following the C-A classification of data, show similar patterns, with higher values in correspondence of the volcanic lithotypes (i.e., within the perimeter of the volcanic centres and in correspondence with the pyroclastic covers) and lower values in correspondence with sedimentary (mostly siliciclastic) formations. However, as already seen for the TGDR values, throughout the whole area, the flux estimates based on radiometric data are, generally, higher than the ones based on

geochemical data. As a matter of fact, $^{222}Rn\ flux_{rad}$ and $^{222}Rn\ flux_{geoc}$ show a mean value of 16.19 mBq m^{-2} s^{-1} and 12.69 mBq m^{-2} s^{-1}, respectively (Table 5.3). However, these latter values both result abundantly below the average world value of 33 mBq m^{-2} s^{-1} proposed for an ideal mass of homogeneous dry soil by UNSCEAR (2000), and in accordance with the mean worldwide flux of 15.75 mBq m^{-2} s^{-1} proposed by Wilkening et al. (1972) and the global average of the Rn exhalation rate of 18.0 mBq m^{-2} s^{-1} calculated by Goto et al. (2008) assuming an invariable ^{226}Ra concentration in soil.

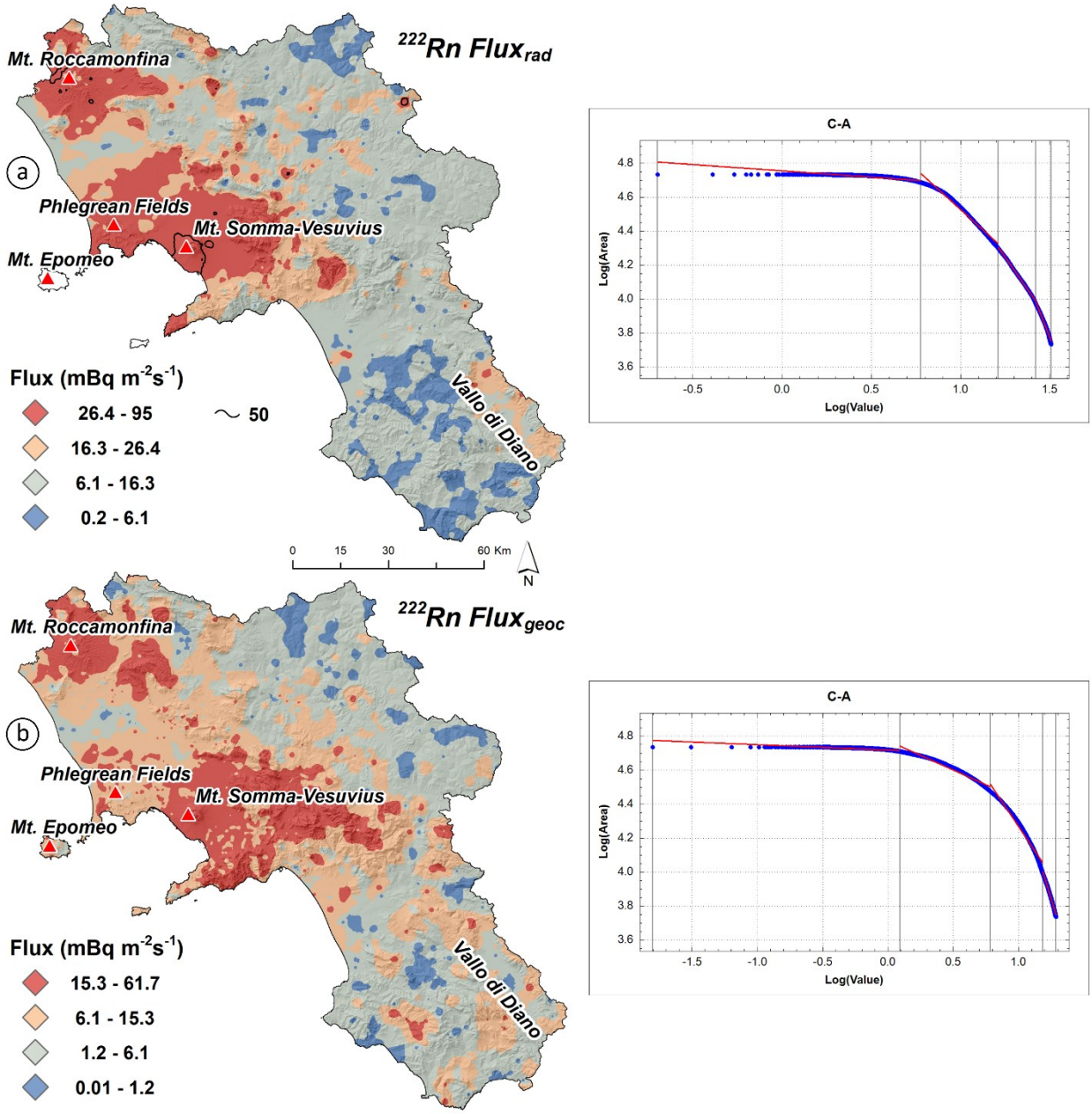

Figure 5.5 ^{222}Rn flux interpolated maps relative to (a) radiometric data and (b) geochemical data.

By analysing the patterns more in details, the ^{222}Rn $flux_{rad}$ shows a neater separation among volcanic areas, featured by values above 16.3 mBq m^{-2} s^{-1}, and the inner territories where siliciclastic materials are predominant.

The lowest values of the flux feature the extreme north-eastern sector of the region and some areas in the south-western territories with values below 6.1 mBq m^{-2} s^{-1}. However, close to these latter areas, some singularities (i.e., areas of limited extension whose values differ from the spatial context in which they are located) are also present in the map with values above 16.3 mBq m^{-2} s^{-1}.

The map of ^{222}Rn $flux_{geoc}$, on the overall similar to the ^{222}Rn $flux_{rad}$, presents a sort of transition buffer featured by values between 6.1 and 15.3 mBq m^{-2} s^{-1} moving from the volcanic toward the sedimentary domain; this interval roughly corresponds to those areas with the presence of pyroclastic covers over sedimentary lithologies and to most of the Phlegrean Fields territory and its surrounding areas.

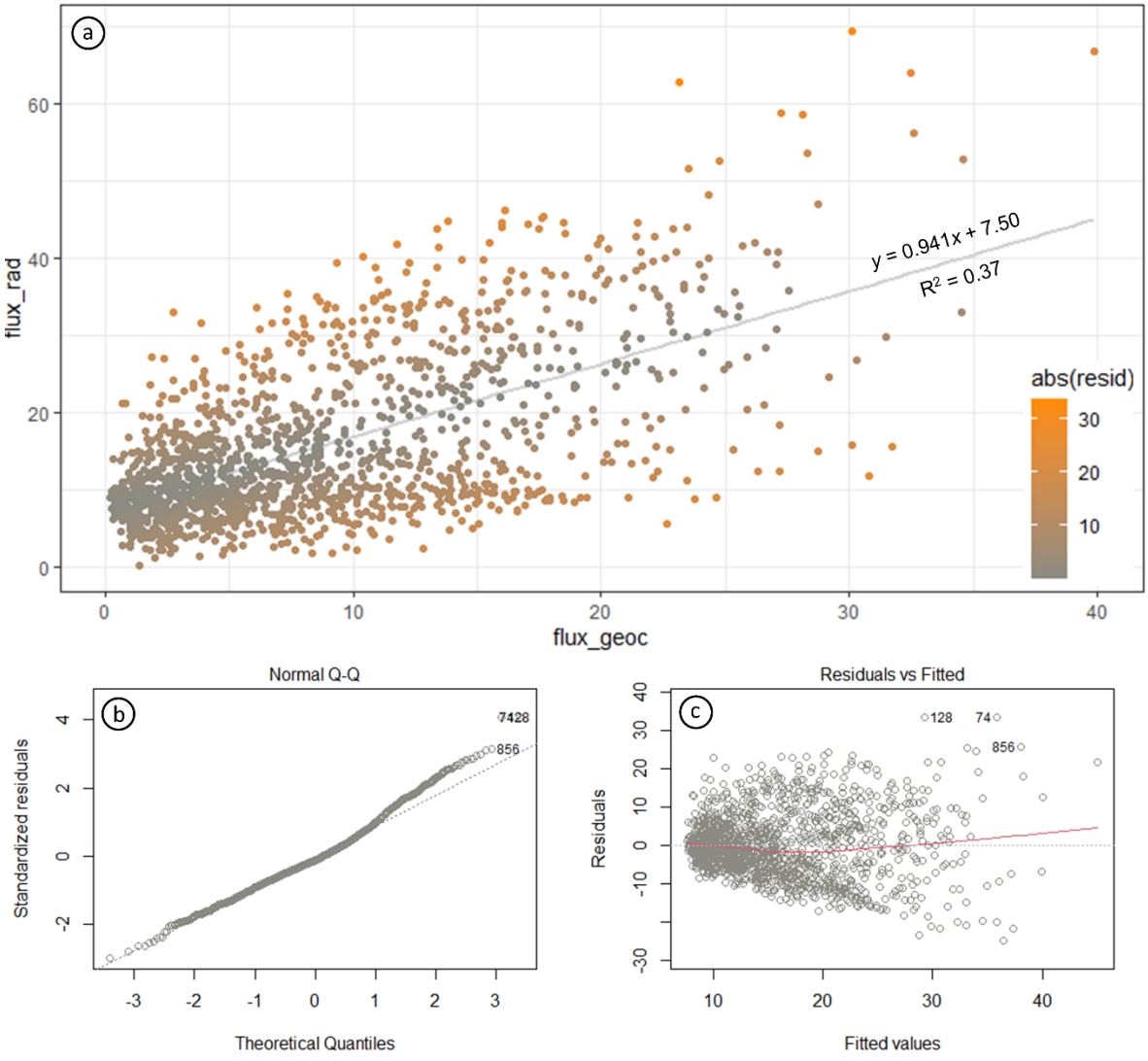

Figure 5.6 ^{222}Rn flux from radiometric data vs. ^{222}Rn flux from concentration data: (a) Scatter plot with regression line and observations coloured on the basis of the corresponding residual absolute values, (b) Normal Q-Q Residuals plot and (c) Residuals vs Fitted values plot.

5.4.3 Analysis of residuals and similarities

The function determined by the linear regression applied among ^{222}Rn flux$_{geoc}$ and ^{222}Rn flux$_{rad}$ show a coefficient of determination (R-squared) of 0.367, which means that the predictor variable (^{222}Rn flux$_{geoc}$) can explain 37% of the variance of the response variable (^{222}Rn flux$_{rad}$) (Fig. 5.6a).

The p-value of 2.2E-16 clearly indicates that there is a statistically significant relationship between the two variables even though the total variance is not fully explained by the relationship.

Standardised residuals seem to be quite normally distributed (Fig. 5.6b), although they are slightly right-skewed, indicating that higher values tend to deviate from the expected distribution.

The plot of residuals vs fitted values (Fig. 5.6c) (estimated according to the linear function found through regression analysis) does not show any markedly discernible pattern around the "zero" value line confirming the general linear assumption; however, a closer look at the details allows to discriminate both a linear trend for some negative residuals, in correspondence of the fitted values within the lower part of points cloud, and some outliers on the right sector of the plot, as confirmed by the local regression curve (in red) and in accordance with the distribution of the standardised residuals in Fig. 5.6b.

The map of residuals (Fig. 5.7a) represents a valuable tool to interpret their variability based on their spatial distribution. Markedly positive residuals (ranging from 6.55 and 33.31 mBq m^{-2} s^{-1}) are mostly detectable in correspondence with the northern coastal sector of the region where the volcanic centres are located (i.e., Mt. Somma-Vesuvius, Mt. Roccamonfina, Phlegrean Fields). Considering that the measured gamma-ray activity levels (and related TGDR) are a function of the amount of radioelement-bearing minerals contained in the geological materials being gauged and the activity estimated from geochemical data is directly related to elemental concentrations of U, Th and K in the analysed sample, we can infer that the high residuals of volcanic areas depends not so much by the pyroclastic nature of the pedological coverages but rather by the presence of thick layers of lavas and other volcanic lithoid materials below the surface (Vitale and Ciarcia, 2018).

As a matter of fact, the Scintrex GRS-500, among the others, processes gamma radiations within the energy windows between 1.65 and 1.87 MeV and between 2.45 and 2.79 MeV, respectively; hence, measurements include gamma radiation associated to ^{214}Bi (at 1.76 MeV) and ^{208}Tl (at 2.62 MeV), which are considered daughter decay products of ^{222}Rn (in the U series) and ^{220}Rn (in the Th series), respectively. Therefore, whereas the ^{222}Rn flux$_{geoc}$ estimates exclusively depends on the concentration of U and Th (and K) in soils, the ^{222}Rn flux$_{rad}$ is also related to other radionuclides (belonging to the same chains) whose presence in soil partially depends on the migration toward the surface of ^{222}Rn and ^{220}Rn from underground radioactive layers.

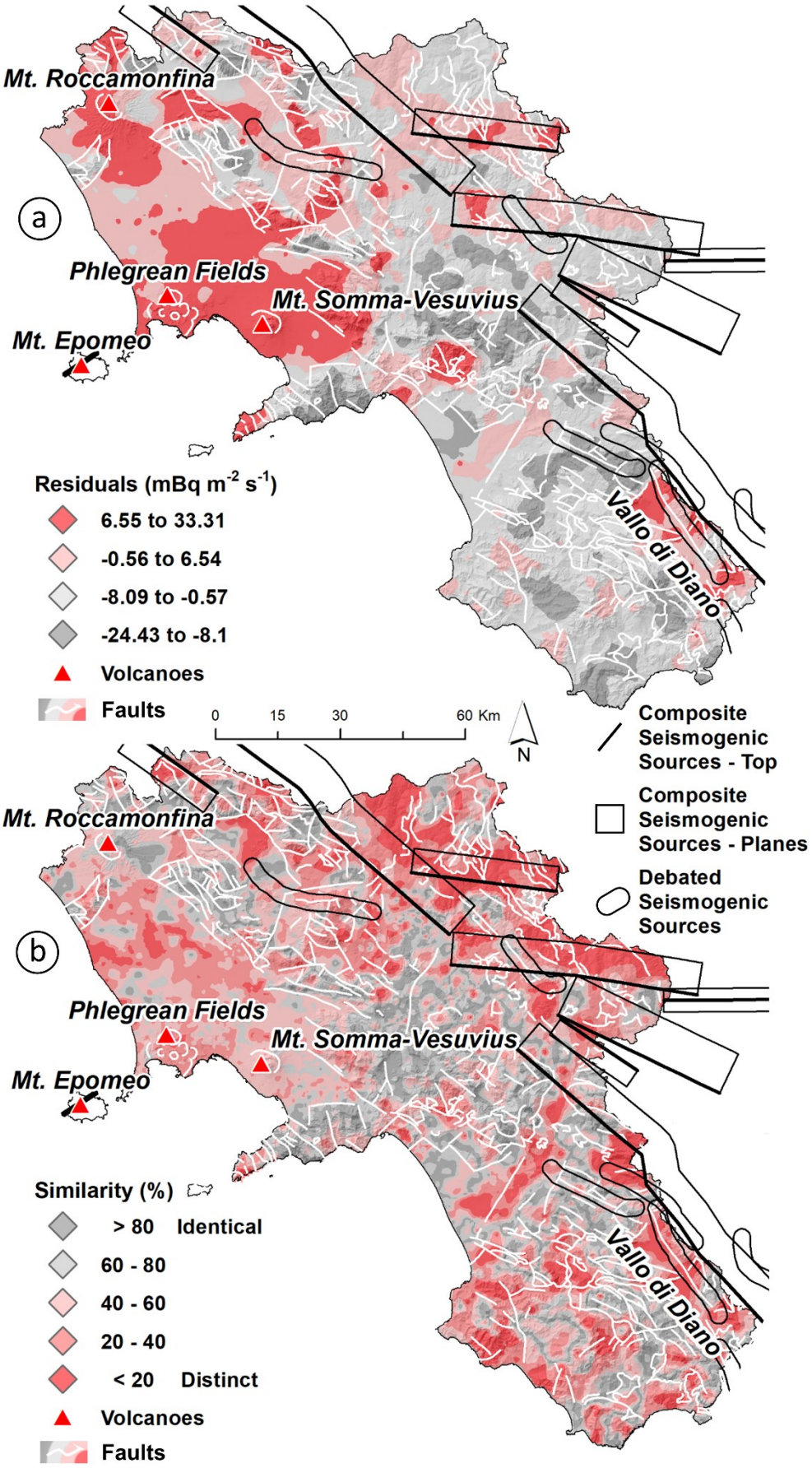

Figure 5.7 ^{222}Rn flux maps comparison: (a) residuals map (b) and similarity map of flux determined from geochemical data and radiometric data.

As for the slightly positive residuals (<6.54 mBq m^{-2} s^{-1}) characterizing the Apennine reliefs (mantled by loose pyroclastic deposits) and the Campania plain (where alluvial sediments are partly made of transported volcanic materials proceeding from the same reliefs), the differences could be related to the mineral composition of soil. In fact, some minerals which contain high concentration of U and Th, such as zircon or monazite, are not completely dissolved by aqua regia extraction and so the measurement by ICP-MS can underestimate the content of such elements (Lima et al., 2005), while this does not happen measuring radioactivity on field.

Slightly high and high positive residuals also characterize the terrains of Vallo di Diano, an upland in the south-eastern sector of the region, and other areas of limited extensions in the north-eastern regional territory where, in contrast with the coastal areas, siliciclastic lithologies are predominant. In these latter cases, a ^{222}Rn $flux_{rad}$ higher than the expected value (hence positive residuals) could be associated with the presence of seismogenic sources (DISS Working Group, 2018) in accordance with the hypothesis that radon flux density at the Earth's surface can be accentuated by a high stress and strain state of the geological environment (King et al., 1996; Yakovleva and Karataev, 2007; Chen et al., 2018; Sun et al., 2018).

Although the graphical patterns of the map of residuals (Fig. 5.7a) are roughly kept in the similarity distribution map (Fig. 5.7b), it is worth noting that, in general, the areas featured by the highest positive values of residuals are, in contrast, characterized by a higher similarity among maps of ^{222}Rn $flux_{geoc}$ and ^{222}Rn $flux_{rad}$ whereas, the areas with less marked positive residuals are featured by a stronger dissimilarity. In facts, the lowest values of similarity feature the inner portions of the Campania territory where the presence of seismogenic sources was considered as a potential factor influencing the increase of ^{222}Rn $flux_{rad.}$

5.4.4 Risk assessment

Aiming at determining the distribution of the potential regional hazard associated with ^{222}Rn using its flux estimates, we decided to compare our results with available national or international guidelines. Since there is no regulation that establishes a limit threshold either at national or European level, we considered the Chinese and Russian regulations. The first one, the "code for Indoor Environmental Pollution Control of Civil Building Engineering in China" (GB 50325–2010), establishes a level of 50 mBq m^{-2} s^{-1} below which there is no need of prevention and control of Rn flux density; the second one, the "basic sanitary rules of radiation safety" (OSPORB-99/2010), establishes a recommended limit of 80 mBq m^{-2} s^{-1} for construction sites. Among the two available options, we selected the most conservative one to be used as a reference, and, in view of the

abovementioned considerations, all regional areas showing a flux above 50 mBq m^{-2} s^{-1}, in accordance with the Chinese regulation (GB 50325-2010), were delimited in fig. 4a. Among the others, an area of 90 km^2 on the south-western sector of the Mt. Somma-Vesuvius complex is characterized by ^{222}Rn flux overcoming the considered threshold; this area includes most of the urbanized territory of two populous towns (Torre del Greco and Torre Annunziata) inhabited by about 130.000 persons with an average density of more 3000 pop./km^2. Consequently, considering that the average regional population density is about 420 pop./km^2, the latter area could be associated with a relevant public health risk due to environmental exposure to ^{222}Rn.

An analysis of the data on lung cancer incidence for the decade 2008-2018 in the population of the southern sector of the metropolitan area of Naples (Available at https://www.registrotumorinapoli3sud.it/it/, last accessed on 22nd May 2021), including the territory of Torre Annunziata and Torre del Greco, shows that the sanitary districts to which the two municipalities belong are featured by a Standardized Incidence Rate (SIR) of 125 and 129, respectively; this values are slightly above the local average value (124) and reflect the general tendency of the areas belonging to the volcanic district of Mt. Somma-Vesuvius to be featured by SIR values above 100 (which refers to the European population).

Another smallest area, on the north-western sector of Mt. Roccamonfina, is also characterized by ^{222}Rn fluxes above the chosen reference threshold; however, since in this area there are only small villages (belonging to the municipality of Sessa Aurunca) where a very small number of people use to live, the overall ^{222}Rn risk can be considered limited.

5.5 Conclusions

The cross-analysis of the results obtained made it possible to discriminate in more detail the nature of the different sources that potentially contribute to the surface radon fluxes in Campania. It is to be assumed that the flux estimates based on radiometric measurements ($^{222}Rn\ flux_{rad}$) have a greater adherence to the real flux values, which are the subject of a survey activity still in progress in the region.

However, it has been possible to ascertain that, considering some limits of the geochemical data in evaluating ^{222}Rn fluxes, the comparison (by means of adequate statistical tools) of flux estimates (from radiometric and geochemical data) can facilitate the understanding of some peculiarities found in the distribution patterns of $^{222}Rn\ flux_{rad}$. In fact, based on residuals and similarities, it was possible to hypothesize an underground contribution to the surficial ^{222}Rn flux for some regional areas characterized by the presence of deep volcanic layers and/or by the presence of active tectonic

structures. Obviously, since these are estimates, the results obtained from the present study must be seen as preliminary pending confirmation from direct field measurements.

As a matter of fact, if the results of the proposed technique will be verified by the field checks, the availability of previously gathered geochemical and radiometric data could make it possible to assess and, possibly, interpret the distribution patterns of ^{222}Rn flux for large areas where direct measurements are missing and cannot be carried out.

This last consideration could assume great relevance especially from a health safety perspective since, as demonstrated for the Campania region, the estimates of fluxes, where considered reliable, could be used to discriminate areas for which the risks from exposure to ^{222}Rn could be relevant for the local population. Furthermore, if the comparison among $^{222}Rn\ flux_{rad}$ and $^{222}Rn\ flux_{geoc}$ would be confirmed as a tool to locate seismogenic sources and buried radioactive layers, the existence of debated hidden geological features could be confirmed by applying the technique presented here. Of course, in case direct measurements of flux would be available, the comparison of this latter with $^{222}Rn\ flux_{geoc}$ could be even more effective in finding sources not related to the compositional characteristics of soils but with underlying geological bodies and structures.

References

Ahmed, R.S., Mohammed, R.S., Abdaljalil, R.O., 2018. The Activity Concentrations and Radium Equivalent Activity in Soil Samples Collected from the Eastern Part of Basrah Governorate in Southern Iraq. Int. J. Anal. Chem. https://doi.org/10.1155/2018/2541020

Albanese, S., Cicchella, D., De Vivo, B., Lima, A., Civitillo, D., Cosenza, A., Grezzi, G., 2011. Advancements in urban geochemical mapping of the Naples Metropolitan Area: colour composite maps and results from an urban brownfield site. In: Mapping the Chemical Environment of Urban Areas, 410–423.

Albanese, S., De Vivo, B., Lima, A., Cicchella, D., 2007. Geochemical background and baseline values of toxic elements in stream sediments of Campania region (Italy). J. Geochem. Explor. 93 (1), 21-34. https://doi.org/10.1016/j.gexplo.2006.07.006.

Baubron, J.C., Allard, P., Sabroux, J.C., Tedesco, D., Toutain, J.P., 1991. Soil gas emanations as precursory indicators of volcanic eruptions. J. Geol. Soc. London 148 (3), 571-576. https://doi.org/10.1144/gsjgs.148.3.0571

Bochicchio, F., Campos-Venuti, G., Piermattei, S., Nuccetelli, C., Risica, S., Tommasino, L., Torri, G., Magnoni, M., Agnesod, G., Sgorbati, G., Bonomi, M., Minach, L., Trotti, F., Malisan, M.R., Maggiolo, S., Gaidolfi, L., Giannardi, C., Rongoni, A., Lombardi, M., Cherubini, G., D'Ostilio, S., Cristofaro, C. , Pugliese, M., Martucci, V., Crispino, A., Cuzzocrea, P., Sansone Santamaria, A., Cappai, M., 2005. Annual average and seasonal variations of residential radon concentration for all the Italian Regions. Radiat. Meas. 40, 686–694.

Buccianti, A., Lima, A., Albanese, S., Cannatelli, C., Esposito, R., De Vivo, B., 2015. Exploring topsoil geochemistry from the CoDA (Compositional Data Analysis) perspective: the multi-element data archive of the Campania Region (Southern Italy). J. Geochem. Explor. 159, 302-316.

Cheng, Q., 1999. Spatial and scaling modelling for geochemical anomaly separation. J. Geochem. Explor. 65, 175–194.

Cheng, Q., Agterberg, F.P., Ballantyne, S.B., 1994. The separation of geochemical anomalies from background by fractal methods. J. Geochem. Explor. 51 (2), 109-130. https://doi.org/10.1016/0375-6742(94)90013-2.

Chen, Z., Li, Y., Liu, Z., Wang, J., Zhou, X., Du, J., 2018. Radon emission from soil gases in the active fault zones in the Capital of China and its environmental effects. Scientific Reports 8, 16772. https://doi.org/10.1038/s41598-018-35262-1

Cinelli, G., Tollefsen, T., Bossew, P., Gruber, V., Bogucarskis, K., De Felice, L., De Cort, M., 2019. Digital version of the European Atlas of natural radiation. J. Environ. Radioact. 196, 240–252.

Countess, R.J., 1976. 222Rn Flux Measurements with a Charcoal Canister. Health Phys. 31 (5), 455-456.

De Vivo, B., Cicchella, D., Lima, A., Albanese, S., 2006. Atlante geochimico-ambientale della Regione Campania (Geochemical Environmental Atlas of Campania Region). Aracne Editrice, p. 216. ISBN: 978-88-548-0819-5

De Vivo, B., Lima, A., Albanese, S., Cicchella, D., Rezza, C., Civitillo, D., Minolfi, G., Zuzolo, D., 2016. Atlante geochimico-ambientale dei suoli della Campania (Environmental Geochemical Atlas of Campania soils). Aracne Editrice, p. 364. ISBN: 978-88-548-9744-1

De Vivo, B., Petrosino, P., Lima, A., Rolandi, Belkin, H.E., 2010. Research progress in volcanology in Neapolitan area, southern Italy: a review and alternative views. Mineral. Petrol. 99, 1–28.

De Vivo, B., Rolandi, G., Gans, P.B., Calvert, A., Bohroson, W.A., Spera, F.J., Belkin, H.E., 2001. New constraints on the pyroclastic eruptive history of the Campanian volcanic Plain (Italy). Mineral. Petrol. 73, 47–65.

De Vos, W., Tarvainen, T., 2006. Geochemical Atlas of Europe. Part 2 – Interpretation of Geochemical Maps, Additional Tables, Figures, Maps, and Related Publications. Geological Survey of Finland, Espoo 692 pp. http://weppi.gtk.fi/publ/foregsatlas/

Demoury, C., Ielsch, G., Hemon, D., Laurent, O., Laurier, D., Clavel, J., Guillevic, J., 2013. A statistical evaluation of the influence of housing characteristics and geogenic radon potential on indoor radon concentrations in France. J. Environ. Radioact. 126, 216–225.

DISS Working Group, 2018. Database of Individual Seismogenic Sources (DISS), Version 3.2.1: A compilation of potential sources for earthquakes larger than M 5.5 in Italy and surrounding areas. http://diss.rm.ingv.it/diss/, Istituto Nazionale di Geofisica e Vulcanologia; doi:10.6092/INGV.IT-DISS3.2.1

Duchi, V., Minissale, A., Vaselli, O., Ancillotti, M., 1995. Hydrogeochemistry of the Campania region in southern Italy. J. Volcanol. Geoth. Res. 67, 313 – 328.

Goto, M., Moriizumi, J., Yamazawa, H., Iida, T., Zhuo, W., 2008. Estimation of global radon exhalation rate distribution. AIP Conference Proceedings 1034 (1), 169-172. https://doi.org/10.1063/1.2991199

Guagliardi, I., Zuzolo, D., Albanese, S., Lima, A., Cerino, P., Pizzolante, A., Thiombane, M., De Vivo, B., Cicchella, D., 2020. Uranium, thorium and potassium insights on Campania region (Italy) soils: Sources patterns based on compositional data analysis and fractal model. J. Geochem. Explor. 212, 106508. https://doi.org/10.1016/j.gexplo.2020.106508

Guida, D., Guida, M., Cuomo, A., Guadagnuolo, D., Siervo, V., 2013. Assessment and Mapping of Radon-prone Areas on a regional scale as application of a Hierarchical Adaptive and Multi-scale Approach for the Environmental Planning. Case Study of Campania Region, Southern Italy. WSEAS Transactions on Systems 2 (12), 105-120. E-ISSN: 2224-2678

IAEA, 2013. Measurement and Calculation of Radon Releases from NORM Residues. International Atomic Energy Agency. IAEA Technical Reports Series 474, IAEA, Vienna.

IARC, 1988. Monographs on the evaluation of carcinogenic risks to humans. Man-made mineral fibres and radon. International Agency for Research on Cancer. IARC Scientific Publications 43, 173–259.

ICRP, 2007. The 2007 Recommendations of the International Commission on Radiological Protection. ICRP Publication 103. Ann. ICRP 37 (2-4).

Ielsch, G., Ferry, C., Tymen, G., Robe, M.C., 2002. Prediction of areas presenting a high radon exhalation potential: A new methodology based on the properties of geological formations and soils. Radioprotection 37, C1-1211.

King, C.Y., King, B.S., Evans, W.C., Zhang, W., 1996. Spatial radon anomalies on active faults in California. Appl. Geochem. 11, 497-510.

Lemercier, M., Gurriaran, R., Bouisset, P., Cagnat, X., 2007. Specific activity to H*(10) conversion coefficients for in situ gamma spectrometry. Radiat. Prot. Dosim. 128 (1), 83-9.

Lima, A., Albanese, S., Cicchella, D., 2005. Geochemical baselines for the radioelements K, U, and Th in the Campania region, Italy: a comparison of stream-sediment geochemistry and gamma-ray surveys. Appl. Geochem. 20 (3), 611 – 625.

Manohar, S.N., Meijer, H.A.J., Herber, M.A., 2013. Radon flux maps for The Netherlands and Europe using terrestrial gamma radiation derived from soil radionuclides. Atmos. Environ. 81, 399-412. http://dx.doi.org/10.1016/j.atmosenv.2013.09.005

Miles J., 1998. Development of maps of radon-prone areas using radon measurements in houses. J. Hazard. Mater. 61(1), 53–58

Minolfi, G., Albanese, S., Lima, A., Tarvainen, T., Fortelli, A., De Vivo, B., 2018. A regional approach to the environmental risk assessment - human health risk assessment case study in the Campania region. J. Geochem. Explor. 184 (B), 400-416.

Navas, A., Machín, J., Soto, J., 2005. Mobility of Natural Radionuclides and Selected Major and Trace Elements Along A Soil Toposequence in the Central Spanish Pyrenees. Soil Science 170 (9), 743-757. doi: 10.1097/01.ss.0000185906.18460.65

Nazaroff, W.W., 1992. Radon transport from soil to air. Rev. Geophys. 30 (2), 137-160.

Nieder, R., Benbi, D.K., Reichl, F.X., 2018. Soil-Borne Gases and Their Influence on Environment and Human Health, in: Soil Components and Human Health. Springer, 179-221. https://doi.org/10.1007/978-94-024-1222-2_4

Peccerillo, A., 2005. Plio-quaternary Volcanism in Italy. Petrology, Geochemistry, Geodynamics. Springer-Verlag, Berlin Heidelberg. ISBN 978-3-540-29,092-6

Petrik, A., Albanese, S., Lima, A., De Vivo, B., 2018. The spatial pattern of beryllium and its possible origin using compositional data analysis on a high-density topsoil data set from the Campania Region (Italy). Appl. Geochem. 91, 162 – 173.

Quarto, M., Pugliese, M., Roca, V., 2013. Gamma dose rate measurements in dwellings of Campania region, South Italy. J. Environ. Radioact. 115, 114-117.

Reimann, C., Filzmoser, P., Garrett, R., Dutter, R., 2008. Statistical Data Analysis Explained: Applied Environmental Statistics with R. Wiley. ISBN: 978-0-470-98581-6

RISK 2013. Map Comparison Kit User Manual. Research Institute for Knowledge Systems.

Sabbarese, C., Ambrosino, F., D'Onofrio, A., Pugliese, M., La Verde, G., D'Avino, V., Roca, V., 2021. The first radon potential map of the Campania region (southern Italy). Appl. Geochem. 126, 104890. https://doi.org/10.1016/j.apgeochem.2021.104890

Sabbarese, C., Ambrosino, F., D'Onofrio, A., Roca, V., 2020. Radiological characterization of natural building materials from the Campania region (Southern Italy). Construct. Build. Mater., 121087. https://doi.org/10.1016/j.conbuildmat.2020.121087

Saito, K., Jacob, P., 1995. Gamma ray fields in the air due to sources in the ground. Radiat. Prot. Dosimetry 58 (1), 29-45.

Salminen, R., Tarvainen, T., Demetriades, A., Duris, M., Fordyce, F.M., Gregorauskiene, V., Kahelin, H., Kivisilla, J., Klaver, G., Klein, H., Larson, J.O., Lis, J., Locutura, J., Marsina, K., Mjartanova, H., Mouvet, C., O'Connor, P., Odor, L., Ottonello, G., Paukola, T., Plant, J.A., Reimann, C., Schermann, O., Siewers, U., Steenfelt, A., Van der Sluys, J., De Vivo, B., Williams, L., 1998. FOREGS Geochemical Mapping Field Manual. Geological Survey of Finland, Espoo Guide 47.

Sarra, A., Fontanella, L., Valentini, P., Palermi, S., 2016. Quantile regression and Bayesian cluster detection to identify radon prone areas. J. Environ. Radioact. 164, 354 – 364.

Scintrex Limited, 1997. GRS-500 operation manual.

Somma, R., Ebrahimi, P., Troise, C., De Natale, G., Guarino, A., Cicchella, D., Albanese, S., 2021. The first application of compositional data analysis (CoDA) in a multivariate perspective for detection of pollution source in sea sediments: The Pozzuoli Bay (Italy) case study. Chemosphere 274, 129955. https://doi.org/10.1016/j.chemosphere.2021.129955.

Stavitskaya, K., Ryzhakova, N., Udalov, A., Almyakov, P., 2019. Comparative analysis of the measuring results of the Radon flux density and Ra-226 specific activity for different soils types. AIP Conference Proceedings, 2101 (1), 020013. https://doi.org/10.1063/1.5099605

Stieff, L.R., Kotrappa, P., Bigu, J., 1996. Passive E-PERM Radon Flux Monitors for Measuring Undisturbed Radon Flux from the Ground. 1996 International Radon Symposium.

Sun, X., Yang, P., Xiang, Y., Si, X., Liu, D., 2018. Across-fault distributions of radon concentrations in soil gas for different tectonic environments. Geosciences Journal 22 (2), 227-239. http://dx.doi.org/10.1007/s12303-017-0028-2

Szegvary, T., Conen, F., Stöhlker, U., Dubois, G., Bossew, P., de Vries, G., 2007a. Mapping terrestrial γ-dose rate in Europe based on routine monitoring data. Radiat. Meas. 42, 1561–1572. https://doi.org/10.1016/j.radmeas.2007.09.002

Szegvary, T., Leuenberger, M., Conen, F., 2007b. Predicting terrestrial 222Rn flux using gamma dose rate as a proxy. Atmos. Chem. Phys. 7 (11), 2789-2795. https://hal.archives-ouvertes.fr/hal-00296241/document

UNSCEAR, 2000. Sources and effects of ionizing radiation. United Nations Scientific Committee on the Effects of Atomic Radiation, UN, New York. Report to General Assembly, with Annexes.

Vitale, S., Ciarcia, S., 2018. Tectono-stratigraphic setting of the Campania region (southern Italy). J. Maps 14 (2), 9-21. https://doi.org/10.1080/17445647.2018.1424655

Yakovleva, V. S., Karataev, V. D., 2007. Radon Flux Density at the Earth's Surface as a Possible Indicator of the Stress and Strain State of the Geological Environment. J. of Volcano. and Seismic. 1 (1), 67–70. https://doi.org/10.1134/S0742046307010058

Wilkening, M.H., Clements, W.E., Stanley, D., 1972. Radon222 flux measurements in widely separated regions, in: The Natural Radiation Environment II, 717-730. CONF-720805-P2.

Zahorowski, W., Whittlestone, S., 1996. A Fast Portable Emanometer for Field Measurement of Radon and Thoron Flux. Radiat. Portect. Dosim. 67, 109-120.

Zeeb, H., Shannoun, F., World Health Organization, 2009. WHO handbook on indoor radon: a public health perspective. World Health Organization. ISBN: 9789241547673.

Zuo, R., Wang, J., 2020. ArcFractal: An ArcGIS Add-In for Processing Geoscience Data Using Fractal/Multifractal Models. Nat. Resour. Res. 29, 3-12. https://doi.org/10.1007/s11053-019-09513-5

Zuzolo, D., Cicchella, D., Albanese, S., Lima, A., Zuo, R., De Vivo, B., 2018. Exploring uni-element geochemical data under a compositional perspective. Appl. Geochem. 91, 174–184.

Zuzolo, D., Cicchella, D., Lima, A., Guagliardi, I., Cerino, P., Pizzolante, A., Thiombane, M., De Vivo, B., Albanese, S., 2020. Potentially Toxic Elements in soils of Campania region (Southern Italy): combining raw and compositional data. J. Geochem. Explor. 213, 106524.

CHAPTER 6 – Collaborations

6.1 Radon and carbon dioxide contents in Phlegraean Fields volcanic aquifer

The results of this activity were published/presented in:

Ebrahimi, P., Guarino, A., Allocca, V., Caliro, S., Cicchella, D., Albanese, S., under review. The dissolved radon and carbon dioxide contents in Phlegraean Fields volcanic aquifer: a follow-up study. Chemosphere.

6.1.1 Summary of the work

Phlegraean Fields, south Italy, are one of the most active volcanic areas in the world, where the spatial distribution of radon and carbon dioxide in groundwater and statistical relationships between the dissolved gases and other variables deserve further attention to assess the potential proxies of volcanic-related phenomena. The Phlegraean Fields caldera is a large active volcanic system (about 12 km in diameter; Fig. 6.1) along the coastline of Tyrrhenian Sea. Campanian Ignimbrite and Neapolitan Yellow Tuff explosive eruptions (39 and 12 ka B.P., respectively) influenced the present morphology. There were several centuries of deflation after the last eruption at Monte Nuovo (Fig. 6.1) in 1538 AD, but land deformation and seismic unrest since the 1950s (which led to bradyseismic crises at the end of the last century) highlighted the importance of volcanological studies to prepare for an emergency.

Previous studies in soil and groundwater revealed that Rn concentrations in Phlegraean Fields and Ischia are higher than those of Vesuvius (Avino et al., 1999). A recent regional-scale investigation also confirmed association between the greatest Rn flux from soil and the volcanic centers, including Phlegarean Fields (Guarino et al., 2022).

The objectives of this study were capturing spatial distribution of Rn and CO_2 in the central part of the Phlegraean Fields caldera together with respecting compositional data structure to investigate the statistical relationship between the dissolved gases, major ions and other physicochemical characteristics of the groundwater body.

Compositional data analysis (CoDA) (Aitchison, 1982, 1986) was proposed at the end of last century and further developed in the last decades for reliable data mining, but its potential has not been fully explored for characterization of the groundwater aquifers affected by hydrothermal activity. Based on a prospecting campaign aimed at the determination of both radon and carbon dioxide in Phlegraean Fields groundwater, this work explored the spatial patterns of these gases in the local aquifer system and used a CoDA approach to extract the relevant information and determine the meaningful geochemical associations.

The results show that both dissolved gases share almost similar spatial distributions, but the logratio transformed CO_2 distinguishes bicarbonate-rich groundwater better than the raw values. Average concentration of radon in the chlorine-rich group is higher than that of bicarbonate-rich group. Principal component analysis reveals two associations: 1) Ca^{2+}, Mg^{2+}, K^{+}, SO_4^{2-}, HCO_3^{-}+CO_2 and pH; and 2) Na^{+}, Cl^{-}, As, B, Li, Rn, TDS and T. It highlights that the groundwater composition is generally influenced by two main factors: 1) meteoric water, which is modified by CO_2–rich magmatic fluids in some cases; and 2) upflow of hydrothermal fluid and/or seawater through the fault and fracture system. The results are in agreement with literature and application of CoDA is recommended in future investigations because the study area is highly populated and considering compositional nature of geochemical data might help to propose new tools for characterizing volcanic eruption more efficiently.

Further details can be found in Ebrahimi et al. (under review).

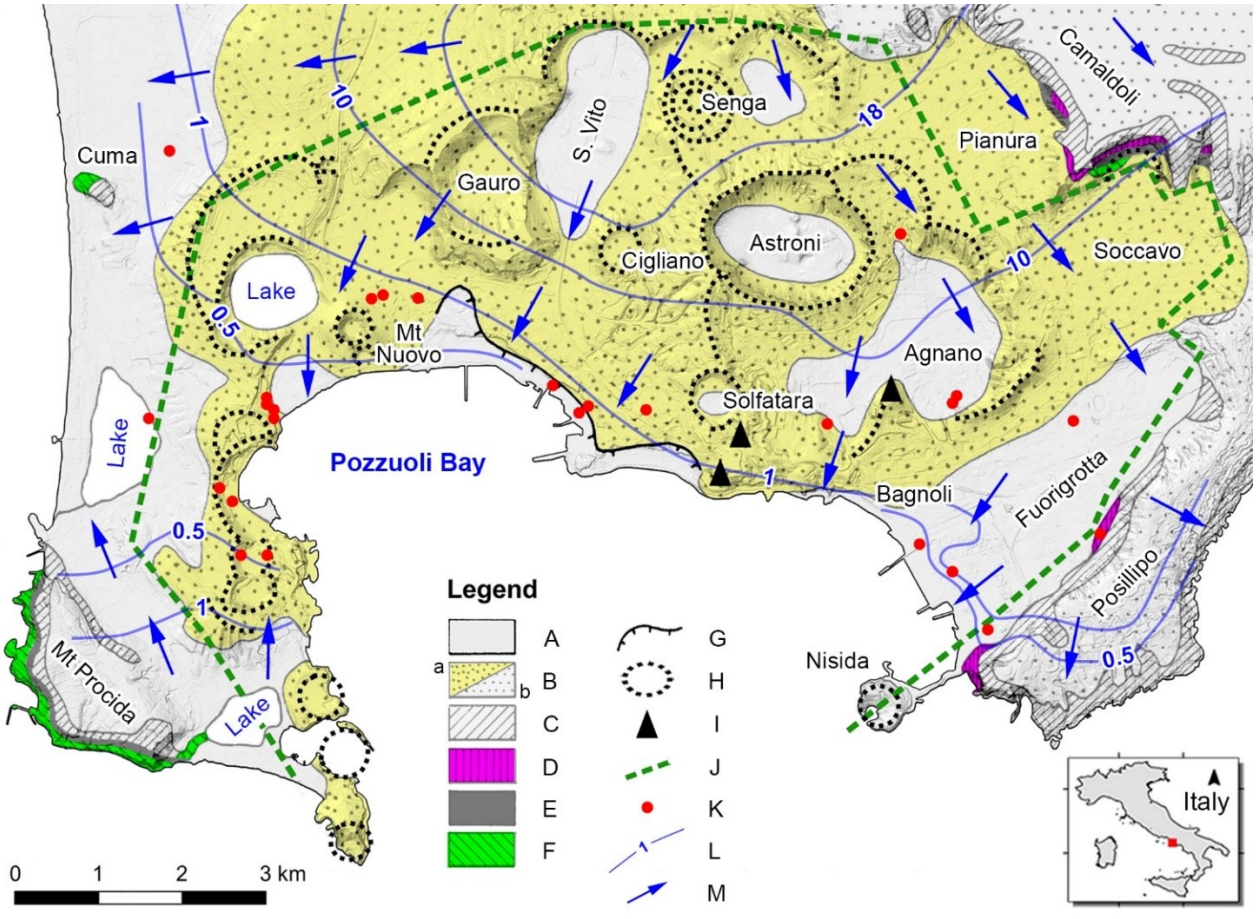

Figure 6.1 Map of Phlegraean Fields with location of the sampling points: (A) Recent active continental sediments; (B) Volcanics younger than 12 ka: "a" and "b" show proximal and distal deposits, respectively; (C) Neapolitan Yellow Tuff (NYT; 12 ka B.P.); (D) Volcanics erupted 35-12 ka B.P.; (E) Campanian Ignimbrite (CI; 35 ka B.P.); (F) Volcanics older than 35 ka; (G) Edge of La Starza marine cliff; (H) Crater rims of volcanoes younger than 12 ka (ISPRA, 2018); (I) Lava domes; (J) NYT caldera rim (Vitale and Isaia, 2014); (K) Groundwater sampling points; and (L) Piezometric contour lines (m a.s.l.; De Vita et al., 2018); (M) Groundwater flow direction.

6.1.2 Personal contribution

My personal contribution to that work has been the logistics of field activity, sampling, and chemical analysis (in situ and in laboratory).

Because the highest Rn values in groundwater were observed in the central part of the Phlegraean Fields caldera (Avino et al., 1999), twenty-six groundwater samples from thermal springs and private wells that mostly occur inside Neapolitan Yellow Tuff (NYT) caldera and a seawater sample from Porto di Baia (Pozzuoli Bay) were collected in November and December 2020 (Fig. 6.1).

At each station, two aliquots were collected following 0.45-µm filtration and HNO_3 acidification for determination of cations and metal(loid)s, and four unfiltered and unacidified aliquots were collected for anions, alkalinity, Rn and CO_2 measurements (Fig. 6.2 A). Well purging was performed before sampling to ensure that the samples were representative of the groundwater in the vicinity of the well. The sampling bottles were rinsed three times with the water from the exact site of sampling prior to filling them. Airtight sealed containers were utilized for the aliquots that underwent Rn and CO_2 determinations. All containers were made of high-density polyethylene, but the aliquot for Rn measurement was stored in glass bottles (Fig. 6.2 A). Total dissolved solids (TDS), temperature (Fig. 6.2 B) and pH (Fig. 6.2 C) were recorded in situ with portable devices.

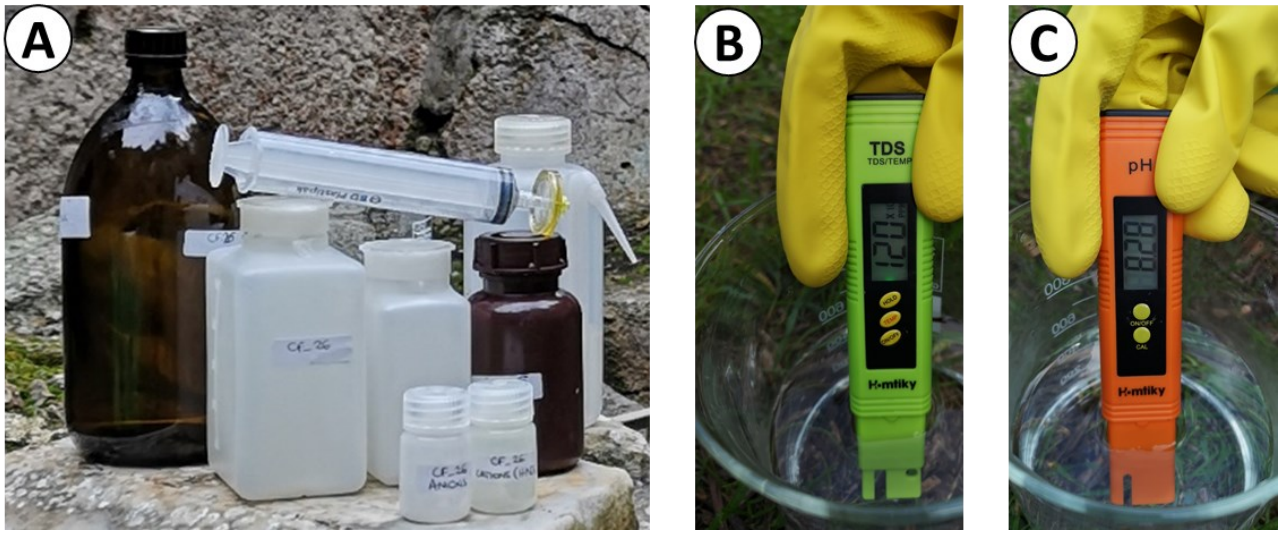

Figure 6.2 (A) Containers for the collection of the different aliquots of water samples, with the syringe and the 0.45-µm filter and the distillate water for the cleaning of the devices; (B) TDS-meter; (C) pH-meter.

On the same day of sample collection, alkalinity, Rn and CO_2 were determined at the Environmental Geochemistry Laboratory (EGL) of the Department of Earth, Environmental and Resources Sciences (DiSTAR), University of Naples Federico II (UNINA). Alkalinity was measured

by titration of 100 ml of a given sample with HCl (0.1 N) (Fig. 6.3B) and the values are expressed as HCO_3^-.

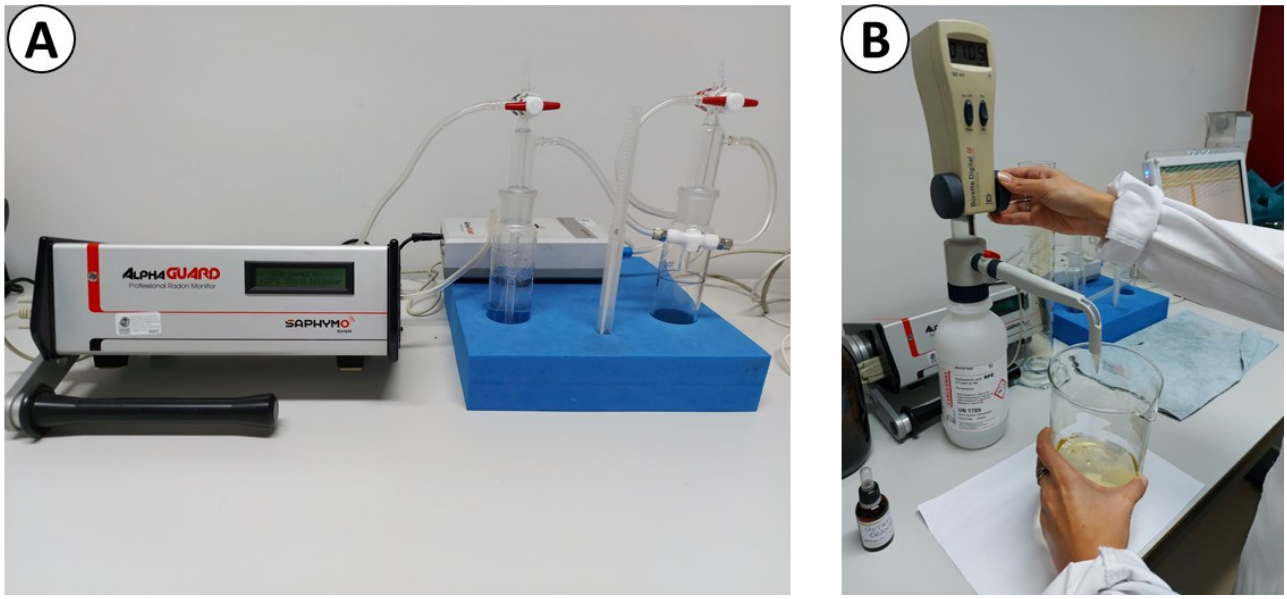

Figure 6.3 (A) AlphaGUARD device connected to the AquaKIT accessories (i.e., AlphaPUMP and vessels); (B) precision burette for titration.

Rn concentrations were measured with the AquaKIT accessory (which is composed of a degassing vessel, a security vessel, a pump and tubes) for the radon monitoring system AlphaGUARD PQ2000 PRO (Fig. 6.3 A). Briefly, the "empty" measurement set-up is assembled, AlphaPUMP is turned on with the flow rate of 1 L/min and the system is rinsed with room air for 10 min. The gas cycle is then closed, AlphaPUMP is turned on with the flow rate of 0.5 L/min, AlphaGUARD is switched on in "FLOW, 1min" operation mode and the background Rn level is detected in the "empty" measurement set-up for 10 min. Subsequently, the sample is injected in the system, AlphaPUMP is turned on with the flow rate of 0.5 L/min, AlphaGUARD is switched on in "FLOW, 1min" operation mode and the dissolved Rn level is detected for 20 min. Finally, water temperature is determined and Rn concentration (c_{Water}; Bq/l) in groundwater sample is calculated as follows:

$$c_{Water} = \frac{c_{Air} \times \left(\frac{V_{System} - V_{Sample}}{V_{Sample}} + k \right) - c_0 \times \left(\frac{V_{System} - V_{Sample}}{V_{Sample}} \right)}{1000} \quad \text{[Eq 6.1]}$$

Where:

- c_{Air} is Rn concentration (Bq/m³) in the measurement set-up after sample introduction and expelling the dissolved gas;

- c_0 is the background Rn concentration (Bq/m³) in the measurement set-up before sample introduction;
- V_{System} is the interior volume (ml) of the measurement set-up;
- V_{Sample} is the volume (ml) of the introduced water sample;
- k is Rn distribution coefficient water/air obtained from the temperature dependency curve of Rn diffusion coefficient based on water temperature (with falling temperature, the amount of Rn soluble in water and the k-value increase).

In this study, V_{System} and V_{Sample} are 1102 and 100 ml, respectively. It is worth mentioning that AlphaGUARD records a value every minute and the time period in which the readings are almost stable is considered to compute the average Rn concentration (i.e., c_{Air} or c_0) for a given sample.

Equation 6.1 is also applicable to the dissolved CO_2 content, but carbon dioxide concentration needs to be detected via ECOPROBE 5 and some parameters in the above-mentioned formula should be adjusted. Briefly, after rinsing the "empty" measurement set-up with room air using AlphaPUMP with the flow rate of 1 L/min for 10 min, the gas cycle is closed, ECOPROBE 5 is turned on with the flow rate of 0.5 L/min and the background CO_2 level is detected in the "empty" measurement set-up for 3 min. Subsequently, the sample is injected in the system, ECOPROBE 5 is turned on with the flow rate of 0.5 L/min and the dissolved CO_2 level is detected for 3 min. Finally, water temperature is determined and CO_2 concentration (c_{Water}; mg/l) in water sample is calculated via equation 6.1. For carbon dioxide calculation via the equation 6.1:

- c_{Air} is CO_2 concentration (mg/m^3) in the measurement set-up after sample introduction and expelling the dissolved gas;
- c_0 is the background CO_2 concentration (mg/m^3) in the measurement set-up before sample introduction;
- V_{System} is the interior volume (ml) of the measurement set-up;
- V_{Sample} is volume (ml) of the introduced water sample;
- k is CO2 distribution coefficient water/air obtained from the temperature dependency curve of CO2 diffusion coefficient (Carroll and Mather, 1991) based on water temperature.

In this study, V_{System} and V_{Sample} are 404 and 100 ml, respectively. It is noteworthy that ECOPROBE 5 records a value each 0.5 second.

As, B, Cd, Mn, Fe, Pb, Zn, Ba, Cu, Co, Ni, Cr and Ti were measured with inductively coupled plasma–optical emission spectroscopy (ICP-OES) at the chemistry laboratory of DiSTAR (UNINA). The 20 ml solutions prepared for the analysis were composed by 5 ml of sample + 0.1 ml HNO3 + 0.2 ml internal standard (100 mg/kg Y) + the remaining portion (ca. 14.7 ml) of ultrapure water (0.055

μS/cm) (Fig. 6.4 A and B). Every four or five samples, 1 blank and 1 standard sample were analysed for the auto-calibration of the instrument (Fig. 6.4 C).

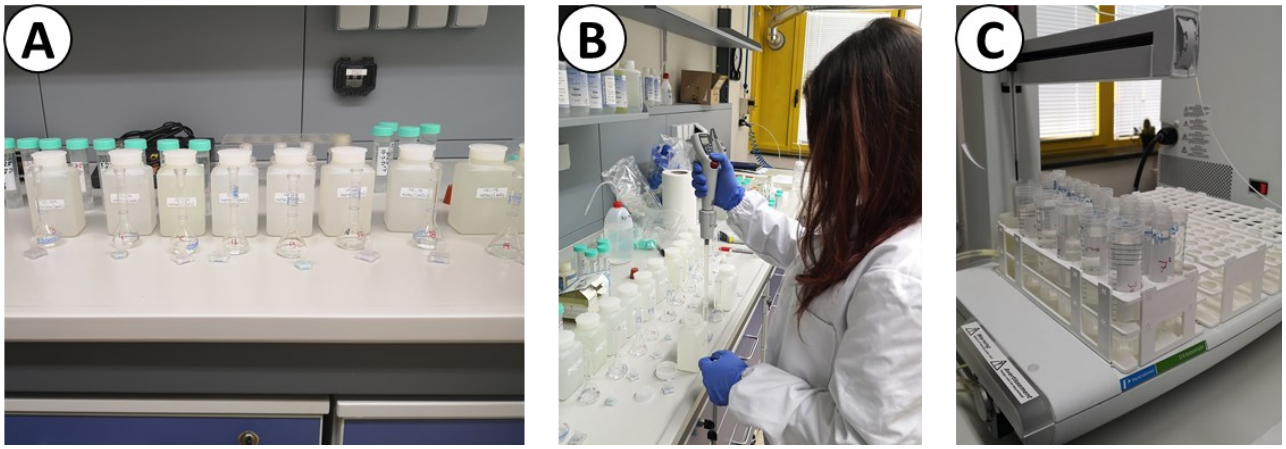

Figure 6.4 (A and B) Preparation of the solutions to be analysed; (C) solutions, standards and blanks ready to be analysed.

In addition, major ions and other elements were determined via ion chromatography in the laboratory of fluid geochemistry at the INGV-Osservatorio Vesuviano, Napoli, Italy. Blank, duplicate, and certified standard solutions were analyzed to check quality of the analytical results.

6.2 Hydrogeochemistry of Campi Flegrei volcanic aquifer (south Italy).

The results of this activity were published/presented in:

Ebrahimi, P., Guarino, A., Allocca, V., Caliro, S., Avino, R., Bagnato, E., Capecchiacci, F., Carandente, A., Minopoli, C., Santi, A., Albanese, S., 2022. Hierarchical clustering and compositional data analysis for interpreting groundwater hydrogeochemistry: The application to Campi Flegrei volcanic aquifer (south Italy). Journal of Geochemical Exploration.

Ebrahimi, P., Guarino, A., Allocca, V., Caliro, S., Avino, R., Bagnato, E., Capecchiacci, F., Carandente, A., Minopoli, C., Santi, A., Albanese, S, 2021. Fluoride in Campi Flegrei volcanic aquifer, south Italy: A comparison between water and rock composition. BeGeo scientists 2021, Naples. https://doi.org/10.3301/ABSGI.2021.04

6.2.1 Summary of the work

Comprehensive hydrogeochemical studies have been conducted in the Campi Flegrei volcanic aquifer since late 20th century due to the volcanic unrest (Chiodini et al., 2010, 2012). In the last decade, studies showed that hydrogeochemical processes in the volcanic aquifer could be preliminarily understood using the dominant anion species (i.e., bicarbonate, sulfate and chloride) to explain the general hydrogeochemical processes (Valentino and Stanzione, 2003; Aiuppa et al., 2006). Groundwater samples were collected from Campi Flegrei aquifer, analysed to determine the content in major ions, Li, As, B, pH, electric conductivity and temperature, to geochemically and spatially capture the main characteristics of the groundwater body. The main objective of this work was taking advantage of the long history of hydrogeochemical research in the study area to apply hierarchical cluster analysis (HCA) (Reimann et al., 2008) and compositional data analysis (CoDA) (Aitchison, 1982) for investigating groundwater geochemistry, which might provide new tools for monitoring volcanic activity more accurately and mitigating risk of volcanic eruption more effectively.

The hierarchical clustering algorithm was then performed on ratios of bicarbonate, sulfate and chloride, and the optimum number of clusters were determined regarding the results of deep hydrogeochemical investigations published in the past. The collected samples were categorized in the following groups: (1) bicarbonate-rich groundwater; (2) chlorine-rich groundwater; (3) sulfate-rich groundwater; and (4) mixed groundwater.

The first group (As = 158.2 ± 169 µ g/l, electric conductivity = 1,732.1 ± 1,086 µ S/cm and temperature = 25.6 ± 8 ◦ C) is mainly derived from poor arsenic meteoric water, but there is significant thermal/seawater contribution in the second one (As = 1,457.8 ± 2,210 µ g/l, electric conductivity =

20,118.3 ± 11,139 µ S/cm and temperature = 37.1 ± 20 ◦ C). Interaction of the bicarbonate-rich groundwater and hydrothermal vapors gives rise to the sulfate-rich groundwater (As = 847.2 ± 679 µ g/l, electric conductivity = 3,940.0 ± 540 µ S/cm and temperature = 82.8 ± 3 ◦ C) around Solfatara volcano. The mixed groundwater (As = 451.4 ± 388 µ g/l, electric conductivity = 4,482.9 ± 4,027 µ S/cm and temperature = 37.1 ± 16 ◦ C) is observed where the three main groundwater groups undergo a mixing process, depending on the hydrogeology of the volcanic aquifer.

Contrary to the bicarbonate- and sulfate-rich groundwaters, the chlorine-rich and mixed groundwaters generally occurs at low piezometric levels (approximately < 1 m above sea level) near the coastline. The hierarchical cluster analysis provides more information about the volcanic aquifer, particularly when compositional data analysis is applied to study hydrogeochemistry of the homogeneous groundwater groups and to uncover the relationships between variables. Addressing compositional nature of data is recommended in the future studies for developing new tools that help deeper understanding of groundwater evolution in volcanic aquifers and identifying promising precursors of volcanic eruption.

Further details can be found in Ebrahimi et al. (2022).

6.2.2 Personal contribution

The contribution made for this work was prevalently the review and editing processes and collaboration with the sampling procedures.

A total of 44 water samples are collected in May 2019 from wells and springs mostly located in the NYT caldera (Fig. 6.5). Alkalinity, electric conductivity (EC), pH and temperature were measured with portable instruments in situ. The water samples were filtered with 0.45 µm filters and collected in 30 ml high-density polyethylene (HDPE) bottles for chemical analyses. One aliquot was acidified (1%) with Suprapure 36% HCl for determination of the major cations, whereas the aliquot for minor and trace elements was acidified (1%) with Suprapure 63% HNO3.

Samples were analyzed for Li, Ca^{2+}, Mg^{2+}, Na^{+}, K^{+}, SO_4^{2-}, Cl^{-}, NO_3^{-} and F^{-} by ion chromatography standard technique, using a Dionex ICS3000 system at the laboratory of fluid geochemistry at the INGV-Osservatorio Vesuviano, Napoli. Measurement accuracy is better than ± 5%, obtained by analyzing certified standard solutions, and the detection limits are better than 0.1 mg/l.

Arsenic and boron contents were detected using inductively coupled plasma-optical emission spectrometry (ICP-OES) at the Department of Earth, Environmental and Resources Sciences in the University of Naples Federico II, following 0.45- µm filtration and HNO_3 acidification of another

aliquot in the field. Measurement accuracy is better than ± 5%, obtained by analysing certified standard solutions, and the detection limits are 3.0 µg/l.

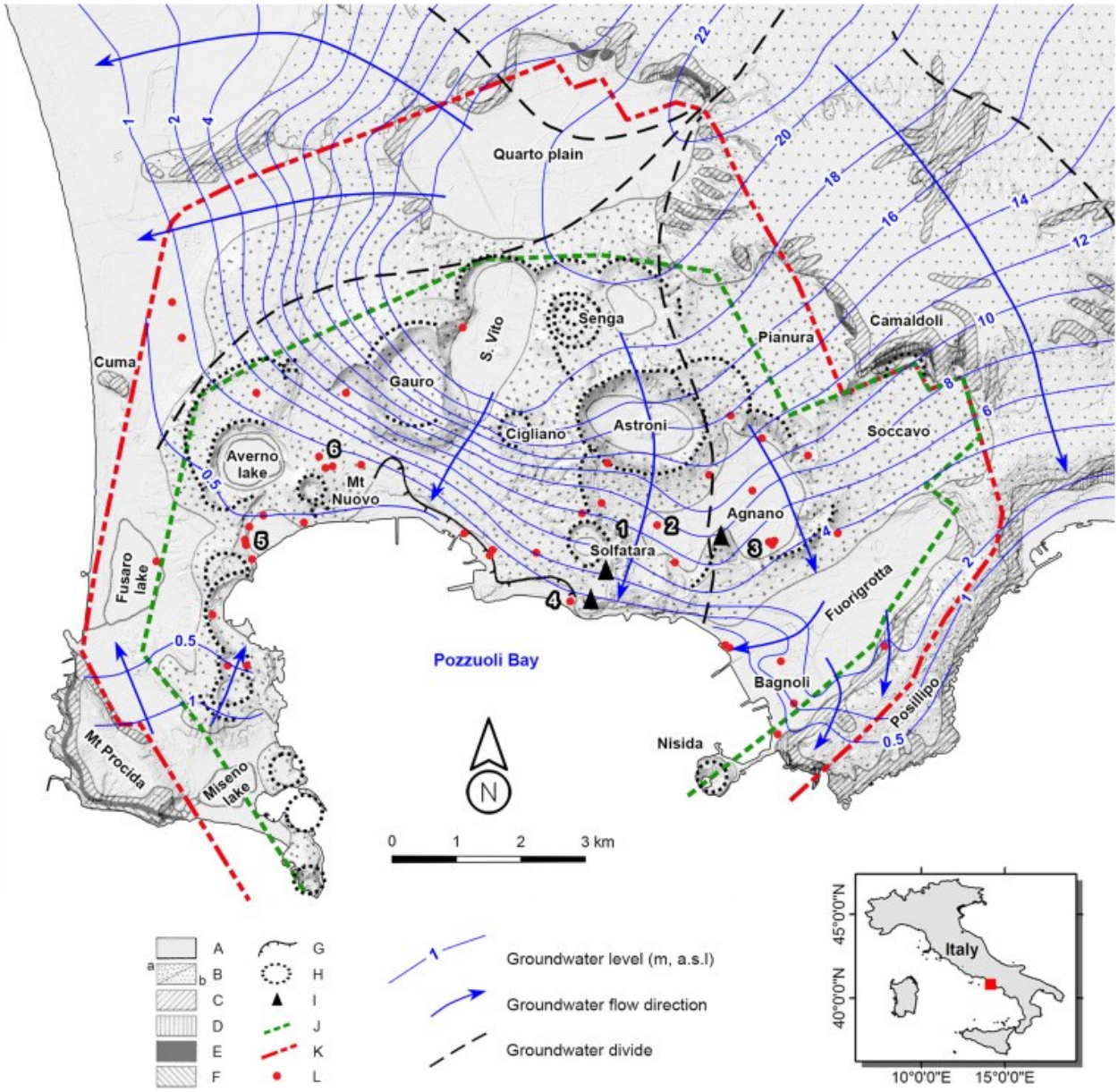

Figure 6.5 The simplified geological map of Campi Flegrei (after Valentino et al., 1999). The groundwater level, groundwater flow direction, groundwater divide (after De Vita et al., 2018) together with location of (1) Pisciarelli, (2) Hotel Tennis, (3) Agnano Terme, (4) Terme Puteolane, (5) Stufe di Nerone and (6) Damiani are also represented. Legend: (A) Recent active continental sediments; (B) Volcanics younger than 12 ka: (a) proximal, mostly pyroclastic-flow and surge deposits, (b) distal, mostly fallout deposits; (C) Neapolitan Yellow Tuff (NYT; 12 ka B.P.); (D) Volcanics erupted 35–12 ka B.P.; (E) Campanian Ignimbrite (CI; 35 ka B.P.); (F) Volcanics older than 35 ka; (G) Edge of La Starza marine cliff; (H) Crater rims of volcanoes younger than 12 ka (ISPRA, 2018); (I) Lava domes; (J) NYT caldera rim (Vitale and Isaia, 2014); (K) CI caldera rim (Vitale and Isaia, 2014); and (L) sampling points.

6.3 Detecting pollution source in sea sediments using compositional data analysis (CoDA): the Pozzuoli Bay (Italy) case study

The results of this activity were published/presented in:

Somma, R., Ebrahimi, P., Troise, C., De Natale, G., Guarino, A., Cicchella, D., Albanese, S., 2021. The first application of compositional data analysis (CoDA) in a multivariate perspective for detection of pollution source in sea sediments: The Pozzuoli Bay (Italy) case study. Chemosphere 274. DOI: 10.1016/j.chemosphere.2021.129955.

Ebrahimi, P., Somma R., Troise C., De Natale G., Guarino A., Cicchella D., Albanese S., 2021. Characterising source of arsenic in the sediments of Pozzuoli Bay (south Italy) using compositional data analysis (CoDA). Goldschmidt Virtual 2021, Lyon. DOI: 10.7185/gold2021.6152

6.3.1 Summary of the work

Pozzuoli Bay is a part of Campi Flegrei caldera, an active volcano with intensive hydrothermal activity. Due to co-existence of natural processes (e.g., underwater fumaroles, minerals and sub-marine groundwater discharge) and anthropogenic activities (for instance, industrial activity in the past, the ineffective coastal landfill and the seepages) across the area, in the last decades, investigating geochemistry of sea sediments has been challenging in the eastern sector of the bay, and a debate about the source of some potentially toxic elements (PTEs) (particularly As) has been ongoing.

Compositional data analysis (CoDA) was applied to uncover the statistically meaningful relationships and discriminate between pollution sources in sea sediments. CoDA was used because the results are independent of the measurement unit, the selected subgroup of elements and the order of chemicals in the dataset (Aitchison, 1982).

Specifically, sediments were collected from 0-50 cm depth range in the proximal zone (PZN) and 0-20 cm depth interval in the distal zone (DZN) of shoreline (Fig. 6.6), in a sector of the bay where a steelwork has been active until 90's. The samples were analysed for major and trace elements, grain size and organic matter (OM) content. A robust principal component analysis (PCA) was separately applied to PZN and DZN datasets. OM and the shortest distance of sample locations to fumaroles, coastline and seepages were considered as external variables.

For both zones, the first two principal components (PC1 and PC2) retained >89% of the total variance. The robust variant of PCA (Filzmoser et al., 2009) indicated that Hg, Cd, Cu, Pb and Zn were positively correlated with mud and organic matter in the sediments deposited in front of the former industrial site. Concentrations of these metals decrease along the cores and in the distal zone.

Nevertheless, Al, As, V, Fe, Cr, Ni and sand form an association along the coast which strengthens with increasing distance from fumaroles in the proximal zone. It suggests that arsenic was mainly originated from the pyroclastic deposits of Campi Flegrei and some of the seepages with hydrothermal component, supported by low contribution of the variables in robust PCA of the sediments from distal zone.

It seems that submarine groundwater discharge, underwater fumaroles and the coastal landfill do not play the major role in arsenic geochemistry. Despite almost similar associations in DZN, low contribution of variables in the robust PCA probably suggests that the main sources of elements are spatially located in the proximal zone.

Therefore, this pioneering article suggests CoDA as a powerful tool for answering the long-lasting questions over sediment geochemistry in polluted areas.

Further details can be found in Somma et al. (2021).

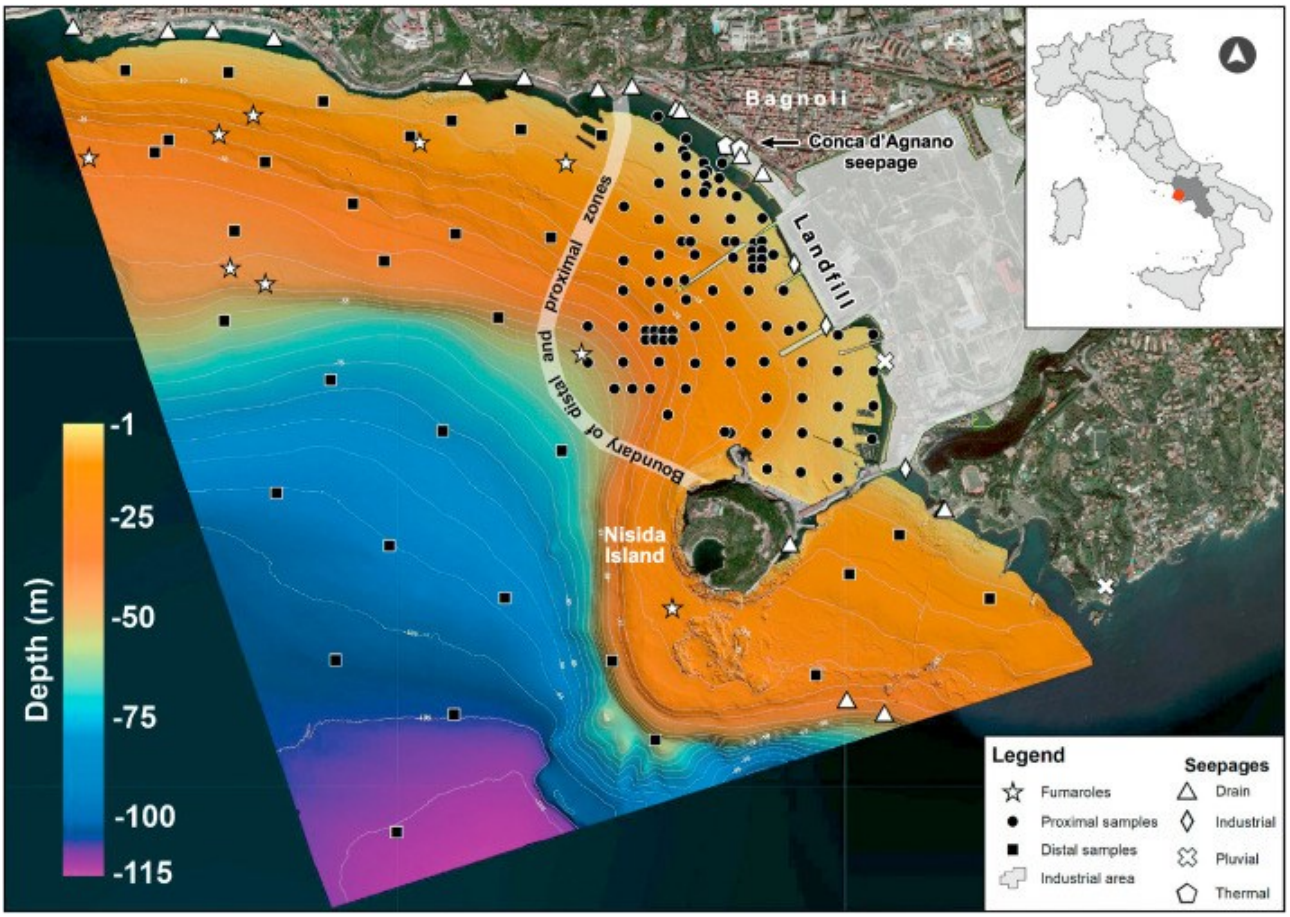

Figure 6.6 Location of the study area, bathymetry of the coastal environment, the sediment samples of proximal and distal zones (PZN and DZN, respectively) and location of seepages and fumaroles.

6.3.2 Personal contribution

The personal contribution in the scope of the work has been the production of the interpolated maps of the raw and the clr-trasformed data by mean of the multifractal method approach. Specifically, the interpolated maps of the variable Al, Fe, Zn, Pb, V, As, Cr, Cu, Ni, Cd, Hg, sand, mud, organic matter, principal component (PC) scores and standardised residuals were produced.

The geochemical mapping was performed by the multifractal inverse distance weighted (MIDW) method. The search radius was set to 300 m for proximal zone and 1000 m for distal zone, and the 4 nearest sample points were used to generate the maps with output cell size of 10 m. Because distribution of geochemical data has a fractal nature, the interpolated surfaces were then reclassified through the concentration–area (C–A) model (Cheng et al., 1994) already discussed in previous chapters (Fig. 6.7).

Since a non-negative dataset is required for MIDW mapping, a data treatment was proposed to deal with the negative clr coefficients. First, the variables (i.e., Al, Fe and Zn) with positive clr values (clr.element) were scaled (clr_{scl1}.element and clr_{scl2}.element) using equations 6.1 and 6.2:

$$clr_{scl1}.element = (clr.element - Min_{clr.element}) + 0.1 \quad \text{[Eq. 6.1]}$$

$$clr_{scl2}.element = (clr.element + Min_{clr.element}) + 0.1 \quad \text{[Eq. 6.2]}$$

Then, the spatial distributions of clr.element, clr_{scl1}.element and clr_{scl2}.element were prepared and reclassified according to the fractal approach. The upper and lower values of each class were subsequently back-transformed to the original clr.element by the equations 6.3 and 6.4:

$$clr.element = (clr_{scl1}.element + Min_{clr.element}) - 0.1 \quad \text{[Eq. 6.3]}$$

$$clr.element = (clr_{scl2}.element - Min_{clr.element}) - 0.1 \quad \text{[Eq. 6.4]}$$

It was illustrated that applying the proposed formulas to scale the clr coordinates does not significantly affect the spatial patterns. Therefore, whenever a negative clr.element is present in a variable, Eq. (6.1) is utilized to obtain the threshold concentrations by fractal analysis which will be back-transformed to the original clr coefficients via equation 6.3. The above-mentioned approach was also utilized for mapping grain size fractions, principal component scores (Fig. 6.8) and standardized residuals (Fig. 6.9). The MIDW mapping was performed using the ArcFractal Plugin in ArcGIS 10.4.1 software (Zuo and Wang, 2020).

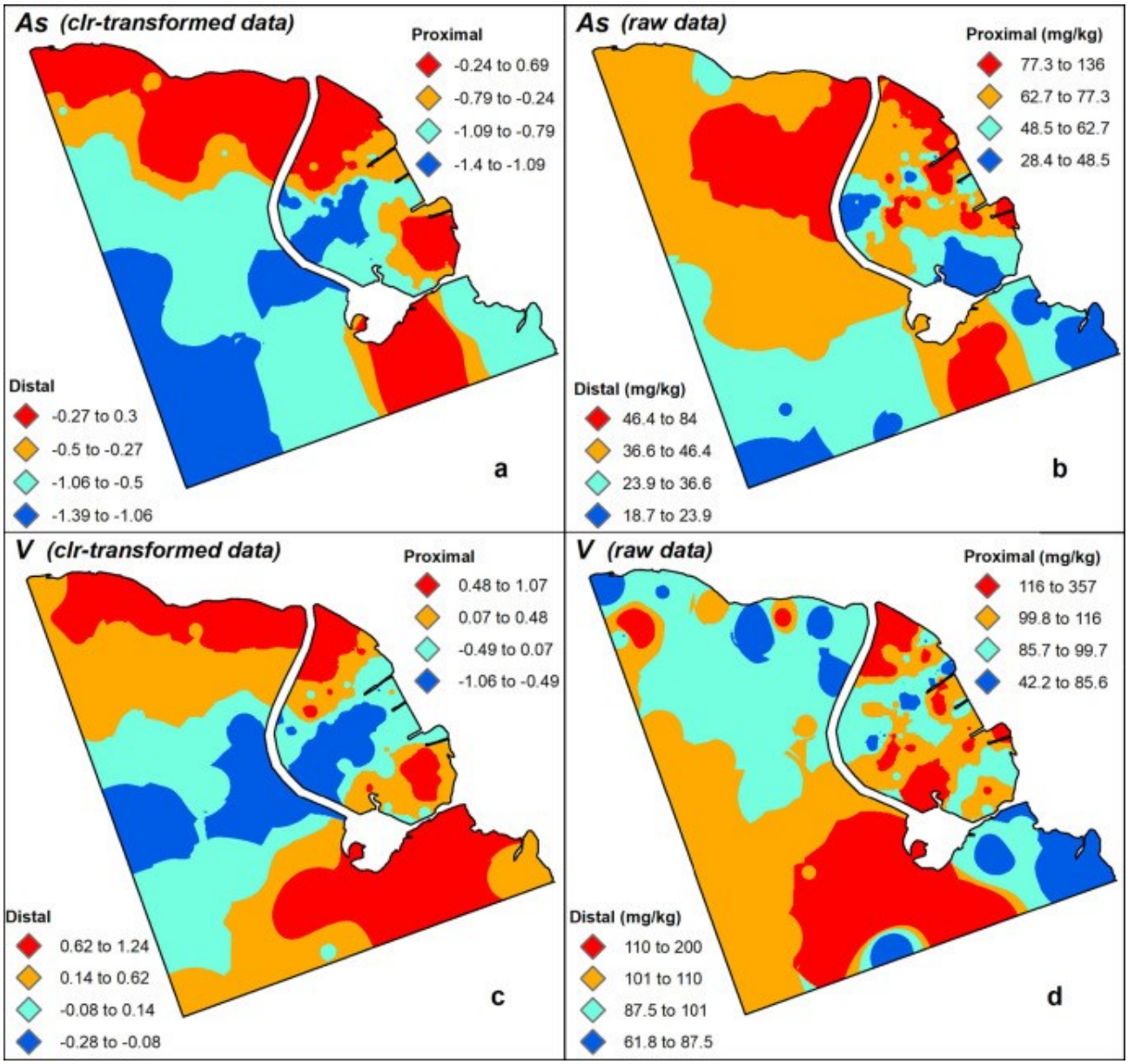

Figure 6.7 Arsenic and vanadium geochemical maps produced by clr-transformed data (a and c) and raw data (b and d). Opening the data noticeably impacted spatial patterns of the PTEs.

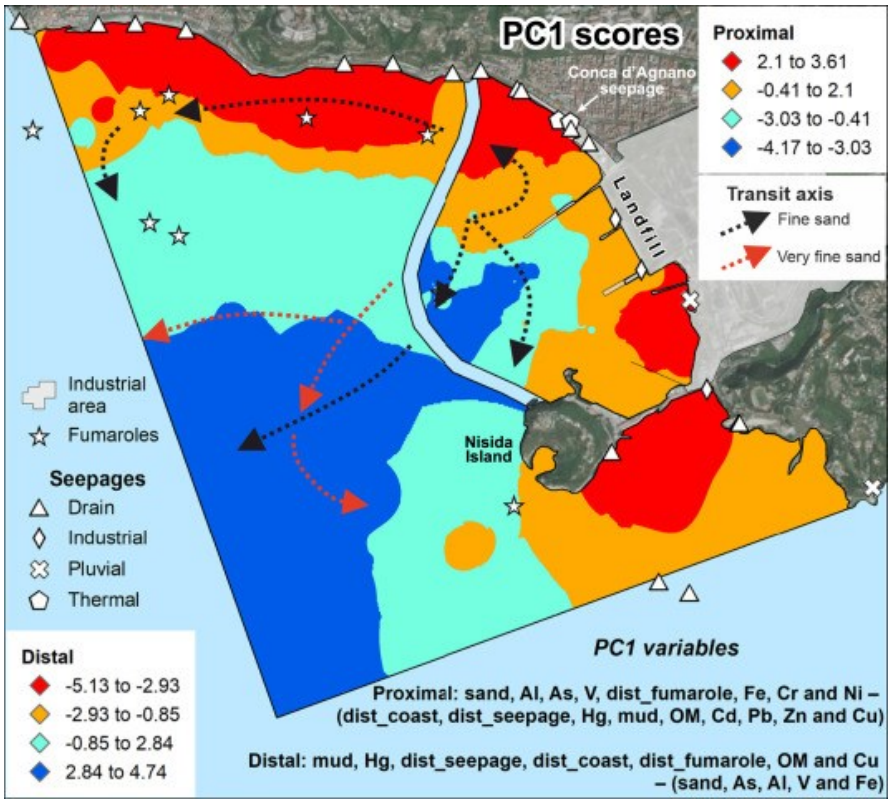

Figure 6.8 PC1 score map of the sediments collected from the proximal (0–50 cm) and distal (0–20 cm) zones. Due to low contribution of Cd in robust PCA and very low correlation of Ni, Cr, Pb and Zn with PC1, they were excluded from PC1 of the DZN. The transit axes of fine and very fine sand (Arienzo et al., 2017) are also illustrated.

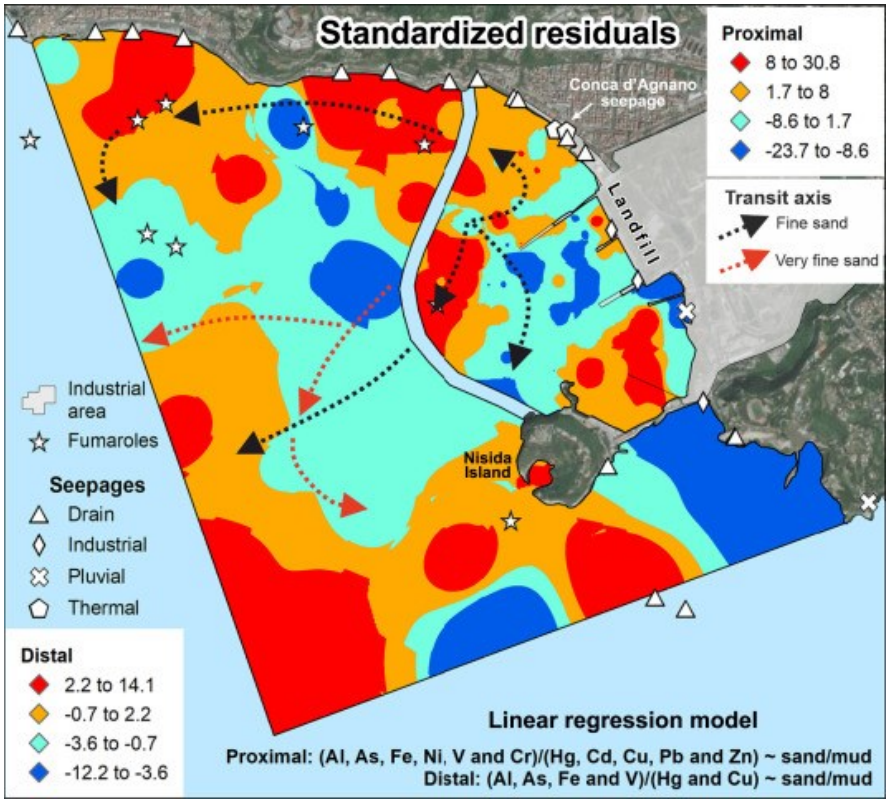

Figure 6.9 Spatial distribution of the standardized residuals in the proximal and distal zones. The transit axes of fine and very fine sand (Arienzo et al., 2017) are depicted as well.

6.4 PTEs distribution in stream sediments of the Sabato River Catchment Basin (southern Italy)

The results of this activity were published/presented in:

Dominech, S., Guarino, A., Aruta, A., Ebrahimi, P., Yang, S., Albanese, S., 2020. Potentally toxic elements (PTEs) distribution and main geochemical processes in Sabato River Catchment Basin (southern Italy): a focus on cadmium. Conference proceedings, Proscience vol. 7. ISSN: 2283-5954.

Dominech, S., Yang, S., Ebrahimi, P., Aruta, A., Guarino, A., Gramazio, A., Albanese, S., 2021. A new approach to determine geochemical fingerprint of contaminants in stream sediments of Southern Italy. Goldschmidt Virtual 2021, Lyon. DOI: 10.13140/RG.2.2.35044.91523

Dominech, S., Guarino A., Aruta A., Ebrahimi P., Yang S., Albanese S., 2020. Potentally toxic elements (PTEs) distribution and main geochemical processes in Sabato River Catchment Basin (southern Italy). GEOHEALTH 2020 - INTERNATIONAL MEETING OF GEOHEALTH SCIENTISTS, Bari. Scientific Research Abstracts Vol. 10, p. 16. ISSN 2464-9147.

6.4.1 Summary of the work

The catchment basin of Sabato River (with an area of ca. 459 km²), located in a large industrial and urbanized area of the Campania region (Southern Italy), between the cities of Avellino and Benevento, has been historically characterized by the presence of urban settlements and industrial development areas along its course (with a total length of 50 km). Thus, a study on the distribution of Potentially Toxic Elements (PTEs) and their potential sources was done.

For the purpose, 35 stream sediment samples were collected in 2019 from the main course of the river right after any tributaries inlet and upstream and downstream of the main industrial and urbanized areas within the basin (Fig. 6.10). Thus, a sample catchment basin (SCB) approach (Carranza and Hale, 1997) was applied.

After their collection, samples were oven-dried (temperature was kept below 37°C to preserve Hg content) and sieved (< 200 mesh) at the Environmental Geochemistry Laboratory (EGL) of University of Napoli Federico II; an aliquot of each sample was sent to Bureau Veritas Laboratories (Vancouver, Canada) for chemical analysis where the concentrations of 53 elements were determined through a combination of Inductively Coupled Plasma Mass Spectrometry (ICP-MS) and Inductively Coupled Plasma Emission Spectroscopy (ICP-ES) following a modified aqua regia digestion. Grain size analysis was also performed at Nanjing University (China).

Geochemical data have been processed according to Compositional Data Analysis (CoDA) fundamentals (Aitchison, 1984) and the dataset has undergone a centred log-ratio (clr) transformation due to its capability of preserving both geometric properties and one-to-one relationship within the variables.

In this study, we focused on the particular behaviour of Cadmium (Cd), due to its toxic effects on the kidneys as well as the skeletal and respiratory systems. Firstly, we compared the raw geochemical dataset and the log-ratio (clr) transformed one, found that the latter can improve the readability of the Cd data distribution. Both Cd raw geochemical data and clr values have been plotted, from source to sink (Fig. 6.11). Applying a linear regression between the clr-values and the log-transformed cumulative area (estimated by the sample catchment basin approach), we emphasized a possible contaminant source at the headwaters followed by a decreasing trend, potentially explained by a downstream dilution effect.

Since there is no evidence of any Cd-related industrial activity at the headwaters, and anomalies seem to be highly localized in the southern part of the basin, we supposed that its main source could be found in the use of some phosphate fertilizers for local agricultural practice.

Further details can be found in Dominech et al. (2020).

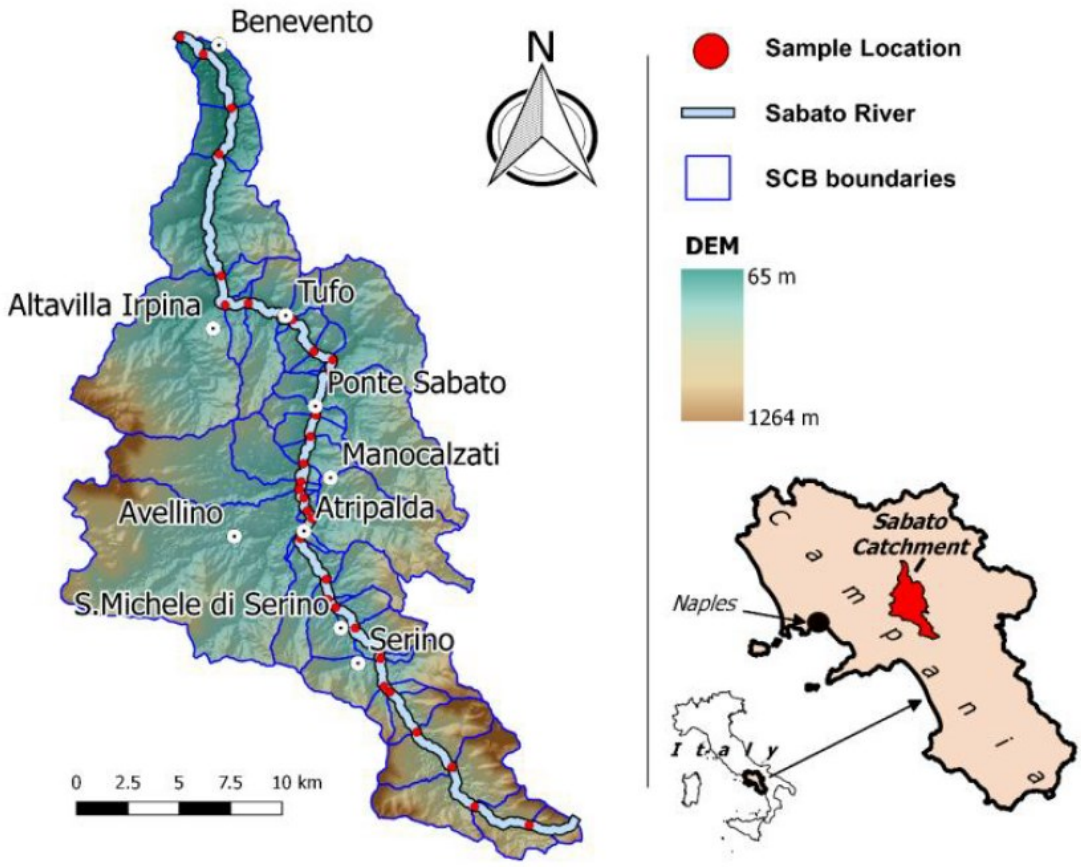

Figure 6.10 Framing of the study area. The Digital Elevation Model (DEM) of the catchment area was used to outline the Sample Catchment Basins (SCBs)

6.4.2 Personal contribution

The contribution in the framework of the work has been the calculations of the anomaly thresholds.

Both raw chemical data and clr values of a subset of potentially toxic elements (PTEs – As, Cd, Cr, Cu, Hg, Pb, Zn) has been plotted, from source to sink (S2S) (Fig. 6.11). For each element of interest, raw concentrations have been compared with the Upper Baseline Limits (UBLs) estimated by Albanese et al. (2007) for Campania region to determine potential anomalies (which is equal to 0.69 mg/kg for Cd). Furthermore, since in literature there are no reference values for log-ratio transformed data, the anomaly thresholds (ATs) for clr-transformed data have been established applying the approach proposed by Reimann et al. (2005), which replaces the arithmetic mean with the median and the standard deviations with the median absolute deviation (MAD):

$$AT = \tilde{X} + 2[\text{median}\ (|\ X_i - \tilde{X}\ |)] \qquad [\text{Eq. } 6.5]$$

Where:

- $\tilde{X}$ is the median clr value for Cd based on all the samples in the dataset;
- X_i is the clr value for Cd of the i-esim sample;
- [median ($|\ X_i - \tilde{X}\ |$)] is defined as median absolute deviation (MAD).

These estimators are strongly suggested as they are robust against extreme values.

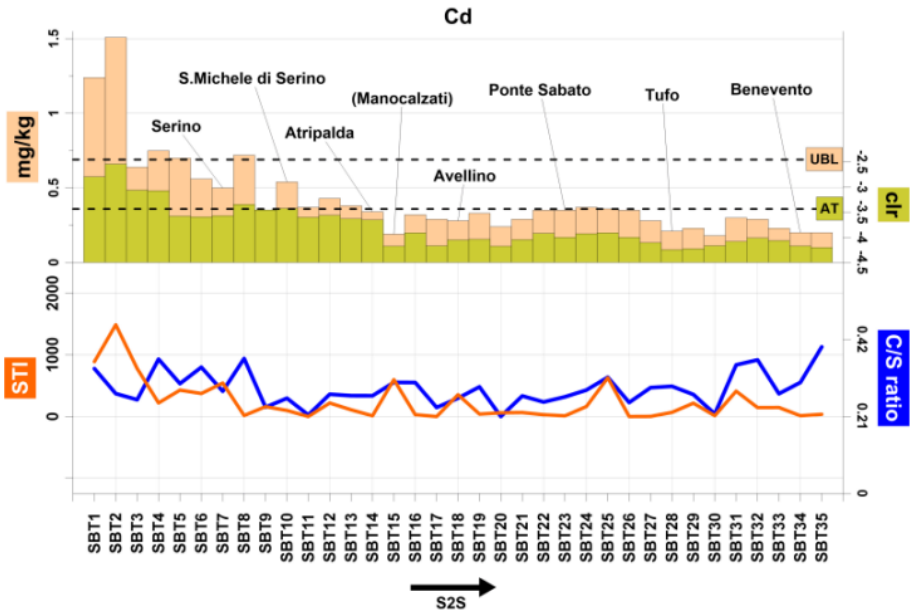

Figure 6.11 S2S distribution of raw concentrations (pink) and clr values (green). Data variations along the river course were also compared with the clay/silt ratio (C/S ratio) and sedimentation transport index (STI) (Mehnatkesh et al., 2013) to recognize any hydrogeological effect on concentration distribution.

6.5 Enrichment of PTEs in sediments from the Changjiang (Yangtze) River (China)

The results of this activity were published/presented in:

Dominech, S., Albanese, S., Guarino, A., Yang, S., submitted. Using compositional data analysis and multivariate statistics to indicate the enrichments of potentially toxic elements (PTEs) in sediments from the Changjiang (Yangtze) River. Geochemical Transactions

6.5.1 Summary of the work

Several studies have investigated the temporal and spatial distributions of PTEs concentrations in the Changjiang (Yangtze River) catchment which is one of the largest catchments in the world, suggesting that PTEs enrichment has become severe over the last two decades (Dong et al., 2012) due to the rapid economic development of China (Shen et al., 2006). The Changjiang is one of the largest rivers (6380 km long) in the world and originates in the eastern Tibetan Plateau and discharges suspended sediment and water into the East China Sea through one of the largest estuaries in the world (Fig. 6.12).

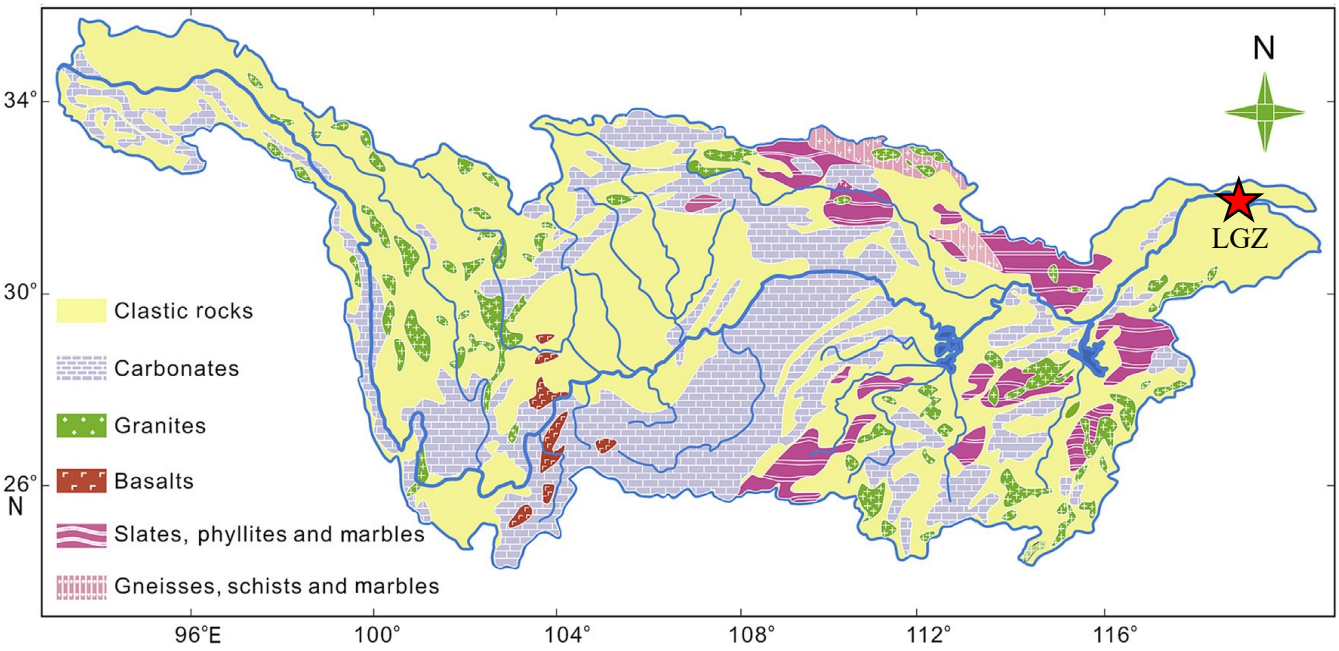

Figure 6.12 Simplified geological map (Shao et al., 2012) showing the Changjiang drainage basins, major tributaries, and the location of the LGZ core

This study measured the concentration of PTEs in 101 samples collected, at the sampling interval of 1-2 cm, from Core LGZ (of about 2 m) located in the mid-channel near the Changjiang River mouth (Fig. 6.12), far from any industrial activity, and aimed to find a novel and more complete approach in determining PTEs contamination levels. It also may give interesting insights in reconstructing the historical events that occurred in this large drainage basin over the last 150 years.

The parameters measured on the samples are: PTEs concentrations (estimated through the XRF), ^{137}Cs and ^{210}Pb for dating measurements, sediment grain size (analyzed by the laser size analyzer Coulter LS230), total organic carbon (TOC) and total nitrogen (TN).

The fundamentals of the Compositional Data Analysis (CoDA), together with multivariate statistics (robust principal factor analysis and fuzzy cluster analysis), were used for identifying baseline values and the reference group of geochemical elements used in the assessment of the modified enrichment factors (mEFs), estimated working with ratios among groups of elements that can be more representative of geochemical processes (Dominech et al., 2020). Log-ratio transformations and symmetrical balances were useful in an early-stage exploratory analysis to investigate the several relationships among geochemical trends and identify the first-order group of elements, also minimizing the variables available.

The robust principal factor analysis (RPCA) produced a three-component model (Na-Mg vs P-Si suggesting variations due to natural seasonal processes; Pb-Sc vs Zr-Sr-Ca showing high correspondence with the main flood events; Pb-Zn-Zr vs Y-Ca-Co indicating the anthropic impact in the study area) that mainly confirmed the multi-element associations already found adopting the symmetrical pivot coordinates (Na-Mg; Y-Rb; Si-P; Ti-La; Ca-Sr-Zr; Co-Fe-Sc-V; Zn-Pb).

Right after estimating the enrichment factors, the majority of considerable variations are related to the strong flood events, which have a great potential to alter the geochemical concentrations in a riverine environment. However, focusing on the upper (youngest) sector of the core, the noticeable anthropic impact on the catchment in the last few decades is quite evident.

Further details can be found in Dominech et al. (submitted).

6.5.2 Personal contribution

The contribution made for this work was prevalently the review and editing processes and the calculation of the baseline values, used in the estimate of the mEFs.

A clustering analysis was applied on the resulting principal component scores to identify several sample (observations) groups based on their relative affinity with one component over the others. The analysis performed in R allowed to detect 5 clusters. Among them, two clusters were identified as

potentially natural, or better, mainly influenced by geogenic (weathering, seasonal variation, chemical precipitation) processes, based on a deep geological interpretation and the sampling depth.

The baseline geochemical concentrations for all the selected elements were thus evaluated on the samples belonging to these two clusters through the ProUCL software (USEPA, 2014; Singh and Nocerino, 2002), estimated using the 95% UTL with 95% Coverage approach (Singh et al., 2006).

For this study, baselines values were preferred over background ones since any anthropogenic impact cannot be excluded in a short period (~150 years) for such a historically populated area like the Changjiang river basin.

References

Aitchison, J., 1982. The statistical analysis of compositional data. J R Stat Soc Series B Stat Methodol, 44(2), 139-160.

Aitchison J., 1984. The statistical analysis of geochemical compositions. J. Int. Assoc. Math. Geol. 16(6), 531–564. doi.org/10.1007/BF01029316.

Aitchison J., 1986. The statistical analysis of compositional data. London: Chapman & Hall, 416 pp.

Aiuppa, A., Avino, R., Brusca, L., Caliro, S., Chiodini, G., D'Alessandro, W., Favara, R., Federico, C., Ginevra, W., Inguaggiato, S., Longo, M., Pecoraino, G., Valenza, M., 2006. Mineral control of arsenic content in thermal waters from volcano-hosted hydrothermal systems: insights from island of Ischia and Phlegrean Fields (Campanian Volcanic Province, Italy). Chem. Geol. 229(4), 313 – 330.

Albanese S., De Vivo B., Lima A., Cicchella D., 2007. Geochemical background and baseline values of toxic elements in stream sediments of Campania region (Italy). J. Geochem. Explor. 93(1), 21–34.

Arienzo, M., Donadio, C., Mangoni, O., Bolinesi, F., Stanislao, C., Trifuoggi, M., Toscanesi, M., Di Natale, G., Ferrara, L., 2017. Characterization and source apportionment of polycyclic aromatic hydrocarbons (PAHs) in the sediments of gulf of Pozzuoli (Campania, Italy). Mar. Pollut. Bull. 12(1), 480-487.

Avino, R., Capaldi, G., Pece, R., 1999. Radon in active volcanic areas of Southern Italy. Il Nuovo Cimento, 22 C (3-4), 379-385.

Carranza E.J.M., Hale M., 1997. A catchment basin approach to the analysis of reconnaissance geochemical-geological data from Albay Province, Philippines. J. Geochem. Explor. 60(2), 157–171. doi.org/10.1016/S0375-6742(97)00032-0.

Cheng, Q., 1994. Multifractal modelling and spatial analysis with GIS: Gold potential estimation in the Mitchell-Sulphurets area. Northwestern British Columbia - Unpublished PhD thesis. University of Ottawa, Ottawa, 268 pp.

Chiodini, G., Caliro, S., Cardellini, C., Granieri, D., Avino, R., Baldini, A., Donnini, M., Minopoli, C., 2010. Long-term variations of the Campi Flegrei, Italy, volcanic system as revealed by the monitoring of hydrothermal activity. J. Geophys. Res. Solid Earth 115 (B3).

Chiodini, G., Caliro, S., De Martino, P., Avino, R., Gherardi, F., 2012. Early signals of new volcanic unrest at Campi Flegrei caldera? Insights from geochemical data and physical simulations. Geology 40(10), 943 – 946.

De Vita, P., Allocca, V., Celico, F., Fabbrocino, S., Mattia, C., Monacelli, G., Musilli, Celico, P., 2018. Hydrogeology of continental southern Italy. Journal of Maps, 14(2), 230-241. https://doi.org/10.1080/17445647.2018.1454352

Dominech, S., Guarino, A., Aruta, A., Ebrahimi, P., Yang, S., Albanese, S., 2020. Potentally toxic elements (PTEs) distribution and main geochemical processes in Sabato River Catchment Basin (southern Italy): a focus on cadmium. Conference proceedings, Proscience vol. 7. ISSN: 2283-5954.

Dong, A., Zhai, S., Matthias, Z., Yu, Z., Zhang, H., Liu, F., 2012. Heavy metals in Changjiang estuarine and offshore sediments: Responding to human activities. Acta Oceanol. Sin. 31, 88–101. https://doi.org/10.1007/s13131-012-0195-y

Ebrahimi, P., Guarino, A., Allocca, V., Caliro, S., Cicchella, D., Albanese, S., submitted. The dissolved radon and carbon dioxide contents in Phlegraean Fields volcanic aquifer: a follow-up study. Chemosphere

Ebrahimi, P., Guarino, A., Allocca, V., Caliro, S., Avino, R., Bagnato, E., Capecchiacci, F., Carandente, A., Minopoli, C., Santi, A., Albanese, S., 2022. Hierarchical clustering and compositional data analysis for interpreting groundwater hydrogeochemistry: The application to Campi Flegrei volcanic aquifer (south Italy). J. Geochem. Explor. 233. https://doi.org/10.1016/j.gexplo.2021.106922

Filzmoser, P., Hron, K., Reimann, C., 2009. Principal component analysis for compositional data with outliers. Environmetrics 20(6), 621-632.

Guarino, A., Lima, A., Cicchella, D., Albanese, S., 2022. Radon flux estimates, from both gamma radiation and geochemical data, to determine sources, migration pathways, and related health risk: The Campania region (Italy) case study. Chemosphere 287(1), 132233. https://doi.org/10.1016/j.chemosphere.2021.132233

ISPRA (Istituto superiore per la protezione e la ricerca ambientale), 2018. Carta Geologica d'Italia. 563 1:50,000 Sheets: 446-447 Napoli.

Mehnatkesh A., Ayoubi S., Jalalian A. Sahrawat, K.L., 2013. Relationships between soil depth and terrain attributes in a semi-arid hilly region in western Iran. J. Mt. Sci. 10(1), 163–172.

Reimann C., Filzmoser P., Garrett R.G., 2005. Background and threshold: Critical comparison of methods of determination. Sci. Total Environ. 346(1–3), 1–16. doi.org/10.1016/j.scitotenv.2004.11.023.

Reimann, C., Filzmoser, P., Garrett, R.G., Dutter, R., 2008. Statistical Data Analysis Explained: Applied Environmental Statistics with R. Wiley, Chichester, UK.

Shao, L., Li, C.A., Yuan, S., Kang, C., Wang, J., Li, T., 2012. Neodymium isotopic variations of the late Cenozoic sediments in the Jianghan Basin: Implications for sediment source and evolution of the Yangtze River. https://doi.org/10.1016/j.jseaes.2011.09.018

Shen, M., Yu, H.X., Deng, X.H., 2006. Heavy metals in surface sediments from lower reach of the Yangtze River. The Administration and Technique of Environmental Monitor- ing 18, 15–18 (In Chinese).

Singh, A., Maichle, R., Lee, S., 2006. On the computation of a 95% upper confidence limit of the unkown population mean upon data sets with below detection limit observations.

Singh, A., Nocerino, J., 2002. Robust estimation of mean and variance using environmental data sets with below detection limit observations. Chemom. Intell. Lab. Syst. 60, 69–86. https://doi.org/10.1016/S0169-7439(01)00186-1

Somma, R., Ebrahimi, P., Troise, C., De Natale, G., Guarino, A., Cicchella, D., Albanese, S., 2021. The first application of compositional data analysis (CoDA) in a multivariate perspective for detection of pollution source in sea sediments: The Pozzuoli Bay (Italy) case study. Chemosphere 274. DOI: 10.1016/j.chemosphere.2021.129955

USEPA, 2014. ProUCL 5.0.00 Statistical Software for Environmental Applications for Datasets with and without Nondetect. Observations. Office of Research and Development, US Environmental Protection Agency (US EPA), August 2014. http://www.epa.gov/esd/tsc/TSC_form.htm

Valentino, G.M., Stanzione, D., 2003. Source processes of the thermal waters from the Phlegraean Fields (Naples, Italy) by means of the study of selected minor and trace elements distribution. Chem. Geol. 194(4), 245 – 274.

Valentino, G.M., Cortecci, G., Franco, E., Stanzione, D., 1999. Chemical and isotopic compositions of minerals and waters from the Campi Flegrei volcanic system, Naples, Italy. J. Volcanol. Geotherm. Res. 91(2 – 4), 329 – 344.

Vitale, S., Isaia, R., 2014. Fractures and faults in volcanic rocks (Campi Flegrei, southern Italy): insight into volcano-tectonic processes. Int. J. Earth Sci. 103(3), 801 – 819.

Zuo, R., Wang, J., 2020. ArcFractal: An ArcGIS Add-In for Processing Geoscience Data Using Fractal/Multifractal Models. Nat. Resour. Res. 29, 3-12. https://doi.org/10.1007/s11053-019-09513-5.

Conclusions

The work carried out during the PhD project and presented in this thesis was made possible thanks to the collaborations that the Environmental Geochemistry Working Group (EGWG), based at the Department of Earth, Environment and Resources Sciences, University of Naples Federico II, is carrying out since several years with numerous national and international research institutions.

Specifically, among the others, the activities involved collaborations with the State Key Laboratory of Marine Geology of the Tongji University (Shanghai, PR China), the National Institute of Geophysics and Volcanology - Vesuvius Observatory (INGV-OV) (Naples, Italy), the Experimental Zooprophylactic Institute of Southern Italy (IZSM) (Portici, Naples, Italy) and last but not least the Center for Ecological-Noosphere Studies (CENS) (Yerevan, Armenia) thanks to which I accomplished a three-month virtual Erasmus+ program from September to December 2021.

The objectives of the project, which were predominantly the study of specific scientific problems of great relevance and interest in the field of environmental geochemistry and medical geology (e.g., the determination of background/baseline values at both regional and local scale that allows the definition of the contamination level of an area, the study of bioavailable fraction of elements that could enter the food chain and represent a potential hazard for human health, the study of the distribution of radioelements in regional soils, the determination of the source origins of several PTEs and POPs) have been totally fulfilled.

The work done, which allowed me to acquire a greater scientific and personal maturity, represents another piece to add to the geochemical knowledge of the Campania region.

Although Campania is, to date, the most monitored Italian region, this study conducted on various topics, from the definition of background values to the assessment of potential danger and from the definition of the factors that influence the bioavailability of the elements to the study of natural radioactivity in regional soils, does not represent the end of the design of environmental assessment but rather the starting point for an even more efficient and exhaustive characterization of the territory.

The hope is to reach not only the representative bodies, providing tools for the correct management of the territory, but also to raise awareness among the population by making available tools for the knowledge of the nature of issues affecting the territories that surround them.

Publications in the framework of the PhD program

Contributions to international peer-reviewed journals

- **Guarino A**., Albanese S., Cicchella D., Ebrahimi P., Dominech S., Allocca C., Romano N., De Vivo B., Lima A., submitted. Selected major and potentially toxic elements bioavailability in agricultural soils of Campania region (Italy): spatial patterns and influencing factors. Journal of Geochemical Exploration
- Dominech S., Albanese S., **Guarino A.**, Yang S., submitted. Using compositional data analysis and multivariate statistics to indicate the enrichments of potentially toxic elements (PTEs) in sediments from the Changjiang (Yangtze) River. Geochemical Transactions
- Ebrahimi P., **Guarino A.**, Allocca V., Caliro S., Cicchella D., Albanese S., under review. The dissolved radon and carbon dioxide contents in Phlegraean Fields volcanic aquifer: a follow-up study. Chemosphere.
- Ebrahimi P., **Guarino A.**, Allocca V., Caliro S., Avino R., Bagnato E., Capecchiacci F., Carandente A., Minopoli C., Santi A., Albanese S., 2022. Hierarchical clustering and compositional data analysis for interpreting groundwater hydrogeochemistry: The application to Campi Flegrei volcanic aquifer (south Italy). Journal of Geochemical Exploration. https://doi.org/10.1016/j.gexplo.2021.106922
- **Guarino A.**, Lima A., Cicchella D., Albanese S., 2022. Radon flux estimates, from both gamma radiation and geochemical data, to determine sources, migration pathways, and related health risk: The Campania region (Italy) case study. Chemosphere 287(1):132233 https://doi.org/10.1016/j.chemosphere.2021.132233
- Somma R., Ebrahimi P., Troise C., De Natale G., **Guarino A.**, Cicchella D., Albanese S., 2021. The first application of compositional data analysis (CoDA) in a multivariate perspective for detection of pollution source in sea sediments: The Pozzuoli Bay (Italy) case study. Chemosphere 274. DOI: 10.1016/j.chemosphere.2021.129955

Contribution to national scientific volumes

- Aruta A., **Guarino A**., 2020. The European and Italian experience in the global geochemical baseline mapping and some related activities: soils, waters and sediments. GIS DAY 2018, pp 79-100. ISBN: 978-88-255-2952-4.

- Albanese S., **Guarino A.**, Pizzolante A., Nicodemo F., Ragone G., Iorio R., D'Antonio A., Ferraro A., 2022. The use of natural geochemical background values for the definition of local environmental guidelines: the case study of the Vesuvian plain. In: Baldi, D., and Uricchio, F. (Eds.), Le bonifiche ambientali nell'ambito della transizione ecologica, Società Italiana di Geologia Ambientale (SIGEA) and Consiglio Nazionale delle Ricerche (CNR).

Monographies

- De Vivo B., Cicchella D., Lima A., Fortelli A., **Guarino A.**, Zuzolo D., Esposito M., Cerino P., Pizzolante A., Albanese S., 2021. Monitoraggio Geochimico-Ambientale dei suoli della Regione Campania – Volume 1 (Elementi Potenzialmente Tossici e loro Biodisponibilità, Elementi Maggiori e in Traccia; distribuzione in suoli superficiali e profondi). Aracne Editrice, Roma. ISBN: 978-88-255-4036-9.
- De Vivo B., Albanese S., Lima A., Qu C., Fortelli A., **Guarino A.**, Zuzolo D., Esposito M., Pizzolante A., Cerino P., Hope D., Pond P., Cicchella D., 2021. Monitoraggio Geochimico-Ambientale dei suoli della Regione Campania – Volume 2 (Composti Organici Persistenti: Idrocarburi Policiclici Aromatici, Policlorobifenili, Pesticidi). Aracne Editrice, Roma. ISBN: 978-88-255-4107-6.
- De Vivo B., Cicchella D., Albanese S., Qu C., **Guarino A.**, Fortelli A., Esposito M, Cerino P., Pizzolante A., Hope D., Pond P., Lima A., 2022. Monitoraggio geochimico-ambientale della matrice aria della Regione Campania. Il Piano Campania Trasparente. Volume 3. Idrocarburi Policiclici Aromatici (IPA), Policlorobifenili (PCB), Pesticidi (OCP), Eteri di Polibromobifenili (PBDE), Elementi Potenzialmente Tossici (EPT). Aracne Editrice, Roma. ISBN: 979-12-5994-733-8, 676 pag.
- De Vivo B., Cicchella D., Lima A., **Guarino A.**, Qu C., Fortelli A., Esposito M, Cerino P., Pizzolante A., Albanese S., 2022. Sintesi del monitoraggio dei suoli e dell'aria della regione Campania, a scala regionale e locale. Piano Campania Trasparente. Volume 4: Elementi potenzialmente tossici (EPT) e loro biodisponibilità elementi maggiori e in traccia, Idrocarburi Policiclici Aromatici (IPA), Policlorobifenili (PCB), Pesticidi (OCP), Eteri di Polibromobifenili (PBDE). Aracne Editrice, Roma. ISBN: 979-12-5994-735-2, 240 pag.

Conference proceedings

- **Guarino A.**, Aruta A., Ebrahimi P., Dominech S., Lima A., De Vivo B., Qi S., Albanese S., 2020. Potentially Harmful Elements and Polycyclic Aromatic Hydrocarbons in the soils of Acerra, southern Italy. Conference proceedings, Proscience vol. 7. ISSN: 2283-5954.
- Dominech S., **Guarino A**., Aruta A., Ebrahimi P., Yang S., Albanese S., 2020. Potentally toxic elements (PTEs) distribution and main geochemical processes in Sabato River Catchment Basin (southern Italy): a focus on cadmium. Conference proceedings, Proscience vol. 7. ISSN: 2283-5954.

Conference abstracts

- **Guarino A.**, Aruta A., Ebrahimi P., Dominech S., Lima A., Cicchella D., Albanese S., 2021. Radon fluxes estimate from geochemical data and gamma radiation in Campania region (Italy). BeGeo scientists 2021, Naples. https://doi.org/10.3301/ABSGI.2021.04
- Ebrahimi P., **Guarino A.,** Allocca V., Caliro S., Avino R., Bagnato E., Capecchiacci F., Carandente A., Minopoli C., Santi A., Albanese S, 2021. Fluoride in Campi Flegrei volcanic aquifer, south Italy: A comparison between water and rock composition. BeGeo scientists 2021, Naples. https://doi.org/10.3301/ABSGI.2021.04
- **Guarino A.**, Aruta A., Ebrahimi P., Dominech S., Lima A., Cicchella D., Albanese S., 2021. Estimating radon fluxes through different datasets to discriminate sources and assess health risks in Campania region (Italy). Environmental Geochemistry and Health 2021
- Albanese S., **Guarino A.**, De Mascellis R., Perreca C., Fagnano M., Vingiani S., 2021. Use of proximal sensors and pedo-geochemical survey in a outdoor shooting range for the assessment of spatial variability and fate of contaminants in soils. Eurosoil 2021.
- **Guarino A.**, Pizzolante A., Nicodemo F., Ragone G., D'Antonio A, Ferraro A., Albanese S., 2021. The definition of geochemical background values at local scale as a key procedure to set reliable guidelines for contaminated land management. Goldschmidt Virtual 2021, Lyon. DOI: 10.7185/gold2021.3810
- Ebrahimi P., Somma R., Troise C., De Natale G., **Guarino A**., Cicchella D., Albanese S., 2021. Characterising source of arsenic in the sediments of Pozzuoli Bay (south Italy) using compositional data analysis (CoDA). Goldschmidt Virtual 2021, Lyon. DOI: 10.7185/gold2021.6152

- Dominech S., Yang S., Ebrahimi P., Aruta A., **Guarino A.**, Gramazio A., Albanese S., 2021. A new approach to determine geochemical fingerprint of contaminants in stream sediments of Southern Italy. Goldschmidt Virtual 2021, Lyon. DOI: 10.13140/RG.2.2.35044.91523
- **Guarino A.,** Aruta A., Ebrahimi P., Dominech S., Lima A., De Vivo B., Qi S., Albanese S., 2021. Organochlorine pesticides in the soils of the Acerra plain: concentration and distribution of DDT isomers and metabolites. European Geosciences Union General Assembly 2021, Vienna. DOI: 10.5194/egusphere-egu21-5739
- Albanese S., **Guarino A.,** Aruta A., De Mascellis R., Perreca C., Fagnano M., Vingiani S., 2021. Soil pollution in a decommissioned shooting range: a preliminary survey of the spatial variability of legacy pollutants. European Geosciences Union General Assembly 2021, Vienna. DOI: 10.5194/egusphere-egu21-4969
- Aruta A., **Guarino A.**, Ebrahimi P., Dominech S., Belyaeva O., Tepanosyan G., Albanese S., 2021. Low-level ionising radiation and associated risk in an urban environment: the importance of both paving and building materials. European Geosciences Union General Assembly 2021, Vienna. DOI: 10.5194/egusphere-egu21-5566
- **Guarino A.**, Aruta A., Ebrahimi P., Dominech S., Zuzolo D., Lima A., Cicchella D., Albanese S., 2020. Pedogenic radon fluxes predictions from geochemical data and gamma ray: the Campania region experiment. GEOHEALTH 2020 - INTERNATIONAL MEETING OF GEOHEALTH SCIENTISTS, Bari. Scientific Research Abstracts Vol. 10, p. 26. ISSN 2464-9147.
- Zuzolo D., Albanese S., Iannone A., Ebrahimi P., Melito R., **Guarino A.**, Aruta A., Cicchella D., 2020. Reconnaisance soil gas radon survey in Campania region (Italy): preliminary results. GEOHEALTH 2020 - INTERNATIONAL MEETING OF GEOHEALTH SCIENTISTS, Bari. Scientific Research Abstracts Vol. 10, p. 51. ISSN 2464-9147.
- Dominech S., **Guarino A**., Aruta A., Ebrahimi P., Yang S., Albanese S., 2020. Potentally toxic elements (PTEs) distribution and main geochemical processes in Sabato River Catchment Basin (southern Italy). GEOHEALTH 2020 - INTERNATIONAL MEETING OF GEOHEALTH SCIENTISTS, Bari. Scientific Research Abstracts Vol. 10, p. 16. ISSN 2464-9147.
- Aruta A., **Guarino A.**, Ebrahimi P., Dominech S., Belyaeva O., Tepanosyan G., Albanese S., 2020. Radiological risk induced by road paving and building materials in the city of Naples, south Italy. GEOHEALTH 2020 - INTERNATIONAL MEETING OF GEOHEALTH SCIENTISTS, Bari. Scientific Research Abstracts Vol. 10, p. 2. ISSN 2464-9147.
- **Guarino A**., Aruta A., Ebrahimi P., Dominech S., Lima A., De Vivo B., Qi S., Albanese S., 2020. Potentially Harmful Elements and Polycyclic Aromatic Hydrocarbons in the soils of

Acerra, southern Italy. GEOHEALTH 2020 - INTERNATIONAL MEETING OF GEOHEALTH SCIENTISTS, Bari. Scientific Research Abstracts Vol. 10, p. 25. ISSN 2464-9147.

- **Guarino A**., Aruta A., Ebrahimi P., Dominech S., Albanese S., 2020. The "Triangle of Death": a case study from Campania region (Italy). Goldschmidt Virtual 2020, Honolulu. DOI: 10.46427/gold2020.897.
- Albanese S., **Guarino A.**, Zuzolo D., Aruta A., Cicchella D., Iannone A., Melito R., Verrilli F., Fedele Gianvito A., 2020. Extending the concept of background to soil gas: natural radon concentrations in soils of Campania region. European Geosciences Union General Assembly 2020, Vienna. DOI: 10.5194/egusphere-egu2020-22687.

Tutoring activities

Co-tutored master (Ms) and bachelor (Bc) theses

- Liguori, F., 2021. Determination of surficial fluxes and concentrations of Radon in the surface soils and groundwater of the municipalities of the plain north of Vesuvius. (**Ms**)
- Pacifico, L.R., 2021. Interpreting geochemical patterns of some major and trace elements in Campania region topsoils using Compositional Data Analysis (CoDA) in a multivariate perspective. (**Ms**)
- De Falco, A., 2020. Geological origin and pedogenic fluxes of Radon in Campania. The municipality of Saviano (Na) case study. (**Bc**)
- Garofalo, F.F., 2019. Cartographic and statistical analysis of geochemical data for the determination of the main sources of anthropogenic anomalies in the province of Caserta. (**Ms**)

Teaching support

- "Geochemistry" course (2020/2021; 2021/2022). Priciples of thermodynamics. (**Bc**)
- "Geochemical prospecting" course (2020/2021; 2021/2022). Priciples of geochemical mapping. (**Ms**)
- "Environmental geochemistry" course (2019/2020; 2020/2021; 2021/2022). Priciples of geochemical mapping. (**Ms**)

Acknowledgments

I would like to express my deep gratitude to the members of the Environmental Geochemistry Working Group (EGWG) Prof. Annamaria Lima, my supervisor, Prof. Stefano Albanese and Prof. Domenico Cicchella, my co-supervisor, and Prof. Benedetto De Vivo. They have always been kind and helpful, giving me many opportunities to increase my skills through active participation in various research activities.

A heartfelt thanks goes to Prof. Stefano Albanese without whom I probably would not have started this PhD program. Thank you for believing in me, for giving me so many opportunities and for being able to create a collaborative work environment while managing to be a mentor and a colleague at the same time.

Thanks to my colleagues, the junior members of the EGWG, Salvatore, Antonio, Pooria, Andrea and Lucy, for the crazy moments spent together both on the field and in the office.

Thanks to the referees of my thesis, Prof. Paolo Valera and Dr. Gevorg Tepanosyan, for their valuable advice for improving my work and for their kind words of appreciation.

A big thanks to my parents, mes oncles and my grandmothers for loving me and always being there. They were not convinced of my choice to enrol in geology, but I hope I made you proud of me.

My warm thanks to Jessica, Leonardo, Lollo, Gessica and Mariagiulia. A book would not be enough to tell all the adventures spent together and what you mean to me. Thanks to you I know the value of the word "brotherhood".

Thanks to all my friends, old and new, those I met at the Bachelor's and Master's, those I met in Erasmus and those I met by chance. It would be impossible to list you all, but thanks for sharing joys, sorrows, anxieties, happy moments with me, or even just an aperitif, a bruschetta, a "cena de pesce", a trip or a crazy birthday.

Last, but not least, to my partner, best friend, boyfriend Attilio. Thanks for everything. Thanks for putting up with me and supported me in these nine years, for having been by my side even when you were not convinced of my choices, for having been the light in the dark moments, for helping me to grow and at the same time allowing me to remain a child. “A dream you dream alone is only a dream. A dream you dream together is reality.”